D.J. Staziker

Water Wave Scattering by Undulating Bed Topography.

February 1995

Abstract

The purpose of this thesis is to investigate the scattering of a train of small amplitude harmonic surface waves on water by undulating one-dimensional bed topography.

The computational efficiency of an integral equation procedure that has been used to solve the mild-slope equation, an approximation to wave scattering, is improved by using a new choice of trial function. The coefficients of the scattered waves given by the mild-slope equation satisfy a set of relations. These coefficients are also shown to satisfy the set of relations when they are given by any approximation to the solution of the mild-slope equation.

A new approximation to wave scattering is derived that includes both progressive and decaying wave mode terms and its accuracy is tested. In particular, this approximation is compared with older approximations that only contain progressive wave mode terms such as the mild-slope approximation. The results given by the new approximation are shown to agree much more closely with known test results over steep topography, where decaying wave modes are significant. During this analysis, a new set of boundary conditions is found for the mild-slope equation and the subsequent results give much better agreement with established test results.

Finally, the full wave scattering problem over a hump, that is, a local elevation in an otherwise flat uniform bed, is examined. Green's theory is used to convert the problem into an integral equation and a variational approach is then used to obtain approximations to the coefficients of the scattered waves. The results are used to further test the accuracy of previous approximations to wave scattering.

Contents

Chapter 1

Introduction

A long-standing but persistent problem in the area of water wave theory is the determination of the effect of bed topography and obstacles on a given wave field. An example of a practical problem faced by coastal engineers is to predict the amplitude of waves in harbours, where both man-made breakwaters and the shape of the sea bed affect the wave behaviour. Such problems involve the scattering, diffraction and refraction of waves and are mathematically formidable for linearised theory, even with relatively simple bed and/or obstacle geometries.

The work presented in this thesis is solely concerned with the effect of bed topography on an incident wave train. We do not address problems where an obstacle, such as a barrier, affects an incident wave train, except for mentioning them in this introduction and noting the solution methods used. The effect of variations in the still-water depth on an incident wave train is examined using linearised theory. We prescribe the incident wave train and the deviation in the still-water depth, and seek the additional waves, the scattered waves, caused by this deviation. A typical problem requires the determination of a velocity potential satisfying Laplace's equation within the fluid, a mixed boundary condition on the free surface, and a given normal velocity on rigid boundaries. If the fluid domain extends to infinity, a radiation condition is required to ensure uniqueness. This boundary-value problem is well known and is formally presented in Chapter 2. We shall refer to the problem of finding a solution of the boundary-value problem as the full linear problem. Analytic solutions of the full linear problem are rare for any deviation from the constant water depth case, that is, for any

deviation from a flat sea bed. Problems where analytic solutions exist are usually for a limited selection of straightforward geometries which include horizontal and/or vertical boundaries.

In Chapters 3 and 5 we are faced with solving second-kind and first-kind integral equations respectively. Many problems in water wave theory, where an incident wave train is influenced by bed topography and/or obstacles, can be reduced to integral equations. It is useful to review some of these two-dimensional and quasi-two-dimensional wave scattering problems here.

The two-dimensional scattering of surface waves by fixed vertical barriers has seen much attention over recent decades. In water of infinite depth, that is, water deep enough that the bed has no significant effect on surface waves, Dean [13] considered the case of a submerged semi-infinite barrier, whose upper edge was a finite depth below the surface. His solution procedure used the reduction method, which consists of replacing the velocity potential by another function which is chosen to simplify the boundary conditions. Dean showed that the reflected wave is small, unless the edge of the barrier is very near the edge of the surface, when the wave motion is no longer oscillatory and there is a rapid flow over the barrier when a crest arrives. Ursell [58] solved this problem, and its complement in which the barrier extends from above the free surface to a finite depth, by an integral equation procedure for which exact solutions were found. In water of finite depth, these two problems become more difficult and have been solved numerically by Mei and Black [4] using a variational method employed by Miles [39] when he considered wave scattering due to an infinite step.

The problem of two submerged, semi-infinite barriers placed an arbitrary distance apart was addressed by Jarvis [23]. He found expressions for the coefficients of the reflected and transmitted waves in terms of four definite integrals. Jarvis evaluated these integrals by numerical approximation and showed that total transmission could be achieved at certain wavelengths. Evans and Morris [18] considered the complementary problem of two surface piercing barriers immersed to a given depth by a quite different, integral equation, procedure. Approximate solutions were found by using Ursell's [58] exact solution for a single barrier as a trial function in the integral equation. Their analysis revealed that total trans-

mission or total reflection is possible. This approximation method proved less accurate when the ratio of barrier separation to barrier length became small. Newman [43] addressed this case, by a different approach which involved matching solutions both near the two obstacles and in the far field. Newman also found that both total transmission or total reflection is possible.

Another problem of much interest concerns the flow around vertical barriers containing gaps. Tuck [57] considered the problem of a thin, semi-infinite impermeable barrier extending downwards from the fluid surface and having at some depth a small gap. He constructed an approximation to the transmission coefficient under the assumption that the gap was small. Porter [47] considered the same problem using a reduction method and an integral equation procedure and his analysis showed that both approaches relied on the same basic step. Porter calculated several reflection and transmission coefficients without needing to make any restrictions on the gap width. A more general problem of this form, where an arbitrary number of thin barriers (one above the next, with the uppermost barrier allowed to intersect the free surface and the lowest allowed to extend infinitely far into the fluid) are allowed to oscillate with the same frequency as the incident wave, was considered by Porter [48]. The resulting boundary-value problem was converted into an integral equation, from which the amplitudes of the scattered waves could be readily determined. The case of two parallel semi-infinite barriers that pierce the free surface and extend downwards throughout the fluid having at some depth a small gap, was addressed by Evans [17] using an integral equation approach. The numerical results again showed the possibility of total transmission or total reflection occurring for an infinite number of configurations of barrier spacing, gap width and incident wavelength.

The more general problem for surface waves in deep water incident on an arbitrary number of evenly spaced, identical, thin vertical barriers, each containing arbitrarily positioned gaps was addressed by Porter [49]. Expressions for the transmission and reflection coefficients were derived by approximation methods for two special cases. The first was for each barrier containing a single small gap and the second was for the separation between adjacent barriers greatly exceeding the wavelength. In both cases it was found that there existed band-

s of wavelengths for which total transmission of the incident wave is possible, and the insertion of an additional barrier resulted in an infinity of wavelengths corresponding to zero reflection.

These problems with barriers that contain gaps become more difficult when the water is not assumed to be deep, as the motion is then also affected by the bed. Macaskill [34] considered the reflection of water waves by a thin vertical barrier of arbitrary permeability in water of finite depth. An integral equation for the horizontal fluid velocity was derived by an application of Green's theorem and was solved by collocation methods. A serious problem for the solution process to overcome involved the numerical difficulty of evaluating a Green's function given by an infinite series. We are faced with the same problem in Chapter 5.

In Porter [50], there is a general discussion about the refraction/diffraction problem for vertical-sided breakwaters of finite depth, in relation to Green's theory and integral equation methods. Examination of several special cases for the class of problems where the breakwaters are straight, parallel walls containing gaps showed that the resulting integral equations are conducive to straightforward numerical solution techniques. Indeed, a very efficient computational method which solves the problem of diffraction of a plane wave train through a gap in an infinite straight breakwater, and the complementary problem of diffraction by a finite strip, was given by Chu and Porter [11]. The solution procedure involved the conversion of known first-kind equations for these problems into second-kind equations which are much more amenable to numerical techniques. This was an early example of the use of the technique of invariant imbedding in water wave theory.

For all the problems discussed so far, the geometries have involved vertical boundaries in water of infinite or constant depth. Allowing the water depth to vary increases the difficulty of the problem, and consequently exact solutions are exceedingly rare for such problems. The exceptions to this are limiting cases such as shallow water, where the wavelength is assumed to be much larger than the water depth.

Lamb [28] derived an exact expression for the reflection coefficient for the problem of waves incident on a vertical step in shallow water. Bartholomeusz [1]

considered the same problem without the shallow water assumption. By matching eigenfunction expansions, Bartholomeusz derived a first-kind integral equation for the horizontal fluid velocity. After transforming this equation into a second-kind integral equation for which extensive theory exists, Bartholomeusz showed that the solution reduced to that obtained by Lamb [28] in the shallow water limit, so giving a verification of this theory.

Newman [42] considered the propagation of water waves over an infinite step, where the vertical part of the step extends down to infinity. By matching solutions for the two fluid regions at the cut above the step, Newman derived an integral equation for the horizontal velocity component on the cut. Newman recast this integral equation as an infinite system of equations and solved it by truncation. Miles [39] considered the more difficult problem of a finite step which Bartholomeusz [1] solved in the shallow water limit. Miles used a variational technique to obtain approximate solutions of the first-kind integral equation for the horizontal fluid velocity. By taking the limit of the vertical part of the step to infinity, Miles found that his results showed excellent agreement with those obtained by Newman.

Allowing the depth profile to vary smoothly, rather than changing abruptly as in the case of a step, creates further difficulties in the wave scattering problem. As far as is known, the only analytic expression for the velocity potential in a problem of this type has been given by Roseau [53]. He obtained an explicit solution for the reflection and transmission of waves across a shelf of a special profile which asymptotically joins two regions of constant, but unequal, depth. According to Wehausen and Laitone [59], a proof of the existence and uniqueness of a velocity potential in a general problem of this type had yet to be given. Evans [16] addressed this problem in considering the transmission of water waves over a shelf of arbitrary profile. He used Green's theorem to derive a second-kind integral equation for the velocity potential. The associated Green's function which Evans derived is very complicated and the kernel of the integral equation was given in terms of the normal derivative, on the shelf, of this function. By suitably restricting the shelf profile, Evans was able to prove that the velocity potential exists and is unique, except possibly for certain discrete values of the

parameters of the problem corresponding to trapping modes over the shelf. The complexity of this integral equation is well illustrated by the fact that no one has so far found a suitable numerical method to solve it.

Fitz-Gerald [20] investigated wave scattering by a region of varying depth. He used a Fourier transform procedure to convert the boundary -value problem satisfied by the velocity potential into a pair of integro-differential equations. The required solution was then given by a linear combination of the solutions of the integro-differential equations. Fitz-Gerald was able to prove the existence and uniqueness of the velocity potential in two limiting cases and presented the associated asymptotic results.

The propagation of long waves over water of slowly varying depth for the two and three-dimensional cases was treated by Harband [22]. Asymptotic expressions were found for the scattered long waves under the assumption that the water is shallow compared with the wavelength.

Finding an accurate solution of the full linear problem of water wave scattering due to an arbitrary varying bed has proved so difficult and computationally expensive that various types of approximation to this problem have been proposed which can be solved accurately. One of the earliest and most widely used approximations is that of linearised shallow-water theory, in which the vertical structure of the fluid motion is ignored. A derivation of this approximation from first principles can be found in Stoker [55] and one example of its application is given by Lautenbacher [30], who considered the run-up of tsunamis on Hawaiian islands. Lautenbacher used Green's theorem to convert the governing differential equation into an integral equation and then found approximate solutions of the integral equation by using a numerical (finite difference) technique.

In water where the depth is not assumed to be shallow, one of the earliest approximations to the full linear problem was given by Eckart [15]. He derived his approximation by converting the full linear problem for the velocity potential into an integro-differential equation. Eckart showed that this equation was approximated by a partial differential equation by discarding a presumably small integral, 'without examining the justification of this approximation'. Eckart showed that his approximate equation reduces to the linearised shallow-water e-

quation in the shallow water limit. Through this work, Eckart also discovered a useful approximation to the root of the well known 'dispersion relation', a transcendental equation which connects the deep-water wave number to the wave number in finite water depth. Eckart did not pursue his approximation to the full linear problem further possibly, according to Miles [40], because he had obtained a rather unsatisfactory approximation to the group velocity in his 1951 lecture notes.

A more recent and very popular approximation of the full linear problem was given by Berkhoff [2] & [3], whose 'combined refraction-diffraction' equation has now become known as the mild-slope equation. There have been many subsequent derivations of the mild-slope equation, which typically approximate the vertical structure of the motion and restrict the bed slope to be 'small' or 'mild' in a sense to be described later. The derivation given by Berkhoff [3] is a clarification of the original derivation given in Berkhoff [2]. However, the mathematical approach used in Berkhoff [3], which is a perturbation procedure in terms of two small parameters, is still not rigorous. Smith and Sprinks [54] gave a more mathematically sound derivation of the mild-slope equation, by expanding the vertical dependence of the velocity potential in terms of an orthogonal set of functions and removing the dependence on the vertical co-ordinate by integration over the depth. The final step of their derivation still requires physical intuition to justify the neglect of terms on the basis that the bed slope is 'small' or 'mild enough'. Other derivations of the mild-slope equation have been given by Lozano and Meyer [32] and Massel [35], but perhaps the most elegant was given by Miles [40]. He uses a variational approach which, through a suitable choice of trial function, can be used to generate the linearised shallow-water, the Eckart and the mild-slope equations. Miles [40] goes on to compare the mild-slope and Eckart equations through the calculation of reflection from a gently sloping beech and of edge-wave eigenvalues for a uniform slope. He finds that Eckart's equation is inferior to the mild-slope equation for the amplitude in the reflection problem, but is superior in the edge-wave problem.

Another test of the accuracy of the mild-slope approximation was given by Booij [5], when he considered the problem of wave scattering due to a talud as its

steepness was varied. Booij compared the amplitude of the reflected wave given by the mild-slope approximation with values he computed using full linearised theory. From his results, Booij suggested that the mild-slope approximation gave results in 'good agreement' with those he had computed using full linearised theory for talud gradients up to one third. The results Booij [5] computed using full linearised theory have been well used by authors proposing new approximations to the velocity potential, because, as far as is known, these are the only published estimates of the reflection coefficient for the full linear wave scattering problem over a bed of varying depth.

The numerical methods that have been used to solve the boundary-value problem resulting from the mild-slope approximation are mainly finite difference (for example, Ebersole [14], Li and Anastasiou [31]) and finite element (for example, Berkhoff [2], [3] and Booij [5]) methods. An alternative solution method was given by Chamberlain [7], who converted the mild-slope boundary-value problem into a second-kind Fredholm integral equation. Through a powerful variational method which used problem-dependent trial functions, Chamberlain was able to find solutions that were machine accurate. The maximum trial space dimension required to achieve this accuracy was only six for all the problems he considered.

Wave tank experiments have also been carried out as another means of testing the accuracy of approximations, such as the mild-slope, to the velocity potential satisfying the full linear problem. One such set of wave tank experiments was conducted by Davies and Heathershaw [12], who measured the scattering of water waves by a finite patch of small amplitude ripples set in an otherwise horizontal bed. It was found that the mild-slope approximation gave a poor estimate of the peaks in the reflected amplitudes that arise in ripple bed problems when the water wave number is approximately twice the ripple wave number. Such peaks in the amplitude are known as Bragg resonance peaks. Improvements have therefore been sought to the mild-slope approximation, by attempting to improve the mild-slope approximation itself and by finding new approximations to the velocity potential.

To overcome this deficiency in the mild-slope approximation, Kirby [26] presented a model in which the depth profile was expressed in terms of a slowly

varying (mild-slope) component onto which a rapidly varying component of small amplitude is superimposed. Kirby then used a vertical integration procedure to derive what is now called the extended mild-slope equation. He verified that it gave much better agreement with the experimental data at the Bragg peaks for ripple bed problems than the mild-slope approximation. However, this improvement to the mild-slope approximation is only valid for ripple bed problems.

A further improvement to the mild-slope equation, which is valid over arbitrary depth profiles, was given by Chamberlain [6]. He followed the same procedure which Lozano and Meyer [32] used to derive the mild-slope equation. In other words, Chamberlain approximated the vertical structure of the velocity potential and removed the dependence on the vertical co-ordinate by integration over the depth. Chamberlain does not make the further assumption that the bed slope is mild, and consequently finds a new approximation to the velocity potential. Chamberlain and Porter [9] formalised the derivation of this new approximation, giving derivations using a variational approach and a Galerkin approach. They named the resulting equation the modified mild-slope equation, and showed that it reduced to the mild-slope equation when the bed slope is assumed to be mild. Chamberlain and Porter [9] also show that for ripple bed problems the modified mild-slope equation subsumes the extended mild-slope equation too. They found that the results given by the modified mild-slope equation are in better agreement with the full linear results for Booij's [5] talud problem than those given by the mild-slope equation. Chamberlain and Porter also found that in ripple bed problems, the results from the modified mild-slope equation gave excellent agreement with the experimental data at the Bragg peaks. Indeed, Chamberlain and Porter [10] use the well-known symmetry properties between the coefficients of the reflected and transmitted waves to obtain results for the modified mild-slope equation over any number of ripples from knowing the results for just one ripple. These symmetry properties were first derived for the full linear problem by Kreisel [27] and Newman [41] and Chamberlain [8] derived them for the mild-slope approximation. Chamberlain and Porter [10] show that these symmetry properties are an intrinsic part of the problem rather than of its exact solution, in the sense that they are automatically satisfied regardless of the accuracy of the

solution.

Massel [36] also uses a Galerkin approach to derive an approximation to the full linear velocity potential that included decaying wave mode terms too. He named the resulting system of second-order differential equations the extended refraction-diffraction equation. In this paper, Massel only gives solutions when the decaying wave mode terms are neglected, leaving the solution of the full problem incorporating decaying modes to a subsequent paper which has yet to appear. The system of second-order differential equations derived by Massel [36] reduces to a single equation when the decaying wave mode terms are omitted, which turns out to be the modified mild-slope equation. Massel noticed that this equation reduced to the mild-slope equation on the assumption that the slope of the bed is mild and also showed it was superior to the mild-slope equation for Booij's [5] talud problem and for ripple bed problems.

Other approximations of the full linear problem that include decaying wave mode terms have been given by O'Hare and Davies [45] and Rey [52]. Both sets of authors use a similar approach to derive the approximation to the velocity potential. The common approach involves approximating the bed profile as a series of horizontal shelves separated by abrupt vertical steps. The well-known flat bed infinite series representation of the velocity potential is used to represent the potential over each horizontal shelf. Continuity of the velocity potential and its horizontal derivative is imposed throughout the depth at the ends of each shelf, which gives a matrix system to be solved. This approximation can be computationally expensive as a large number of steps are required to obtain reliable results. In O'Hare and Davies [45], the approximation assumes that the steps are sufficiently far apart that the decaying modes generated at one step are negligible at neighbouring steps. O'Hare and Davies applied their approximation to ripple bed problems and noted that the results were in good agreement with known wave tank data. In a subsequent paper, O'Hare and Davies [46] compared their approximation against the extended mild-slope equation (Kirby [26]) for ripple bed problems. They found that their approximation provides a more explicit formulation of the problem and gave better agreement with the wave tank data than the extended mild-slope equation, but was much more computationally ex-

pensive. In Rey [52], the series of steps which approximates the depth profile is subdivided into smaller subsystems called patches. In each patch, the decaying modes generated at one step are not assumed negligible at neighbouring steps in the patch. However, the decaying modes generated in one patch are assumed negligible at neighbouring patches. This seems to be a superior approximation to that used by O'Hare and Davies [45]. Rey [52] goes on to test his approximation on Booij's [5] talud problem, finding good agreement with the full linear results computed by Booij. He also found that his results were quite different to those given by the mild-slope approximation, even for taluds with gradient less than one third, for which Booij [5] had claimed were in good agreement with the full linear model. Rey [52] also tested his approximation on ripple beds, finding good agreement with wave tank data.

After re-establishing the well-known full linearised equations for the scattering of waves by varying topography in Chapter 2, we go on to state the mild-slope equation and briefly review the integral equation procedure that Chamberlain [7] used to solve it.

Noting that coastal engineers require only about three decimal place accuracy in solutions of water wave problems, we go on, in Chapter 3, to improve the computational efficiency of Chamberlain's integral equation solution method. This is done by using a new choice of trial function and seeking solution accuracy to three decimal places rather than the machine accuracy achieved by Chamberlain. We also reinvestigate Eckart's [15] approximation and the symmetry properties of the coefficients of the reflected and transmitted waves.

The purpose of Chapter 4 is to derive a new approximation to the full linear velocity potential that includes both progressive and decaying wave mode terms and test its accuracy. We compare this new approximation with older approximations that only contain progressive wave mode terms, such as the mild-slope and the modified mild-slope approximations, as the steepness of the depth profile is varied. We investigate if the new approximation is better for steeper bed profiles as the steeper the bed profile the more significant the decaying wave modes become. In the course of this analysis a new set of boundary conditions is found for the modified mild-slope and mild-slope equations. The subsequent results give

much better agreement with the results that have been obtained using full linear theory and those found by Rey [52] than the results obtained using the original boundary conditions.

In Chapter 5, we consider the full linear wave scattering problem over an arbitrary hump. The term hump is used to describe a local elevation in an otherwise flat uniform bed. Using Green's theory, the boundary-value problem for the velocity potential is converted into a second-kind integral equation. Initially, an approximation in this equation is tried, but it proves to be rather inaccurate. It is found, however, that the second-kind integral equation for the potential can be converted into a first-kind integral equation for the tangential fluid velocity. The kernel of the first-kind equation is much easier to evaluate numerically than that of the second-kind equation. A variational approach is then used to obtain approximations to the coefficients of the reflected and transmitted waves which are second-order accurate compared to the approximation of the solution of the integral equation. These results are then used to test the accuracy of the new 'decaying mode' approximation derived in Chapter 4 and also to test the accuracy of the modified mild-slope and mild-slope approximations.

A summary of the work presented, together with conclusions and suggestions for future research concludes this thesis.

Chapter 2

Background Fluid Dynamics

In this chapter we present the linearised equations satisfied by the velocity potential for the irrotational flow of an incompressible, homogeneous fluid over a bed of varying depth. It is assumed that the fluid occupies a region which extends to infinity in every horizontal direction. The fluid is also bounded below by a bed of given permanent shape and above by a free surface whose shape is sought. A harmonic time dependence is removed from the velocity potential Φ. Separation solutions of the boundary-value problem satisfied by the time independent part of Φ are examined in the special case where the depth is constant.

However, analytic solutions are rare when there is any departure from the constant depth case. Therefore, three vertically integrated approximations of these equations are then considered: the well-known mild-slope and shallow water approximations, and the less familiar Eckart approximation.

Some of the subsequent work in this thesis revolves around solving integral equation forms of the one-dimensional mild-slope, Eckart and shallow water equations. This chapter therefore concludes with a review of an integral equation procedure which requires only 2- or 3- dimensional trial spaces to give excellent approximations to the solutions of these vertically integrated models.

2.1 The linearised boundary-value problem

Let x and y be horizontal cartesian co-ordinates and z a vertical co-ordinate measured positively upwards with the undisturbed free surface at $z = 0$. Let

the fluid velocity at time t and a given point (x, y, z) in the fluid be denoted by $\underline{q}(x, y, z, t)$. Assuming the fluid motion starts from rest, with gravity the only external force acting, then $\underline{q}$ is necessarily irrotational. It follows that there exists a velocity potential $\Phi(x, y, z, t)$ such that $\underline{q} = -\tilde{\nabla}\Phi$ where $\tilde{\nabla} = (\frac{\partial}{\partial x}, \frac{\partial}{\partial y}, \frac{\partial}{\partial z})$. The assumption of the fluid being homogeneous and incompressible reduces the continuity equation to

$$\tilde{\nabla} \, . \, \underline{q} = 0$$

and hence Φ satisfies Laplace's equation,

$$\tilde{\nabla}^2 \Phi = 0 \ , \tag{2.1}$$

in the fluid.

The bed is assumed to be fixed and impermeable and is defined by $z = -h(x, y)$, as depicted in Fig.2.1. As the fluid cannot flow through the bed, the normal derivative of the velocity potential on the bed must be zero, giving rise to the boundary condition

$$\frac{\partial \Phi}{\partial n} = 0 \qquad \text{on } z \ = \ -h(x, y) \tag{2.2}$$

where $\frac{\partial}{\partial n}$ denotes the outward normal derivative on $z = -h(x, y)$.

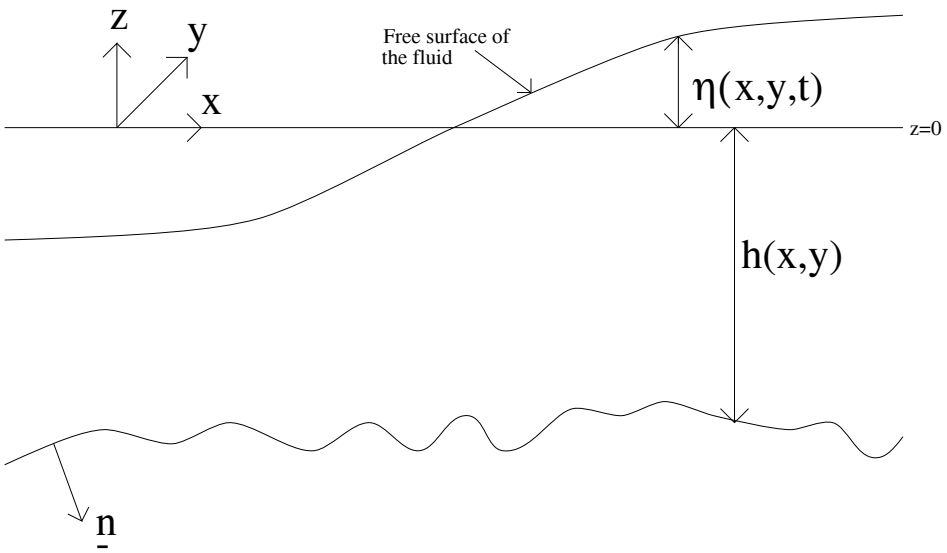

Figure 2.1: Vertical cross section of the fluid domain.

By considering the Stokes derivative $\frac{D}{Dt} = \frac{\partial}{\partial t} + \underline{q} \, . \, \tilde{\nabla}$ which denotes differentiation following the motion of the fluid, this boundary condition may be rewritten

as a so-called 'kinematic boundary condition' as follows. On any fluid boundary given by $f(x,y,z,t)=0$ we have

$$\frac{Df}{Dt}=0 \tag{2.3}$$

as otherwise there would be a finite flow of fluid across the boundary (Lamb [28]). The bed is defined by $z=-h(x,y)$, so substituting $f=z+h(x,y)$ into (2.3) delivers

$$\frac{\partial\Phi}{\partial z}+\nabla h\ .\ \nabla\Phi=0 \qquad \text{on } z=-h(x,y)\ , \tag{2.4}$$

where $\nabla=(\frac{\partial}{\partial x},\frac{\partial}{\partial y})$ is the gradient operator with respect to the horizontal co-ordinates only. Comparing equations (2.2) and(2.4) shows that

$$\frac{\partial}{\partial n}=-\frac{\frac{\partial}{\partial z}+\nabla h\ .\ \nabla}{(1+(\nabla h)^2)^{\frac{1}{2}}}\ , \tag{2.5}$$

where the denominator appears on the right hand side so that the outward unit normal, $\underline{n}$, given by

$$\underline{n}=-\frac{1}{(1+(\nabla h)^2)^{\frac{1}{2}}}\,(h_x,h_y,1)$$

satisfies the requirement $|\underline{n}|=1$.

Similarly, equation (2.3) must hold at the free surface given by $z=\eta(x,y,t)$. Substituting $f=z-\eta$ into (2.3) gives

$$\frac{\partial\eta}{\partial t}=-\frac{\partial\Phi}{\partial z}+\nabla\Phi\ .\ \nabla\eta \qquad \text{on } z=\eta. \tag{2.6}$$

A further condition at the free surface is delivered by considering Bernoulli's equation for unsteady, incompressible, homogeneous flows, namely

$$\frac{p}{\rho}=\frac{\partial\Phi}{\partial t}-\frac{1}{2}q^2-gz+f(t)\ , \tag{2.7}$$

where p is the pressure, ρ the constant density and g the acceleration due to gravity. Now, as Φ is defined by $\underline{q}=-\tilde{\nabla}\Phi$, $f(t)$ can be absorbed into $\dfrac{\partial\Phi}{\partial t}$ and similarly, assuming that surface pressure is constant, then on $z=\eta$ the left-hand side of (2.7) can also be absorbed into $\dfrac{\partial\Phi}{\partial t}$, reducing (2.7) to

$$\frac{\partial\Phi}{\partial t}=g\eta+\frac{1}{2}q^2 \qquad \text{on } z=\eta\ . \tag{2.8}$$

Equations (2.6) and (2.8) are linearised by expanding about $z=0$ and neglecting second-order terms, yielding, respectively,

$$\frac{\partial\Phi}{\partial z}=-\frac{\partial\eta}{\partial t} \qquad \text{on } z=0 \tag{2.9}$$

and

$$\frac{\partial \Phi}{\partial t} = g\eta \qquad \text{on } z = 0 \ . \tag{2.10}$$

On eliminating η from (2.9) and (2.10) we obtain the final boundary condition of the linear boundary-value problem, which is given by

$$\begin{aligned} \tilde{\nabla}^2 \Phi &= 0 \qquad && -h < z < 0 \ , \\ \frac{\partial \Phi}{\partial z} + \frac{1}{g}\frac{\partial^2 \Phi}{\partial t^2} &= 0 \qquad && \text{on } z = 0 \ , \\ \frac{\partial \Phi}{\partial z} + \nabla h \ . \ \nabla \Phi &= 0 \qquad && \text{on } z = -h(x,y) \ , \end{aligned} \tag{2.11}$$

together with a radiation condition imposed as $x^2 + y^2 \to \infty$. If we write $\Phi = \Phi_i + \Phi_s$ where Φ_i represents the incident wave field, then the radiation condition causes Φ_s to represent only outgoing waves as $x^2 + y^2 \to \infty$. Evans [16] has shown that when the bed is given by a shelf of arbitrary profile, then the solution Φ of the above problem is unique except possibly for certain discrete values of the parameters of the problem which correspond to trapped modes over the shelf.

2.2 Time-independent solutions

A harmonic time dependence can be removed from the velocity potential Φ by setting

$$\begin{aligned} \Phi(x,y,z,t) &= \phi_1(x,y,z)\cos(\sigma t) + \phi_2(x,y,z)\sin(\sigma t) \\ &= Re(\phi(x,y,z)e^{-i\sigma t}) \ , \end{aligned} \tag{2.12}$$

where $\phi(x,y,z) = \phi_1(x,y,z) + i\ \phi_2(x,y,z)$, $i = \sqrt{-1}$, and σ is an assigned angular frequency.

Defining $\nu = \sigma^2/g$, it follows that if Φ satisfies (2.11) together with a radiation condition then ϕ satisfies

$$\begin{aligned} \tilde{\nabla}^2 \phi &= 0 \qquad && -h < z < 0 \ , \\ \frac{\partial \phi}{\partial z} - \nu\phi &= 0 \qquad && \text{on } z = 0 \ , \\ \frac{\partial \phi}{\partial z} + \nabla h \ . \ \nabla \phi &= 0 \qquad && \text{on } z = -h(x,y) \ , \end{aligned} \tag{2.13}$$

together with a radiation condition.

The free surface elevation may be recovered by combining equations (2.10) and (2.12) to give

$$\eta(x,y,t) = Re\left\{-\frac{i\sigma}{g}\phi(x,y,0)e^{-i\sigma t}\right\} \tag{2.14}$$

2.3 Separation solutions

We have already noted that analytic solutions of (2.13) are rare. However, assuming that ϕ is independent of y, then in the flat bed case where h (the undisturbed fluid depth) is the constant h_0, separation solutions of (2.13) are easily found. These can be combined to give the general solution

$$\phi(x,z) = \sum_{n=0}^{\infty} \phi_n(x) w_n(z) \ , \tag{2.15}$$

where

$$\phi_0(x) \ = \ C_0 e^{ik_0 x} + D_0 e^{-ik_0 x} \ , \ \phi_n(x) = C_n e^{-B_n^0 x} + D_n e^{B_n^0 x} \quad (n \in \mathbb{N}),$$

$$w_0(z) \ = \ \frac{\cosh\left(k_0(z+h_0)\right)}{\cosh\left(k_0 h_0\right)} \ , \ w_n(z) = \frac{\cos\left(B_n^0(z+h_0)\right)}{\cos\left(B_n^0 h_0\right)} \quad (n \in \mathbb{N}),$$

and where k_0 is the real, positive root of the relation

$$\nu = k_0 \tanh\left(k_0 h_0\right) \tag{2.16}$$

and $B_n^0 \quad (n \in \mathbb{N})$ are the real, positive roots of the relation

$$-\nu = B_n^0 \tan\left(B_n^0 h_0\right) \ , \tag{2.17}$$

arranged in ascending order of magnitude.

Once an incident wave has been assigned, the arbitrary constants C_n and $D_n \quad (n+1 \in \mathbb{N})$ are specified. As already mentioned, the radiation condition enforces that ϕ is bounded as $|x| \to \infty$, causing the constants to be chosen so that, $\forall n \in \mathbb{N}$, $|\phi_n| \to 0$ as $|x| \to \infty$. Thus, the terms $\phi_n w_n \quad (n \in \mathbb{N})$ are called the decaying or evanescent modes (see for example, Mei [37]). Therefore $\phi_0 w_0$ is the only mode which propagates as a wave throughout the domain and is thus called the progressive wave mode.

Denoting the wavelength by λ, then using the fact that $\lambda = 2\pi/k_0$ allows (2.16) to be rewritten as

$$\left(\frac{\sigma}{k_0}\right)^2 = \frac{g\lambda}{2\pi}\tanh\left(\frac{2\pi}{\lambda}h_0\right) \ ,$$

where σ/k_0 is the wave speed. An interpretation of this equation is that waves of different lengths travel at different speeds. In other words they are dispersive, and hence (2.16) is known as a dispersion relation.

The following approximations to the full linear problem for ϕ use the assumption that the evanescent modes are negligibly small $\forall x \in (-\infty \ , \ \infty)$ when h is suitably restricted.

2.4 Approximations to time independent velocity potential ϕ

As previously stated, analytic solutions for the time-independent velocity potential ϕ satisfying (2.13) for any departure from the constant depth are rare. This naturally leads to the pursuit of an approximation to ϕ. As discussed in Chapter 1, the mild-slope approximation to ϕ is very well-known, with many authors using various procedures to establish the approximation. The mild-slope approximation to ϕ suitably restricts the depth profile h so that the decaying mode parts of ϕ are assumed to be negligibly small. Thus the mild-slope approximation to ϕ seeks to approximate the propagating mode of ϕ. This is achieved by approximating its dependence on the z co-ordinate, and discarding terms of $O(\nabla^2 h, \ |\nabla h|^2)$ on the basis of the mild-slope assumption $|\nabla h| \ll kh$ (Meyer [38]), where $h = h(x,y)$ is the undisturbed fluid depth and $k = k(x,y)$ is the local wave number satisfying the local dispersion relation,

$$\nu = k\tanh(kh) \ . \tag{2.18}$$

Omitting the details of a derivation here, the mild-slope approximation to ϕ is given by

$$\phi(x,y,z) = \phi_0(x,y)w(z,h) \ , \tag{2.19}$$

where

$$w(z,h) = \frac{\cosh\left(k(z+h)\right)}{\cosh\left(kh\right)} \ . \tag{2.20}$$

ϕ_0 satisfies the differential equation

$$\nabla.u\nabla\phi_0 + k^2 u\phi_0 = 0 \ , \tag{2.21}$$

where

$$u(h) = \int_{-h}^{0} w^2 \ dz = \frac{1}{2k}\tanh\left(kh\right)\left(1 + \frac{2kh}{\sinh\left(2kh\right)}\right) \ , \tag{2.22}$$

and the differential equation (2.21) satisfied by ϕ_0 is known as the mild-slope equation .

In Chapter 4, a variational approach similar to Miles [40] is employed, in which a variational principle and an n term trial function are used to obtain an approximation to ϕ that includes the decaying wave mode terms too. It will be shown that if a one-term trial function is used in this variational principle, and terms of $O(\nabla^2 h, \ |\nabla h|^2)$ are neglected, then the mild-slope equation is derived.

It should be noted that under the further assumption that $kh \ll 1$, so that $\tanh(kh)$ and $\sinh(2kh)$ are approximated by their arguments, the mild-slope equation (2.21) reduces to

$$\nabla.h\nabla\phi_0 \ + \ \nu\phi_0 = 0 \ . \tag{2.23}$$

This is another well-known equation – the linearised shallow water equation – which can, of course, be derived from first principles using the shallow water approximation (Stoker [55]). However, forming (2.23) as a limit of (2.21) is justified as the assumptions of the shallow water approximation imply mildness of slope. Jonsson et al [25] give some detail as to what constitutes 'small kh', and show that (2.23) is valid if $kh < \pi/10$.

Another vertically integrated approximation to ϕ was proposed some forty years ago by Carl Eckart [15], in which the linearised boundary-value problem for ϕ given by (2.13) is transformed into an integro-differential equation. Here the integral term is assumed small (without justification) in some cases, and is thus discarded. After neglecting third and higher derivatives of the depth function h, an approximation for linear gravity waves in water of variable depth $h = h(x,y)$

is arrived at in the form

$$\nabla.u\nabla\phi_0 \; + \; k^2 u\phi_0 = 0 \; , \tag{2.24}$$

where $Re(\phi_0 e^{-i\sigma t})$ is an approximation to the free surface shape,

$$u(h) \;\; = \;\; \frac{1-e^{-2\nu h}}{2\nu} \; , \tag{2.25}$$

$$k^2 \;\; = \;\; \nu^2 \coth(\nu h) \; , \tag{2.26}$$

and $\nu = \frac{\sigma^2}{g}$ is the deep water wave number.

Eckart's equation (2.24) also reduces to the linearised shallow water equation under the same assumption as in the mild-slope case. Eckart notes that (2.26) actually approximates the root of the dispersion relation (2.18) to within 4% for all values of kh. However, he seemed to be discouraged from further development of his approximation due to the unsatisfactory approximation to the group velocity he obtained. Recently, Miles [40] has shed new light on Eckart's approximation, deriving (2.24) as well as (2.21) and (2.23), via an elegant variational procedure. Miles notes that the direct calculation of the group velocity from Eckart's dispersion relation (2.26), gives an approximation to the ratio of group velocity to phase velocity within 1% of the exact value for all values of kh. Miles also notes that while the mild-slope approximation conserves wave energy, Eckart's approximation does not (except in uniform depth). Also, on a gently sloping beach, Eckart's approximation is inferior to the mild-slope approximation in predicting the amplitude of the reflected wave. However, in the calculation of edge wave eigenvalues over a beach of uniform (and not necessarily small) slope, Eckart's approximation is superior to the mild-slope approximation. We will return to Eckart's approximation in Chapter 3 where it will be compared to the mild-slope approximation. Some ideas will then be proposed to improve the Eckart prediction of the amplitude of the reflected wave.

Most numerical methods used to solve the mild-slope equation (2.21) have been based on either finite difference (for example, Ebersole [14], Li and Anastasiou [31]) or finite element methods (for example, Berkhoff [2], Booij [5]). Efficiency of methods and accuracy of solution are obviously of considerable importance. Chamberlain [7] has used a different approach in which the one-dimensional mild-slope equation is converted into two integral equations, the

solutions of which are approximated by variational techniques. For a specified incident wave, this procedure can calculate highly accurate approximations of the coefficients of the resulting transmitted and reflected waves, and of the free surface shape, with only 2- or 3- dimensional (problem-dependent) trial spaces. As work in the following chapters uses this integral approach, it is convenient to give a brief description of Chamberlain's solution method for 1-dimensional scattering problems.

2.5 The 1-dimensional mild-slope equation

Let x and y be horizontal cartesian co-ordinates as defined in section 2.1. The class of depth profiles now considered is such that h is independent of y and varies only in some finite interval of x, so that

$$h(x) = \begin{cases} h_0 & \forall x \leq 0 \ , \\ h_1 & \forall x \geq l \ , \end{cases}$$

where h_0 and h_1 are constants for a given problem, and $h(x)$ is assumed to be continuous on $(-\infty, \infty)$. In the case of a localised hump in the bed, h_0 and h_1 are equal; they may, however, be unequal when the bed profile is that of a localised

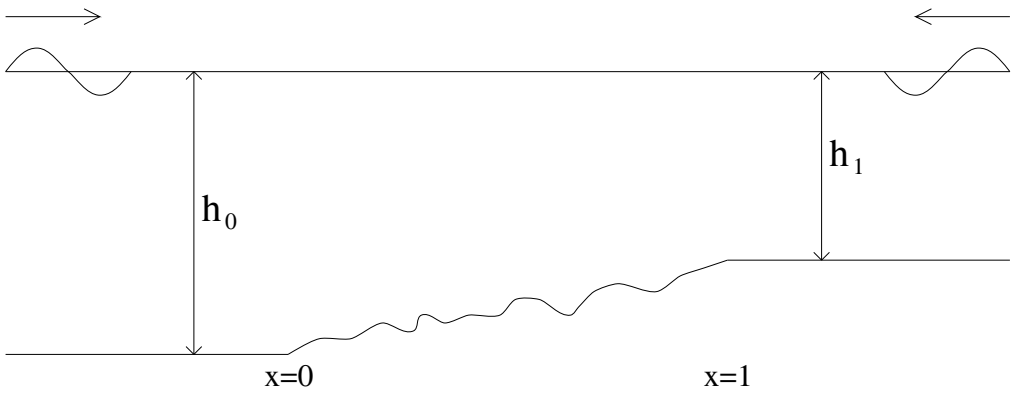

Figure 2.2: Vertical cross section of the fluid domain.

talud, as depicted in Fig. 2.2. In the wave motion, it is assumed that the crests are parallel to the y axis – this implying that $\phi_0 = \phi_0(x)$.

The mild-slope equation is now scaled using the non-dimensionalisation pro-

cess outlined by Chamberlain [7], which may be summarised as follows. Let

$$\hat{x} = \frac{x}{l} ,$$

$$U(\hat{x}) = \frac{1}{h_0} u(l\hat{x}) ,$$

$$H(\hat{x}) = \frac{1}{h_0} h(l\hat{x}) ,$$

$$\hat{\phi}_0(\hat{x}) = \frac{1}{\sigma l^2} \phi_0(l\hat{x}) .$$

The following account discards the accents from these definitions in the pursuit of a simple notation. In the above circumstances, the mild-slope equation (2.21) may be written as

$$\frac{d}{dx}\left(U\frac{d\phi_0}{dx}\right) + \kappa^2 U\phi_0 = 0 , \tag{2.27}$$

where

$$U(x) = \frac{\tanh(\kappa\tau H)}{2\kappa\tau}\left(1 + \frac{2\kappa\tau H}{\sinh(2\kappa\tau H)}\right) ,$$

and $\kappa = \kappa(x)\,(= k(x)l)$ – the dimensionless localised wave number – is the positive real root of

$$\alpha_0{}^2\tau = \kappa\tanh(\kappa\tau H) , \tag{2.28}$$

and where α_0 and τ are two dimensionless parameters given by

$$\alpha_0 = \frac{\sigma l}{\sqrt{g h_0}} \quad , \quad \tau = h_0/l .$$

This scaling process will be used throughout this text.

The process of converting the differential equation (2.27) and its boundary conditions into an integral equation is made much simpler by converting (2.27) into normal form. This is done by introducing a new variable ζ defined by

$$\zeta(x) = \phi_0(x)\sqrt{\frac{U(x)}{U(0)}} . \tag{2.29}$$

Then ζ satisfies

$$\zeta'' + \kappa_0{}^2\zeta = \rho\zeta , \tag{2.30}$$

where, for the rest of this chapter, the prime denotes differentiation with respect to x,

$$\rho(x) = \frac{U''(x)}{2U(x)} - \left(\frac{U'(x)}{2U(x)}\right)^2 + \kappa_0^2 - \kappa^2(x),$$

and where the notation $\kappa_0 = \kappa(0)$ (and $\kappa_1 = \kappa(1)$) is used.

The coefficients appearing in the differential equation (2.30) are uniquely defined once H, α_0 and τ are assigned. The only remaining information necessary is the choice of incident waves. On the flat bed for $x \leq 0$, the non-dimensional mild-slope equation (2.27) reduces to $\phi_0'' + {\kappa_0}^2\phi_0 = 0$. Similarly, on the flat bed for $x \geq 1$, (2.27) reduces to $\phi_0'' + {\kappa_1}^2\phi_0 = 0$. Therefore, we suppose in general, that there are two incident waves with known coefficients $A^{\pm}$ propagating from $x = \pm\infty$ respectively. This will result in two outgoing waves, with unknown coefficients $B^{\pm}$, propagating towards $x = \pm\infty$ respectively. Hence, on the flat beds, we take

$$\phi_0(x) = \begin{cases} A^- e^{i\kappa_0 x} + B^- e^{-i\kappa_0 x} & \forall x \leq 0 \ , \\ A^+ e^{-i\kappa_1 x} + B^+ e^{i\kappa_1 x} & \forall x \geq 1 \ , \end{cases}$$

and using (2.29) we see that the corresponding form for ζ is

$$\zeta(x) = \begin{cases} A^- e^{i\kappa_0 x} + B^- e^{-i\kappa_0 x} & \forall x \leq 0 \ , \\ (A^+ e^{-i\kappa_1 x} + B^+ e^{i\kappa_1 x})\sqrt{\dfrac{U(1)}{U(0)}} & \forall x \geq 1 \ . \end{cases} \tag{2.31}$$

We use jump conditions at $x = 0$ and $x = 1$ (as H' is allowed to be discontinuous at the ends of the varying bed) to eliminate $B^{\pm}$ between ζ and ζ', yielding

$$\begin{aligned} \zeta'(0) + i\kappa_0\zeta(0) &= 2i\kappa_0\hat{a} \ , \\ \zeta'(1) - i\kappa_0\zeta(1) &= -2i\kappa_0 e^{-i\kappa_0}\hat{b} \ , \end{aligned} \tag{2.32}$$

where

$$\begin{aligned} \hat{a} &= c_1 + c_2\zeta(0) + c_3\zeta(1) \ , \\ \hat{b} &= c_4 + c_5\zeta(0) + c_6\zeta(1) \ . \end{aligned}$$

The complex numbers c_j $(j = 1, \ldots, 6)$ are given by

$$\begin{aligned} c_1 &= A^- \ , \\ c_2 &= -\frac{iU'(0+)}{4\kappa_0 U(0)} \ , \\ c_3 &= 0 \ , \\ c_4 &= A^+ e^{i(\kappa_0 - \kappa_1)}\frac{\kappa_1}{\kappa_0}\sqrt{\frac{U(1)}{U(0)}} \ , \\ c_5 &= 0 \ , \\ c_6 &= \left(\frac{iU'(1-)}{4\kappa_0 U(1)} + \frac{\kappa_0 - \kappa_1}{2\kappa_0}\right)e^{i\kappa_0} \ , \end{aligned} \tag{2.33}$$

where the terms involving U' are the consequences of allowing slope discontinuities in H at $x = 0, 1$. Greater detail of the derivation of these boundary conditions and the merit of writing them in the form of (2.32) can be found in Chamberlain [6].

Linearity allows superposition of solutions corresponding to waves incident from the left with solutions corresponding to waves incident from the right. This removes the need to solve the problem with two incident waves. By removing one incident wave, the amplitude of the remaining incident wave may be set equal to unity, without loss of generality. Accordingly the two reflection and transmission coefficients, denoted by R and T, for this problem are defined as follows.

$$\text{If } A^+ = 0 \text{ then } R_1 = \frac{B^-}{A^-} \quad \text{and} \quad T_1 = \frac{B^+}{A^-} \ .$$

$$\text{If } A^- = 0 \text{ then } R_2 = \frac{B^+}{A^+} \quad \text{and} \quad T_2 = \frac{B^-}{A^+} \ .$$

The subscripts distinguish between waves incident from the left(1) or the right(2). Now we define ζ_1 to be the solution of (2.30) and (2.32) for an incident wave from the left (requiring $A^+ = 0$ in (2.32)). ζ_2 is defined to be the solution for an incident wave from the right (requiring $A^- = 0$ in (2.32)). Using the equations (2.31), the reflection and transmission coefficients can now be defined in terms of ζ_j $(j = 1, 2)$ in the following way.

If $A^+ = 0$:

$$\begin{aligned} R_1 &= \frac{\zeta_1(0)}{A^-} - 1 \ , \\ T_1 &= \frac{\zeta_1(1)e^{-i\kappa_1}}{A^-}\sqrt{\frac{U(0)}{U(1)}} \ . \end{aligned} \tag{2.34}$$

If $A^- = 0$:

$$\begin{aligned} R_2 &= \frac{\zeta_2(1)e^{-i\kappa_1}}{A^+}\sqrt{\frac{U(0)}{U(1)}} - e^{-2i\kappa_1} \ , \\ T_2 &= \frac{\zeta_2(0)}{A^+} \ . \end{aligned} \tag{2.35}$$

The outgoing wave coefficient B^+ comprises of two parts – that part of A^- transmitted beyond the talud and that part of A^+ reflected back from the talud. We can make a similar statement about B^-, and these resulting relationships can be summarised as

$$\begin{pmatrix} B^+ \\ B^- \end{pmatrix} = \begin{pmatrix} T_1 & R_2 \\ R_1 & T_2 \end{pmatrix} \begin{pmatrix} A^- \\ A^+ \end{pmatrix} \ .$$

The matrix on the right-hand side of this equation is called the scattering matrix. Clearly, as soon as the reflection and transmission coefficients have been found, then $B^{\pm}$ can be determined for any $A^{\pm}$.

2.6 Integral equations and variational principles

A variation of parameters procedure shows that the boundary-value problem for ζ given by (2.30) and (2.32) is equivalent to the integral equation

$$\zeta(x) = \hat{a}e^{i\kappa_0 x} + \hat{b}e^{-i\kappa_0 x} - \frac{i}{2\kappa_0}\int_0^1 e^{i\kappa_0|x-t|}\rho(t)\zeta(t)\,dt\ . \tag{2.36}$$

With some simple algebra, this integral equation can be rewritten in terms of the integral equation with a real-valued kernel,

$$\zeta(x) = Me^{i\kappa_0 x} + Ne^{-i\kappa_0 x} + \frac{1}{2\kappa_0}\int_0^1 \sin\left(\kappa_0|x-t|\right)\rho(t)\zeta(t)\,dt\ , \tag{2.37}$$

where

$$\begin{aligned}
M &= \hat{a} - (b_4 + b_5\zeta(0) + b_6\zeta(1))\ ,\\
N &= \hat{b} - (b_1 + b_2\zeta(0) + b_3\zeta(1))\ ,\\
b_1 &= \tfrac{1}{2}(c_1 + c_4)\ ,\\
b_2 &= \tfrac{1}{2}(c_2 + c_5 - 1)\ ,\\
b_3 &= \tfrac{1}{2}(c_3 + c_6),\\
b_4 &= \tfrac{1}{2}(c_1 + c_4e^{-2i\kappa_0})\ ,\\
b_5 &= \tfrac{1}{2}(c_2 + c_5e^{-2i\kappa_0})\ ,\\
b_6 &= \tfrac{1}{2}(c_3 + c_6e^{-2i\kappa_0} - e^{-i\kappa_0}),
\end{aligned}$$

and where

$$b_4 + b_5\zeta(0) + b_6\zeta(1) = \frac{i}{4\kappa_0}\int_0^1 e^{-i\kappa_0 t}\rho(t)\zeta(t)\,dt\ , \tag{2.38}$$

$$b_1 + b_2\zeta(0) + b_3\zeta(1) = \frac{i}{4\kappa_0}\int_0^1 e^{i\kappa_0 t}\rho(t)\zeta(t)\,dt\ . \tag{2.39}$$

Full details of this derivation can be found in Chamberlain [6].

The equation (2.37) can be written as an operator equation in the Hilbert space $L_2(0,1)$, with inner product

$$(f,g) = \int_0^1 f(t)\overline{g(t)}\,dt\ ,$$

on defining two self-adjoint operators L and P by

$$(L\zeta)(x) = \frac{1}{2\kappa_0} \int_0^1 \sin(\kappa_0|x-t|)\, \zeta(t)\, dt$$

and

$$(P\zeta)(x) = \rho(x)\zeta(x) \ .$$

Then $\zeta \in L_2(0,1)$ satisfies

$$\zeta = Mf^+ + Nf^- + LP\zeta \ ,$$

where

$$f^{\pm} = e^{\pm i\kappa_0 x}$$

and since ρ is bounded and L is a compact operator, then LP is also compact.

It follows that if there exists a solution $\zeta \in L_2(0,1)$ of this operator equation, it determines the desired function $\zeta(x)$ of (2.37). This issue and others which arise from using Hilbert space methods can be found in Porter and Stirling [51].

A summary is now presented of the approximation method employed by Chamberlain [6] for integral equations of the form (2.37) where the function ζ is sought. The apparent difficulty posed by the free term, where end-point values of the unknown function ζ are contained in the constants M and N, is circumvented by exploiting linearity. It can be shown that

$$\zeta(x) = (M+N)\chi_1(x) + i(M-N)\chi_2(x) \ , \tag{2.40}$$

where the functions χ_j $(j = 1,2)$ are the solutions of real-valued integral equations, that can be expressed in operator form as

$$A\chi_j = f_j \qquad (j = 1,2) \ , \tag{2.41}$$

where $A = I - LP$ (I being the identity operator) and the free terms f_j $(j = 1,2)$ are given by

$$f_1(x) = \cos(\kappa_0 x)$$

and

$$f_2(x) = \sin(\kappa_0 x) \ .$$

It follows that once χ_1 and χ_2 are determined, the unknown function ζ can also be determined through (2.40) once the end-point values $\zeta(0)$ and $\zeta(1)$, and

thus the coefficients in (2.40) have been found. Also, on finding $\zeta(0)$ and $\zeta(1)$, then the reflection and transmission coefficients are known through (2.34) and (2.35).

On substituting the above equation (2.40) for ζ into the right hand side of equations (2.38) and (2.39) and rearranging them, it can be shown that $\zeta(0)$ and $\zeta(1)$ are determined by solving the rank 2 system of equations

$$\left(\begin{pmatrix} b_2 & b_3 \\ b_5 & b_6 \end{pmatrix} - i \begin{pmatrix} B_1 & B_2 \\ \overline{B}_2 & B_1 \end{pmatrix} \begin{pmatrix} c_5 - b_2 & c_6 - b_3 \\ c_2 - b_5 & c_3 - b_6 \end{pmatrix}\right) \begin{pmatrix} \zeta(0) \\ \zeta(1) \end{pmatrix}$$

$$= - \begin{pmatrix} b_1 \\ b_4 \end{pmatrix} + i \begin{pmatrix} B_1 & B_2 \\ \overline{B}_2 & B_1 \end{pmatrix} \begin{pmatrix} c_4 - b_1 \\ c_1 - b_4 \end{pmatrix} \tag{2.42}$$

in which

$$B_1 = \tfrac{1}{2}(A_{11} + A_{22}) \quad \text{and} \quad B_2 = \tfrac{1}{2}(A_{11} + 2iA_{12} - A_{22})$$

and

$$A_{jk} = \frac{1}{2\kappa_0} \int_0^1 \chi_j(t)\rho(t)f_k(t)\ dt \ = \frac{1}{2\kappa_0}(\chi_j, Pf_k) \qquad (j,k = 1,2).$$

Stationary principles are used to generate approximations to the inner products A_{jk} $(j,k = 1,2)$ with upper and lower bounds by firstly ensuring that the function ρ is entirely one-signed. This allows the non-self-adjoint operator A in the integral equations (2.41) to be replaced by a self-adjoint one. In general, ρ does not possess this property, but can be made to do so by adding to it or subtracting from it a known quantity. This process requires a slight change in the boundary conditions (2.32) which causes the definitions of the c_j $(j = 1, \ldots 6)$ in (2.33) to be amended. Full details of this device are in Chamberlain [6]. With ρ one-signed, a new self-adjoint operator S can be defined by

$$(S\chi)(x) = s(x)\chi(x)\ ,$$

where

$$s(x) = \sqrt{\lambda\rho(x)}$$

and

$$\lambda = \mathrm{sgn}(\rho) \qquad \text{(that is } \lambda = \pm 1)\ .$$

Then the integral equations for χ_j $(j = 1, 2)$ given by (2.41) can be rewritten as

$$\hat{A}\hat{\chi}_j = Sf_j \qquad (j = 1, 2) \ , \tag{2.43}$$

where

$$\hat{\chi}_j = S\chi_j \qquad (j = 1, 2)$$

and

$$\hat{A} = I - \lambda SLS \ .$$

Clearly $\hat{A}$ is self-adjoint and as S is bounded, SLS is a compact operator.

It is easy to show that the functionals

$$\begin{aligned} J_k &: L_2(0,1) \to \mathbb{R} \qquad (k = 1, 2), \\ J_3 &: L_2(0,1) \times L_2(0,1) \to \mathbb{R} \end{aligned}$$

given by

$$J_k(p) = 2(p, Sf_k) - (\hat{A}p, p) \qquad (k = 1, 2) \ , \tag{2.44}$$

$$J_3(p_1, p_2) = (Sf_1, p_2) + (p_1, Sf_2) - (\hat{A}p_1, p_2) \tag{2.45}$$

have stationary values

$$\begin{aligned} (\hat{\chi}_k, Sf_k) &= \lambda(\chi_k, Pf_k) \qquad (k = 1, 2) \ , \\ (\hat{\chi}_1, Sf_2) &= \lambda(\chi_1, Pf_2) \end{aligned}$$

respectively. Problem-dependent, N-dimensional trial functions $\tilde{p}_1$ and $\tilde{p}_2$ given by

$$\tilde{p}_k = \sum_{n=1}^{N} a_n^k (LP)^{n-1} f_k \qquad (k = 1, 2) \tag{2.46}$$

are used to approximate χ_1 and χ_2 respectively, for some $a_n^k \in \mathbb{R}$ $(n = 1, \ldots, N)$. Substituting $\tilde{p}_1$ and $\tilde{p}_2$ in the above functionals generates approximations to the inner products A_{jk} $(j, k = 1, 2)$ which are second-order accurate compared with the approximations to the unknown functions χ_1 and χ_2. The unknown constants, $a_n^k (n = 1, \ldots, N)$, are chosen so as to make the functionals (2.44) and (2.45) stationary within the N-dimensional trial spaces (see Chamberlain [6] for details). To clarify the notation, we shall denote the functions $\tilde{p}_k$ $(k = 1, 2)$ determined by the first functional (2.44) as ξ_k $(k = 1, 2)$ respectively, and the functions

$\tilde{p}_k$ $(k = 1, 2)$ determined by the second functional (2.45) as μ_k $(k = 1, 2)$ respectively.

The further assumption that there exists $b > 0$ such that $\forall p \in L_2(0, 1)$,

$$b \|p\|^2 \leq (\hat{A}p, p) \leq a \|p\|^2 \ , \tag{2.47}$$

where the existence of an $a > 0$ is guaranteed since $\hat{A}$ is a bounded operator, establishes the following upper and lower bounds on the inner products of interest:

$$J_k(\xi_k) + \frac{1}{a} \left\| \hat{A}\xi_k - Sf_k \right\|^2 \leq (\hat{\chi}_k, Sf_k) \leq J_k(\xi_k) + \frac{1}{b} \left\| \hat{A}\xi_k - Sf_k \right\|^2 \quad (k = 1, 2) \tag{2.48}$$

and

$$G(\mu_1, \mu_2) - R(\mu_1, \mu_2) \leq (\hat{\chi}_1, Sf_2) \leq G(\mu_1, \mu_2) + R(\mu_1, \mu_2) \ , \tag{2.49}$$

where the functionals G and R are given by

$$G(\mu_1, \mu_2) = J_3(\mu_1, \mu_2) + \frac{1}{2} \left(\frac{1}{b} + \frac{1}{a} \right) (\hat{A}\mu_1 - Sf_1, \hat{A}\mu_2 - Sf_2)$$

and

$$R(\mu_1, \mu_2) = \frac{1}{2} \left(\frac{1}{b} - \frac{1}{a} \right) \left\| \hat{A}\mu_1 - Sf_1 \right\| \left\| \hat{A}\mu_2 - Sf_2 \right\| \ .$$

An excellent derivation of these upper and lower bounds may be found in Porter and Stirling ([51],pp.254-257,261-263). Approximations to a and b can be found in Chamberlain [6]. Disappointingly, the approximation to b can be negative in certain cases, resulting in just a stationary approximation to the inner products with no upper and lower bounds.

The implementation of the solution process follows by firstly assigning H, α_0, τ and the direction of the incident wave. Then, after ensuring ρ is one-signed (by adjusting it to make it so if necessary) and choosing the dimension of the trial space, the trial functions given by (2.46) are generated and the approximations $J_1(\xi_1), J_2(\xi_2)$ and $J_3(\mu_1, \mu_2)$ to the inner products $(\chi_j, \ Pf_k)$ $(j, k = 1, 2)$ are calculated. Upper and lower bounds to the inner products are also calculated if $b > 0$. Then the rank 2 system (2.42) is solved to give the approximations to $\zeta(0)$ and $\zeta(1)$. Finally (2.34) and (2.35) are used to deliver approximations to the reflection and transmission coefficients, and when $b > 0$, upper and lower bounds on the reflected and transmitted amplitudes are also found. The approximation to ζ, and thus the free surface shape, can then be found through (2.40).

Chamberlain [7] has shown that 2- or 3- dimensional trial spaces can result in the determination of approximations to the reflection and transmission coefficients to machine accuracy.

This integral approach can also be used with the linearised shallow water equation and Eckart's equation with certain modifications. Chamberlain [6] has done this for the linearised shallow water equation, and the necessary modifications required to use this integral approach to solve Eckart's equation are given in Chapter 3.

Chapter 3

Further development of Chamberlain's theory

In this chapter some extensions to the work appearing in Chamberlain [7] & [8] are presented. A new computationally cheap integral equation solution method is developed for the three model equations mentioned in Chapter 2, namely the mild-slope equation, Eckart's equation and the linearised shallow water equation, over a range of parameter values. This method uses the approximation methods discussed in section 2.6 but with a new choice of trial functions. Eckart's equation is further investigated and improvements to it are suggested. Finally, the symmetry properties of the solutions of the three model equations are studied, and an unexpected property is discovered that any approximations of the solutions still possess the symmetry properties.

3.1 Introduction to approximation methods

This section begins by illustrating the interest in solving the model equations over a continuous range of their parameters for a specified bed shape. Booij [5] provided some experimental evidence concerning the accuracy of the mild-slope approximation to the velocity potential ϕ satisfying (2.13). As a part of that paper, a talud problem was considered and a graph (see Fig.3.1) was presented of reflected amplitude ($|R|$) given by the mild-slope equation against W_s, a parameter which denotes the length of Booij's talud. In terms of the notation used

in Chapter 2, the dimensionless parameters of the mild-slope equation are given in terms of W_s by $\alpha_0 = W_s/\sqrt{0.6}$ and $\tau = 0.6/W_s$ (See Chamberlain [6] p.114 for details). Booij computed $|R|$ using full linearised theory and superimposed it onto his graph, observing that the two sets of results coincide for talud slopes with gradient $< 1/3$ (that is, for values of $W_s > 1.2$).

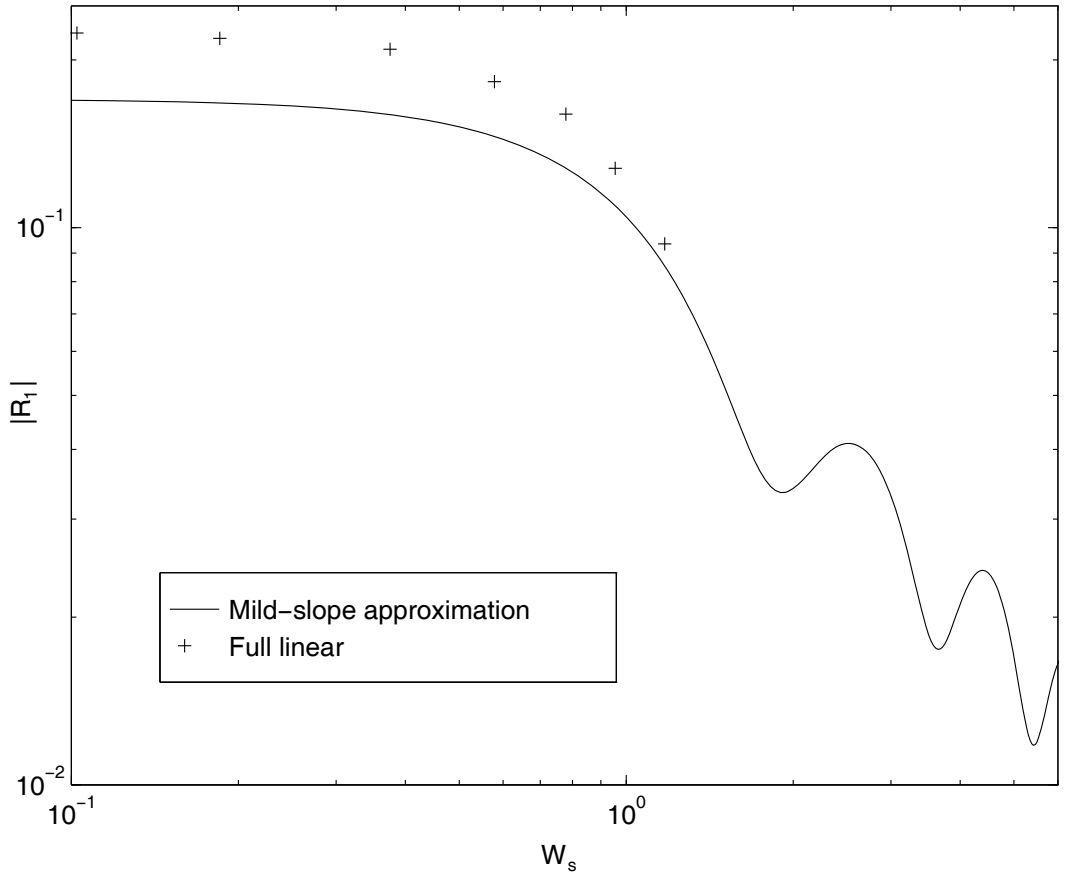

Figure 3.1: Reflected amplitude over the depth profile $H(x) = 1 - 2/3x\,(0 \leq x \leq 1)$.

In the absence of any analytical estimates of the accuracy of the mild-slope approximation, experimental evidence, such as this provided by Booij, has become invaluable.

Another property coastal engineers are interested in is the wave number at which, for a given shape of bed, a significant part of the wave is transmitted. An easy way to find this information is to solve the model equations over a wide range of wave numbers and present the results graphically, as in Fig.3.1.

So, it is obvious that there exists much interest in finding solutions of our

three model equations over a range of their parameters. From Chapter 2, we know that in a fluid, of undisturbed depth $H = H(x)$, the non-dimensional mild-slope equation is given by

$$\frac{d}{dx}\left(U\frac{d\phi_0}{dx}\right) + \kappa^2 U\phi_0 = 0 \ , \tag{3.1}$$

where

$$U(x) = \frac{\tanh(\kappa\tau H)}{2\kappa\tau}\left(1 + \frac{2\kappa\tau H}{\sinh(2\kappa\tau H)}\right) \ , \tag{3.2}$$

and $\kappa = \kappa(x)$ is the positive real root of the dispersion relation

$$\alpha_0{}^2\tau = \kappa\tanh(\kappa\tau H) \ . \tag{3.3}$$

The integral equation method, given in section 2.6, can be used to solve the mild-slope equation for a wave incident from $x = \pm\infty$ on a given depth profile for some α_0 and τ and gives extremely accurate approximations to the coefficients of the resulting reflected and transmitted waves. These coefficients are defined in Chapter 2, and are denoted by R_k and T_k $(k = 1, 2)$, where the subscripts distinguish between waves incident from $x = -\infty$ (1) and $x = \infty$ (2). The integral equation method involves using variational principles to generate approximations to the inner products (χ_j, Pf_k) $(j, k = 1, 2)$ and approximations to the solutions χ_k $(k = 1, 2)$ $\in L_2(0, 1)$ of the integral equations

$$(I - LP)\chi_k = f_k \qquad (k = 1, 2) \ . \tag{3.4}$$

Here, the operators L and P are defined by

$$(L\chi)(x) = \frac{1}{2\kappa_0}\int_0^1 \sin(\kappa_0|x - t|)\,\chi(t)\,dt \qquad \text{and} \qquad (P\chi)(x) = \rho(x)\chi(x) \ , \tag{3.5}$$

with $\kappa_0 = \kappa(0)$, the solution of the dispersion relation (3.3) at $x = 0$, and $\rho = \rho(x)$ given by

$$\rho(x) = \frac{U''(x)}{2U(x)} - \left(\frac{U'(x)}{2U(x)}\right)^2 + \kappa_0^2 - \kappa^2(x), \tag{3.6}$$

where, for the rest of this chapter, the prime denotes differentiation with respect to x and the functions U and κ are defined by (3.2) and (3.3) respectively. The free terms f_k $(k = 1, 2)$ in (3.4) are defined by

$$f_1(x) = \cos(\kappa_0 x) \qquad \text{and} \qquad f_2(x) = \sin(\kappa_0 x) \ . \tag{3.7}$$

The results presented in Fig.3.1 were obtained by using the integral equation method to find extremely accurate approximations to R_k and T_k $(k = 1, 2)$ given by the mild-slope equation at 170 values of α_0 and τ.

In Chapter 2, we used maximum principles to generate approximations to (χ_k, Pf_k) $(k = 1, 2)$ and approximations ξ_k $(k = 1, 2)$ to the unknown functions χ_k $(k = 1, 2)$ respectively. A stationary principle is also used to generate an approximation to (χ_1, Pf_2) and approximations μ_k $(k = 1, 2)$ to χ_k $(k = 1, 2)$ respectively. We also saw that when the operator $\hat{A}$ is bounded above and below – that is $\forall p \in L_2(0, 1)$,

$$b \|p\|^2 \leq (\hat{A}p, p) \leq a \|p\|^2 \ ,$$

where $b > 0$, then we can find upper and lower bounds on our approximations to (χ_j, Pf_k) $(j, k = 1, 2)$. The maximum error in the estimates of $|R_k|$ and $|T_k|$ $(k = 1, 2)$ can then be calculated. We have also shown in Chapter 2 that the approximations to the inner products (χ_j, Pf_k) $(j, k = 1, 2)$ and therefore the approximations to R_k and T_k $(k = 1, 2)$ are second-order accurate compared with the approximations to the unknown functions χ_1 and χ_2. In other words, requiring the maximum error in $|R_k|$ and $|T_k|$ $(k = 1, 2)$ to be $O(10^{-8})$ is approximately equivalent to requiring the maximum norm of the residual errors (that is $\max_{k=1,2} \{\|(I - LP)\xi_k - f_k\|\ ,\ \ \|(I - LP)\mu_k - f_k\|\}$) to be $O(10^{-4})$. Examples illustrating this can be found in Porter and Stirling ([51] Chap. 8).

For the results presented in Fig.3.1, at values of α_0 and τ where our approximation to b is greater than zero, extremely accurate approximations to R_k and T_k $(k = 1, 2)$ are such that the maximum error in $|R_k|$ and $|T_k|$ $(k = 1, 2)$ is $O(10^{-8})$ for all values of α_0 and τ. In the case where our approximation to b is negative, then we do not have any upper and lower bounds on our approximations to (χ_j, Pf_k) $(j, k = 1, 2)$. However, we still know that the approximations to these inner products (and hence to R_k and T_k $(k = 1, 2)$) are second-order accurate compared with the approximations of χ_1 and χ_2. Therefore, at values of α_0 and τ where no upper and lower bounds exist, we use the fact that the error in $|R_k|$ and $|T_k|$ $(k = 1, 2)$ is approximately $O(\max_{k=1,2} \left\{\|(I - LP)\xi_k - f_k\|^2\right.$, $\left.\|(I - LP)\mu_k - f_k\|^2\right\})$. Hence for the results presented in Fig.3.1, where no

upper and lower bounds exist, extremely accurate approximations to R_k and T_k $(k = 1, 2)$ are such that $\max_{k=1,2} \{\|(I - LP)\xi_k - f_k\|, \ \|(I - LP)\mu_k - f_k\|\}$ is $O(10^{-4})$ for all values of α_0 and τ.

In future, whenever we specify the accuracy in the approximations to the reflection and transmission coefficients of any of the model equations, we shall just give the maximum error in $|R_k|$ and $|T_k|$ $(k = 1, 2)$. In the case where the upper and lower bounds do not exist, this will imply that $\max_{k=1,2} \left\{\|(I - LP)\xi_k - f_k\|^2, \ \|(I - LP)\mu_k - f_k\|^2\right\}$ is the same order of magnitude as the maximum allowable error in $|R_k|$ and $|T_k|$ $(k = 1, 2)$. This will not be mentioned again in the next sections, but it is the policy employed whenever the approximation to b is negative.

Many coastal engineers would consider approximations to the reflection and transmission coefficients generated by Chamberlain's method as too accurate for applications. Instead, approximations that are correct to two significant figures (2.s.f.) would be considered quite adequate. So we now arrive at the following question: can the accuracy of the Chamberlain solutions be relaxed, enabling less accurate solutions of the model equations to be generated over a parameter range at a much reduced computational cost?

Sections (3.2) and (3.3) show that this is indeed possible for all three model equations of interest. We shall concentrate on developing the new approximation method to solve the mild-slope equation. Once this has been completed, the minor changes required for the method to encompass the other model equations, the Eckart equation and the shallow water equation, will be given.

3.2 A one-dimensional trial space approximation

3.2.1 Outline of method

Chamberlain's method, summarised in Chapter 2, solves the mild-slope equation by converting it into an integral equation. The solution of the integral equation was found through a rank two system of equations, once approximations

to the solutions χ_1 and χ_2, of the real-valued integral equations (3.4) and to the inner products (χ_j, Pf_k) $(j,k=1,2)$ had been obtained. For convenience, we shall recap the variational method used to obtain approximations to χ_1, χ_2 and (χ_j, Pf_k) $(j,k=1,2)$, as this is where we shall seek to make computational savings.

Now, with the ρ function one-signed, we define a new self-adjoint operator S by

$$(S\chi)(x) = \sqrt{\lambda\rho(x)}\chi(x) \ ,$$

where $\lambda = \mathrm{sgn}(\rho)$ (that is, $\lambda = \pm 1$). The integral equations for χ_k $(k=1,2)$ given by (3.4) can be rewritten as

$$\hat{A}\hat{\chi}_k = Sf_k \qquad (k=1,2) \ ,$$

where $\hat{\chi}_k = S\chi_k$ and $\hat{A} = I - \lambda SLS$.

The functionals $J_k : L_2(0,1) \to \mathbb{R}$ $(k=1,2)$ and $J_3 : L_2(0,1)\times L_2(0,1) \to \mathbb{R}$ given by

$$J_k(p) = 2(p, Sf_k) - (\hat{A}p, p) \qquad (k=1,2) \ , \tag{3.8}$$

$$J_3(p_1,p_2) = (Sf_1, p_2) + (p_1, Sf_2) - (\hat{A}p_1, p_2) \tag{3.9}$$

have stationary values

$$(\hat{\chi}_k, Sf_k) = \lambda(\chi_k, Pf_k) \qquad (k=1,2) \ ,$$

$$(\hat{\chi}_1, Sf_2) = \lambda(\chi_1, Pf_2)$$

respectively. Problem-dependent, N-dimensional trial functions $\tilde{p}_1$ and $\tilde{p}_2$ given by

$$\tilde{p}_k = \sum_{n=1}^{N} a_n^k (LP)^{n-1} f_k \qquad (k=1,2) \tag{3.10}$$

are used as approximations to χ_1 and χ_2 respectively, for some a_n^k $(n=1,\ldots,N)$. We generate approximations to the inner products $(\chi_j,\ Pf_k)$ $(j,k=1,2)$ by substituting $\tilde{p}_1$ and $\tilde{p}_2$ into the functionals given by (3.8) and (3.9). The approximations to $(\chi_j,\ Pf_k)$ $(j,k=1,2)$ are second-order accurate compared with the approximations $\tilde{p}_1$ and $\tilde{p}_2$ to the unknown functions χ_1 and χ_2. The unknown constants, $a_n^k (n=1,\ldots,N)$, are chosen so as to make the functionals (3.8) and

(3.9) stationary within the N-dimensional trial spaces. We shall denote the functions $\tilde{p}_k$ $(k = 1, 2)$ determined by (3.8) as ξ_k $(k = 1, 2)$ respectively, and the functions $\tilde{p}_k$ $(k = 1, 2)$ determined by (3.9) as μ_k $(k = 1, 2)$ respectively.

As already noted, the Chamberlain solutions, ξ_k and μ_k $(k = 1, 2)$, are very accurate approximations to the solutions χ_1 and χ_2 of the integral equations (3.4), but they also require considerable computer time to determine. The integral equation solution method we have used to solve the mild-slope equation at each value of α_0 and τ employs this expensive process of generating the Chamberlain solutions. Instead of this, we shall use the Chamberlain solutions at a chosen α_0 and τ to approximate χ_1 and χ_2 in the neighbourhood of α_0 and τ. In the present circumstances, we only need to consider problems where τ is either fixed or is a function of α_0, as in the problem considered by Booij [5] given in section 3.1, where $\tau = \sqrt{0.6}/\alpha_0$. In the following we shall only refer to the value of α_0 at which we are solving the problem, and we shall not mention τ as we automatically know its value once α_0 is assigned.

A superscript is now introduced into our established notation to denote the value of α_0 at which each operator, function and functional is evaluated.

We introduce the 1-dimensional trial functions

$$p_k = r_k \xi_k^{\alpha_0} \qquad (k = 1, 2) \tag{3.11}$$

as approximations to $\chi_1^{\hat{\alpha_0}}$ and $\chi_2^{\hat{\alpha_0}}$, for some $r_k \in \mathbb{R}$ $(k = 1, 2)$ determined so as to make the functional (3.8) stationary. Therefore, substituting (3.11) into (3.8), we see that

$$J_k^{\hat{\alpha_0}}(p_k) = J_k^{\hat{\alpha_0}}(r_k) = 2r_k \left(\xi_k^{\alpha_0},\ S^{\hat{\alpha_0}} f_k^{\hat{\alpha_0}}\right) - r_k^2 \left(\hat{A}^{\hat{\alpha_0}} \xi_k^{\alpha_0},\ \xi_k^{\alpha_0}\right) \qquad (k = 1, 2)$$

regarded as a function of r_k, is stationary where

$$\frac{dJ_k^{\hat{\alpha_0}}}{dr_k} = 0 \qquad (k = 1, 2)\ .$$

Hence the constants r_k $(k = 1, 2)$ are given by

$$r_k = \frac{\left(\xi_k^{\alpha_0},\ S^{\hat{\alpha_0}} f_k^{\hat{\alpha_0}}\right)}{\left(\hat{A}^{\hat{\alpha_0}} \xi_k^{\alpha_0},\ \xi_k^{\alpha_0}\right)} \qquad (k = 1, 2)$$

and the approximations to the inner products $\left(\chi_k^{\hat{\alpha_0}},\ P^{\hat{\alpha_0}} f_k^{\hat{\alpha_0}}\right)$ $(k = 1, 2)$ are

$$J_k^{\hat{\alpha_0}}(p_k) = \frac{\left(\xi_k^{\alpha_0},\ S^{\hat{\alpha_0}} f_k^{\hat{\alpha_0}}\right)^2}{\left(\hat{A}^{\hat{\alpha_0}} \xi_k^{\alpha_0},\ \xi_k^{\alpha_0}\right)} \qquad (k = 1, 2)$$

respectively.

To find an approximation to the inner product $\left(\chi_1^{\hat{\alpha_0}},\ P^{\hat{\alpha_0}} f_2^{\hat{\alpha_0}}\right)$, we use the 1-dimensional trial functions

$$q_k = \gamma_k \mu_k^{\alpha_0} \qquad (k = 1, 2) \tag{3.12}$$

as approximations to $\chi_1^{\hat{\alpha_0}}$ and $\chi_2^{\hat{\alpha_0}}$, for some $\gamma_k \in \mathbb{R}$ $(k = 1, 2)$ determined so as to make the functional (3.9) stationary. Therefore, substituting (3.12) into (3.9), we see that

$$\begin{aligned} J_3^{\hat{\alpha_0}}(q_1, q_2) &= J_3^{\hat{\alpha_0}}(\gamma_1, \gamma_2) \\ &= \gamma_2 \left(S^{\hat{\alpha_0}} f_1^{\hat{\alpha_0}},\ \mu_2^{\alpha_0}\right) + \gamma_1 \left(\mu_1^{\alpha_0},\ S^{\hat{\alpha_0}} f_2^{\hat{\alpha_0}}\right) - \gamma_1 \gamma_2 \left(\hat{A}^{\hat{\alpha_0}} \mu_1^{\alpha_0},\ \mu_2^{\alpha_0}\right) \end{aligned}$$

is stationary where

$$\frac{\partial J_3^{\hat{\alpha_0}}}{\partial \gamma_k} = 0 \qquad (k = 1, 2).$$

Hence the constants γ_j $(j = 1, 2)$ are given by

$$\gamma_1 = \frac{\left(S^{\hat{\alpha_0}} f_1^{\hat{\alpha_0}},\ \mu_2^{\alpha_0}\right)}{\left(\hat{A}^{\hat{\alpha_0}} \mu_1^{\alpha_0},\ \mu_2^{\alpha_0}\right)}$$

and

$$\gamma_2 = \frac{\left(\mu_1^{\alpha_0},\ S^{\hat{\alpha_0}} f_2^{\hat{\alpha_0}}\right)}{\left(\hat{A}^{\hat{\alpha_0}} \mu_1^{\alpha_0},\ \mu_2^{\alpha_0}\right)}$$

and the approximation to the inner product $\left(\chi_1^{\hat{\alpha_0}},\ P^{\hat{\alpha_0}} f_2^{\hat{\alpha_0}}\right)$ is

$$J_3^{\hat{\alpha_0}}(q_1, q_2) = \frac{\left(S^{\hat{\alpha_0}} f_1^{\hat{\alpha_0}},\ \mu_2^{\alpha_0}\right)\left(\mu_1^{\alpha_0},\ S^{\hat{\alpha_0}} f_2^{\hat{\alpha_0}}\right)}{\left(\hat{A}^{\hat{\alpha_0}} \mu_1^{\alpha_0},\ \mu_2^{\alpha_0}\right)}\ .$$

The approximations to $\chi_1^{\hat{\alpha_0}}$ and $\chi_2^{\hat{\alpha_0}}$ given by (3.11) and (3.12) are very much quicker to compute than the N-dimensional Chamberlain solutions, given by (3.10), when $N > 1$. It is clear that the approximate solutions (3.11) and (3.12) will not be accurate enough if $|\hat{\alpha_0} - \alpha_0|$ is too large. So, where the error exceeds a given tolerance, we choose a new α_0, find the Chamberlain solutions there, and then the approximate solutions (3.11) and (3.12) in its neighbourhood. This

process, of solving the mild-slope equation over a range of values of α_0, can be continued in such a way as to minimise the number of Chamberlain solutions required. Remember, from section 3.1, that the tolerance in the error will be given by the maximum allowable error in the amplitudes of the reflection and transmission coefficients.

We note that after this new choice of trial functions has been used to generate the approximations to $\chi_1^{\hat{\alpha_0}}$, $\chi_2^{\hat{\alpha_0}}$ and $\left(\chi_j^{\hat{\alpha_0}}, P^{\hat{\alpha_0}} f_k^{\hat{\alpha_0}}\right)$ $(j,k = 1,2)$, we revert back to the same stage in the integral equation procedure given in Chapter 2 to find the resulting reflection and transmission coefficients.

Now we are in a position to use this method. It is implemented by firstly assigning the depth profile H, the tolerance in the error, the initial and final values of α_0 and the increment to be added to α_0 to give the next α_0 at which a solution is to be found. Chamberlain's method, outlined in Chapter 2, is used to solve the mild-slope equation at the initial α_0, to give the extremely accurate solutions, remarked about in section 3.1. The increment is then added to α_0 and we now use the new 1-dimensional method to generate the solutions at this α_0. The solutions are then checked to make sure the error is within the user specified tolerance. We carry on in this manner until the error exceeds the given tolerance, and at this α_0 we use Chamberlain's method again to generate extremely accurate solutions. Then at the next α_0 we revert back to the new 1-dimensional trial functions to generate the solutions again, and we carry on in this manner until solutions of the mild-slope equation have been found over the desired α_0 range.

3.2.2 Results

Solutions of the mild-slope equation can be obtained using this new 1-dimensional trial space method in a greatly reduced computational run-time compared with using solely Chamberlain's procedure at each successive α_0. However, the α_0 range over which these 'cheap' solutions can be obtained has an upper limit, $\alpha_{\max}$. This means that whatever the tolerance specified in the error of the 'cheap' solutions, the new method still has to use Chamberlain's procedure to generate the solutions at all the desired solution points α_0, where $\alpha_0 > \alpha_{\max}$. Therefore no more computational savings are possible at these α_0. The value of $\alpha_{\max}$ decreases

as we increase the tolerance in the error (and so increase the accuracy) of the 'cheap' solutions. Also, for a fixed tolerance in the error, we find that the value of $\alpha_{\max}$ varies from one depth profile to another.

Consider, for example, the solution of the mild-slope equation (MSE) for the test problem of Booij [5], mentioned in section 3.1, for an incident wave of unit amplitude from the left. Here the depth profile is given by

$$H(x) = 1 - \frac{2}{3}x \qquad (0 \leq x \leq 1) \ .$$

In section 3.1, Chamberlain's method was used in generating extremely accurate solutions of the MSE for this problem with α_0 taking values between 0.05 and 8.5 at intervals of 0.05 (with τ given at each value of α_0 by $\tau = \sqrt{0.6}/\alpha_0$) to produce the results seen in Fig.3.1. This required the use of a 3-dimensional trial space for $\alpha_0 < 2$ and a 6-dimensional trial space for $\alpha_0 > 4$. The total CPU run-time required to generate all these results was 51m 55s. It should be noted that the same Sun 1 workstation was used to generate all the CPU run-times for all the methods used in this chapter.

The new method is now used to solve this problem for the mild-slope equation over the same α_0 range. We choose the tolerance in the error to be a minimum of 2.s.f. accuracy in $|R_k|$ and $|T_k|$ $(k = 1, 2)$. The new method produces 'cheap' solutions at the 29 values of α_0 in the range $[0.05, 1.45]$. For all $\alpha_0 > \alpha_{\max} = 1.45$, our new method has to use Chamberlain's method to generate the solutions. Fig.3.2 depicts the amplitude of the reflected wave, generated by both methods over the α_0 range from 0.05 to 1.45, against W_s (the parameter used by Booij [5] in his corresponding graph), where $W_s = \sqrt{0.6}\alpha_0$. As one would expect with these prescribed tolerances in the error, there is practically no difference in the two sets of results. The new method uses Chamberlain solutions at 5 values of α_0, which are

$$\alpha_0 = 0.05,\ 0.95,\ 1.2,\ 1.4 \text{ and } 1.45 \ ,$$

to generate results over the α_0 range from 0.05 to 1.45. Thus the number of Chamberlain solutions required to generate the results is reduced from 29 to 5, that is, by a factor of 6. This significant decrease in the number of Chamberlain solutions required is reflected in the decrease of the CPU run-times. The total

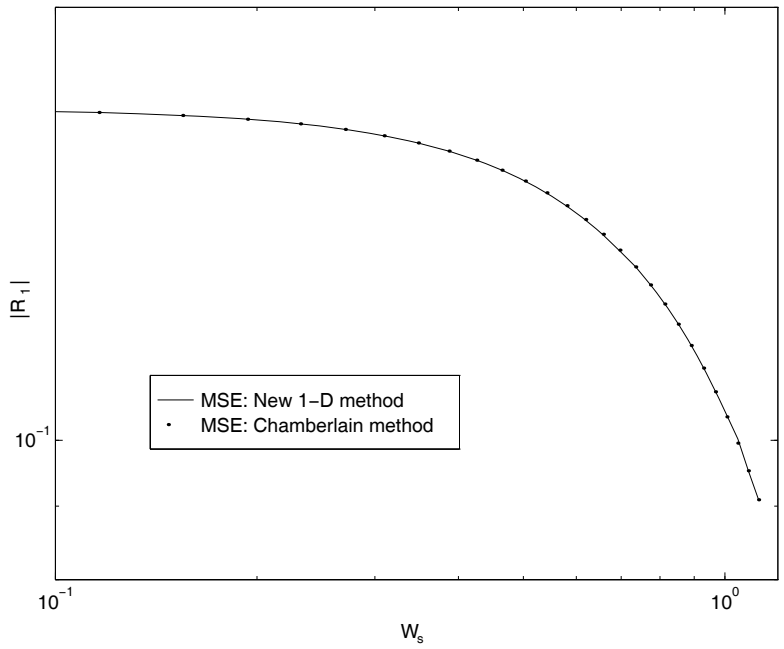

Figure 3.2: Reflected amplitude for the depth profile $H(x) = 1 - 2/3x$ $(0 \leq x \leq 1)$.

CPU run-time to generate these results by Chamberlain's method is 7m 39s. The total CPU run-time required by the new method is 3m 54s and so the total CPU run-time has been reduced by 49%. This large reduction in CPU run-times is not as significant as the reduction in the number of Chamberlain solutions used, because at the values of α_0 where Chamberlain solutions are not used, the solutions generated by the new one-dimensional trial functions still have to be calculated there.

Similar results were found in tests with other bed profiles. So the new method produces solutions accurate to 2.s.f. in a greatly reduced CPU run-time over an α_0 range where the largest α_0 value is still small (< 2).

However, if solutions of the MSE, that are accurate to 2.s.f., are desired over a range of α_0 where the initial $\alpha_0 > \alpha_{\max}$, then clearly the new method achieves no computational savings. In order to resolve this problem, we need to understand the reason why the new method cannot generate accurate enough solutions at $\alpha_0 > \alpha_{\max}$.

Chamberlain [7] notes that the dimension of trial space required to achieve a constant level of accuracy rises as α_0 increases. This happens because $\|P\|$

and hence $\|LP\|$ increase with α_0, making more terms in the trial functions $\tilde{p}_k$ $(k = 1, 2)$ given by (3.10) (and consequently larger trial spaces) necessary to be assured of the desired accuracy. Correspondingly, the new approximation method has to resolve the problem via Chamberlain's method at more frequent intervals for larger α_0. This occurs because as α_0 increases, $\|P\|$ increases and hence $\rho(x)$ and the solutions, $\chi_1^{\alpha_0}$ and $\chi_2^{\alpha_0}$, of the integral equations (3.4) change more rapidly from one value of α_0 to the next. Fig.3.3 depicts the approximations, $\xi_1^{\alpha_0}$ and $\xi_2^{\alpha_0}$, to the solutions $\chi_1^{\alpha_0}$ and $\chi_2^{\alpha_0}$ of (3.4) from the previous example at two different values of α_0. At the smaller value of α_0, the $\xi_2^{\alpha_0}$ approximation has a zero, whilst at the larger α_0, both approximations have zeros and the position of the zero in the $\xi_2^{\alpha_0}$ approximation is different from that in the smaller α_0 case.

Thus, it is easy to understand why there is a maximum value of $\alpha_0 = \alpha_{\max}$ for which at any $\hat{\alpha_0} > \tilde{\alpha_0} > \alpha_{\max}$ the trial approximations $C_1\xi_1^{\tilde{\alpha_0}}$ and $C_2\xi_2^{\tilde{\alpha_0}}$, where C_j $(j = 1, 2)$ are some constants, will be a poor approximation to $\chi_1^{\hat{\alpha_0}}$ and $\chi_2^{\hat{\alpha_0}}$. Hence the minimum practical trial space dimension is two.

3.3 A two-dimensional trial space approximation

3.3.1 Outline of method

The one-dimensional trial space method described in section 3.2 used Chamberlain solutions at a chosen α_0 to approximate the solutions of the integral equations (3.4) in the neighbourhood of α_0. The two-dimensional trial space method uses Chamberlain solutions at two particular choices of α_0, denoted by $\tilde{\alpha_0}$ and $\tilde{\tilde{\alpha_0}}$ (with $\tilde{\alpha_0} < \tilde{\tilde{\alpha_0}}$), to approximate $\chi_1^{\hat{\alpha_0}}$ and $\chi_2^{\hat{\alpha_0}}$ at the intermediate values $\hat{\alpha_0}$, that is at $\hat{\alpha_0} \in (\tilde{\alpha_0},\ \tilde{\tilde{\alpha_0}})$. So we use the two-dimensional trial functions

$$p_k = r_k\xi_k^{\tilde{\alpha_0}} + s_k\xi_k^{\tilde{\tilde{\alpha_0}}} \qquad (k = 1, 2) \tag{3.13}$$

as approximations to $\chi_1^{\hat{\alpha_0}}$ and $\chi_2^{\hat{\alpha_0}}$, for some r_k and $s_k \in \mathbb{R}$ $(k = 1, 2)$ determined so as to make the functionals (3.8) stationary. Therefore, substituting (3.13) into

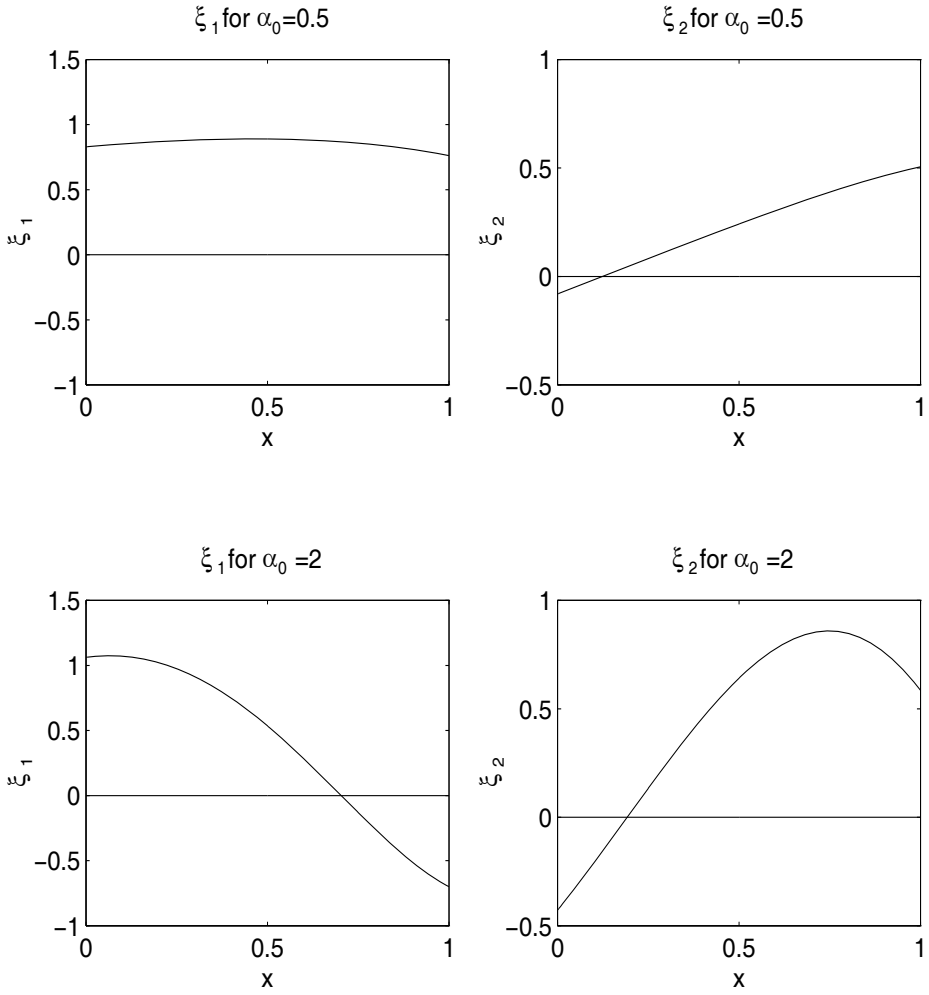

Figure 3.3: Comparison of Chamberlain solutions at two values of α_0

the functional (3.8), we see that

$$\begin{aligned} J_k^{\hat{\alpha_0}}(p_k) = \;& J_k^{\hat{\alpha_0}}(r_k, s_k) \\ = \;& 2\left[r_k\left(\xi_k^{\tilde{\alpha_0}},\ S^{\hat{\alpha_0}} f_k^{\hat{\alpha_0}}\right) + s_k\left(\xi_k^{\tilde{\tilde{\alpha_0}}},\ S^{\hat{\alpha_0}} f_k^{\hat{\alpha_0}}\right)\right] \qquad (k=1,2) \\ & -\left[r_k^2\left(\hat{A}^{\hat{\alpha_0}}\xi_k^{\tilde{\alpha_0}},\ \xi_k^{\tilde{\alpha_0}}\right) + 2r_k s_k\left(\hat{A}^{\hat{\alpha_0}}\xi_k^{\tilde{\alpha_0}},\ \xi_k^{\tilde{\tilde{\alpha_0}}}\right) + s_k^2\left(\hat{A}^{\hat{\alpha_0}}\xi_k^{\tilde{\tilde{\alpha_0}}},\ \xi_k^{\tilde{\tilde{\alpha_0}}}\right)\right] , \end{aligned}$$

regarded as a function of r_k and s_k $(k=1,2)$, is stationary where

$$\frac{\partial J_k^{\hat{\alpha_0}}}{\partial r_k} = 0 \qquad \text{and} \qquad \frac{\partial J_k^{\hat{\alpha_0}}}{\partial s_k} = 0 \qquad (k=1,2)\ .$$

Hence the constants r_k and s_k $(k=1,2)$ are given by the rank two system,

$$\begin{pmatrix} \left(\hat{A}^{\hat{\alpha_0}}\xi_k^{\tilde{\alpha_0}},\ \xi_k^{\tilde{\alpha_0}}\right) & \left(\hat{A}^{\hat{\alpha_0}}\xi_k^{\tilde{\alpha_0}},\ \xi_k^{\tilde{\tilde{\alpha_0}}}\right) \\ \left(\hat{A}^{\hat{\alpha_0}}\xi_k^{\tilde{\alpha_0}},\ \xi_k^{\tilde{\tilde{\alpha_0}}}\right) & \left(\hat{A}^{\hat{\alpha_0}}\xi_k^{\tilde{\tilde{\alpha_0}}},\ \xi_k^{\tilde{\tilde{\alpha_0}}}\right) \end{pmatrix} \begin{pmatrix} r_k \\ s_k \end{pmatrix} = \begin{pmatrix} \left(\xi_k^{\tilde{\alpha_0}},\ S^{\hat{\alpha_0}} f_k^{\hat{\alpha_0}}\right) \\ \left(\xi_k^{\tilde{\tilde{\alpha_0}}},\ S^{\hat{\alpha_0}} f_k^{\hat{\alpha_0}}\right) \end{pmatrix} \quad (k=1,2)\ .$$

The approximation to the inner products $\left(\chi_k^{\hat{\alpha_0}},\ P^{\hat{\alpha_0}} f_k^{\hat{\alpha_0}}\right)$ $(k = 1, 2)$ are therefore given by $J_k^{\hat{\alpha_0}}(p_k)$ $(k = 1, 2)$ respectively.

To find an approximation to the inner product $\left(\chi_1^{\hat{\alpha_0}},\ P^{\hat{\alpha_0}} f_2^{\hat{\alpha_0}}\right)$, we use the two-dimensional trial functions

$$q_k = \gamma_k \mu_k^{\tilde{\alpha_0}} + \delta_k \mu_k^{\tilde{\tilde{\alpha_0}}} \qquad (k = 1, 2) \tag{3.14}$$

as approximations to $\chi_1^{\hat{\alpha_0}}$ and $\chi_2^{\hat{\alpha_0}}$, for some γ_k and $\delta_k \in \mathbb{R}$ $(k = 1, 2)$ determined so as to make the functional (3.9) stationary. Therefore, substituting (3.14) into the functional (3.9), we see that

$$\begin{aligned} J_3^{\hat{\alpha_0}}(q_1, q_2) = &\ J_k^{\hat{\alpha_0}}(\gamma_1, \gamma_2, \delta_1, \delta_2) \\ = &\ \gamma_2 \left(S^{\hat{\alpha_0}} f_1^{\hat{\alpha_0}},\ \mu_2^{\tilde{\alpha_0}}\right) + \delta_2 \left(S^{\hat{\alpha_0}} f_1^{\hat{\alpha_0}},\ \mu_2^{\tilde{\tilde{\alpha_0}}}\right) \\ &+ \gamma_1 \left(\mu_1^{\tilde{\alpha_0}},\ S^{\hat{\alpha_0}} f_2^{\hat{\alpha_0}}\right) + \delta_1 \left(\mu_1^{\tilde{\tilde{\alpha_0}}},\ S^{\hat{\alpha_0}} f_2^{\hat{\alpha_0}}\right) \\ &- \Big[\gamma_1\gamma_2 \left(\hat{A}^{\hat{\alpha_0}} \mu_1^{\tilde{\alpha_0}},\ \mu_2^{\tilde{\alpha_0}}\right) + \gamma_1\delta_2 \left(\hat{A}^{\hat{\alpha_0}} \mu_1^{\tilde{\alpha_0}},\ \mu_2^{\tilde{\tilde{\alpha_0}}}\right) \\ &\quad + \delta_1\gamma_2 \left(\hat{A}^{\hat{\alpha_0}} \mu_1^{\tilde{\tilde{\alpha_0}}},\ \mu_2^{\tilde{\alpha_0}}\right) + \delta_1\delta_2 \left(\hat{A}^{\hat{\alpha_0}} \mu_1^{\tilde{\tilde{\alpha_0}}},\ \mu_2^{\tilde{\tilde{\alpha_0}}}\right)\Big] , \end{aligned}$$

regarded as a function of γ_k and δ_k $(k = 1, 2)$, is stationary where

$$\frac{\partial J_3^{\hat{\alpha_0}}}{\partial \gamma_k} = 0 \qquad \text{and} \qquad \frac{\partial J_3^{\hat{\alpha_0}}}{\partial \delta_k} = 0 \qquad (k = 1, 2) \ .$$

Hence the constants γ_1 and δ_1 are given by the rank two system,

$$\begin{pmatrix} \left(\hat{A}^{\hat{\alpha_0}} \mu_1^{\tilde{\alpha_0}},\ \mu_2^{\tilde{\alpha_0}}\right) & \left(\hat{A}^{\hat{\alpha_0}} \mu_1^{\tilde{\tilde{\alpha_0}}},\ \mu_2^{\tilde{\alpha_0}}\right) \\ \left(\hat{A}^{\hat{\alpha_0}} \mu_1^{\tilde{\alpha_0}},\ \mu_2^{\tilde{\tilde{\alpha_0}}}\right) & \left(\hat{A}^{\hat{\alpha_0}} \mu_1^{\tilde{\tilde{\alpha_0}}},\ \mu_2^{\tilde{\tilde{\alpha_0}}}\right) \end{pmatrix} \begin{pmatrix} \gamma_1 \\ \delta_1 \end{pmatrix} = \begin{pmatrix} \left(S^{\hat{\alpha_0}} f_1^{\hat{\alpha_0}},\ \mu_2^{\tilde{\alpha_0}}\right) \\ \left(S^{\hat{\alpha_0}} f_1^{\hat{\alpha_0}},\ \mu_2^{\tilde{\tilde{\alpha_0}}}\right) \end{pmatrix} ,$$

and the constants γ_2 and δ_2 are given by the rank two system,

$$\begin{pmatrix} \left(\hat{A}^{\hat{\alpha_0}} \mu_1^{\tilde{\alpha_0}},\ \mu_2^{\tilde{\alpha_0}}\right) & \left(\hat{A}^{\hat{\alpha_0}} \mu_1^{\tilde{\alpha_0}},\ \mu_2^{\tilde{\tilde{\alpha_0}}}\right) \\ \left(\hat{A}^{\hat{\alpha_0}} \mu_1^{\tilde{\tilde{\alpha_0}}},\ \mu_2^{\tilde{\alpha_0}}\right) & \left(\hat{A}^{\hat{\alpha_0}} \mu_1^{\tilde{\tilde{\alpha_0}}},\ \mu_2^{\tilde{\tilde{\alpha_0}}}\right) \end{pmatrix} \begin{pmatrix} \gamma_2 \\ \delta_2 \end{pmatrix} = \begin{pmatrix} \left(\mu_1^{\tilde{\alpha_0}},\ S^{\hat{\alpha_0}} f_2^{\hat{\alpha_0}}\right) \\ \left(\mu_1^{\tilde{\tilde{\alpha_0}}},\ S^{\hat{\alpha_0}} f_2^{\hat{\alpha_0}}\right) \end{pmatrix} .$$

The approximation to the inner product $\left(\chi_1^{\hat{\alpha_0}},\ P^{\hat{\alpha_0}} f_2^{\hat{\alpha_0}}\right)$ is therefore given by $J_3^{\hat{\alpha_0}}(q_1, q_2)$. Once approximations to $\chi_1^{\hat{\alpha_0}}$, $\chi_2^{\hat{\alpha_0}}$ and $\left(\chi_j^{\hat{\alpha_0}}, P^{\hat{\alpha_0}} f_k^{\hat{\alpha_0}}\right)$ $(j, k = 1, 2)$, have been obtained, we revert back to the same stage in the integral equation procedure given in Chapter 2 to find the resulting reflection and transmission coefficients.

Clearly, the approximations to $\chi_1^{\hat{\alpha_0}}$ and $\chi_2^{\hat{\alpha_0}}$ given by (3.13) and (3.14) are very much quicker to calculate than the N-dimensional Chamberlain solutions, given by (3.10), when $N > 1$. We shall refer to the solutions generated by the trial functions (3.13) and (3.14) as the 'cheap' solutions. It is obvious that the approximations (3.13) and (3.14) to $\chi_1^{\hat{\alpha_0}}$, $\chi_2^{\hat{\alpha_0}}$ will not be accurate enough for all $\hat{\alpha_0} \in (\tilde{\alpha_0},\ \tilde{\tilde{\alpha}}_0)$ if $(\tilde{\tilde{\alpha}}_0 - \tilde{\alpha_0})$ becomes too large. We recall from section 3.2, that as α_0 increases, $\|P\|$ increases and so $\rho(x)$ and the solutions of the integral equations (3.4) vary more rapidly from one value of α_0 to the next. Therefore the length of the interval $(\tilde{\alpha_0},\ \tilde{\tilde{\alpha}}_0)$, where the error in the 'cheap' solutions found at the intermediate $\hat{\alpha_0} \in (\tilde{\alpha_0},\ \tilde{\tilde{\alpha}}_0)$ is within the specified tolerance, will decrease as $\tilde{\alpha_0}$ increases.

The worst approximations to the functions $\chi_1^{\hat{\alpha_0}}$, $\chi_2^{\hat{\alpha_0}}$ and the inner products $\left(\chi_j^{\hat{\alpha_0}}, P^{\hat{\alpha_0}} f_k^{\hat{\alpha_0}}\right)$ $(j,k = 1,2)$ will occur when $\hat{\alpha_0}$ has a value close to the mid-point of the interval $(\tilde{\alpha_0},\ \tilde{\tilde{\alpha}}_0)$. Therefore a check is made to see whether the error in the 'cheap' solution at $\hat{\alpha_0} = \frac{1}{2}(\tilde{\alpha_0} + \tilde{\tilde{\alpha}}_0)$ is within the specified tolerance. If the error at $\hat{\alpha_0} = \frac{1}{2}(\tilde{\alpha_0} + \tilde{\tilde{\alpha}}_0)$ is within the given tolerance, then the trial functions (3.13) and (3.14) are used to generate the solutions at all the $\hat{\alpha_0} \in (\tilde{\alpha_0},\ \tilde{\tilde{\alpha}}_0)$. In the unlikely case that the error in one of these 'cheap' solutions does exceed the tolerance, we proceed as if the error in the 'cheap' solution at the mid-point of $(\tilde{\alpha_0},\ \tilde{\tilde{\alpha}}_0)$, that is, at $\hat{\alpha_0} = \frac{1}{2}(\tilde{\alpha_0} + \tilde{\tilde{\alpha}}_0)$, has exceeded the given tolerance.

If the error in the 'cheap' solution at $\hat{\alpha_0} = \frac{1}{2}(\tilde{\alpha_0} + \tilde{\tilde{\alpha}}_0)$ exceeds the given tolerance, the Chamberlain solutions at $\tilde{\tilde{\alpha}}_0$ are saved and a new set of Chamberlain solutions are found at $\alpha_0 = \frac{1}{2}(\tilde{\alpha_0} + \tilde{\tilde{\alpha}}_0)$, and we check the error in the 'cheap' solution at the mid-point of the interval $[\tilde{\alpha_0},\ \frac{1}{2}(\tilde{\alpha_0} + \tilde{\tilde{\alpha}}_0)]$. This process is repeated until an interval $[\tilde{\alpha_0},\ \alpha_0^*]$ has been found in which the error of the 'cheap' solution at all the intermediate $\hat{\alpha_0}$ is within the specified tolerance. We now move onto the next interval $[\alpha_0^*,\ \alpha_0^{**}]$, where the Chamberlain solutions are known at $\alpha_0 = \alpha_0^*$ and the value of α_0^{**} has to be chosen. If we suppose we know the Chamberlain solutions at values of α_0 given by

$$\alpha_0^* < \alpha_0{}^{(1)} < \alpha_0{}^{(2)} < \ldots < \alpha_0{}^{(n)} < \tilde{\tilde{\alpha}}_0 \ ,$$

then we choose $\alpha_0^{**} = \alpha_0{}^{(1)}$ and the whole process starts again. If no Chamberlain solutions are known at values of $\alpha_0 > \alpha_0^*$, then α_0^{**} is chosen according to the size

of the maximum error in all the 'cheap' solutions found in the previous interval $[\tilde{\alpha_0},\ \alpha_0^*]$. We use the following 'rule of thumb' to choose α_0^{**}. If the maximum error in the 'cheap' solutions found in the interval $[\tilde{\alpha_0},\ \alpha_0^*]$ is 2 (or more) orders of magnitude smaller than the specified tolerance, then α_0^{**} is chosen so that the length of the interval $[\alpha_0^*,\ \alpha_0^{**}]$ is greater than the length of the interval $[\tilde{\alpha_0},\ \alpha_0^*]$. If the maximum error is the same order of magnitude as the specified tolerance, then α_0^{**} is chosen so that the length of the interval $[\alpha_0^*,\ \alpha_0^{**}]$ is less than the length of the interval $[\tilde{\alpha_0},\ \alpha_0^*]$. Otherwise α_0^{**} is chosen so that the length of the interval $[\alpha_0^*,\ \alpha_0^{**}]$ is equal to the length of the interval $[\tilde{\alpha_0},\ \alpha_0^*]$. The Chamberlain solutions are then found at α_0^{**} and the whole process starts again.

We clarify this situation in the following example. Fig.3.4 depicts a typical situation. In this case, the errors in all the 'cheap' solutions found in Interval

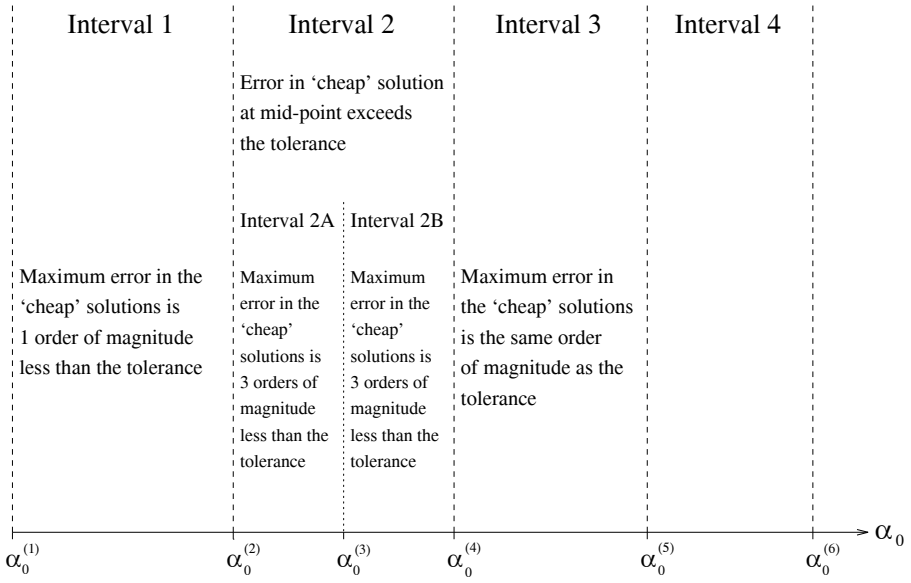

Figure 3.4: An example situation depicting the values of α_0 at which Chamberlain solutions are found.

1 are within the specified tolerance. No Chamberlain solutions are known at $\alpha_0 > \alpha_0{}^{(2)}$ and the maximum error of all these 'cheap' solutions is 1 order of magnitude less than the tolerance. Therefore, the next value of α_0 at which Chamberlain solutions are found is chosen so that the length of Interval 2 is equal to the length of Interval 1. This value of α_0 is denoted by $\alpha_0{}^{(4)}$ in Fig.3.4. The error in the 'cheap' solution at the mid-point of Interval 2 is not within the tolerance. Consequently, Chamberlain solutions at α_0 =mid-point of Interval 2

are found. This value of α_0 is denoted by $\alpha_0{}^{(3)}$ in Fig.3.4. The errors in the 'cheap' solutions in Interval 2A are within the tolerance, and as the Chamberlain solutions are known at $\alpha_0 = \alpha_0{}^{(4)} > \alpha_0{}^{(3)}$, the next interval is 2B. Here the errors in the 'cheap' solutions are also within the tolerance. No Chamberlain solutions are known at $\alpha_0 > \alpha_0{}^{(4)}$ and the maximum error of all the 'cheap' solutions found in Interval 2B is 3 orders of magnitude less than the tolerance. Therefore, the next value of α_0 at which Chamberlain solutions are found, which is denoted by $\alpha_0{}^{(5)}$ in Fig.3.4, is chosen so that

$$\text{length of Interval 2B} < \text{length of Interval 3} < \text{length of Interval 2}.$$

Here, the upper bound arises because sufficiently accurate 'cheap' solutions could not be obtained at all values of α_0 in Interval 2, and therefore could not be obtained in Interval 3 if it had the same length as Interval 2. The errors in the 'cheap' solutions found in Interval 3 are within the tolerance, with the maximum error being the same order of magnitude as the tolerance. As no Chamberlain solutions are known at $\alpha_0 > \alpha_0{}^{(5)}$, the next Chamberlain solutions are found at $\alpha_0 = \alpha_0{}^{(6)}$, where $\alpha_0{}^{(6)}$ is chosen to make the length of Interval 4 less than the length of Interval 3. The process continues like this until solutions have been found for the required α_0 range.

We are now in a position to use this method. It is implemented by firstly assigning the depth profile H, the tolerance in the error, the initial α_0 range $(\tilde{\alpha_0},\ \tilde{\tilde{\alpha_0}})$, the final value of α_0, the relationship between α_0 and τ and the increment to be added to α_0 to give the next α_0 at which a solution is to be found. Chamberlain solutions are then found at $\alpha_0 = \tilde{\alpha_0}$ and at $\alpha_0 = \tilde{\tilde{\alpha_0}}$ and the method outlined in the last few pages is used to generate solutions of the mild-slope equation over the desired α_0 range.

3.3.2 Results

The two-dimensional trial space method works excellently with the mild-slope equation, in the sense that solutions satisfying a minimum accuracy requirement can be obtained over an α_0 range, using a small number of Chamberlain solutions, in much less CPU time than just using Chamberlain's procedure at each successive

α_0. The problem of the one-dimensional trial space method concerning the small range of values of α_0 over which 'cheap' solutions could be obtained does not arise.

Let us consider the example we tested the one-dimensional trial space method on. Here we seek the solution of the MSE for an incident wave of unit amplitude from $x = -\infty$ over the depth profile given by

$$H(x) = 1 - \frac{2}{3}x \qquad (0 \leq x \leq 1) \ .$$

We shall use the two-dimensional method to solve this problem for the 170 values of α_0 between 0.05 and 8.5 at intervals of 0.05 (with τ given at each value of α_0 by $\tau = \sqrt{0.6}\alpha_0$). We again choose the tolerance in the error to be a minimum of 2.s.f. accuracy in $|R_k|$ and $|T_k|$ $(k = 1, 2)$. The two-dimensional method produces 'cheap' solutions over the α_0 range $[0.05, 8.5]$, and uses Chamberlain solutions at 18 values of α_0, given by

$$\begin{aligned} \alpha_0 = \ & 0.05, 2.0, 2.5, 3.0, 3.7, 4.05, 4.4, 4.7, \\ & 5.0, 5.5, 6.0, 6.5, 6.75, 7.0, 7.4, 7.8, 8.2 \text{ and } 8.5 \ . \end{aligned}$$

Thus, the number of Chamberlain solutions required to generate the results has been reduced from 170 to 18, that is, by a factor of 9. This significant decrease in the number of Chamberlain solutions required to generate the results is reflected in the large decrease of the CPU run-times. The total CPU run-time to generate these results by Chamberlain's method is 51m 55s. The total CPU run-time required by the new method is 34m 48s, which represents a saving of 33%. This reduction in CPU run-times is not as significant as the reduction in the number of Chamberlain solutions used, because at the values of α_0 where Chamberlain solutions are not used, the solutions generated by the new two-dimensional trial functions still have to be calculated. The solid, higher line in Fig.3.5 depicts the reflected amplitude given by the mild-slope equation plotted against the parameter W_s (as used by Booij [5]) generated by both methods. As one would expect with these prescribed tolerances in the error, there is practically no difference between the two sets of results.

Now that we have a method that works well with the mild-slope equation, we are in a position to make slight amendments so that it encompasses the other two

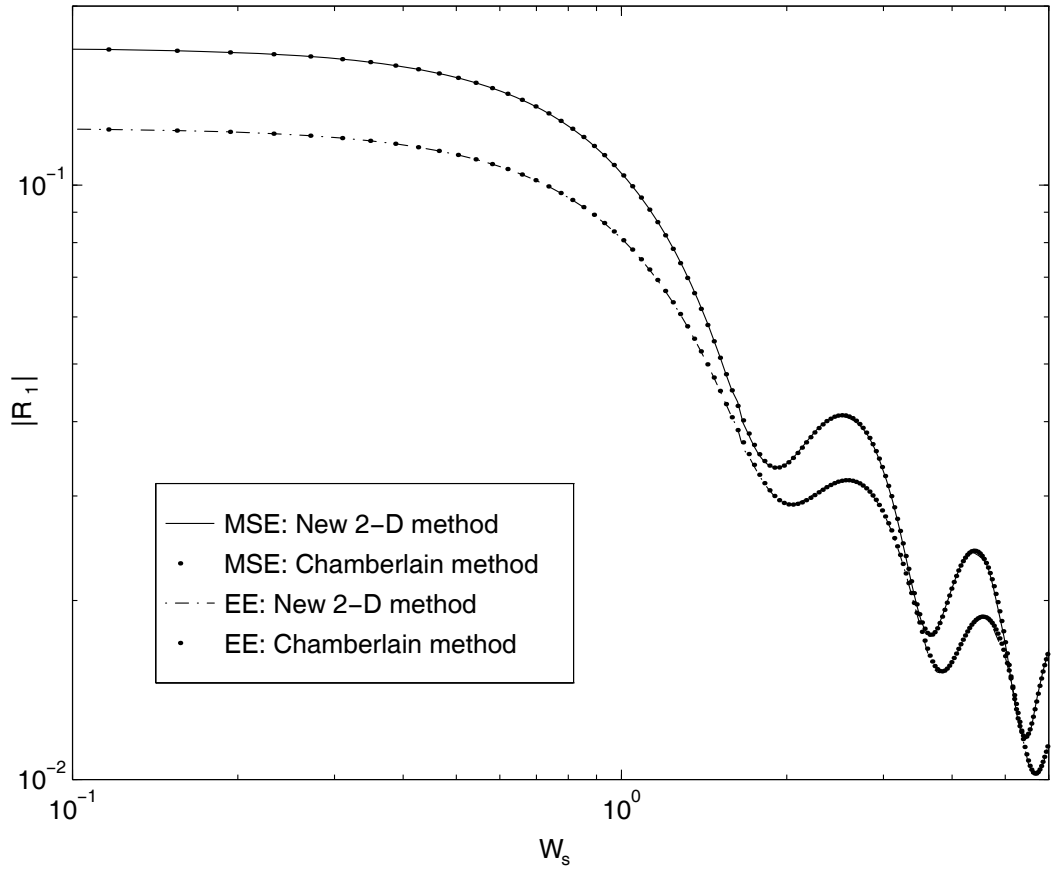

Figure 3.5: Reflected amplitude over the depth profile $H(x) = 1 - 2/3x\,(0 \leq x \leq 1)$.

model equations. In fact, all that is required is to replace the mild-slope U and κ functions given by (3.2) and (3.3) by the corresponding Eckart and shallow water ones. Thus in the case of Eckart's equation we use

$$U(x) = \frac{1 - e^{-2(\alpha_0 \tau)^2 H}}{2(\alpha_0 \tau)^2}$$

and

$$\kappa(x) = \sqrt{(\alpha_0{}^2 \tau)^2 \coth\left((\alpha_0 \tau)^2 H\right)}\ .$$

In the case of the shallow water equation we use $\kappa(x) = \alpha_0$ and $U(x) = H(x)$.

In order to compare the mild-slope and Eckart results, we shall also solve Eckart's equation over the talud with depth profile given by

$$H(x) = 1 - \frac{2}{3}x \qquad (0 \leq x \leq 1)\ ,$$

for a wave of unit amplitude incident from $x = -\infty$. We seek the solution of Eckart's equation for values of α_0 between 0.05 and 8.5 at intervals of 0.05 (with

τ given at each value of α_0 by $\tau = \sqrt{0.6}\alpha_0$). Using Chamberlain's method to generate extremely accurate solutions of Eckart's equation, with three-dimensional trial spaces for $\alpha_0 < 2$ and six-dimensional trial spaces for $\alpha_0 > 4$, has a total CPU run-time of 49m 37s. The two-dimensional trial space method with the tolerance in the error set to be a minimum of 2.s.f. accuracy in $|R_k|$ and $|T_k|$ $(k = 1, 2)$, uses Chamberlain solutions at 19 values of α_0, given by

$$\begin{aligned}\alpha_0 = \quad & 0.05, 1.5, 2.0, 2.5, 3.2, 3.55, 3.9, 4.2, 4.5, \\ & 5.0, 5.5, 6.0, 6.5, 6.75, 7.0, 7.4, 7.8, 8.2 \text{ and } 8.5 \ .\end{aligned}$$

Therefore, the number of Chamberlain solutions required has been again reduced by a factor of 9. The total CPU run-time required is 33m 52s, which represents a saving of 32% in CPU time compared with using Chamberlain solutions at each value of α_0. The dashed, lower line in Fig.3.5 depicts the reflected amplitude given by the Eckart's equation plotted against the parameter W_s (as used by Booij [5]) generated by both methods. Again, with these prescribed tolerances in the error, there is practically no difference in the two sets of results. The difference in the Eckart and mild-slope results are discussed in section 3.4.

As a different example, we shall solve the shallow water equation (SWE) over the trench whose depth profile is given by

$$H(x) = 1 + x(1 - x^2) \qquad (0 \leq x \leq 1) \ ,$$

for a wave of unit amplitude incident from $x = -\infty$. We seek the solution of the SWE for the 200 values of α_0 between 0.05 and 10.0 at intervals of 0.05. Using Chamberlain's method with three-dimensional trial spaces for $\alpha_0 < 2$ and six-dimensional trial spaces for $\alpha_0 > 4$, has a total CPU run-time of 58m 58s. The two-dimensional trial space method with the tolerance in the error set to be a minimum of 2.s.f. accuracy in $|R_k|$ and $|T_k|$ $(k = 1, 2)$, uses Chamberlain solutions at 19 values of α_0, given by

$$\begin{aligned}\alpha_0 = \quad & 0.05, 2.0, 3.0, 4.0, 4.5, 5.0, 5.7, 6.4, 6.75, 7.1, \\ & 7.6, 8.1, 8.35, 8.6, 9.0, 9.2, 9.4, 9.7 \text{ and } 10.0 \ .\end{aligned}$$

Now the number of Chamberlain solutions required has been reduced by a factor of 10, and the total CPU run-time is 38m 26s. This represents a saving of 35% in

CPU time compared with using Chamberlain solutions at each value of α_0, which is slightly higher than that achieved in the mild-slope and Eckart examples due to the larger decrease in the number of Chamberlain solutions used. From Fig.3.6, we notice that there is no observable difference in the results, as expected with

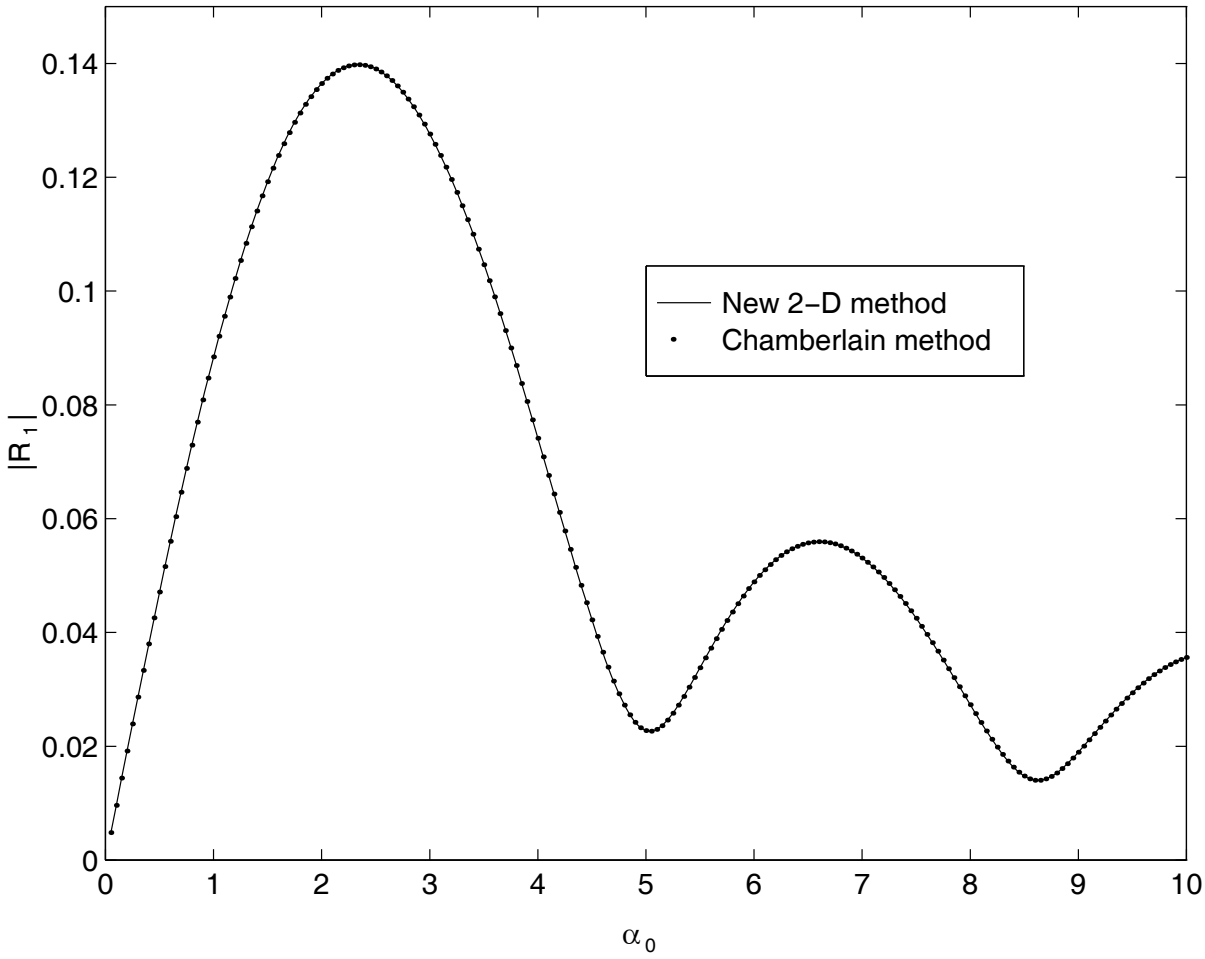

Figure 3.6: SWE reflected amplitude for depth profile $H(x) = 1 + x(1 - x^2)(0 \leq x \leq 1)$.

the choice in the tolerance of the errors. Similar percentage savings have been found for all three model equations on all bed profiles tested, with the tolerance in the error as specified above.

This section has shown that the two-dimensional trial space method significantly reduces CPU run-times by approximately one third for all three model equations on all depth profiles tested. Although this is an excellent improvement, we can do even better as shown in the next subsection.

3.3.3 Extra computational saving

A further source of computational saving can be effected without compromising the approximations already described. As already mentioned in this chapter, by substituting trial functions $\xi_k^{\alpha_0}$ $(k = 1, 2)$ into the functionals $J_k^{\alpha_0}$ $(k = 1, 2)$, given by

$$J_k^{\alpha_0}(\xi_k^{\alpha_0}) = 2(\xi_k^{\alpha_0}, S^{\alpha_0} f_k^{\alpha_0}) - (\hat{A}^{\alpha_0}\xi_k^{\alpha_0}, \xi_k^{\alpha_0}) \qquad (k = 1, 2) \ ,$$

we generate approximations to the inner products

$$(\chi_k^{\alpha_0},\ P^{\alpha_0} f_k^{\alpha_0}) \qquad (k = 1, 2) \ . \tag{3.15}$$

Similarly, by substituting trial functions $\mu_k^{\alpha_0}$ $(k = 1, 2)$ into the functional $J_3^{\alpha_0}$, given by

$$J_3^{\alpha_0}(\mu_1^{\alpha_0}, \mu_2^{\alpha_0}) = (\mu_1^{\alpha_0}, S^{\alpha_0} f_2^{\alpha_0}) + (S^{\alpha_0} f_1^{\alpha_0}, \mu_2^{\alpha_0}) - (\hat{A}^{\alpha_0}\mu_1^{\alpha_0}, \mu_2^{\alpha_0}) \ ,$$

we generate an approximation to the inner product

$$(\chi_1^{\alpha_0},\ P^{\alpha_0} f_2^{\alpha_0}) \ . \tag{3.16}$$

The trial functions $\xi_k^{\alpha_0}$ $(k = 1, 2)$ are determined by making the functionals $J_k^{\alpha_0}$ $(k = 1, 2)$ stationary within their respectful trial spaces. Similarly, the trial functions $\mu_k^{\alpha_0}$ $(k = 1, 2)$ are determined by making the functional $J_3^{\alpha_0}$ stationary within its trial space. It was noticed that if $\xi_k^{\alpha_0}$ $(k = 1, 2)$ were used in the functional $J_3^{\alpha_0}$ to estimate $(\chi_1^{\alpha_0},\ P^{\alpha_0} f_2^{\alpha_0})$, this estimate was the same, to 5.s.f., as that obtained when $\mu_k^{\alpha_0}$ $(k = 1, 2)$ are used in $J_3^{\alpha_0}$. The previous tests that we have used to check the accuracy of the reflection and transmission coefficients revealed that the maximum error in $|R_k|$ and $|T_k|$ $(k = 1, 2)$ using both choices of trial function in $J_3^{\alpha_0}$ was the same order of magnitude, with neither choice always giving the smallest error. Porter and Stirling [51] (p. 154-163) show how to obtain approximations to the inner products of the form (3.15) and (3.16) and the errors incurred. However, they did not investigate whether the trial functions generated by the functionals $J_k^{\alpha_0}$ $(k = 1, 2)$ gave as good an estimate to $(\chi_1^{\alpha_0},\ P^{\alpha_0} f_2^{\alpha_0})$ when substituted into the functional $J_3^{\alpha_0}$, as the trial functions generated by the functional $J_3^{\alpha_0}$.

It turns out that $J_3^{\alpha_0}(\xi_1^{\alpha_0}, \xi_2^{\alpha_0})$ and $J_3^{\alpha_0}(\mu_1^{\alpha_0}, \mu_2^{\alpha_0})$ correspond to at least 5.s.f. in all problems undertaken so far for the mild-slope, Eckart and shallow water equations. However this result still remains to be proved in full generality. As only very approximate solutions are being looked for here, then the approach of only using the trial functions $\xi_k^{\alpha_0}$ $(k = 1, 2)$ to estimate $\left(\chi_j^{\alpha_0}, P^{\alpha_0} f_k^{\alpha_0}\right)$ $(j, k = 1, 2)$ is quite justified. Computationally this device gives a great saving because it reduces the work load in the 'cheap' solution method by nearly one third. We now test the two-dimensional method with this device incorporated, which we shall refer to as the streamlined two-dimensional method.

3.3.4 Results

We return to the solution of the MSE for an incident wave of unit amplitude from $x = -\infty$ over the depth profile given by

$$H(x) = 1 - \frac{2}{3}x \qquad (0 \leq x \leq 1) \ .$$

We use the streamlined two-dimensional method to solve this problem with α_0 taking values between 0.05 and 8.5 at intervals of 0.05 (with τ given at each value of α_0 by $\tau = \sqrt{0.6}\alpha_0$). We again choose the tolerance in the error to be a minimum of 2.s.f. accuracy in $|R_k|$ and $|T_k|$ $(k = 1, 2)$. The streamlined two-dimensional method uses Chamberlain solutions at the same values of α_0 as the original two-dimensional method. However, the total CPU run-time is now reduced to 22m 19s, which represents a saving of 57% in CPU time compared with using Chamberlain solutions at each value of α_0. The reflected amplitude given by the MSE is depicted in Fig.3.7 and again there is no difference in the results.

Similarly, if we now solve the above problem for Eckart's equation instead of the MSE, then the streamlined two-dimensional method reduces the total CPU run-time to 22m 58s, which represents a saving of 54% in CPU time compared with using Chamberlain solutions at each value of α_0. Finally , if we now solve the previous shallow water problem, given in subsection 3.3.2, using the streamlined two-dimensional method, the total CPU run-time is reduced to 25m 4s. This represents a saving of 57% in CPU time compared to using Chamberlain solutions

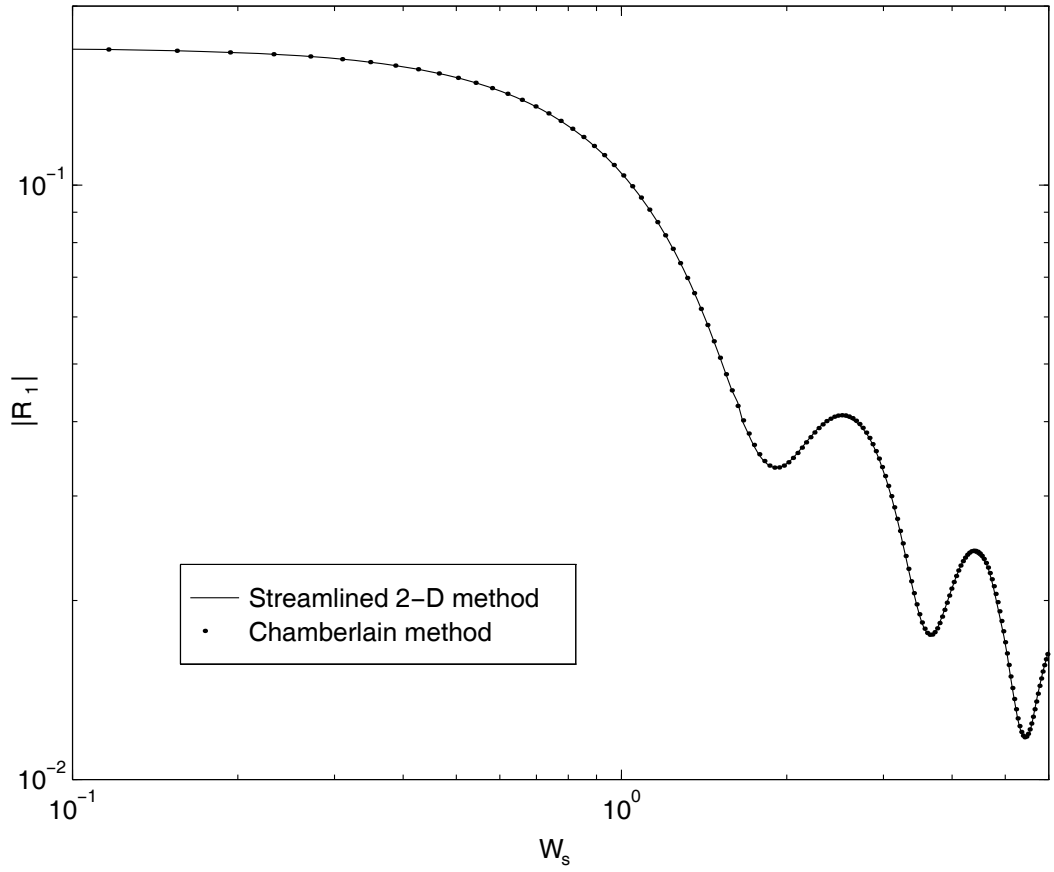

Figure 3.7: MSE reflected amplitude for depth profile $H(x) = 1 - 2/3x$ $(0 \leq x \leq 1)$.

at each value of α_0.

We note that further reduction of the tolerance in the errors of the 'cheap' solutions, enabling fewer Chamberlain solutions to be found over the α_0 range, will only effect a small reduction in CPU run-times already obtained with the 2.s.f. tolerance in the error. This is because the major saving in CPU run-time was achieved by reducing the total number of Chamberlain solutions found over an α_0 range by a factor of 9 or 10. In the examples given in this section, the two-dimensional methods use 20 (or less) Chamberlain solutions to find solutions of the model equations at 170 (or more) values of α_0. Therefore, any further reduction in the number of Chamberlain solutions used in the two-dimensional methods will only give rise to a small percentage ($< 3\%$) decrease in the previously obtained CPU run-times. Also a reduction in the tolerance will make the error in the 'cheap' solutions noticeable in graphical displays of solutions. We do not

therefore, pursue this issue further.

In conclusion, we can see that this new approach has been very successful, with very large savings in CPU run-times being achieved without loosing any observable accuracy in the solutions.

We now turn our attention to Eckart's equation.

3.4 Eckart's equation

Eckart's equation, which gives an alternative approximation to flow over topography, has non-dimensional form,

$$\frac{d}{dx}\left(U\frac{d\phi_0}{dx}\right) + \kappa^2 U\phi_0 = 0 \ , \tag{3.17}$$

where $\mathrm{Re}(\phi_0(x)e^{-i\sigma t})$ is an approximation to the free surface elevation,

$$U(x) = \frac{1 - e^{-2\lambda\tau H}}{2\lambda\tau} \ , \tag{3.18}$$

and $\kappa = \kappa(x)$ is given by

$$\kappa(x) = \lambda\sqrt{\coth(\lambda\tau H)} \ , \tag{3.19}$$

with the dimensionless parameters λ, α_0 and τ given by

$$\lambda = \frac{\sigma^2 l}{g} = {\alpha_0}^2\tau \quad , \quad \alpha_0 = \frac{\sigma l}{\sqrt{gh_0}} \quad \text{and} \quad \tau = \frac{h_0}{l} \ .$$

The same scaling process used in section 2.5 with the mild-slope equation, has been employed here to convert Eckart's equation given in section 2.4 to the above non-dimensional form.

We notice that the terms in Eckart's equation (3.17) are all given explicitly and so (3.17) is much more computationally attractive than the mild-slope equation (3.1), in which the wave number κ is given implicitly by the dispersion relation (3.3). An advantage of the explicit nature of (3.17) is reflected in the CPU run-times for solving the mild-slope and Eckart equations. Consider the example given in section 3.3.3, where the mild-slope and Eckart equations are solved over the talud with depth profile $H(x) = 1 - \frac{2}{3}x \ \ (0 \le x \le 1)$. Using Chamberlain's method to solve both equations at 170 values of α_0 and τ, the mild-slope equation

had a run-time of 51m55s and Eckart's equation had one of 49m37s. Miles [40] also revived Eckart's equation, when he derived it from a new variational approach. Miles' notes that Eckart's equation conserves wave action but, unlike the mild-slope equation, does not conserve wave energy (except for uniform depth). Miles compares the two approximations through the calculation of reflection from a gently sloping beach of finite offshore depth and finds that Eckart's equation is inferior to the mild-slope equation in its prediction of the amplitude in the reflection problem if the offshore depth is neither shallow or deep. This agrees with the evidence appearing in Fig.3.5 where the reflected amplitudes of the mild-slope and Eckart approximations are compared over a talud with depth profile $H(x) = 1 - \frac{2}{3}x$ $(0 \leq x \leq 1)$. The similarity of the mild-slope and Eckart solutions, depicted in Fig.3.5 for the depth profile $H(x) = 1 - \frac{2}{3}x$ $(0 \leq x \leq 1)$ encouraged attempts to improve Eckart's approximation without compromising its advantageous explicit form.

The depth profiles of concern here are the ones which vary only in the interval $(0, 1)$, and have flat bed depths $H_0 = 1$ for $x \leq 0$ and $H_1 = \frac{h_0}{h_1}$ for $x \geq 1$. Thus, at each value of α_0 and τ in Eckart's equation, the travelling waves on the left(right) of the undulating region have wave numbers $\kappa_0^e(\kappa_1^e)$ defined as

$$\kappa_0^e = \lambda\sqrt{\coth(\lambda\tau H_0)} \quad (\ \kappa_1^e = \lambda\sqrt{\coth(\lambda\tau H_1)}\ )\ .$$

Eckart [15] notes that the positive real root x of the dispersion relation

$$a = x\tanh(x) \tag{3.20}$$

is approximated by

$$x = a\sqrt{\coth(a)} \tag{3.21}$$

with a maximum difference of 5% for any value of a. Thus at each α_0 and τ, the wave number of a left (right) incident wave, κ_0^e (κ_1^e), is not quite the same as the correct wave number, κ_0^m (κ_1^m), used in the mild-slope equation, where κ_0^m (κ_1^m) is the positive real root of the dispersion relation

$${\alpha_0}^2\tau = \kappa_0^m\tanh(\kappa_0^m\tau H_0) \qquad ({\alpha_0}^2\tau = \kappa_1^m\tanh(\kappa_1^m\tau H_1)\ )\ .$$

So, in effect, at each value of α_0 and τ, the mild-slope and Eckart equation are solving different problems. The difference in the mild-slope and Eckart wave

numbers could be resolved by simply using the correct wave number, given by the positive real root of the dispersion relation (3.3) in Eckart's equation instead of Eckart's approximation to it, which is given by (3.19). However, this device defeats the advantage offered by Eckart's equation – that each term in the equation was explicit. So the issue is whether a new, explicit approximation to the positive real root of (3.20) can be generated which is more accurate than (3.21). This is indeed possible.

A direct approach is used in which the solution x of (3.20) is approximated by adding a small correction term to (3.21). Thus x is approximated in the form

$$x = x_0 + x_1$$

where $x_0 = a\sqrt{\coth(a)}$ and x_1 is a small correction term. Substituting for x in (3.20) gives

$$a = (x_0 + x_1)\tanh(x_0 + x_1) \ ,$$

that is,

$$a = (x_0 + x_1)\left[\frac{\tanh(x_0) + \tanh(x_1)}{1 + \tanh(x_0)\tanh(x_1)}\right] \ . \tag{3.22}$$

Then, using the expansion $\tanh(x_1) = x_1 + O(x_1^3)$,

$$\begin{aligned}
& a(1 + \tanh(x_0)\tanh(x_1)) \\
&= a + a\tanh(x_0)\tanh(x_1) \\
&= a + (x_0 + x_1)\left[\frac{\tanh(x_0) + \tanh(x_1)}{1 + \tanh(x_0)\tanh(x_1)}\right]\tanh(x_0)\tanh(x_1) \\
&= a + (x_0 + x_1)\left[\frac{\tanh(x_0) + x_1 + O(x_1^3)}{1 + [x_1 + O(x_1^3)]\tanh(x_0)}\right]\tanh(x_0)[x_1 + O(x_1^3)] \\
&= a + [x_0\tanh^2(x_0)]x_1 + O(x_1^2) \ ,
\end{aligned}$$

and

$$(x_0 + x_1)[\tanh(x_0) + \tanh(x_1)] = x_0\tanh(x_0) + x_1(x_0 + \tanh(x_0)) + O(x_1^2) \ .$$

Thus (3.22) becomes

$$a + [x_0\tanh^2(x_0)]x_1 = x_0\tanh(x_0) + x_1(x_0 + \tanh(x_0)) + O(x_1^2) \ ,$$

and neglecting second and higher order terms in x_1 (as x_1 is assumed to be small) gives

$$x_1 = \frac{a - x_0\tanh(x_0)}{x_0 + \tanh(x_0) - x_0\tanh^2(x_0)} \ .$$

Thus, the new two-term explicit approximation to (3.20) is given by

$$\begin{aligned} x &= x_0 + x_1 \\ &= x_0 + \frac{a - x_0 \tanh(x_0)}{x_0 + \tanh(x_0) - x_0 \tanh^2(x_0)} \ , \end{aligned}$$

which simplifies to

$$x = \frac{x_0^2 \mathrm{sech}^2(x_0) + a}{x_0 \mathrm{sech}^2(x_0) + \tanh(x_0)} \ . \tag{3.23}$$

Computations have shown that (3.23) gives the solution x of (3.20) to machine accuracy for $a > 3.1$, and for $0 < a < 3.1$, the maximum difference is 0.04%. Thus (3.23) is a new explicit approximation to (3.20) which is a significant improvement on (3.21).

We shall now replace the function $\kappa = \kappa(x)$ defined by (3.19) by

$$\kappa(x) = \frac{1}{\tau H} \left(\frac{[v \mathrm{sech}(v)]^2 + \lambda \tau H}{v \mathrm{sech}^2(v) + \tanh(v)} \right) \ , \tag{3.24}$$

where $v = v(x) = \lambda \tau H \sqrt{\coth(\lambda \tau H)}$, in Eckart's equation, and call the resulting equation the new Eckart equation. We now find the solution of the new Eckart equation for an incident wave of unit amplitude from $x = -\infty$ over the depth profile given by

$$H(x) = 1 - \frac{2}{3}x \qquad (0 \leq x \leq 1) \ .$$

We use the streamlined two-dimensional method to solve this problem with α_0 taking values between 0.05 and 8.5 at intervals of 0.05 (with τ given at each value of α_0 by $\tau = \sqrt{0.6}\alpha_0$). We choose again the tolerance in the error to be a minimum of 2.s.f. accuracy in $|R_k|$ and $|T_k|$ $(k = 1, 2)$. The amplitude of the reflected wave given by the new Eckart equation is depicted in Fig.3.8, along with the corresponding results from the mild-slope and Eckart's equations. We see that the peaks and troughs of the reflected amplitudes predicted by the mild-slope and new Eckart equations are almost in line. The size of the reflected amplitude predicted by the new Eckart equation is also an increase on that given by Eckart's equation. However, the reflected amplitude given by the new Eckart equation is still not as large as that given by the mild-slope equation. The difference in results from both is now due to the difference of the mild-slope and Eckart U functions. As yet, no approximation has been found, such as the one used in conjunction with the wave number functions, that can rectify this difference. The new Eckart

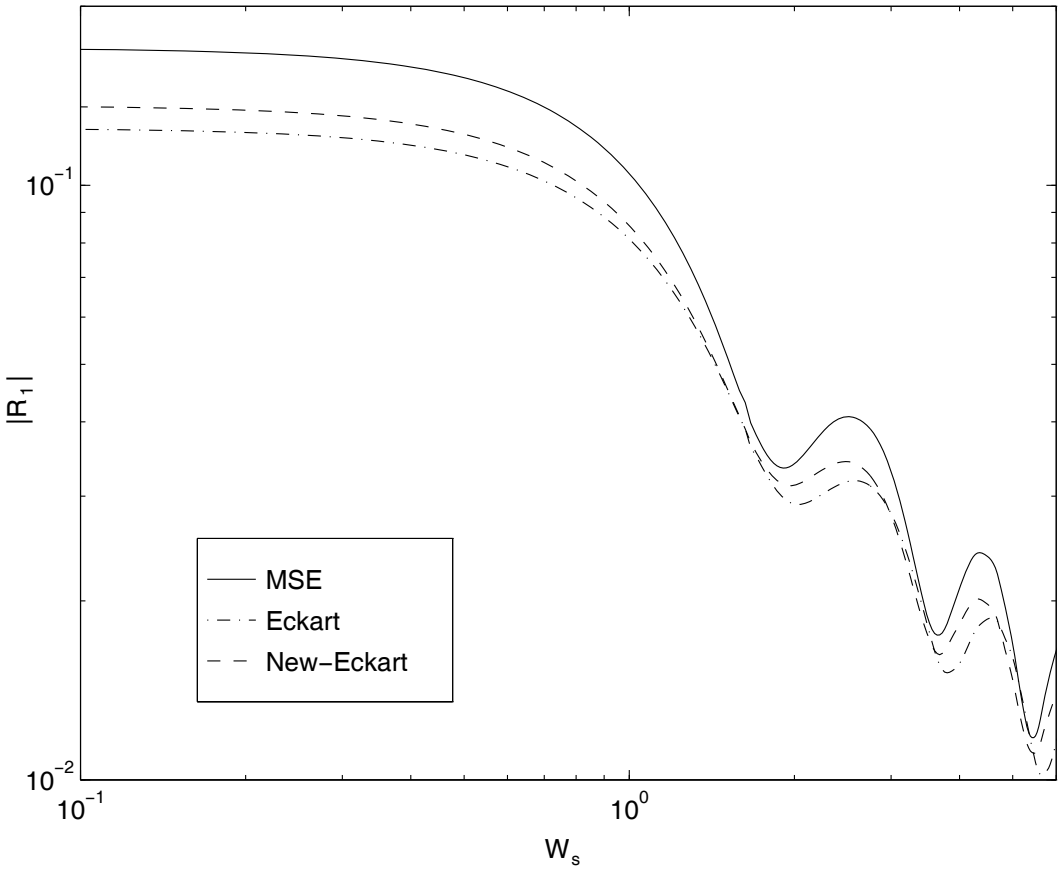

Figure 3.8: Reflected amplitude over the depth profile $H(x) = 1 - 2/3x$ $(0 \leq x \leq 1)$.

equation is therefore an amalgamation of two approximations. The approach most likely to produce the U corresponding to the new κ (3.24) is to use the variational principle of Miles [40] with the trial function that generates the κ function as given by (3.24). However, such a trial function has not as yet been found.

Other attempts have been undertaken to overcome the inferiority in the reflected amplitude of Eckart's equation for the problem over a depth profile given by

$$H(x) = 1 - \frac{2}{3}x \qquad (0 \leq x \leq 1) \ .$$

In Eckart's original equation (3.17) – (3.19), the manoeuvre of employing (3.24) instead of (3.19) to ensure that the Eckart and mild-slope wave numbers are the same at α_0 and τ, was replaced by using a variety of artificial bed shapes. An approach of this type would also affect the Eckart U function (3.18), as it depends

on the bed shape and so it was hoped that this device would bring the reflected amplitude into line. The flat bed depths for the Eckart problem in $0 \leq x$ and $x \geq 1$ were chosen so that the Eckart and mild-slope wave numbers were identical at each α_0 and τ over these flat regions. This guaranteed that at each value of α_0 and τ, the mild-slope and Eckart problems had the same incident wave. A variety of choices of depth profile for joining the two flat bed regions together were used. However, none of the results over any of the artificial beds caused the reflected amplitude predicted by Eckart's approximation to be any closer to that predicted by the mild-slope approximation than the reflected amplitude obtained using (3.24) in Eckart's approximation instead of (3.19).

Employing (3.24) in Eckart's equation ensures that this approximation has practically the correct wave number at each value of α_0 and τ, and thus the mild-slope and Eckart equations have practically identical solutions over a flat bed. Currently, this is the best possible improvement to Eckart's equation, but it still has an inferior reflected amplitude problem as compared with the MSE. The discovery of a trial function for the variational principle by Miles [40] which delivers the κ function (3.24) and a new corresponding U function, should remove this problem.

A final point of interest in Eckart's approximation is the method by which it was derived. Eckart obtained his equation (2.24) by firstly transforming the linear boundary-value problem (2.13) for the time-independent velocity potential ϕ into an integral equation. He then discarded, without justification, an assumed small integral and converted the resulting approximate problem back to a differential equation. It was hoped that an investigation into this method would yield an error bound between the full linear integral equation and Eckart's approximate integral equation. However, the complexity of the discarded term (an integral whose integrand contained a differential operator amongst its terms) stopped this line of approach. So an error bound which shows how accurately the mild-slope, Eckart and shallow water models approximate ϕ still does not exist.

In this section, we have seen that for wave scattering problems, Eckart's approximation gives an inferior reflected amplitude compared with that given by the mild-slope approximation. Currently, the best possible improvement to Eckart's

approximation is effected by replacing the κ function (3.19) in Eckart's equation by (3.24). The new equation still gives a slightly inferior reflected amplitude than that given by the MSE. The very accurate, explicit approximation (3.23) to the root of the dispersion relation (3.20) has never been seen before, and is an excellent first term to use in an iteration method to give machine accurate solutions of (3.20). (See Newman [44] for details of such iterative methods.)

3.5 Symmetry Properties

Here, certain intrinsic properties of a particular type of second-order differential system, referred to as symmetry properties, are derived. When the second-order system is specified to be one of the model equations, mild-slope, Eckart or shallow water, the well-known symmetry properties of the reflection and transmission coefficients are found. These properties were first derived by Newman [41] for the full linear problem. More recently, Chamberlain [8] used integral equation methods to derive these properties for the mild-slope approximation.

Consider the general second-order differential equation in the form

$$-(L\phi)(x) + \mu r(x)\phi(x) = m(x) \ , \tag{3.25}$$

where the differential operator L is defined by

$$(L\phi)(x) = -(p(x)\phi'(x))' + q(x)\phi(x) \ , \tag{3.26}$$

and where $p,\ q,\ r$ and m are continuous, real-valued functions, p is differentiable and μ is a given real parameter; the prime denotes differentiation with respect to x. Suppose that ϕ satisfies the boundary conditions

$$\begin{aligned} a_0\phi(0) + b_0\phi'(0) &= c_0 \ , \\ a_1\phi(1) + b_1\phi'(1) &= c_1 \ , \end{aligned} \tag{3.27}$$

where the constants $a_i,\ b_i$ and $c_i\ (i = 0, 1)\ \in \mathbb{C}$.

Now suppose that ψ satisfies (3.25) together with the boundary conditions

$$\begin{aligned} e_0\psi(0) + f_0\psi'(0) &= g_0 \ , \\ e_1\psi(1) + f_1\psi'(1) &= g_1 \ , \end{aligned} \tag{3.28}$$

where the constants $e_i,\ f_i$ and $g_i\ (i = 0, 1)\ \in \mathbb{C}$.

Then an application of Green's theorem on $[0, 1]$, that is,

$$\int_0^1 (\psi L\phi - \phi L\psi)\ dx = \Big[p(\phi\psi' - \psi\phi')\Big]_0^1\ ,$$

yields

$$\begin{aligned}\int_0^1 m(\phi - \psi)\ dx\ &=\ \Big[p(\phi\psi' - \psi\phi')\Big]_0^1\ ,\\ &=\ p(1)\left\{\phi(1)\psi(1)\left[\frac{a_1}{b_1} - \frac{e_1}{f_1}\right] + \frac{g_1}{f_1}\phi(1) - \frac{c_1}{b_1}\psi(1)\right\}\\ &\quad -p(0)\left\{\phi(0)\psi(0)\left[\frac{a_0}{b_0} - \frac{e_0}{f_0}\right] + \frac{g_0}{f_0}\phi(0) - \frac{c_0}{b_0}\psi(0)\right\}. \quad (3.29)\end{aligned}$$

If $m(x)$ is set identically to zero, then (3.29) gives relations between the end-point values of solutions of the differential equation (3.25)

We are considering the scattering of plane harmonic waves normally incident on a given scaled bed profile $H = H(x)$, that varies only in some finite interval of x, so that

$$H(x) = \begin{cases} H_0 & \forall x \le 0\ , \\ H_1 & \forall x \ge 1\ , \end{cases}$$

where H_0 and H_1 are constants for a given problem, and $H(x)$ is assumed to be continuous on $(-\infty, \infty)$. In these circumstances, all three model equations, mild-slope, Eckart and shallow water, can be written in the general form

$$(U\phi_0')' + \kappa^2 U\phi_0 = 0\ , \qquad (3.30)$$

where $Re(\phi_0(x)e^{-i\sigma t})$ is an approximation to the free surface elevation. The functions $U = U(x)$ and $\kappa = \kappa(x)$ are as previously defined in each of the model equation cases. The differential equation (3.30) reduces to $\phi_0'' + {\kappa_0}^2\phi_0 = 0\ \ \forall x \le 0$ and to $\phi_0'' + {\kappa_1}^2\phi_0 = 0\ \ \forall x \ge 1$, where $\kappa_0 = \kappa(0)$ and $\kappa_1 = \kappa(1)$. Therefore, as in Chapter 2, we take

$$\phi_0(x) = \begin{cases} A^- e^{i\kappa_0 x} + B^- e^{-i\kappa_0 x} & \forall x \le 0\ , \\ A^+ e^{-i\kappa_1 x} + B^+ e^{i\kappa_1 x} & \forall x \ge 1\ , \end{cases} \qquad (3.31)$$

where $A^{\pm}$ denotes the prescribed amplitudes of the incident plane waves propagating from $x = \pm\infty$ respectively and $B^{\pm}$ denotes the unknown amplitudes of the

scattered waves propagating towards $x = \pm\infty$ respectively. As already noted in Chapter 2, the reflection and transmission coefficients for an incident wave from the left ($A^+ = 0$) are defined by

$$R_1 = \frac{B^-}{A^-} \qquad \text{and} \qquad T_1 = \frac{B^+}{A^-} \tag{3.32}$$

and those for an incident wave from the right ($A^- = 0$) are defined by

$$R_2 = \frac{B^+}{A^+} \qquad \text{and} \qquad T_2 = \frac{B^-}{A^+} \tag{3.33}$$

Using the equations (3.31) and enforcing the continuity of ϕ_0 and ϕ_0' at $x = 0$ and $x = 1$ gives the boundary conditions

$$\begin{aligned} \phi_0'(0) + i\kappa_0\phi_0(0) &= 2A^- i\kappa_0 \ , \\ \phi_0'(1) - i\kappa_1\phi_0(1) &= -2A^+ i\kappa_1 e^{-i\kappa_1} \ . \end{aligned} \tag{3.34}$$

Choosing $p,\ q,\ r$ and m of the differential equation (3.25) to be the corresponding terms in differential equation (3.30), that is, $p = U,\ q = \kappa^2 U,\ r = 0$ and $m = 0$, reduces (3.29) to the identity

$$\begin{aligned} 0 \ = \ & U(1)\left\{\phi(1)\psi(1)\left[\frac{a_1}{b_1} - \frac{e_1}{f_1}\right] + \frac{g_1}{f_1}\phi(1) - \frac{c_1}{b_1}\psi(1)\right\} \\ & - U(0)\left\{\phi(0)\psi(0)\left[\frac{a_0}{b_0} - \frac{e_0}{f_0}\right] + \frac{g_0}{f_0}\phi(0) - \frac{c_0}{b_0}\psi(0)\right\} \ . \end{aligned} \tag{3.35}$$

Now the symmetry relations of the reflection and transmission coefficients can be easily found. Firstly, choose ϕ to be the solution of (3.30) and (3.34) for an incident wave of unit amplitude from the left (so $A^- = 1,\ A^+ = 0$) and choose ψ to be the complex conjugate of ϕ. Hence ψ satisfies (3.30) and the constants in the boundary conditions (3.27) and (3.28) satisfied by ϕ and ψ respectively are given by

$$\begin{aligned} a_0 = i\kappa_0 = \overline{e}_0 \quad &, \quad b_0 = 1 = f_0 \ , \quad c_0 = 2i\kappa_0 = \overline{g}_0 \quad , \\ a_1 = -i\kappa_1 = \overline{e}_1 \quad &, \quad b_1 = 1 = f_1 \ , \qquad c_1 = 0 = \overline{g}_1 \quad . \end{aligned} \tag{3.36}$$

and from (3.31) and (3.32) we see that the functions ϕ and ψ have end-point values

$$\phi(0) = 1 + R_1 = \overline{\psi(0)} \quad \text{and} \quad \phi(1) = T_1 e^{i\kappa_1} = \overline{\psi(1)} \ . \tag{3.37}$$

Substituting (3.36) and (3.37) into the identity (3.35) gives

$$0 = U(1)\left(-2i\kappa_1 T_1 \overline{T}_1\right) - U(0)\left(2i\kappa_0(R_1\overline{R}_1 - 1)\right) \ ,$$

which is easily rearranged to give the relation

$$|R_1|^2 + \frac{\kappa_1 U(1)}{\kappa_0 U(0)}|T_1|^2 = 1 \ . \tag{3.38}$$

For the same ϕ, choose ψ to be the solution of (3.30) and (3.34) for an incident wave of unit amplitude from the right (so $A^- = 0,\ A^+ = 1$). This results in the constants in the boundary condition (3.28) satisfied by ψ to be redefined as

$$\begin{aligned} e_0 = i\kappa_0 \quad &, \quad f_0 = 1 \ , \quad g_0 = 0 \quad , \\ e_1 = -i\kappa_1 \quad &, \quad f_1 = 1 \ , \quad g_1 = -2i\kappa_1 e^{-i\kappa_1} \quad . \end{aligned} \tag{3.39}$$

ψ now has end-point values given by

$$\psi(0) = T_2 \quad \text{and} \quad \psi(1) = e^{-i\kappa_1} + R_2 e^{i\kappa_1} \ . \tag{3.40}$$

Substituting (3.39) and (3.40) into the identity (3.35) gives the relation

$$\kappa_1 U(1) T_1 = \kappa_0 U(0) T_2 \ . \tag{3.41}$$

Now choose ψ to be the complex conjugate of the solution of (3.30) and (3.34) for an incident wave of unit amplitude from the right. This redefines the constants of (3.28) to be the complex conjugate of those defined by (3.39). Similarly, the end-point values of ψ are just the complex conjugate of those defined by (3.40). Substituting into the identity (3.35) results in the relation

$$\kappa_1 U(1) \overline{R}_2 T_1 = -\kappa_0 U(0) \overline{T}_2 R_1 \ . \tag{3.42}$$

The final symmetry relation is derived by choosing ϕ to be the solution of (3.30) and (3.34) for an incident wave of unit amplitude from the right and retaining the most recent ψ. The constants in the boundary conditions (3.27) satisfied by ϕ are given by

$$\begin{aligned} a_0 = i\kappa_0 \quad &, \quad b_0 = 1 \ , \quad c_0 = 0 \quad , \\ a_1 = -i\kappa_1 \quad &, \quad b_1 = 1 \ , \quad c_1 = -2i\kappa_1 e^{-i\kappa_1} \quad . \end{aligned}$$

ϕ now has end-point values given by

$$\phi(0) = T_2 \quad \text{and} \quad \phi(1) = e^{-i\kappa_1} + R_2 e^{i\kappa_1} \ .$$

Substituting into the identity (3.35) gives the final symmetry relation

$$|R_2|^2 + \frac{\kappa_0 U(0)}{\kappa_1 U(1)}|T_2|^2 = 1 \ . \tag{3.43}$$

Therefore, the reflection and transmission given by the three approximations satisfy these symmetry relations, with the κ and U functions defined according to the approximation used.

These symmetry relations can also be derived within the framework of integral equations using an integral equation form of the identity (3.35) with the same choices of input functions. Chamberlain [8] has used this approach and it is briefly reiterated here.

From Chapter 2 we recall the integral equation (2.36), namely,

$$\zeta_j(x) = \hat{a}_j e^{i\kappa_0 x} + \hat{b}_j e^{-i\kappa_0 x} - \frac{i}{2\kappa_0}\int_0^1 e^{i\kappa_0|x-t|}\rho(t)\zeta_j(t)\,dt \quad (j = 1, 2), \tag{3.44}$$

where the 1,2 subscripts have been introduced to denote incident wave direction from the left or right respectively. Therefore from Chapter 2 we see that the constants $\hat{a}_j$ and $\hat{b}_j$ $(j = 1, 2)$ are defined by

$$\begin{aligned} \hat{a}_1 &= 1 - \left(\frac{iU'(0+)}{4\kappa_0 U(0)}\right)\zeta_1(0) \ , \\ \hat{b}_1 &= \left(\frac{iU'(1-)}{4\kappa_0 U(1)} + \frac{\kappa_0 - \kappa_1}{2\kappa_0}\right) e^{i\kappa_0}\zeta_1(1) \ , \end{aligned} \tag{3.45}$$

$$\begin{aligned} \hat{a}_2 &= -\left(\frac{iU'(0+)}{4\kappa_0 U(0)}\right)\zeta_2(0) \ , \\ \hat{b}_2 &= e^{i(\kappa_0-\kappa_1)}\frac{\kappa_1}{\kappa_0}\sqrt{\frac{U(1)}{U(0)}} + \left(\frac{iU'(1-)}{4\kappa_0 U(1)} + \frac{\kappa_0 - \kappa_1}{2\kappa_0}\right) e^{i\kappa_0}\zeta_2(1) \ . \end{aligned} \tag{3.46}$$

It follows that $\zeta_j \in L_2(0,1)$ satisfies

$$\zeta_j = \hat{a}_j f^+ + \hat{b}_j f^- + KP\zeta_j \qquad (j = 1, 2) \ , \tag{3.47}$$

where the operators K and P are defined by

$$(K\zeta)(x) = \frac{-i}{2\kappa_0}\int_0^1 e^{i\kappa_0|x-t|}\zeta(t)\,dt \qquad \text{and} \qquad (P\zeta)(x) = \rho(x)\zeta(x) \ ,$$

and all the other constants, functions and operators are as defined in Chapter 2 . Noting that if ζ satisfies the differential equation and boundary conditions that give rise to the ζ integral equation (3.44), namely,

$$\zeta'' \ + \ {\kappa_0}^2\zeta \ = \ \rho\zeta \ ,$$

and

$$\begin{aligned} \zeta'(0) + i\kappa_0\zeta(0) &= 2i\kappa_0\hat{a} \ , \\ \zeta'(1) - i\kappa_0\zeta(1) &= -2i\kappa_0 e^{-i\kappa_0}\hat{b} \ , \end{aligned}$$

then $\overline{\zeta}$ also satisfies the same differential equation and the complex conjugate of the boundary conditions. Therefore, $\overline{\zeta}$ satisfies the integral equation (3.44) with $\hat{a}_j$ and $\hat{b}_j$ replaced by $\tilde{a}_j$ and $\tilde{b}_j$, where

$$\begin{aligned} \tilde{a}_1 &= -1 + \left(1 - \frac{iU'(0+)}{4\kappa_0 U(0)}\right)\overline{\zeta_1(0)} \ , \\ \tilde{b}_1 &= \left(1 + \frac{iU'(1-)}{4\kappa_0 U(1)} - \frac{\kappa_0 - \kappa_1}{2\kappa_0}\right) e^{i\kappa_0}\overline{\zeta_1(1)} \ , \end{aligned} \tag{3.48}$$

$$\begin{aligned} \tilde{a}_2 &= \left(1 - \frac{iU'(0+)}{4\kappa_0 U(0)}\right) \ \overline{\zeta_2(0)} \ , \\ \tilde{b}_2 &= -e^{i(\kappa_0+\kappa_1)}\frac{\kappa_1}{\kappa_0}\sqrt{\frac{U(1)}{U(0)}} + \left(1 + \frac{iU'(1-)}{4\kappa_0 U(1)} - \frac{\kappa_0 - \kappa_1}{2\kappa_0}\right) e^{i\kappa_0}\overline{\zeta_2(1)} \ . \end{aligned} \tag{3.49}$$

Now suppose that $\psi_j \ \in \ L_2(0,1)$ $(j = 1,2)$ satisfies

$$\psi_j = g_j + KP\psi_j \qquad (j = 1,2) \ ,$$

where $g_j = \alpha_j f^+ + \beta_j f^-$ for some α_j and β_j $(j = 1,2)$ and consider the functional S given by

$$-2i\kappa_0 S(\psi_1, \psi_2) = (\psi_1, P\overline{g}_2) - (\psi_2, P\overline{g}_1) \ .$$

We denote the adjoint of an operator T by T^*. Then, as $P = P^*$, we see that

$$\begin{aligned} -2i\kappa_0 S(\psi_1, \psi_2) &= (\psi_1, P(I - K^*P)\overline{\psi}_2) - (\psi_2, P(I - K^*P)\overline{\psi}_1) \\ &= (P(I - KP)\psi_1, \overline{\psi}_2) - (P(I - KP)\psi_1, \overline{\psi}_2) \\ &= 0 \ . \end{aligned}$$

Substituting $x = 0$ and $x = 1$ into the integral equation satisfied by ψ_j $(j = 1, 2)$ yields

$$\frac{i}{2\kappa_0}\int_0^1 f^+(t)\rho(t)\psi_j(t)\,dt = \alpha_j + \beta_j - \psi_j(0)\ ,$$
$$\frac{i}{2\kappa_0}\int_0^1 f^-(t)\rho(t)\psi_j(t)\,dt = \alpha_j + \beta_j e^{-2i\kappa_0} - e^{-i\kappa_0}\psi_j(1)\ ,$$

and hence it follows that

$$S(\psi_1, \psi_2) = \alpha_1\psi_2(0) - \alpha_2\psi_1(0) + (\beta_1\psi_2(1) - \beta_2\psi_1(1))e^{-i\kappa_0} = 0\ . \tag{3.50}$$

This identity is equivalent to the identity (3.35) which was derived within the framework of differential equations. Before the symmetry relations are rederived, the definitions of the reflection and transmission coefficients, as given previously in Chapter 2, are restated here for convenience as follows:

$$\begin{aligned} R_1 &= \zeta_1(0) - 1\ , \\ T_1 &= \zeta_1(1)e^{-i\kappa_1}\sqrt{\frac{U(0)}{U(1)}}\ . \end{aligned} \tag{3.51}$$

$$\begin{aligned} R_2 &= \zeta_2(1)e^{-i\kappa_1}\sqrt{\frac{U(0)}{U(1)}} - e^{-2i\kappa_1}\ , \\ T_2 &= \zeta_2(0)\ , \end{aligned} \tag{3.52}$$

where the subscripts 1, 2 distinguish between waves incident from the left or the right respectively.

Substituting $\psi_1 = \zeta_1$ (and therefore $\alpha_1 = \hat{a}_1\ ,\ \beta_1 = \hat{b}_1$) and $\psi_2 = \overline{\zeta_1}$ (and therefore $\alpha_2 = \tilde{a}_1\ ,\ \beta_2 = \tilde{b}_1$) in S gives

$$S(\zeta_1, \overline{\zeta}_1) = \overline{\zeta_1(0)} + \zeta_1(0) - |\zeta_1(0)|^2 - \frac{\kappa_1}{\kappa_0}|\zeta_1(1)|^2 = 0\ ,$$

and employing (3.51) reduces this to the symmetry relation (3.38) , namely,

$$|R_1|^2 + \frac{\kappa_1 U(1)}{\kappa_0 U(0)}|T_1|^2 = 1\ .$$

By the same procedure

$$\begin{aligned} S(\zeta_1, \zeta_2) &= 0 \quad \text{implies} \quad \kappa_1 U(1)T_1 = \kappa_0 U(0)T_2\ , \\ S(\zeta_1, \overline{\zeta_2}) &= 0 \quad \text{implies} \quad \kappa_1 U(1)\overline{R}_2 T_1 = -\kappa_0 U(0)\overline{T}_2 R_1\ , \\ S(\zeta_2, \overline{\zeta_2}) &= 0 \quad \text{implies} \quad |R_2|^2 + \frac{\kappa_0 U(0)}{\kappa_1 U(1)}|T_2|^2 = 1\ . \end{aligned}$$

In the final part of this section, we need to recall the rank two system of equations defined in Chapter 2. This relates $\zeta_j(0)$ and $\zeta_j(1)$ $(j = 1, 2)$, the end point values of the solutions ζ_j $(j = 1, 2)$ of the integral equation (3.44) with the inner products (χ_j, Pf_k) $(j, k = 1, 2)$. The χ_j $(j = 1, 2) \in L_2(0, 1)$ are the solutions of the real valued integral equations

$$(I - LP)\chi_j = f_j \qquad (j = 1, 2) \ ,$$

where I is the identity operator and the operators L and P are defined by

$$(L\chi)(x) = \frac{1}{2\kappa_0} \int_0^1 \sin(\kappa_0 |x - t|)\, \chi(t)\, dt \qquad \text{and} \qquad (P\chi)(x) = \rho(x)\chi(x) \ ,$$

and where the free terms are defined by $f_1(x) = \cos(\kappa_0 x)$ and $f_2(x) = \sin(\kappa_0 x)$. In Chapter 2 and the first part of Chapter 3 , we have used variational techniques to approximate the values of these inner products. For convenience we give the rank two system of equations here, namely,

$$\begin{aligned} &\left(\begin{pmatrix} b_2 & b_3 \\ b_5 & b_6 \end{pmatrix} - i \begin{pmatrix} B_1 & B_2 \\ \overline{B}_2 & B_1 \end{pmatrix} \begin{pmatrix} c_5 - b_2 & c_6 - b_3 \\ c_2 - b_5 & c_3 - b_6 \end{pmatrix} \right) \begin{pmatrix} \zeta_j(0) \\ \zeta_j(1) \end{pmatrix} \\ &= - \begin{pmatrix} b_1 \\ b_4 \end{pmatrix} + i \begin{pmatrix} B_1 & B_2 \\ \overline{B}_2 & B_1 \end{pmatrix} \begin{pmatrix} c_4 - b_1 \\ c_1 - b_4 \end{pmatrix} \qquad (j = 1, 2) \ , \end{aligned} \tag{3.53}$$

where the values of known constants b_i and c_i $(i = 1, \ldots, 6)$ are chosen according to whether ζ_j corresponds to the solution of the integral equation (3.44) for an incident wave from the left or right, or the complex conjugate of the solution of (3.44) for an incident wave from the left or right (as seen earlier in this section), and

$$B_1 = \tfrac{1}{2}(A_{11} + A_{22}) \ \text{ and } \ B_2 = \tfrac{1}{2}(A_{11} + 2iA_{12} - A_{22})$$

and

$$A_{jk} = \frac{1}{2\kappa_0}(\chi_j, Pf_k) \qquad (j, k = 1, 2).$$

Now the reflection and transmission coefficients are defined by (3.51) and (3.52) in terms of $\zeta_j(0)$ and $\zeta_j(1)$ $(j = 1, 2)$ and therefore , through the rank two system of equations (3.53), in terms of the inner products (χ_j, Pf_k) $(j, k = 1, 2)$. When calculating the reflection and transmission coefficients, it was noticed that

even by using poor approximations to the inner products (χ_j, Pf_k) $(j,k=1,2)$, the resulting reflection and transmission coefficients still satisfied the symmetry relations. This property is explained by the following theorem.

THEOREM 3.1 *The reflection and transmission coefficients defined by (3.51) and (3.52) satisfy the symmetry relations (3.38), (3.41), (3.42), (3.43) for any approximation to the values of the inner products* (χ_j, Pf_k) $(j,k=1,2)$.

Proof:

The rank two system of equations (3.53) is used to express $\zeta(0)$ and $\zeta(1)$, and thus the reflection and transmission coefficients, in terms of the inner products (χ_j, Pf_k) $(j,k=1,2)$.

Two approaches can now be used. The direct approach is to invert the rank two system (3.53), and substitute the complicated resulting expressions for R_i and T_i $(i=1,2)$ into the symmetry relations. After some long, but simple, algebraic manipulation one finds that all the terms containing these inner products cancel. Therefore, whatever values these inner products take, the resulting reflection and transmission coefficients, which are defined in terms of them, will always satisfy the symmetry relations.

A second, more illuminating approach follows from rewriting the rank two system in three parts, which are given by

$$\begin{pmatrix} d_j \\ e_j \end{pmatrix} = i \begin{pmatrix} B_1 & B_2 \\ \overline{B}_2 & B_1 \end{pmatrix} \begin{pmatrix} \alpha_j - d_j \\ \beta_j - e_j \end{pmatrix} \qquad (j=1,2)\ , \tag{3.54}$$

where

$$\begin{pmatrix} d_j \\ e_j \end{pmatrix} = \begin{pmatrix} b_2 & b_3 \\ b_5 & b_6 \end{pmatrix} \begin{pmatrix} \zeta_j(0) \\ \zeta_j(1) \end{pmatrix} + \begin{pmatrix} b_1 \\ b_4 \end{pmatrix} \qquad (j=1,2)\ , \tag{3.55}$$

and

$$\begin{pmatrix} \alpha_j \\ \beta_j \end{pmatrix} = \begin{pmatrix} c_5 & c_6 \\ c_2 & c_3 \end{pmatrix} \begin{pmatrix} \zeta_j(0) \\ \zeta_j(1) \end{pmatrix} + \begin{pmatrix} c_4 \\ c_1 \end{pmatrix} \qquad (j=1,2)\ . \tag{3.56}$$

A substitution of (3.55) and (3.56) into (3.54) yields the original rank two system (3.53). For ease of notation, we write (3.54) as

$$\underline{x}_j = iW\underline{y}_j \qquad (j=1,2)\ , \tag{3.57}$$

where

$$\underline{x}_j = \begin{pmatrix} d_j \\ e_j \end{pmatrix} \ , \ \underline{y}_j = \begin{pmatrix} \alpha_j - d_j \\ \beta_j - e_j \end{pmatrix} \text{ and } W = \begin{pmatrix} B_1 & B_2 \\ \overline{B}_2 & B_1 \end{pmatrix} \ .$$

Now as B_1 is real, $W^* = W$, where $*$ denotes the conjugate transpose.
It follows that

$$\underline{y}_2^* \underline{x}_1 = \underline{y}_2^* (iW\underline{y}_1) = (-i\underline{y}_1^* W^* \underline{y}_2)^* = (-i\underline{y}_1^* W \underline{y}_2)^* = (-\underline{y}_1^* \underline{x}_2)^* = -\underline{x}_2^* \underline{y}_1 \ ,$$

and so the identity

$$\underline{y}_2^* \underline{x}_1 + \underline{x}_2^* \underline{y}_1 = 0 \tag{3.58}$$

results. Recapping the above procedure, the two forms of (3.57) have been used to eliminate the W matrix to give the identity (3.58). The inner products (χ_j, Pf_k) $(j,k = 1,2)$ only appear in the W matrix which only occurs in equation (3.57) of our breakdown of the rank two system. So now an identity (3.58), very similar to the previous identity (3.50) found in our integral equation framework, has been derived that relates $\zeta_j(0)$ and $\zeta_j(1)$ $(j = 1,2)$ and is independent of the inner products. Therefore this identity will always be satisfied no matter what values the inner products take. Finally the symmetry relations are found by using similar choices of ζ_j $(j = 1,2)$ in (3.58) to those used earlier. □

One consequence of this theorem is that the symmetry relations can no longer be used as a method of checking the accuracy of the computed reflection and transmission coefficients.

We cannot prove from the Green's identity approach that the reflection and transmission coefficients given by an approximation to the solution of the boundary -value problem (3.30) and (3.34) automatically satisfy the symmetry relations. This is because this approach relies on the fact that the right-hand side of the differential equation (3.30) is zero to derive the symmetry relations. An approximation to the solution of the BVP (3.30) and (3.34) will not satisfy the DE (3.30) exactly and so the right-hand side of (3.30) will no longer be zero. Chamberlain and Porter [10] consider this problem using a different approach. They prove that for an approximation to the full linear wave scattering problem of the form (3.30) and (3.34), the reflection and transmission coefficients given by any approximation to the solution of the BVP (3.30) and (3.34) automatically satisfy

the symmetry relations. It follows that the symmetry relations are an intrinsic part of the problem rather than of its exact solution, in the sense that they are always satisfied whatever the accuracy of the solution.

In this chapter, several extensions to the work appearing in Chamberlain [7] & [8] have been presented. A new integral equation method has been developed which solves the mild-slope, Eckart and linearised shallow water equations over a range of their parameters in less than one half of the CPU time required by Chamberlain's [7] integral equation procedure. Eckart's approximation has been investigated and improved and, as a by-product, a new, explicit and very accurate approximation to the solution of the dispersion relation has also been found. Finally, after rederiving the symmetry relations of the reflection and transmission coefficients of these approximations, we have shown that these coefficients satisfy the symmetry relations even when they are inaccurately calculated, an unexpected property.

Chapter 4

A new approximation to wave scattering

In this chapter, a new approximation to the full linear wave scattering problem is derived. A Galerkin approach is used to derive an approximation to the time-independent velocity potential ϕ which takes account of decaying wave modes as well as progressive wave modes. The present approach uses an n-term approximation based on the propagating wave mode and the first $(n-1)$ decaying wave modes over a flat bed. If none of the decaying wave mode terms are used and if we discard terms that are second-order on the basis of the mild-slope assumption $|\nabla h| \ll kh$, where h is the undisturbed fluid depth and k is the corresponding wave number, then this approach reduces to the mild-slope approximation. The extended approximation is then tested on a selection of beds of varying steepness and the results are compared with the corresponding results given by the mild-slope approximation.

4.1 A Galerkin approximation method

Recall from Chapter 2, that the time-independent velocity potential ϕ satisfies

$$\tilde{\nabla}^2\phi = 0 \qquad -h < z < 0 \,, \tag{4.1}$$

$$\frac{\partial\phi}{\partial z} - \nu\phi = 0 \qquad \text{on } z = 0 \,, \tag{4.2}$$

$$\frac{\partial\phi}{\partial z} + \nabla h \,.\, \nabla\phi = 0 \qquad \text{on } z = -h(x,y) \,, \tag{4.3}$$

where $\tilde{\nabla} = (\frac{\partial}{\partial x}, \frac{\partial}{\partial y}, \frac{\partial}{\partial z})$ and $\nabla = (\frac{\partial}{\partial x}, \frac{\partial}{\partial y})$. We also require additional conditions on lateral boundaries or a radiation condition if the fluid extends to infinity to completely specify ϕ. For the moment, we do not concern ourselves with these additional conditions as our initial aim is to reduce the dimension of the boundary-value problem for ϕ by approximating its dependence on the z co-ordinate. This is achieved via a direct application of the classical Galerkin method.

We seek a weak solution $\xi \approx \phi$ of (4.1) – (4.3) in the sense that the residual $\tilde{\nabla}^2\xi$ is required to be orthogonal to a given function ψ. In other words, we require

$$\iint_D \left(\int_{-h}^{0} \psi \tilde{\nabla}^2 \xi dz \right) dxdy \ = 0 \ ,$$

where D can be any domain in the plane $z = 0$. Integrating by parts gives

$$\iint_D \left(\int_{-h}^{0} \left(\psi \nabla^2 \xi + \xi \psi_{zz} \right) dz \ + [\psi \xi_z - \xi \psi_z]_{z=-h}^{z=0} \right) dxdy \ = 0 \ ,$$

which becomes

$$\iint_D \left(\int_{-h}^{0} \left(\psi \nabla^2 \xi + \xi \psi_{zz} \right) dz - [\xi \left(\psi_z - \nu \psi \right)]_{z=0} + [\xi \psi_z + \psi \nabla h . \nabla \xi]_{z=-h} \right) dxdy \ = 0, \quad (4.4)$$

when boundary conditions (4.2) and (4.3) are imposed on ξ. Equation (4.4) is a weak form of the boundary-value problem (4.1) – (4.3) and can be used to generate approximations to the solution of that problem.

We shall use a Galerkin approximation $\xi \approx \phi$ of the form

$$\xi(x, y, z) = \sum_{j=0}^{n-1} \phi_j(x, y) w_j(x, y, z) \ , \quad (4.5)$$

where w_j $(j = 0, 1, \ldots, n-1)$ are given functions and ϕ_j $(j = 0, 1, \ldots, n-1)$ are to be determined from (4.4). We choose our given function ψ as

$$\psi(x, y, z) = w_k(x, y, z) \ ,$$

for some $k \in (0, 1, \ldots, n-1)$. After some simple manipulation, which includes use of the identity

$$\nabla^2 \left(\phi_j w_j \right) = w_j \nabla^2 \phi_j + 2 \nabla \phi_j \ . \ \nabla w_j + \phi_j \nabla^2 w_j \ ,$$

it is found that the functions ϕ_k $(k = 0, \ldots, n-1)$ must satisfy the coupled system of differential equations

$$\sum_{j=0}^{n-1} \left\{ \nabla^2 \phi_j \int_{-h}^{0} w_j w_k dz \ + \tilde{\mathbf{f}}_{jk} . \nabla \phi_j + \left(\int_{-h}^{0} w_j \frac{\partial^2 w_k}{\partial z^2} dz \ + \tilde{g}_{jk} \right) \phi_j \right\} = 0 \ , \quad (4.6)$$

for $k = 0, 1, \ldots, n-1$, where

$$\tilde{\mathbf{f}}_{jk} = \tilde{\mathbf{f}}_{jk}(w_j, w_k) = \nabla h \left(w_j w_k\right)_{z=-h} + 2\int_{-h}^{0} w_k \nabla w_j dz$$

and

$$\tilde{g}_{jk} = \tilde{g}_{jk}(w_j, w_k) = \left[w_j\left(\nu w_k - \frac{\partial w_k}{\partial z}\right)\right]_{z=0} + \left[w_j \frac{\partial w_k}{\partial z} + w_k \nabla h.\nabla w_j\right]_{z=-h} + \int_{-h}^{0} w_k \nabla^2 w_j dz \ .$$

Chamberlain and Porter [9] have used this Galerkin approach with a 1-term approximation (that is, $n = 1$ in (4.5)) to derive a new approximation to ϕ that contains the mild-slope approximation as a special case. They also show that this new approximation to ϕ can be derived via a variational approach, which is similar to the recent work of Miles [40]. Indeed, Chamberlain and Porter [9] use the same trial function in both the Galerkin and variational approaches. The variational principle used in [9] is $\delta L = 0$ where L is the functional given by

$$L(\xi) = \iint_D \left(\frac{1}{2}\nu(\xi^2)_{z=0} - \frac{1}{2}\int_{-h}^{0}(\tilde{\nabla}\xi)^2 dz\right) dxdy \quad .$$

By considering variations which vanish on the lateral boundary $C \times [-h, 0]$, where C is the boundary of D, it follows that L is stationary at $\xi = \phi$ if and only if ϕ satisfies (4.1) – (4.3). So the variational principle $\delta L = 0$ can be used to generate approximations $\xi \approx \phi$. In particular, if we use the approximation ξ given by (4.5), then after imposing $\delta L = 0$ for all variations in ϕ_k $(k = 0, 1, \ldots, n-1)$ which vanish on $C \times [-h, 0]$, we eventually find after some straightforward manipulation that ϕ_k $(k = 0, 1, \ldots, n-1)$ must satisfy (4.6).

The theory up to this point holds for any w_j $(j = 0, 1, \ldots, n-1)$, but now a particular choice of these functions is made. To do this we now consider wave scattering problems that are independent of the y co-ordinate. The separation solution of (4.1) – (4.3) for uniform depth, given in section 2.3, suggests we choose the functions w_j $(j = 0, 1, \ldots, n-1)$ as

$$w_j = \frac{ig}{\sigma}\tilde{w}_j \ , \qquad \tilde{w}_j = \frac{\cos(B_j(z+h))}{\cos(B_j h)} \qquad (j = 0, 1, \ldots, n-1) \ , \tag{4.7}$$

in which $h = h(x)$ is the undisturbed fluid depth and the functions $B_j = B_j(h) = B_j(x)$ $(j = 1, 2, \ldots, n-1)$ are the first $n-1$ real, positive roots

of the relation

$$-\nu = B_j \tan(B_j h) \ , \tag{4.8}$$

arranged in ascending order of magnitude. Equation (4.8) has an imaginary root $B_0 = -ik$, and so we can write $\tilde{w}_0$ in the form

$$\tilde{w}_0 = \frac{\cosh(k(z+h))}{\cosh(kh)} \ , \tag{4.9}$$

where $k = k(h)$ is the real positive root of the local dispersion relation

$$\nu = k \tanh(kh) \ . \tag{4.10}$$

For each fixed value of ν, the equations (4.8) and (4.10) implicitly define $B_j = B_j(h)$ $(j = 1, \ldots, n-1)$ and $k = k(h)$ respectively. Notice that these w_j $(j = 0, \ldots, n-1)$ are an orthogonal set for $z \in [-h,\ 0]$ and they satisfy the same surface condition as ϕ, namely

$$\nu w_j - \frac{\partial w_j}{\partial z} = 0 \qquad \text{on } z = 0 \qquad (j = 0, 1, \ldots, n-1) \ .$$

It follows that the function $\phi_0 w_0$ is an approximation to the progressive wave mode part of ϕ and the functions $\phi_1 w_1,\ \phi_2 w_2, \ldots,\ \phi_{n-1} w_{n-1}$ are approximations to the $1^{\text{st}},\ 2^{\text{nd}}, \ldots,\ (n-1)^{\text{th}}$ decaying wave mode parts of ϕ respectively.

With this choice for the functions w_j $(j = 0, 1, \ldots, n-1)$, it follows from equations (4.8) and (4.10) that, at each x,

$$\int_{-h}^{0} \tilde{w}_j \tilde{w}_k dz = \begin{cases} 0 & j \neq k \ , \\ u_j(h) & j = k \ . \end{cases}$$

where

$$u_j(h) = \frac{1}{2B_j} \tan(B_j h) \left(1 + \frac{2B_j h}{\sin(2B_j h)} \right) \qquad (j = 0, 1, \ldots, n-1) \ ,$$

with $B_0 = -ik$. The approximate solution $\xi(x,z) = \sum_{j=0}^{n-1} \phi_j w_j \approx \phi$ satisfies the same free surface condition as ϕ, namely

$$\frac{\partial \xi}{\partial z} - \nu \xi = 0 \qquad \text{on } z = 0 \ .$$

We recall from Chapter 2 that over a flat bed, the general solution of (4.1) – (4.3) is given by $\phi = \sum_{j=0}^{\infty} \phi_j w_j$. Hence, over a flat bed, $\phi = \sum_{j=0}^{n-1} \phi_j w_j$ is the only solution

of (4.1) – (4.3) corresponding to the progressive wave mode and the first $(n-1)$ decaying wave modes. Also, since the free surface elevation η is defined by

$$\eta(x,t) = Re\left\{\frac{-i\sigma}{g}\phi(x,0)e^{-i\sigma t}\right\} \ ,$$

then the approximate solution is such that $\eta \approx Re\left\{e^{-i\sigma t}\sum_{j=0}^{n-1}\phi_j\right\}$.

Substituting (4.7) and (4.9) into (4.6) reduces (4.6) to the coupled system

$$u_k\left(\phi_k'' - B_k^2\phi_k\right) + \sum_{j=0}^{n-1}\left\{f_{jk}\phi_j' + g_{jk}\phi_j\right\} = 0 \qquad (k = 0,1,\ldots,n-1) \ , \tag{4.11}$$

where the prime denotes differentiation with respect to x, $B_0(h) = -ik(h)$,

$$f_{jk}(x) = \tilde{f}_{jk}(\tilde{w}_j,\tilde{w}_k) = h'\left[\tilde{w}_j\tilde{w}_k\right]_{z=-h} + 2\int_{-h}^{0}\tilde{w}_k\tilde{w}_j'dz \tag{4.12}$$

and

$$g_{jk}(x) = \tilde{g}_{jk}(\tilde{w}_j,\tilde{w}_k) = \left[\tilde{w}_k h'\tilde{w}_j'\right]_{z=-h} + \int_{-h}^{0}\tilde{w}_k\tilde{w}_j''dz \ . \tag{4.13}$$

If the second step of the mild-slope approximation is used, in which terms $O(h'',\ |h'|^2)$ are assumed to be negligibly small, then the coupled system (4.11) reduces to

$$u_k\left(\phi_k'' - B_k^2\phi_k\right) + \sum_{j=0}^{n-1}\left\{f_{jk}\phi_j'\right\} = 0 \qquad (k = 0,1,\ldots,n-1) \ , \tag{4.14}$$

where the terms g_{jk} $(j,k = 0,1,\ldots,n-1)$ are omitted because

$$g_{jk} = O(h'',\ |h'|^2) \qquad\qquad (j,k = 0,1,\ldots,n-1) \ .$$

(See (4.22) below for details.)

The method we have employed to derive (4.11) clearly shows that the two approximations $\phi \approx \sum_{j=0}^{n-1}\phi_j w_j$ and $g_{jk} \approx 0$ are quite independent. Therefore, we may suppose that the retention of g_{jk} $(j,k = 0,1,\ldots,n-1)$ gives the coupled system (4.11) a wider scope than (4.14), and so we focus our attention on the coupled system (4.11).

In the simple case when (4.5) is just a 1-term trial function, then the coupled system (4.11) reduces to

$$(u_0\phi_0')' + \left(k^2u_0 + g_{00}\right)\phi_0 = 0 \ . \tag{4.15}$$

This is a relatively new approximation to the progressive wave mode part of ϕ and equation (4.15) is known as the modified mild-slope equation (MMSE). This equation was first derived by Chamberlain [6] and more recently by Chamberlain and Porter [9] via the Galerkin and variational procedures given earlier in this section. Investigations of the modified mild-slope equation over a variety of bed profiles are carried out in Chamberlain and Porter [9] and in a subsequent paper by Chamberlain and Porter [10]. Similarly, with the 1-term trial approximation, the coupled system (4.14) reduces to

$$(u_0\phi_0')' + k^2 u_0 \phi_0 = 0 \ , \tag{4.16}$$

the well-known mild-slope equation (MSE). Miles [40] adjusted a variational principle for non-linear free surface flows, due to Luke [33], so that it applied to linearised free surface problems. Miles then used this modified variational principle to derive the mild-slope equation by apparently discarding a term equivalent to g_{00} in the process. The variational principle used by Miles [40] differs from the one used by Chamberlain and Porter [9] in that Miles' variational principle is for a real-valued potential instead.

Massel [36] used the same Galerkin method as used here with the same choice for the functions w_j, but allowed the depth function to vary in both the x and y directions. However, allowing h to vary in this way makes the above choice for the orthogonal functions w_j inappropriate in diffraction problems, for example, as the approximation does not allow for cylindrical waves which arise in these problems. Massel should have reduced the dimension of the problem by one, by removing the y dependence, before making the above choice of the functions w_j because this is the situation that these w_j are appropriate for, as we have already demonstrated. The system of differential equations Massel derives does, however, reduce to the system (4.11) when the y dependence is removed from the problem, although this is not obvious on first reading of the paper because of Massel's complicated notation. In his paper, Massel only solves the system (4.11) in the simplified case of a 1-term trial function. In other words, Massel solves the modified mild-slope equation (4.15). Massel left the solution of (4.11) in the case of an n (> 1) term trial function to another paper which is yet to appear.

Other approximations for wave scattering by a bed of varying topography that include decaying wave mode terms have been given by O'Hare and Davies [45] and Rey [52]. The approximation used by both sets of authors is very similar and involves replacing the bed profile by a series of horizontal shelves joining at vertical steps. Over each flat shelf, the velocity potential has an infinite series representation (see Chapter 2 section 2.3) which contains both progressive and decaying wave mode terms. Continuity of the velocity potential and its horizontal derivative is imposed throughout the fluid depth at the ends of each shelf, which gives a matrix system to solve. As a large number of vertical steps is required in order to obtain reliable results, the resulting matrix system is large and consequently both these methods are computationally expensive.

The complicated notation used by Massel [36] in his version of the system (4.11) is avoided in this approach by evaluating f_{jk} and g_{jk} explicitly.

Differentiating (4.7) and (4.8) with respect to h gives

$$\begin{aligned}\frac{\partial \tilde{w}_j}{\partial h} = \sec(B_j h) \Bigg[\left(h\frac{\partial B_j}{\partial h} + B_j \right) \tan(B_j h) \cos(B_j(z+h)) \\ - \left(\frac{\partial B_j}{\partial h}(z+h) + B_j \right) \sin(B_j(z+h)) \Bigg]\end{aligned} \tag{4.17}$$

and

$$\frac{\partial B_j}{\partial h} = \frac{-2B_j^2}{2B_j h + \sin(2B_j h)} \tag{4.18}$$

for $j = 0, \ldots, n-1$. Now, differentiating (4.17) and (4.18) with respect to h gives

$$\begin{aligned}\frac{\partial^2 \tilde{w}_j}{\partial h^2} = &\frac{\cos(B_j(z+h))}{\cos(B_j h)} \Bigg[\left\{ h\frac{\partial^2 B_j}{\partial h^2} + 2\frac{\partial B_j}{\partial h} + 2(h\frac{\partial B_j}{\partial h} + B_j)^2 \tan(B_j h) \right\} \tan(B_j h) \\ &\qquad -2z\frac{\partial B_j}{\partial h}(h\frac{\partial B_j}{\partial h} + B_j) - z^2 \left(\frac{\partial B_j}{\partial h} \right)^2 \Bigg] \\ &- \frac{\sin(B_j(z+h))}{\cos(B_j h)} \Bigg[2\left(h\frac{\partial B_j}{\partial h} + B_j \right)^2 \tan(B_j h) + h\frac{\partial^2 B_j}{\partial h^2} + 2\frac{\partial B_j}{\partial h} \\ &\qquad + z\left\{ 2\frac{\partial B_j}{\partial h}(h\frac{\partial B_j}{\partial h} + B_j)\tan(B_j h) + \frac{\partial^2 B_j}{\partial h^2} \right\} \Bigg]\end{aligned} \tag{4.19}$$

and

$$\frac{\partial^2 B_j}{\partial h^2} = \left(\frac{2B_j}{2B_j h + \sin(2B_j h)} \right)^3 \left[2B_j h + \sin(2B_j h) \left(1 + \cos^2(B_j h) \right) \right] \tag{4.20}$$

for $j = 0, \ldots, n-1$. It follows that

$$\tilde{w}_j' = \frac{\partial \tilde{w}_j}{\partial h} h' \qquad (j = 0, \ldots, n-1)$$

and

$$\tilde{w}_j'' = \frac{\partial^2 \tilde{w}_j}{\partial h^2}\,(h')^2 + \frac{\partial \tilde{w}_j}{\partial h} h'' \qquad (j = 0, \ldots, n-1)\ .$$

Therefore, the functions f_{jk} and g_{jk} $(j,k = 0, \ldots, n-1)$ defined by (4.12) and (4.13) respectively can be written as

$$f_{jk}(x) = \left(\left[\tilde{w}_j \tilde{w}_k\right]_{z=-h} + 2\int_{-h}^{0} \tilde{w}_k \frac{\partial \tilde{w}_j}{\partial h} dz \right) h' \tag{4.21}$$

and

$$\begin{aligned} g_{jk}(x) = \ & \left(\int_{-h}^{0} \tilde{w}_k \frac{\partial \tilde{w}_j}{\partial h} dz \right) h'' \\ & + \left(\left[\tilde{w}_k \frac{\partial \tilde{w}_j}{\partial h} \right]_{z=-h} + \int_{-h}^{0} \tilde{w}_k \frac{\partial^2 \tilde{w}_j}{\partial h^2} dz \right) (h')^2 \ . \end{aligned} \tag{4.22}$$

A little algebra incorporating the use of relations (4.8) and (4.10) shows that the integrals appearing in (4.21) and (4.22) are given by

$$\int_{-h}^{0} \tilde{w}_k \frac{\partial \tilde{w}_j}{\partial h} dz = \begin{cases} \sec(B_k h)\sec(B_j h) \left(\dfrac{B_j^2}{B_k^2 - B_j^2} \right) & (k \neq j)\ , \\ \dfrac{\sec^2(B_k h)}{4\,(D_k + \sin(D_k))} \Big[\sin(D_k) - D_k \cos(D_k) \Big] & (k = j) \end{cases}$$

and

$$\int_{-h}^{0} \tilde{w}_k \frac{\partial^2 \tilde{w}_j}{\partial h^2} dz = \frac{-4B_j^3 \sec(B_k h)\sec(B_j h)}{D_k + \sin(D_k)} \left(\frac{2B_k^2 + (B_j^2 - B_k^2)\sin^2(B_j h)}{\Big((B_k + B_j)(B_k - B_j)\Big)^2} \right) \qquad (k \neq j)$$

and

$$\begin{aligned} \int_{-h}^{0} \tilde{w}_k \frac{\partial^2 \tilde{w}_k}{\partial h^2} dz = \frac{-B_k \sec^2(B_k h)}{12\,(D_k + \sin(D_k))^3} \Big[\ & (D_k)^4 + 4(D_k)^3 \sin(D_k) \\ & + 3D_k \Big(D_k + 2\sin(D_k)\Big)\Big(\sin^2(D_k) - 2\cos(D_k)\Big) \\ & + 6\sin^2(D_k)\left(1 + 2\cos^2(\tfrac{1}{2}D_k)\right) \Big]\ , \end{aligned}$$

where $D_k = 2B_k h$, and $B_0 = -ik$. It is simple to see that the remaining terms in (4.21) and (4.22) are given by

$$\Big[\tilde{w}_k \tilde{w}_j\Big]_{z=-h} = \sec(B_k h)\sec(B_j h) \qquad (j,k = 0, \ldots, n-1)$$

and

$$\left[\tilde{w}_k \frac{\partial \tilde{w}_j}{\partial h} \right]_{z=-h} = \frac{2\sec(B_k h)\sec(B_j h) B_j \sin^2(B_j h)}{2B_j h + \sin(2B_j h)} \qquad (j,k = 0, \ldots, n-1)\ .$$

4.2 Scaling

We choose the same class of depth profiles as in Chapter 2, which are varying only in some finite interval of x. We assume that

$$h(x) = \begin{cases} h_0 & \forall x \leq 0 \ , \\ h_1 & \forall x \geq l \ , \end{cases}$$

where h_0, h_1 and l are given constants, and where $h(x)$ is continuous on $(-\infty, \infty)$. We allow h to have a slope discontinuity at the ends of the varying bed, that is, at $x = 0$ and $x = l$. At the moment we shall consider the scattering of plane harmonic waves normally incident on a given depth profile. The generalisation to obliquely incident waves will be dealt with later.

The scaling process now employed is the same as that used in Chapter 2. Therefore, we let

$$\begin{aligned}
\hat{x} &= \frac{x}{l} \ , \\
\hat{z} &= \frac{z}{h_0} \ , \\
H(\hat{x}) &= \frac{1}{h_0} h(l\hat{x}) \ , \\
U_k(\hat{x}) &= \frac{1}{h_0} u_k(l\hat{x}) \qquad (k = 0, \ldots, n-1) \ , \\
W_k(\hat{x}, \hat{z}) &= \frac{1}{\sigma l} w_k(l\hat{x}, h_0\hat{z}) \qquad (k = 0, \ldots, n-1) \ , \\
\hat{\phi}_k(\hat{x}) &= \frac{1}{l} \phi_k(l\hat{x}) \qquad (k = 0, \ldots, n-1) \ , \\
F_{jk}(\hat{x}) &= \frac{l}{h_0} f_{jk}(l\hat{x}) \qquad (j, k = 0, \ldots, n-1) \ , \\
G_{jk}(\hat{x}) &= \frac{l^2}{h_0} g_{jk}(l\hat{x}) \qquad (j, k = 0, \ldots, n-1) \ .
\end{aligned}$$

Again, we introduce dimensionless parameters α_0, τ and β_k $(k = 0, \ldots, n-1)$ by

$$\alpha_0 = \frac{\sigma l}{\sqrt{g h_0}} \quad , \quad \tau = h_0/l \quad \text{and} \quad \beta_k = B_k l \ .$$

Remembering that $B_0 = -ik$, we also define the real dimensionless parameter κ by $\kappa = i\beta_0$. As in Chapter 2, we shall discard the accents from the scaled independent variable and from the ϕ_k $(k = 0, \ldots, n-1)$ in the pursuit of a simple notation.

In terms of these dimensionless quantities the coupled system of equations (4.11) is

$$U_k \left(\phi_k'' - {\beta_k}^2 \phi_k\right) + \sum_{j=0}^{n-1} \left\{F_{jk}\phi_j' + G_{jk}\phi_j\right\} = 0 \qquad (k = 0, 1, \ldots, n-1)\ , \tag{4.23}$$

where the prime denotes differentiation with respect to x. The functions U_k are given by

$$U_k = \frac{1}{2\beta_k \tau} \tan(\beta_k \tau H) \left(1 + \frac{2\beta_k \tau H}{\sin(2\beta_k \tau H)}\right) \qquad (k = 0, \ldots, n-1) \tag{4.24}$$

and the functions β_k are the positive real roots of

$$-{\alpha_0}^2 \tau = \beta_k \tan(\beta_k \tau H) \qquad (k = 1, \ldots, n-1), \tag{4.25}$$

arranged in ascending order of magnitude and $\beta_0 = -i\kappa$, where κ is the positive real root of

$$\alpha_0{}^2 \tau = \kappa \tanh(\kappa \tau H)\ . \tag{4.26}$$

For $j, k = 0, \ldots, n-1$, where $j \neq k$, the functions F_{jk} and G_{jk} are given by

$$F_{jk} = \sec(\beta_k \tau H)\sec(\beta_j \tau H) \left(\frac{{\beta_k}^2 + {\beta_j}^2}{{\beta_k}^2 - {\beta_j}^2}\right) H' \tag{4.27}$$

and

$$\begin{aligned} G_{jk} = & \left(\sec(\beta_k \tau H)\sec(\beta_j \tau H) \frac{{\beta_j}^2}{{\beta_k}^2 - {\beta_j}^2}\right) H'' \\ & - \left(\frac{2\beta_j \tau \sec(\beta_k \tau H)\sec(\beta_j \tau H)}{2\beta_j \tau H + \sin(2\beta_j \tau H)}\right) \left(\frac{4{\beta_j}^2 {\beta_k}^2 + ({\beta_j}^4 - {\beta_k}^4)\sin^2(\beta_j \tau H)}{\left((\beta_k + \beta_j)(\beta_k - \beta_j)\right)^2}\right) (H')^2. \end{aligned} \tag{4.28}$$

For $k = 0, \ldots, n-1$ the functions F_{kk} and G_{kk} are given by

$$F_{kk} = \frac{\sec^2(\beta_k \tau H)}{2\left(D_k + \sin(D_k)\right)} \left[3\sin(D_k) + D_k(2 - \cos(D_k))\right] H' \tag{4.29}$$

and

$$
\begin{aligned}
G_{kk} = \quad & \frac{\sec^2(\beta_k \tau H)}{4\,(D_k + \sin(D_k))}\Big[\,\sin(D_k) - D_k\cos(D_k)\Big]\,H'' \\
& -\frac{1}{12}\frac{\beta_k\tau\sec^2(\beta_k\tau H)}{(D_k+\sin(D_k))^3}\Big[\,(D_k)^4 + 4(D_k)^3\sin(D_k) \\
& \qquad -3D_k\Big(D_k + 2\sin(D_k)\Big)\Big(\cos^2(D_k) - 2\cos(D_k) + 3\Big) \\
& \qquad +9\sin(D_k)\sin(2D_k)\,\Big]\,(H')^2 \quad ,
\end{aligned}
\tag{4.30}
$$

where $D_k = 2\beta_k\tau H$.

If we apply the second approximation step of the mild-slope approximation to the coupled system (4.23), then the reduced system is the same as (4.23) with just the G_{jk} terms omitted.

Once H, α_0 and τ have been assigned then all the other quantities in equations (4.24) – (4.30) can be calculated. The functions κ and β_k $(k = 0, \ldots, n-1)$ must be calculated numerically. This can be done using the efficient iterative methods given, for example, by Newman [44].

The only other information we require is the boundary or asymptotic conditions on ϕ_k $(k = 0, \ldots, n-1)$.

4.3 Boundary conditions

On the flat bed for $x \leq 0$, the non-dimensional system of differential equations (4.23) reduces to the decoupled set of equations given by

$$
\begin{aligned}
\phi_0'' + (\kappa_0)^2\,\phi_0 &= 0 \ , \\
\phi_k'' - (\beta_k^0)^2\,\phi_k &= 0 \qquad\qquad (k = 1, \ldots, n-1) \ ,
\end{aligned}
$$

where the notation $\kappa_0 = \kappa(0)$ and $\beta_k^0 = \beta_k(0)$ $(k = 1, \ldots, n-1)$ is used. Similarly, on the flat bed for $x \geq 1$, the system (4.23) reduces to the decoupled set of equations given by

$$
\begin{aligned}
\phi_0'' + (\kappa_1)^2\,\phi_0 &= 0 \ , \\
\phi_k'' - (\beta_k^1)^2\,\phi_k &= 0 \qquad\qquad (k = 1, \ldots, n-1) \ ,
\end{aligned}
$$

where the notation $\kappa_1 = \kappa(1)$ and $\beta_k^1 = \beta_k(1)$ $(k = 1, \ldots, n-1)$ is used. In this section we shall only consider the case of a talud – with the simplification

to a hump arising from putting $h_0 = h_1$ and therefore $\kappa_0 = \kappa_1$ and $\beta_k^0 = \beta_k^1$ $(k = 1, \ldots, n-1)$.

The fluid domain under consideration extends to infinity. Therefore, we prescribe radiation conditions for ϕ_k $(k = 0, \ldots, n-1)$ that are based on the radiation condition for ϕ described in Chapter 2. Hence, we assume that two plane waves propagating from $x = \pm\infty$ with known coefficients $A^{\pm}$ respectively are incident on the talud. The 1-dimensional analogue of the radiation condition for ϕ implies that the outgoing wave solutions must be bounded at $x = \pm\infty$. Hence, there will result 2 outgoing plane waves with unknown coefficients $B_0^{\pm}$ heading towards $x = \pm\infty$ respectively. There will also result $2(n-1)$ outgoing decaying wave modes with $(n-1)$ of these heading towards $x = \infty$ with unknown coefficients B_k^+ $(k = 1, \ldots, n-1)$ and with $(n-1)$ heading towards $x = -\infty$ with unknown coefficients B_k^- $(k = 1, \ldots, n-1)$. Therefore, we assume

$$\phi_0(x) = \begin{cases} A^- e^{i\kappa_0 x} + B_0^- e^{-i\kappa_0 x} & x \leq 0 \ , \\ \\ A^+ e^{-i\kappa_1 x} + B_0^+ e^{i\kappa_1 x} & x \geq 1 \ , \end{cases} \tag{4.31}$$

$$\phi_k(x) = \begin{cases} B_k^- e^{\beta_k^0 x} & x \leq 0 \quad (k = 1, \ldots, n-1) \ , \\ \\ B_k^+ e^{-\beta_k^1 x} & x \geq 1 \quad (k = 1, \ldots, n-1) \ . \end{cases} \tag{4.32}$$

We shall now use this information to give boundary conditions on $(0, 1)$, by returning to our original approximation $\xi \approx \phi$ given by (4.5) and employing the Galerkin procedure again. It follows from (4.31) and (4.32) that our approximation throughout the fluid domain, after scaling, is given by

$$\xi(x,z) = \begin{cases} \xi_1(x,z) & (x \leq 0) \ , \\ \xi_2(x,z) & (0 \leq x \leq 1) \ , \\ \xi_3(x,z) & (x \geq 1) \ , \end{cases}$$

where

$$\xi_1(x,z) = \left(A^- e^{i\kappa_0 x} + B_0^- e^{-i\kappa_0 x}\right) W_0^0 + \sum_{j=1}^{n-1} B_j^- e^{\beta_j^0 x} W_j^0 \ ,$$

$$\xi_2(x,z) = \sum_{j=0}^{n-1} \phi_j W_j \ ,$$

$$\xi_3(x,z) = \left(A^+ e^{-i\kappa_1 x} + B_0^+ e^{i\kappa_1 x}\right) W_0^1 + \sum_{j=1}^{n-1} B_j^+ e^{-\beta_j^1 x} W_j^1 \ .$$

Here, we have used the notation $W_j^0 = W_j(0,z)$, $W_j^1 = W_j(1,z)$ $(j = 0,\ldots,n-1)$, where $W_j = \dfrac{i}{{\alpha_0}^2\tau}\tilde{W}_j$, and the functions $\tilde{W}_j$ $(j = 0,\ldots,n-1)$ are given by

$$\tilde{W}_0(x,z) = \frac{\cosh\left(\kappa\tau(z+H)\right)}{\cosh\left(\kappa\tau H\right)} \quad \text{and} \quad \tilde{W}_j(x,z) = \frac{\cos\left(\beta_j\tau(z+H)\right)}{\cos\left(\beta_j\tau H\right)} \ .$$

The set of functions $\left\{\tilde{W}_j : j+1 \in \mathbb{N}\right\}$ is orthogonal for $z \in [-H,0]$ and in particular

$$\int_{-H}^{0} \tilde{W}_j\tilde{W}_k dz = \begin{cases} 0 & k \neq j \ , \\ U_j & k = j \ , \end{cases}$$

where $U_j = U_j(x)$ is defined by (4.24).

We wish our approximation ξ to possess as many properties of ϕ as possible, and so we certainly need to require that ξ and $\frac{\partial\xi}{\partial x}$ are continuous at the ends of the talud, that is, at $x = 0$ and $x = 1$, throughout the fluid depth. In other words, we require

$$\xi_1 = \xi_2 \ , \qquad \frac{\partial\xi_1}{\partial x} = \frac{\partial\xi_2}{\partial x} \qquad (x = 0; -H(0) \leq z \leq 0) \ ,$$

$$\xi_2 = \xi_3 \ , \qquad \frac{\partial\xi_2}{\partial x} = \frac{\partial\xi_3}{\partial x} \qquad (x = 1; -H(1) \leq z \leq 0) \ .$$

Boundary conditions on ϕ_j $(j = 0,\ldots,n-1)$ are now derived from the above matching equations by employing the same Galerkin procedure used in section 4.1 to derive the differential equation system satisfied by ϕ_j $(j = 0,\ldots,n-1)$.

Invoking the continuity of ξ at $x = 0$ gives

$$\sum_{j=0}^{n-1} C_j^- \tilde{W}_j^0 = \sum_{j=0}^{n-1} \phi_j(0)\tilde{W}_j^0 \qquad (-H(0) \leq z \leq 0) \ , \tag{4.33}$$

where

$$C_j^- = \begin{cases} A^- + B_0^- & (j = 0) \ , \\ B_j^- & (j = 1,\ldots,n-1) \ . \end{cases}$$

Multiplying (4.33) by $\tilde{W}_k^0$ (for some $k \in [0,1,\ldots,n-1]$) and integrating with respect to z from $-H(0)$ to 0 gives

$$C_k^- = \phi_k(0) \qquad (k = 0,\ldots,n-1) \ . \tag{4.34}$$

In the same manner, invoking continuity of ξ at $x = 1$ gives

$$C_k^+ = \phi_k(1) \qquad (k = 0,\ldots,n-1) \ , \tag{4.35}$$

where

$$C_k^+ = \begin{cases} A^+ e^{-i\kappa_1} + B_0^+ e^{i\kappa_1} & (k=0)\ , \\ B_k^+ e^{-\beta_k^1} & (k=1,\ldots,n-1)\ . \end{cases}$$

As we allow the depth function $H(x)$ to have a slope discontinuity at $x=0$ and $x=1$, then it follows that for $j=0,\ldots,n-1$

$$\left.\frac{\partial \tilde{W}_j}{\partial x}\right|_{x=0+} \neq 0\ ,\ \left.\frac{\partial \tilde{W}_j}{\partial x}\right|_{x=0-} = 0\ ,\ \left.\frac{\partial \tilde{W}_j}{\partial x}\right|_{x=1-} \neq 0 \quad \text{and} \quad \left.\frac{\partial \tilde{W}_j}{\partial x}\right|_{x=1+} = 0\ ,$$

since the depth function $H(x)$ is constant for $x \leq 0$ and $x \geq 1$. Therefore, invoking continuity of $\frac{\partial \xi}{\partial x}$ at $x=0$ gives

$$\sum_{j=0}^{n-1} D_j^- \tilde{W}_j^0 = \sum_{j=0}^{n-1} \left\{ \phi_j' \tilde{W}_j + \phi_j \frac{\partial \tilde{W}_j}{\partial x} \right\}_{x=0+}\ , \tag{4.36}$$

where

$$D_j^- = \begin{cases} i\kappa_0 \left(A^- - B_0^- \right) & (j=0)\ , \\ \beta_j^0 B_j^- & (j=1,\ldots,n-1)\ . \end{cases}$$

Multiplying (4.36) by $\tilde{W}_k^0$ (for some $k \in [0,1,\ldots,n-1]$) and integrating with respect to z from $-H(0)$ to 0 gives

$$D_k^- = \phi_k'(0+) + \phi_k(0)[\tau(\beta_k H)' \tan(\beta_k \tau H)]|_{x=0+} - \sum_{j=0}^{n-1} d_{jk}^0 \phi_j(0) \quad (k=0,....n-1)\ ,$$

where

$$d_{jk}(x) = \frac{\tau}{U_k} \int_{-H(x)}^{0} \left(z\beta_j' + (\beta_j H)' \right) \frac{\sin(\beta_j \tau(z+H))}{\cos(\beta_j \tau H)} \frac{\cos(\beta_k \tau(z+H))}{\cos(\beta_k \tau H)} dz$$

and $d_{jk}^0 = d_{jk}(0+)$. Evaluating the integral in the expression for d_{jk} gives

$$d_{jk}(x) = \begin{cases} \dfrac{-(\beta_j)^2 H'}{U_k} \dfrac{\sec(\beta_j \tau H) \sec(\beta_k \tau H)}{(\beta_k + \beta_j)(\beta_k - \beta_j)} & j \neq k\ , \\ \tau(\beta_k H)' \tan(\beta_k \tau H) + \dfrac{\beta_k'}{2\beta_k} - \dfrac{2\tau H \beta_k' \cos^2(\beta_k \tau H)}{\sin(2\beta_k \tau H) + 2\beta_k \tau H} & j = k\ . \end{cases}$$

Similarly, invoking the continuity of $\frac{\partial \xi}{\partial x}$ at $x=1$ gives

$$D_k^+ = \phi_k'(1-) + \phi_k(1)[\tau(\beta_k H)' \tan(\beta_k \tau H)]|_{x=1-} - \sum_{j=0}^{n-1} d_{jk}^1 \phi_j(1) \quad (k=0,....n-1)\ ,$$

where

$$D_k^+ = \begin{cases} -i\kappa_1 \left(A^+ e^{-i\kappa_1} - B_0^+ e^{i\kappa_1} \right) & (k=0)\ , \\ -\beta_k^1 B_k^+ e^{-\beta_k^1} & (k=1,\ldots,n-1)\ , \end{cases}$$

and $d^1_{jk} = d_{jk}(1-)$. Substituting (4.34) into the expression for D^-_k and (4.35) into the expression for D^+_k gives the coupled boundary conditions

$$\phi_0'(0)+\phi_0(0)[i\kappa-\tau(\kappa H)'\tanh(\kappa\tau H)]|_{x=0}-\sum_{j=0}^{n-1} d^0_{j0}\phi_j(0) = \quad 2i\kappa_0 A^-, \qquad (4.37)$$

$$\phi_0'(1)-\phi_0(1)[i\kappa+\tau(\kappa H)'\tanh(\kappa\tau H)]|_{x=1}-\sum_{j=0}^{n-1} d^1_{j0}\phi_j(0) = -2i\kappa_1 e^{-i\kappa_1}A^+, \qquad (4.38)$$

$$\phi_k'(0)-\phi_k(0)[\beta_k-\tau(\beta_k H)'\tan(\beta_k\tau H)]|_{x=0}-\sum_{j=0}^{n-1} d^0_{jk}\phi_j(0) = \quad 0\ , \qquad (4.39)$$

$$\phi_k'(1)+\phi_k(1)[\beta_k+\tau(\beta_k H)'\tan(\beta_k\tau H)]|_{x=1}-\sum_{j=0}^{n-1} d^1_{jk}\phi_j(1) = \quad 0\ , \qquad (4.40)$$

where $k = 0, \ldots, n-1$ and where the derivatives are evaluated inside the interval $(0, 1)$.

The approximation to the free surface elevation is given by

$$\eta(x,t) \approx \mathrm{Re}\left\{e^{-i\sigma t}\xi(x,0)\right\} \qquad (-\infty < x < \infty)\ .$$

These boundary conditions also make the approximation to the free surface continuous at $x = 0$ and $x = 1$. However, the approximation to the slope of the free surface is continuous at $x = 0$ and $x = 1$ only when the slope of the bed is also continuous at $x = 0$ and $x = 1$.

Massel [36] uses the same approach to derive the boundary conditions for his version of the z independent system (4.23). However, in his approach, Massel omits the $\frac{\partial \tilde{W}_j}{\partial x}\Big|_{x=0+}$ terms when he imposes his version of the matching condition $\frac{\partial \xi_1}{\partial x} = \frac{\partial \xi_2}{\partial x}$ at $x = 0$ $(-H(0) \le z \le 0)$ and omits the $\frac{\partial \tilde{W}_j}{\partial x}\Big|_{x=1-}$ terms when he imposes his version of $\frac{\partial \xi_2}{\partial x} = \frac{\partial \xi_3}{\partial x}$ at $x = 1$ $(-H(1) \le z \le 0)$. These omissions imply that Massel's boundary conditions are only correct when

$$\left.\frac{\partial \tilde{W}_j}{\partial x}\right|_{x=0+} = 0 = \left.\frac{\partial \tilde{W}_j}{\partial x}\right|_{x=1-}\ ,$$

that is, when the depth function has a continuous slope at the ends of the talud. Massel [36] only goes on to give solutions in the case of a 1-term approximation. However, as a means of testing the 1-term approximation, he considers the talud problem considered by Booij [5], for which Booij computed solutions of the full linear problem. Unfortunately, this depth function has slope discontinuities where

the talud joins the flat beds. Therefore, the results given by Massel [36] for the 1-term approximation for Booij's test problem are wrong because he uses inappropriate boundary conditions.

In the case of a 1-term approximation, the differential equation system (4.23) reduces to the modified mild-slope equation

$$(U_0\phi_0')' + \left(\kappa^2 U_0 + G_{00}\right)\phi_0 = 0 \ .$$

This is the differential equation that Massel [36] solved with his incorrect boundary conditions. Chamberlain and Porter [10], [9] have also used this equation in a variety of test problems. The above equation reduces to the well-known mild-slope equation if the G_{00} term is omitted. Some of the authors that have used this equation include Berkhoff [2], [3], Smith and Sprinks [54], Booij [5], Kirby [26], O'Hare and Davies [45], Chamberlain [7], [8], Rey [52], Chamberlain and Porter [10] and [9]. For both the modified mild-slope and mild-slope equations, all the above authors have used the boundary conditions which arise from enforcing the continuity of ϕ_0 and ϕ_0' at the junctions where the varying depth region meets the flat beds. For the scaling used in this chapter, these boundary conditions are given by

$$\begin{aligned} \phi_0'(0) + i\kappa_0\phi_0(0) &= 2i\kappa_0 A^- \ , \\ \phi_0'(1) - i\kappa_1\phi_0(1) &= -2i\kappa_1 e^{-i\kappa_1} A^+ \ , \end{aligned} \tag{4.41}$$

where $A^{+(-)}$ denotes the coefficient of the incident wave from the right (left). None of the above authors returned to the approximation $\phi_0 W_0 \approx \phi$ and required $(\phi_0 W_0)$ and $(\phi_0 W_0)_x$ to be continuous throughout the fluid depth at the junctions where the varying depth region meets the flat beds, which is the approach we have used in this section. The boundary conditions used by Massel [36] with the modified mild-slope equation correspond to the above boundary conditions (4.41) and possibly explains why he omits the $\phi_j \frac{\partial \tilde{W}_j}{\partial x}$ terms in his derivation of the boundary conditions.

The boundary conditions that we have derived for the 1-term approximation

are

$$\begin{aligned}
\phi_0'(0+)+\phi_0(0)\left[i\kappa-\left(\frac{1}{2\kappa}-\frac{2\tau H\cosh^2(\kappa\tau H)}{\sinh(2\kappa\tau H)+2\kappa\tau H}\right)\kappa'\right]\Bigg|_{0+} &= 2i\kappa_0 A^-, \\
\phi_0'(1-)-\phi_0(1)\left[i\kappa+\left(\frac{1}{2\kappa}-\frac{2\tau H\cosh^2(\kappa\tau H)}{\sinh(2\kappa\tau H)+2\kappa\tau H}\right)\kappa'\right]\Bigg|_{1-} &= -2i\kappa_1 e^{-i\kappa_1}A^+.
\end{aligned} \tag{4.42}$$

As far as is known, these boundary conditions are completely new and reduce to (4.41) only when the varying bed has a continuous slope at the junctions with the flat beds.

We shall refer to the sets (4.41) and (4.42) of boundary conditions for the mild-slope and modified mild-slope equations as the old set and new set of boundary conditions respectively.

In Section 4.8, we compare results given by the modified mild-slope and mild-slope equations with both the new and old sets of boundary conditions for Booij's [5] test problem. We see that the results given by both equations with the new set of boundary conditions are much closer to the full linear results, justifying the approach we have used here to derive the boundary conditions (4.37) – (4.40).

All that remains to be done in this section is to define the reflection and transmission coefficients of the outgoing plane waves, which we shall denote by R^0 and T^0, and the decay coefficients of the decaying wave modes, which we shall denote by R^k and T^k $(k = 1, \ldots, n-1)$. The definitions we shall use here correspond to the definitions of the reflection and transmission coefficients used in Chapter 2 for the mild-slope approximation. In equation (4.31) we have defined the coefficients of the incident waves from $x = \pm\infty$ as $A^\pm$ respectively. Linearity allows us to superpose (through the scattering matrix given below in (4.47)) solutions corresponding to waves incident from $x = -\infty$ with solutions corresponding to waves incident from $x = \infty$. Therefore, we do not need to solve the problem with two incident waves. Instead, by solving the problem for only one incident wave, its amplitude may be, without loss of generality, set equal to unity. The notation we use is summarised as follows.

$$\text{If } A^+ = 0 \text{ then } R_1^k = \frac{B_k^-}{A^-} \quad \text{and} \quad T_1^k = \frac{B_k^+}{A^-} \qquad (k = 0, \ldots, n-1)\ .$$

$$\text{If } A^- = 0 \text{ then } R_2^k = \frac{B_k^+}{A^+} \quad \text{and} \quad T_2^k = \frac{B_k^-}{A^+} \qquad (k = 0, \ldots, n-1)\ .$$

From equations (4.31) and (4.32) we see that $\phi_0(0) = A^- + B_0^-$, $\phi_0(1) = A^+e^{-i\kappa_1} + B_0^+e^{i\kappa_1}$, $\phi_k(0) = B_k^-$ $(k = 1, \ldots, n-1)$ and $\phi_k(1) = B_k^+e^{-\beta_k^1}$ $(k = 1, \ldots, n-1)$. We can use these expressions to write the reflection, transmission and decay coefficients in terms of the end-point values of ϕ_k $(k = 0, \ldots, n-1)$ as follows.

If $A^+ = 0$:

$$R_1^0 = \frac{\phi_0(0)}{A^-} - 1, \qquad T_1^0 = \frac{\phi_0(1)e^{-i\kappa_1}}{A^-}\ , \tag{4.43}$$

$$R_1^k = \frac{\phi_k(0)}{A^-}, \qquad T_1^k = \frac{\phi_k(1)e^{\beta_k^1}}{A^-} \qquad (k = 1, \ldots, n-1)\ . \tag{4.44}$$

If $A^- = 0$:

$$R_2^0 = \frac{\phi_0(1)e^{-i\kappa_1}}{A^+} - e^{-2i\kappa_1}, \qquad T_2^0 = \frac{\phi_0(0)}{A^+}\ , \tag{4.45}$$

$$R_2^k = \frac{\phi_k(1)e^{\beta_k^1}}{A^+}, \qquad T_2^k = \frac{\phi_k(0)}{A^+} \qquad (k = 1, \ldots, n-1)\ . \tag{4.46}$$

We note that for an incident wave from the left, the transmitted decaying wave mode at $x = 1$ is $T_1^k e^{-\beta_k^1}$ $(k = 1 \ldots, n-1)$ and for an incident wave from the right, the reflected decaying wave mode at $x = 1$ is $R_2^k e^{-\beta_k^1}$ $(k = 1 \ldots, n-1)$. Therefore, these quantities can be calculated regardless of the size of the functions β_k^1 $(k = 1, \ldots, n-1)$. Once the coefficients R_1^k, R_2^k, T_1^k and T_2^k $(k = 0 \ldots, n-1)$ have been determined, then we can deduce values for $B_k^\pm$ $(k = 0 \ldots, n-1)$ (the unknown coefficients of the outgoing plane wave and decaying wave modes) in terms of $A^\pm$ (the given incident wave coefficients). The outgoing plane wave coefficient B_0^+ comprises of two parts – the part of A^- transmitted beyond the talud that is a plane wave and the part of A^+ reflected back from the talud that is a plane wave. A similar argument applies to the other outgoing plane wave coefficient B_0^- and to the decaying wave mode coefficients $B_k^\pm$ $(k = 1, \ldots, n-1)$, and we can summarise these resulting relationships as follows:

$$\begin{pmatrix} B_k^+ \\ B_k^- \end{pmatrix} = \begin{pmatrix} T_1^k & R_2^k \\ R_1^k & T_2^k \end{pmatrix} \begin{pmatrix} A^- \\ A^+ \end{pmatrix} \qquad (k = 0, \ldots, n-1)\ . \tag{4.47}$$

The matrix on the right-hand side of equation (4.47) is called the scattering matrix.

We only need to consider the problem of approximating the reflection, transmission and decay coefficients, and then the $B_k^{\pm}$ $(k = 0 \ldots, n-1)$ can be determined through (4.47) for any $A^{\pm}$.

4.4 A system of Fredholm integral equations

We wish to solve the coupled differential equation system (4.23) together with boundary conditions (4.37) – (4.40). We know from Chamberlain [7] that when the system (4.23) is a scalar equation (that is, when (4.23) is generated using a 1-term approximation) then an integral equation procedure can be used to solve the boundary-value problem to a high degree of accuracy. When the system (4.23) is a vector equation (that is, when (4.23) is generated using an n $(n > 1)$ term approximation) an integral equation solution method is much more difficult to implement. A method of converting the system (4.23) and boundary conditions (4.37) – (4.40) into a system of Fredholm integral equations is now given. The resulting system of integral equations presents serious problems for numerical solution methods and no attempt is made to solve this integral equation system here.

Chamberlain [6] expends much effort in finding a straightforward method to convert the mild-slope equation and its boundary conditions into an integral equation. He uses a variation of parameters method to obtain the integral equation. We can also use this method for our system (4.23) and boundary conditions (4.37) – (4.40). As the idea here is only to indicate the form of the system of integral equations that results, we just give the major steps that occur in the conversion process to the vector integral equation.

We introduce the variable changes

$$\phi_k(x) = \zeta_k(x)\sqrt{\frac{U_k^0}{U_k(x)}} \qquad (k = 0, \ldots, n-1)\ , \tag{4.48}$$

where $U_k^0 = U_k(0)$ $(k = 0, \ldots, n-1)$. Substituting (4.48) into (4.23) and rearranging, we find that the functions ζ_k $(k = 0, \ldots, n-1)$ satisfy the coupled

differential equation system

$$\zeta_k'' - \left(\beta_k^0\right)^2 \zeta_k = \rho_k \zeta_k - \sum_{\substack{j=0 \\ j\neq k}}^{n-1} \left\{ \left[M_{jk} - \frac{U_j'}{2U_j} N_{jk} \right] \zeta_j + N_{jk} \zeta_j' \right\} \ . \tag{4.49}$$

Here, we have used the notation

$$\rho_k = {\beta_k}^2 - \left(\beta_k^0\right)^2 + \frac{U_k''}{2U_k} - \left(\frac{U_k'}{2U_k}\right)^2 - \frac{G_{kk}}{U_k} \qquad (k = 0, \ldots, n-1) \ ,$$

$$M_{jk} = \sqrt{\frac{U_j^0}{U_k^0}} U_j^{-\frac{1}{2}} U_k^{-\frac{1}{2}} G_{jk} \qquad (k = 0, \ldots, n-1) \ ,$$

$$N_{jk} = \sqrt{\frac{U_j^0}{U_k^0}} U_j^{-\frac{1}{2}} U_k^{-\frac{1}{2}} F_{jk} \qquad (k = 0, \ldots, n-1) \ ,$$

where G_{jk} and F_{jk} $(j, k = 0, \ldots, n-1)$ are given by equations (4.27) – (4.30) and the functions β_k $(k = 0, \ldots, n-1)$ are given by equations (4.25) and (4.26). As usual, we have used the notation $\beta_k^0 = \beta_k(0)$, $\beta_k^1 = \beta_k(1)$ and $U_k^0 = U_k(0)$ $(k = 0, \ldots, n-1)$.

The boundary conditions satisfied by the functions ζ_k $(k = 0, \ldots, n-1)$ can be found in exactly the same method as that used to find the boundary conditions for ϕ_k $(k = 0, \ldots, n-1)$ in section 4.3. Omitting the details of this process, it turns out that we can write these boundary conditions in the form

$$\zeta_k'(0+) - \beta_k^0 \zeta_k(0) = -2\beta_k^0 r_k \qquad (k = 0, \ldots, n-1) \ , \tag{4.50}$$

$$\zeta_k'(1-) + \beta_k^0 \zeta_k(1) = 2\beta_k^0 e^{\beta_k^0} s_k \qquad (k = 0, \ldots, n-1) \ , \tag{4.51}$$

where

$$r_0 = \frac{1}{2i\kappa_0} \left\{ 2i\kappa_0 A^- + \zeta_0(0) \left[\frac{U_0'}{2U_0} - \tau(\kappa H)' \tanh(\kappa\tau H) \right] \Big|_{0+} + \sum_{j=0}^{n-1} d_{j0}^0 \zeta_j(0) \right\} \ ,$$

$$s_0 = \frac{e^{i\kappa_0}}{2i\kappa_0} \Bigg\{ 2i\kappa_1 A^+ e^{-i\kappa_1} \sqrt{\frac{U_0^1}{U_0^0}} + \zeta_0(1) \Bigg(i(\kappa_0 - \kappa_1) - \left[\frac{U_0'}{2U_0} - \tau(\kappa H)' \tanh(\kappa\tau H) \right] \Big|_{1-} \Bigg)$$
$$+ \sqrt{\frac{U_0^1}{U_0^0}} \sum_{j=0}^{n-1} \sqrt{\frac{U_j^0}{U_j^1}} d_{j0}^1 \zeta_j(1) \Bigg\} \ ,$$

$$r_k = \frac{-1}{2\beta_k^0} \left\{ \zeta_k(0) \left[\frac{U_k'}{2U_k} - \tau(\beta_k H)' \tan(\beta_k \tau H) \right] \Big|_{0+} + \sum_{j=0}^{n-1} d_{jk}^0 \zeta_j(0) \right\} \ ,$$

$$s_k = \frac{-e^{-\beta_k^0}}{2\beta_k^0}\left\{\zeta_k(1)\left(\beta_k^1-\beta_k^0-\left[\frac{U_k'}{2U_k}-\tau(\beta_k H)'\tan(\beta_k\tau H)\right]\Big|_{1-}\right)\right.$$
$$\left.+\sqrt{\frac{U_k^1}{U_k^0}}\sum_{j=0}^{n-1}\sqrt{\frac{U_j^0}{U_j^1}}d_{jk}^1\zeta_j(1)\right\} ,$$

for $(k=1,\ldots,n-1)$, and where $U_k^1 = U_k(1)$ $(k=0,\ldots,n-1)$.

The merit of writing the boundary conditions for ζ_k $(k=0,\ldots,n-1)$ in the form given by (4.50) and (4.51) is that it is now simple to use a variation of parameters procedure to convert the boundary-value problem (4.49) – (4.51) into the integral equation system given by

$$\zeta_k(x) = r_k e^{-\beta_k^0 x} + s_k e^{\beta_k^0 x} - \frac{1}{2\beta_k^0}\int_0^1 e^{-\beta_k^0|x-t|}\left(\rho_k(t)\zeta_k(t)-\sum_{\substack{j=0\\ j\neq k}}^{n-1}\left\{P_{jk}(t)\zeta_j(t)+N_{jk}(t)\zeta_j'(t)\right\}\right)dt \quad , \tag{4.52}$$

for $k=0,\ldots,n-1$, where for $j,k=0,\ldots,n-1$ and $j\neq k$

$$P_{jk}(t) = M_{jk}(t) - \frac{U_j'(t)}{2U_j(t)}N_{jk}(t) .$$

To convert this into a Fredholm system of integral equations, we need to remove the ζ_j' terms in the integral, which we can do on integrating by parts. Let

$$R = \int_0^1 e^{-\beta_k^0|x-t|}\sum_{\substack{j=0\\ j\neq k}}^{n-1}N_{jk}(t)\zeta_j'(t)dt$$
$$= \sum_{\substack{j=0\\ j\neq k}}^{n-1}\left\{ - N_{jk}(0)\zeta_j(0)e^{-\beta_k^0 x} + N_{jk}(1)\zeta_j(1)e^{-\beta_k^0(1-x)}\right.$$
$$\left. - \int_0^1 e^{-\beta_k^0|x-t|}\left(\mathrm{sgn}(x-t)\beta_k^0 N_{jk}(t) + N_{jk}'(t)\right)\zeta_j(t)dt\right\} .$$

From section 4.1, we recall that for $j\neq k$

$$F_{jk}(x) = \left(\left[\tilde{W}_j\tilde{W}_k\right]_{z=-H} + 2\int_{-H}^0 \tilde{W}_k\frac{\partial\tilde{W}_j}{\partial H}dz\right)H'$$
$$= \sec(\beta_k\tau H)\sec(\beta_j\tau H)\left(\frac{{\beta_k}^2+{\beta_j}^2}{{\beta_k}^2-{\beta_j}^2}\right)H' \qquad (j,k=0,\ldots,n-1) ,$$

where $\tilde{W}_k(z,H) = \cos(\beta_k\tau(z+H))\sec(\beta_k\tau H)$ $(k=0,\ldots,n-1)$ and for $j\neq k$

$$\int_{-H}^0 \tilde{W}_k\frac{\partial\tilde{W}_j}{\partial H}dz = \sec(\beta_k\tau H)\sec(\beta_j\tau H)\left(\frac{{\beta_j}^2}{{\beta_k}^2-{\beta_j}^2}\right) \qquad (j,k=0,\ldots,n-1) .$$

Therefore, it follows that we can rewrite F_{jk} (for $j \neq k$) as

$$F_{jk}(x) = \left(\int_{-H}^{0} \left\{ \tilde{W}_k \frac{\partial \tilde{W}_j}{\partial H} - \tilde{W}_j \frac{\partial \tilde{W}_k}{\partial H} \right\} dz \right) H'(x) \ .$$

Hence, for $j \neq k$, we find that F'_{jk} and G_{jk} are related by

$$\begin{aligned} F'_{jk}(x) = & \left(\int_{-H}^{0} \left\{ \tilde{W}_k \frac{\partial \tilde{W}_j}{\partial H} - \tilde{W}_j \frac{\partial \tilde{W}_k}{\partial H} \right\} dz \right) H''(x) \\ & + \left(\int_{-H}^{0} \left\{ \tilde{W}_k \frac{\partial^2 \tilde{W}_j}{\partial H^2} - \tilde{W}_j \frac{\partial^2 \tilde{W}_k}{\partial H^2} \right\} dz + \left[\tilde{W}_k \frac{\partial \tilde{W}_j}{\partial H} - \tilde{W}_j \frac{\partial \tilde{W}_k}{\partial H} \right]_{z=-H} \right) (H'(x))^2 \\ = & \ G_{jk} - G_{kj} \qquad\qquad (j,k = 0, \ldots, n-1) \ . \end{aligned}$$

For $j \neq k$, we can now see that N'_{jk} is given by

$$N'_{jk}(x) = -\frac{1}{2} \left[\frac{U'_j(x)}{U_j(x)} + \frac{U'_k(x)}{U_k(x)} \right] N_{jk}(x) + M_{jk}(x) - \frac{U_j^0}{U_k^0} M_{kj}(x) \quad (j,k = 0, \ldots, n-1) \ .$$

After substituting R into the system (4.52) and rearranging, we find that the functions ζ_k $(k = 0, \ldots, n-1)$ satisfy the system of Fredholm integral equations given by

$$\begin{aligned} \zeta_k(x) = & \ \tilde{r}_k e^{-\beta_k^0 x} + \tilde{s}_k e^{\beta_k^0 x} \\ & - \frac{1}{2\beta_k^0} \int_0^1 e^{-\beta_k^0 |x-t|} \left(\rho_k(t) \zeta_k(t) - \sum_{\substack{j=0 \\ j \neq k}}^{n-1} Q_{jk}(t) \zeta_j(t) \right) dt \ , \end{aligned} \tag{4.53}$$

for $k = 0, \ldots, n-1$, where

$$\tilde{r}_k = r_k - \frac{1}{2\beta_k^0} \sum_{\substack{j=0 \\ j \neq k}}^{n-1} N_{jk}(0) \zeta_j(0) \qquad (k = 0, \ldots, n-1) \ ,$$

$$\tilde{s}_k = s_k + \frac{e^{-\beta_k^0}}{2\beta_k^0} \sum_{\substack{j=0 \\ j \neq k}}^{n-1} N_{jk}(1) \zeta_j(1) \qquad (k = 0, \ldots, n-1)$$

and, for $j \neq k$,

$$Q_{jk}(x,t) = \frac{U_j^0}{U_k^0} M_{kj}(t) + \left[\frac{U'_k(t)}{2U_k(t)} - \mathrm{sgn}(x-t) \beta_k^0 \right] N_{jk}(t) \qquad (j,k = 0, \ldots, n-1) \ .$$

We can express this equation in operator form as

$$\underline{\zeta}(x) = \underline{f}(x) - \left(L \underline{\zeta} \right)(x) \qquad 0 \leq x \leq 1 \ , \tag{4.54}$$

where

$$\underline{\zeta}(x) = \Big(\zeta_0(x),\ \zeta_1(x), \ldots,\ \zeta_{n-1}(x)\Big)^T \quad ,$$

$$\underline{f}(x) = \Big(\tilde{r}_0 e^{i\kappa_0 x} + \tilde{s}_0 e^{-i\kappa_0 x},\ \tilde{r}_1 e^{-\beta_1^0 x} + \tilde{s}_1 e^{\beta_1^0 x}, \ldots,\ \tilde{r}_{n-1} e^{-\beta_{n-1}^0 x} + \tilde{s}_{n-1} e^{\beta_{n-1}^0 x}\Big)^T \quad ,$$

and the operator L is defined by

$$\Big(L\underline{\zeta}\Big)(x) = \int_0^1 \begin{pmatrix} l_{0\ 0}(x,t) & \ldots & l_{0\ n-1}(x,t) \\ \vdots & \ddots & \vdots \\ l_{n-1\ 0} & \ldots & l_{n-1\ n-1}(x,t) \end{pmatrix} \begin{pmatrix} \zeta_0(t) \\ \vdots \\ \zeta_{n-1}(t) \end{pmatrix} dt \quad ,$$

where the terms in the kernel are defined by

$$l_{jk}(x,t) = \begin{cases} \dfrac{1}{2\beta_j^0} e^{-\beta_j^0 |x-t|} \rho_j(t) & (k=j)\ , \\ \dfrac{-1}{2\beta_j^0} e^{-\beta_j^0 |x-t|} Q_{kj}(x,t) & (k \neq j)\ . \end{cases}$$

It is possible to use a variational approach analogous to that used by Chamberlain [7] and summarised in Chapter 2, to find approximate solutions of (4.53). However, this issue is not pursued here because numerical evaluation of the kernel, which is discontinuous, is formidable and an ideal solution procedure has not been formulated yet. It is for this reason that alternative solution methods were sought.

4.5 Solution procedure

Another approach to solve the system of differential equations (4.23) could be to decouple the system by differentiating with respect to x. However, this process does not advance the cause because the coefficients in the resulting differential equations are a lot more cumbersome than those appearing in (4.23).

The solution procedure we shall employ is to rewrite the second-order boundary -value problem given by the differential equation system (4.23) and boundary conditions (4.37) – (4.40) as a system of first-order differential equations satisfying some initial conditions. There is then a great wealth of numerical solution methods available to solve the first-order system (see, for example, Lambert [29]). We

convert the second-order system (4.23) into a first-order system by introducing the functions

$$\psi_k = \phi_k' \qquad\qquad (k = 0, \ldots, n-1) \ .$$

Therefore, the system (4.23) can be rewritten as

$$\underline{p}' = \underline{q}(x, \underline{p}) \ , \tag{4.55}$$

where the $2n$ vectors $\underline{p}$ and $\underline{q}$ are given by

$$\underline{p} = (\phi_0, \ \phi_1, \ldots, \ \phi_{n-1}, \ \psi_0, \ \psi_1, \ldots, \ \psi_{n-1})^T \ ,$$

$$\underline{q} = \begin{pmatrix} \psi_0 \\ \psi_1 \\ \vdots \\ \psi_{n-1} \\ {\beta_0}^2 \phi_0 - \dfrac{1}{U_0} \displaystyle\sum_{j=0}^{n-1} (F_{j\ 0}\, \psi_j + G_{j\ 0}\, \phi_j) \\ {\beta_1}^2 \phi_1 - \dfrac{1}{U_1} \displaystyle\sum_{j=0}^{n-1} (F_{j\ 1}\, \psi_j + G_{j\ 1}\, \phi_j) \\ \vdots \\ {\beta_{n-1}}^2 \phi_0 - \dfrac{1}{U_{n-1}} \displaystyle\sum_{j=0}^{n-1} (F_{j\ n-1}\, \psi_j + G_{j\ n-1}\, \phi_j) \end{pmatrix} \ .$$

Let $\underline{\chi} = (\phi_0, \ldots, \phi_{n-1})^T$, denote the solution of the boundary-value problem (4.23), (4.37) – (4.40). If we knew the initial conditions that $\underline{\chi}$ and $\underline{\chi}'$ satisfy at $x = 0$, then we would only require a numerical method to solve one initial-value problem, given by (4.55) and these initial conditions, to find an approximation to $\underline{\chi}$ at $x = 1$. However, this is not the case because we only know the boundary-value problem satisfied by $\underline{\chi}$. Therefore, we only know n conditions on $\underline{\chi}$ and $\underline{\chi}'$ at $x = 0$, with the other n conditions on $\underline{\chi}$ and $\underline{\chi}'$ being given at $x = 1$. This means that we have to resort to finding $2n$ independent solutions of (4.55) and then the solution $\underline{\chi}$ of the boundary-value problem is given by the particular linear combination of these independent solutions which satisfies the boundary conditions (4.37) – (4.40).

We can write the boundary conditions (4.37) – (4.40) in vector form as

$$\underline{\chi}'(0) + D_0\underline{\chi}(0) = \underline{s}_0 \tag{4.56}$$

and

$$\underline{\chi}'(1) + D_1\underline{\chi}(1) = \underline{s}_1 \ . \tag{4.57}$$

Here, the $n \times n$ matrices D_0 and D_1 are given by

$$D_0 = \begin{bmatrix} -\beta_0^0 - \tilde{d}_{0\ 0}^0 & -d_{1\ 0}^0 & \dots & -d_{n-1\ 0}^0 \\ -d_{0\ 1}^0 & -\beta_1^0 - \tilde{d}_{1\ 1}^0 & \dots & -d_{n-1\ 1}^0 \\ \vdots & \vdots & \ddots & \vdots \\ -d_{0\ n-1}^0 & -d_{1\ n-1}^0 & \dots & -\beta_{n-1}^0 - \tilde{d}_{n-1\ n-1}^0 \end{bmatrix} ,$$

and

$$D_1 = \begin{bmatrix} \beta_0^1 - \tilde{d}_{0\ 0}^1 & -d_{1\ 0}^1 & \dots & -d_{n-1\ 0}^1 \\ -d_{0\ 1}^1 & \beta_1^1 - \tilde{d}_{1\ 1}^1 & \dots & -d_{n-1\ 1}^1 \\ \vdots & \vdots & \ddots & \vdots \\ -d_{0\ n-1}^1 & -d_{1\ n-1}^1 & \dots & \beta_{n-1}^1 - \tilde{d}_{n-1\ n-1}^1 \end{bmatrix} ,$$

where

$$\tilde{d}_{kk}^0 = d_{kk}^0 - [\tau(\beta_k H)' \tan(\beta_k \tau H)]|_{x=0+} \qquad (k = 0, \dots, n-1)$$

and

$$\tilde{d}_{kk}^1 = d_{kk}^1 - [\tau(\beta_k H)' \tan(\beta_k \tau H)]|_{x=1-} \qquad (k = 0, \dots, n-1) \ .$$

The n vectors $\underline{s}_0$ and $\underline{s}_1$ are given by

$$\underline{s}_0 = \left(-2\beta_0^0 A^-,\ 0, \dots,\ 0\right)^T$$

and

$$\underline{s}_1 = \left(2\beta_0^1 e^{\beta_0^1} A^+,\ 0, \dots,\ 0\right)^T \ .$$

Here, we have employed the usual notation $\beta_j^0 = \beta_j(0)$, $\beta_j^1 = \beta_j(1)$ $(j = 0, \dots, n–1)$ and $\beta_0 = -i\kappa$ with κ and β_j $(j = 1, \dots, n-1)$ the solutions of the relations (4.26) and (4.25) respectively.

Now let $\underline{\chi}_1,\ \underline{\chi}_2, \dots,\ \underline{\chi}_{2n}$ denote linearly independent solutions of (4.55), and therefore also linearly independent solutions of the coupled system (4.23). Then,

as we have already noted, the solution $\underline{\chi}$ of the boundary-value problem is given by

$$\underline{\chi} = c_1\underline{\chi}_1 + c_2\underline{\chi}_2 + \ldots + c_{2n}\underline{\chi}_{2n} \tag{4.58}$$

for some constants $c_j \in \mathbb{C}$ $(j = 1, \ldots, 2n)$. These constants are chosen so that $\underline{\chi}$ given by (4.58) satisfies the boundary conditions (4.56) and (4.57). Therefore, substituting (4.58) into (4.56) and (4.57) leaves a matrix equation for the constants c_j $(j = 1, \ldots, 2n)$, which is given by

$$M\underline{c} = \underline{s} \ , \tag{4.59}$$

where M is a $2n \times 2n$ matrix given by $M = [\underline{m}_1, \underline{m}_2, \ldots, \underline{m}_{2n}]$ with the $2n$ vectors $\underline{m}_j$ $(j = 1, \ldots, 2n)$ and $\underline{s}$ given by

$$\underline{m}_j = \begin{pmatrix} \underline{\chi}_j'(0) + D_0\underline{\chi}_j(0) \\ \\ \underline{\chi}_j'(1) + D_1\underline{\chi}_j(1) \end{pmatrix} \qquad (j = 1, \ldots, 2n)$$

and

$$\underline{s} = \begin{pmatrix} \underline{s}_0 \\ \\ \underline{s}_1 \end{pmatrix} \ .$$

Once (4.59) has been solved, then we can find the value of $\underline{\chi}$, the solution of the boundary-value problem, at $x = 1$ and hence calculate the reflection, transmission and decay coefficients.

All that remains to be done is to find the $2n$ independent solutions of (4.55). We shall use a Runge-Kutta method of the form

$$\underline{p}_{n-1} - \underline{p}_n = h\sum_{j=0}^{R} d_j\underline{q}_j^n \ ,$$

in which h is the step size, $x_0 = 0$, $x_n = x_0 + nh$, $\underline{p}_n \approx \underline{p}(x_n)$ and $\underline{q}_j^n = \underline{q}\left(x_n + \gamma_j h,\ \underline{p}_n + h\sum_{s=1}^{j-1}\eta_{js}\underline{q}_s^n\right)$, to approximate $\underline{p}(1)$. These Runge-Kutta numerical schemes are defined on choosing h, γ_j and η_{js} $(j = 1, \ldots, R$ and $s = 1, \ldots, j)$ and their use is well-documented (see Lambert [29], for example). The results we produce in this chapter will be found using the 6^{th}-stage method $(R = 6)$ given by Fehlberg [19] which is of order 5, that is, accurate to $O(h^5)$. This fifth-order Runge-Kutta procedure uses a corresponding fourth-order Runge-Kutta procedure for step size control. Fehlberg uses the fact that

the difference between his 5^{th}-order Runge-Kutta method and the corresponding 4^{th}-order method provides an approximation of the leading term of the truncation error in the 4^{th}-order method. He assumes that if the truncation error is represented, with sufficient accuracy, by its leading term, then a step size control can easily be implemented into the 5^{th}-order Runge-Kutta procedure. A test is made to see whether the truncation error, as obtained from the difference between the 4^{th} and 5^{th}-order methods, exceeds a certain pre-set tolerable error. If it does, the step size is halved, the step is recomputed and tested again. On the other hand, if the truncation errors are much smaller than the tolerable error, then the step size is doubled. Fehlberg finds this type of step size control is quite reliable because, unlike some other methods incorporating step size control, it is based on a complete coverage of the leading term of the truncation error.

We expect that the use of decaying wave mode terms to approximate the scattering problem will cause greater numerical problems than those which occur when the approximation uses only progressive wave mode terms. This is because for wave scattering problems over any depth profile, the decaying wave mode functions β_k $(k = 1, \ldots, n-1)$ satisfying (4.25) increase with k and are much larger than the corresponding progressive mode function κ, which satisfies (4.26), for any given values of the parameters α_0 and τ. We can see this by noting that the k^{th} root of the equation

$$-(\alpha_0\tau)^2 H = (\beta_k\tau H)\tan(\beta_k\tau H) \qquad (k \in \mathbb{N})$$

can be redefined as

$$\beta_k\tau H = k\pi - \delta_k \qquad (0 < \delta_k < \frac{\pi}{2}) \qquad (k \in \mathbb{N}) \ .$$

It follows that

$$k\pi > \beta_k\tau H > \left(k - \frac{1}{2}\right)\pi \qquad (k \in \mathbb{N}) \ .$$

Therefore

$$\beta_{k+1} > \beta_k + \frac{\pi}{2\tau H} \qquad (k \in \mathbb{N}) \ .$$

For example, with a depth profile given by

$$H(x) = \frac{3}{4} + \frac{1}{4}\cos(\pi x) \qquad (0 \le x \le 1) \ ,$$

and parameter values $\alpha_0 = 3$ and $\tau = 0.1$, the functions κ and β_k $(k = 1, \ldots, 3)$ evaluated at $x = 0$ and $x = 1$ are given by

$$\begin{aligned}
\kappa_0 &= 3.0457 \quad , \quad \kappa_1 = 4.2747 \ , \\
\beta_1^0 &= 31.1269 \quad , \quad \beta_1^1 = 62.5441 \ , \\
\beta_2^0 &= 62.6883 \quad , \quad \beta_2^1 = 125.5203 \ , \\
\beta_3^0 &= 94.1552 \quad , \quad \beta_3^1 = 188.4000 \ .
\end{aligned}$$

Therefore, the inclusion of decaying wave modes is certainly going to make the terms in the coupled system (4.23) more rapidly varying. This means that any numerical solution method will require many more steps in $(0, 1)$ for a problem including decaying wave mode terms than a method which solves the problem without decaying wave mode terms, to achieve the same solution accuracy. Hence, a solution method involving step size control should be more effective in controlling the accuracy of the solution, in a wave scattering problem involving decaying wave mode terms, than a fixed step method.

We shall proceed by choosing the simple initial conditions for the n vectors $\underline{\chi}_j$ $(j = 1, \ldots, 2n)$ given by

$$\left.\begin{aligned} \underline{\chi}_j(0) &= \underline{e}_j \\ \underline{\chi}_j'(0) &= \underline{0} \end{aligned}\right\} \quad j = 1, \ldots, n \tag{4.60}$$

and

$$\left.\begin{aligned} \underline{\chi}_j'(0) &= \underline{e}_{j-n} \\ \underline{\chi}_j(0) &= \underline{0} \end{aligned}\right\} \quad j = n+1, \ldots, 2n \ , \tag{4.61}$$

where the n vectors $\underline{e}_j$ $(j = 1, \ldots, n)$ have a '1' in the j^{th} entry, and zeros in the rest. This choice of initial conditions clearly makes $\underline{\chi}_j$ $(j = 1, \ldots, 2n)$ linearly independent.

The solution procedure is to use the Runge-Kutta method to find approximations to $\underline{\chi}_j(1)$ $(j = 1, \ldots, 2n)$ with $\underline{\chi}_j(0)$, $\underline{\chi}_j'(0)$ $(j = 1, \ldots, 2n)$ given by (4.60) and (4.61). Then we solve the matrix system (4.59) to find the constants c_j $(j = 1, \ldots, 2n)$. The general solution $\underline{\chi}$, given by (4.58), is then constructed, and the reflection, transmission and decay coefficients are found using (4.43) – (4.46).

The solution procedure was implemented on the MATLAB software package (produced by the Math Works Inc.). This was used because it is purpose built for

handling vectors and for solving matrix equations. The Runge-Kutta procedure outlined in this section is the default numerical solution method for first-order systems of differential equations on MATLAB. Full details of how this Runge-Kutta procedure is implemented in MATLAB can be found in Forsythe, Malcolm and Moler [21].

4.6 Numerical results

We now present test examples which use the procedure outlined in section 4.5 to solve the boundary-value problem given by the differential system (4.23) and boundary conditions (4.37) – (4.40). We find results using one, two, three and four decaying wave mode terms and compare them with the existing results given by the mild-slope and modified mild-slope approximations. We examine whether the results converge as the number of decaying mode terms in the approximation is increased. We make no attempt to justify the choices used for the parameters α_0 and τ, as we only wish to see if the numerical method can solve the problem accurately.

In the results presented in this section, and in section 4.7, we refer to the approximation $\xi \approx \phi$ given by

$$\xi(x,z) = \sum_{j=0}^{N-1} \phi_j(x) w_j(x,z)$$

which generates the differential system (4.23), as the 'N-term approximation'. Therefore the 1-term approximation is the modified mild-slope approximation. The results given by the modified mild-slope approximation will be referred to as the results given by the MMSE and the results given by the mild-slope approximation will be referred to as the results given by the MSE. The boundary conditions used with the MMSE and MSE in this section are those given by (4.42), that is, the new boundary conditions that were derived in section 4.3.

For the 2-term approximation, we illustrate the convergence of the numerical method, as we increase the tolerance in the step size control, and go on to give the solutions of interest. We then investigate the behaviour of the initial- value problem solutions $\underline{\chi}_j$ $(j = 1, \ldots, 2n)$ as we increase the number of terms in the trial approximation and for different values of the parameters α_0 and τ.

Example 4.1

Suppose that a wave of unit amplitude is incident from $x = -\infty$ on a talud whose scaled depth profile is given by

$$H(x) = 1 - \frac{1}{2}x^2 \qquad (0 \leq x \leq 1) \ .$$

This depth profile represents a concave talud. We choose parameter values

$$\alpha_0 = 2 \ ,$$
$$\tau = 0.5 \ .$$

(This could represent the physical situation where $h_0 = 1m$, $l = 2m$, $\sigma = \sqrt{g}s^{-1}$). We shall seek approximations to the reflection coefficient of the progressive wave and the coefficients of the reflected decaying wave modes at $x = 0$.

Concentrating on the 2-term approximation, we now use the computer program to generate approximations to $\underline{\chi}_j(1)$ $(j = 1, \ldots, 4)$ for a series of tolerances in the Runge-Kutta method. The results are presented in Table 4.1.

Tolerance	$\underline{\chi}_1$	$\underline{\chi}_2 \times 10^2$	$\underline{\chi}_3$	$\underline{\chi}_4 \times 10^2$
10^{-3}	$\begin{pmatrix} 0.04021 \\ 7.21317 \end{pmatrix}$	$\begin{pmatrix} 0.81801 \\ 6.21359 \end{pmatrix}$	$\begin{pmatrix} 0.02054 \\ -1.42008 \end{pmatrix}$	$\begin{pmatrix} 0.14743 \\ 1.11987 \end{pmatrix}$
10^{-6}	$\begin{pmatrix} 0.04036 \\ 7.21407 \end{pmatrix}$	$\begin{pmatrix} 0.81814 \\ 6.21443 \end{pmatrix}$	$\begin{pmatrix} 0.02051 \\ -1.42025 \end{pmatrix}$	$\begin{pmatrix} 0.14745 \\ 1.12002 \end{pmatrix}$
10^{-9}	$\begin{pmatrix} 0.04037 \\ 7.21415 \end{pmatrix}$	$\begin{pmatrix} 0.81814 \\ 6.21444 \end{pmatrix}$	$\begin{pmatrix} 0.02051 \\ -1.42028 \end{pmatrix}$	$\begin{pmatrix} 0.14745 \\ 1.12003 \end{pmatrix}$

Table 4.1: Approximations to $\underline{\chi}_j(1)$ $(j = 1, \ldots, 4)$

We observe that the step size control on the Runge-Kutta method works well, with the approximations to $\underline{\chi}_j(1)$ $(j = 1, \ldots, 4)$ converging to 5 significant figures (5.s.f.) for a tolerance of 10^{-6}. For all these tolerances, the M matrix in equation (4.59) has a condition number 1.0×10^4. MATLAB can solve (4.59) very accurately to give the constants c_j $(j = 1, \ldots, 4)$ correct to 13.d.p., that is, $M\underline{c} - \underline{s} = O(10^{-13})$. Table 4.2 presents the approximation to the amplitude of the reflected plane wave $|R_1^0|$ and to the amplitude of the reflected decaying wave

mode at $x = 0$ $|R_1^1|$ calculated using the above tolerances in the Runge-Kutta method. We can see that both amplitudes of reflection have converged to 6.d.p.

Tolerance	$\lvert R_1^0\rvert$ $(6d.p.)$	$\lvert R_1^1\rvert$ $(6d.p.)$
10^{-3}	0.064150	0.006390
10^{-6}	0.064150	0.006390
10^{-9}	0.064150	0.006390

Table 4.2: Approximations to $|R_1^0|$ and $|R_1^1|$ for the 2-term approximation

when the tolerance in the Runge-Kutta method is 10^{-3}.

Now, remember that we wish to compare our results with those given by the mild-slope equation (MSE) and the modified mild-slope equation (MMSE). We can either use Chamberlain's integral equation procedure to do this or use the Runge-Kutta method given in this chapter. In keeping with the spirit of this chapter, we use the Runge-Kutta method with a tolerance of 10^{-6} to find the following approximations to the coefficient of the reflected plane wave.

$$\begin{aligned} \text{MSE:}\ \ R_1^0 &= -0.038531 - 0.041166i \qquad (|R_1^0| = 0.056385) \\ \text{MMSE:}\ \ R_1^0 &= -0.047743 - 0.044376i \qquad (|R_1^0| = 0.065181) \end{aligned}$$

These results are accurate to 6.d.p., in the sense that they agree to 6.d.p. with results given by the Runge-Kutta method with an increased tolerance of 10^{-9}. Now with a 2-term trial approximation, the coefficient of the reflected plane wave (using a tolerance of 10^{-6} in the Runge-Kutta method) is given by

$$\text{2-term:}\ \ R_1^0 = -0.052240 - 0.037232i\ .$$

We shall now investigate the solutions of the initial-value problem (4.55), (4.60) and (4.61) as we increase the number of terms in the trial approximation. For the MMSE (that is, the 1-term approximation), the Runge-Kutta method gives approximations to $\underline{\chi}_1(1)$ and $\underline{\chi}_2(1)$ as

$$\underline{\chi}_1(1) = -0.898 \qquad \text{and} \qquad \underline{\chi}_2(1) = 0.209\ .$$

Comparing these solutions of the initial-value problem (4.55),(4.60) and (4.61) with those given in Table 4.1 for the 2-term approximation illustrates that in the

2-term approximation case the solutions of the initial-value problem are growing. From the flat bed solutions of the differential system (4.23), we know that the system has decaying/growing wave mode solutions that behave as decaying/growing exponentials. Applying boundary conditions (4.37) – (4.40) to (4.23) then removes these growing wave mode solutions. In our solution method, as we are solving (4.23) with some initial-values (that do not correspond to the initial- values satisfied by the solution of the BVP (4.23), (4.37) – (4.40)), then these growing wave modes are still present and cause the growth of the initial-value solution from $x = 0$ to $x = 1$. The degree to which these growing wave mode terms affect the solution is certainly dependent on the magnitude of β_k $(k = 1, \ldots, n-1)$. We have already shown that $\beta_{k+1} > \beta_k$ $(k \in \mathbb{N})$. This implies that if we increase the number of terms in the approximation, then the magnitude of the solutions of the initial-value problem (4.55),(4.60) and (4.61) at $x = 1$ will also increase.

If we now use the 3-term approximation, then with a tolerance of 10^{-6} in the Runge-Kutta method, we find that

$$\underline{\chi}_1(1) = \begin{pmatrix} 0.104 \\ -0.560 \\ -1.822 \end{pmatrix} \times 10^3, \qquad \underline{\chi}_2(1) = \begin{pmatrix} 0.247 \\ -1.234 \\ -4.178 \end{pmatrix} \times 10^4, \qquad \underline{\chi}_3(1) = \begin{pmatrix} -0.123 \\ 0.668 \\ 2.141 \end{pmatrix} \times 10^6,$$

$$\underline{\chi}_4(1) = \begin{pmatrix} -0.064 \\ 0.349 \\ 1.126 \end{pmatrix} \times 10^3, \qquad \underline{\chi}_5(1) = \begin{pmatrix} 0.491 \\ -2.471 \\ -8.324 \end{pmatrix} \times 10^3, \qquad \underline{\chi}_6(1) = \begin{pmatrix} -0.100 \\ 0.547 \\ 1.752 \end{pmatrix} \times 10^5,$$

clearly illustrating the large growth in the solutions of the initial- value problem from $x = 0$ to $x = 1$. The condition number of the matrix M in equation (4.59) is now

$$\text{cond}(M) = 7.1 \times 10^7 \ ,$$

and MATLAB can calculate the constants c_j $(j = 1, \ldots, 6)$ correct to 10.d.p. The coefficient of the reflected progressive wave is given by

$$\text{3-term:} \quad R_1^0 = -0.053247 - 0.035397i \qquad (|R_1^0| = 0.063939).$$

The above estimate for R_1^0 agrees to 6.d.p. with that given when the tolerance in the method is increased to 10^{-9}. Notice that this reflection coefficient agrees

with the corresponding reflection coefficient given by the 2-term approximation in the first 2 decimal places.

If we now use the 4-term approximation, then with a tolerance of 10^{-6} in the Runge-Kutta method, we find that

$$\underline{\chi}_1(1) \sim O\left(10^5\right), \quad \underline{\chi}_2(1) \sim O\left(10^7\right), \quad \underline{\chi}_3(1) \sim O\left(10^8\right), \quad \underline{\chi}_4(1) \sim O\left(10^9\right),$$

$$\underline{\chi}_5(1) \sim O\left(10^5\right), \quad \underline{\chi}_6(1) \sim O\left(10^6\right), \quad \underline{\chi}_7(1) \sim O\left(10^7\right), \quad \underline{\chi}_8(1) \sim O\left(10^8\right),$$

again illustrating the large growth in the solutions of the initial- value problem from $x = 0$ to $x = 1$. The condition number of the matrix M in equation (4.59) is now

$$\text{cond}(M) = 2.5 \times 10^{11} \ .$$

MATLAB can still solve (4.59), but the constants c_j $(j = 1, \ldots, 6)$ are only given correct to 7.d.p. The coefficient of the reflected progressive wave is given by

$$\text{4-term:} \ \ R_1^0 = -0.053629 - 0.034675i \qquad (|R_1^0| = 0.063862).$$

The above estimate for R_1^0 agrees to 3.d.p. with that given when the tolerance in the method is increased to 10^{-9}. With a tolerance of 10^{-9} in the Runge-Kutta method, the estimate for R_1^0 is given by

$$\text{4-term:} \ \ R_1^0 = -0.053699 - 0.034580i \qquad (|R_1^0| = 0.063869).$$

This estimate for R_1^0 agrees to 7.d.p. with that given when the tolerance in the method is increased to 10^{-10}. So, as the size of the solutions of the initial-value problem grow, we need to increase the tolerance in the Runge-Kutta method in order to maintain the solution accuracy.

Finally, if we use the 5-term approximation, then with a tolerance of 10^{-9} in the Runge-Kutta method, we find that

$$\underline{\chi}_1(1) \sim O\left(10^8\right), \quad \underline{\chi}_2(1) \sim O\left(10^9\right), \quad \underline{\chi}_3(1) \sim O\left(10^{10}\right),$$

$$\underline{\chi}_4(1) \sim O\left(10^{11}\right), \quad \underline{\chi}_5(1) \sim O\left(10^{12}\right), \quad \underline{\chi}_6(1) \sim O\left(10^8\right),$$

$$\underline{\chi}_7(1) \sim O\left(10^9\right), \quad \underline{\chi}_8(1) \sim O\left(10^9\right), \quad \underline{\chi}_9(1) \sim O\left(10^{10}\right), \quad \underline{\chi}_{10}(1) \sim O\left(10^{11}\right),$$

illustrating huge growth in the solutions of the initial- value problem from $x = 0$ to $x = 1$. The condition number of the matrix M in equation (4.59) is now

$$\text{cond}(M) = 6.0 \times 10^{14} \ .$$

MATLAB can still solve (4.59), but the constants c_j $(j = 1, \ldots, 6)$ are only given correct to 4.d.p. The coefficient of the reflected progressive wave is given by

$$\text{5-term:} \quad R_1^0 = -0.0539 - 0.0341i \qquad (|R_1^0| = 0.0638).$$

The above estimate for R_1^0 agrees to 4.d.p. with that given when the tolerance in the method is increased to 10^{-10}.

With 6 or more terms in the approximation, we find that the solutions of the initial-value problems at $x = 1$ are so large that MATLAB can no longer solve (4.59) and so solutions of the BVP cannot be found. It follows from the relation (4.25) that once α_0 and τ have been prescribed, the maximum value of the functions β_k $(k = 1, \ldots, n-1)$ occurs at the minimum value of H, that is, at the minimum depth. In this example the minimum depth is at $x = 1$ and the maximum values are

$$\beta_1(1) = 11.90 \ , \quad \beta_2(1) = 24.81 \ , \quad \beta_3(1) = 37.49 \ , \quad \beta_4(1) = 50.11 \ , \quad \beta_5(1) = 62.70 \ .$$

Obviously, we wish to stop the solutions of the initial-value problem (4.55), (4.60) and (4.61) growing. To do this we need to know the initial conditions that the solution of the BVP satisfies, as these initial conditions would remove the growing exponential terms from the initial-value problem. However, we do not know these initial conditions and so the question then becomes whether we can improve the situation. In other words, can we choose initial conditions so that the solutions of the first-order system (4.55) do not grow as rapidly as the solutions of (4.55) that satisfy the initial conditions (4.60) and (4.61) ?

We have already noted that the differential equation system (4.23) has decaying/growing wave mode solutions over a flat bed with undisturbed fluid depth $H(0)$ given by

$$\phi_k(x) = S_k e^{\beta_k^0 x} + T_k e^{-\beta_k^0 x} \qquad (0 \le x \le 1) \qquad\qquad (k = 1, \ldots, n-1) \ ,$$

for some constants S_k and T_k $(k = 1, \ldots, n-1)$. Initial conditions of the form

$$\phi_k(0) = 1 \qquad \phi_k'(0) = -\beta_k^0 \qquad (k = 1, \ldots, n-1) \ ,$$

clearly remove the growing exponential term in these flat bed solutions. We have found that if we use these $n-1$ initial conditions with the first-order system (4.55), the solutions of the revised IVP at $x = 1$ are smaller by up to 3 orders in magnitude than the solutions obtained with the original initial conditions,

$$\left.\begin{array}{l} \underline{\chi}_j(0) = \underline{e}_j \\ \underline{\chi}_j'(0) = \underline{0} \end{array}\right\} \quad j = 2, \ldots, n \ .$$

We have not yet found an improved choice for the remaining $n+1$ initial conditions and so we retain the present ones. Therefore, the initial conditions we are now going to employ with the first-order system (4.55) are

$$\left.\begin{array}{l} \underline{\chi}_j(0) = \underline{e}_j \\ \underline{\chi}_j'(0) = \underline{d}_j \end{array}\right\} \quad j = 1, \ldots, n \tag{4.62}$$

and

$$\left.\begin{array}{l} \underline{\chi}_j'(0) = \underline{e}_{j-n} \\ \underline{\chi}_j(0) = \underline{0} \end{array}\right\} \quad j = n+1, \ldots, 2n \ , \tag{4.63}$$

where $\underline{d}_j = -\beta_j^0 \underline{e}_j$ $(j = 2, \ldots, n)$ and $\underline{d}_1$ is the zero vector. With this choice of initial conditions, the functions $\underline{\chi}_j$ $(j = 1, \ldots, 2n)$ are clearly linearly independent.

We now return to the example at hand. For the 2-term approximation, using a tolerance of 10^{-6} in the numerical method, we find that the solution $\underline{\chi}_2$ of (4.59) together with initial condition (4.62) is

$$\underline{\chi}_2(1) = \begin{pmatrix} -0.710 \\ -5.409 \end{pmatrix} \ ,$$

which is a reduction of 2 orders in magnitude on the previous solution. Now $\mathrm{cond}(M) = 1.8 \times 10^3$ which is a reduction of 1 order of magnitude on the previous value.

For the 3-term trial approximation, using a tolerance of 10^{-6} in the numerical method, the solutions $\underline{\chi}_2(1)$ and $\underline{\chi}_3(1)$ of (4.59) with initial conditions given by

(4.62) are

$$\underline{\chi}_2(1) = \begin{pmatrix} -0.276 \\ 1.494 \\ 4.809 \end{pmatrix} \times 10^3 \qquad \underline{\chi}_3(1) = \begin{pmatrix} 0.213 \\ -1.156 \\ -3.714 \end{pmatrix} \times 10^3.$$

So $\underline{\chi}_2(1)$ and $\underline{\chi}_3(1)$ have been reduced by 2 orders of magnitude from the previous solutions. Now $\text{cond}(M) = 5.8 \times 10^6$, which is again a reduction of one order in magnitude from the previous value.

For the 4-term approximation, using a tolerance of 10^{-9} in the numerical method, the solutions $\underline{\chi}_2(1)$, $\underline{\chi}_3(1)$ and $\underline{\chi}_4(1)$ of (4.59) with initial conditions given by (4.62) are now such that

$$\underline{\chi}_2(1) \sim O\left(10^6\right), \quad \underline{\chi}_3(1) \sim O\left(10^6\right), \quad \underline{\chi}_4(1) \sim O\left(10^6\right).$$

So $\underline{\chi}_2(1)$ has been reduced by 1 order of magnitude, $\underline{\chi}_3(1)$ has been reduced by 2 orders of magnitude and $\underline{\chi}_4(1)$ has been reduced by 3 orders of magnitude from the previous solutions. Now $\text{cond}(M) = 1.3 \times 10^{10}$, which is again a reduction of 1 order in magnitude from the previous solution.

For the 5-term approximation, using a tolerance of 10^{-9} in the numerical method, the solutions $\underline{\chi}_2(1)$, $\underline{\chi}_3(1)$ and $\underline{\chi}_4(1)$ of (4.59) with initial conditions given by (4.62) are now such that

$$\underline{\chi}_2(1) \sim O\left(10^9\right), \quad \underline{\chi}_3(1) \sim O\left(10^9\right), \quad \underline{\chi}_4(1) \sim O\left(10^9\right), \quad \underline{\chi}_5(1) \sim O\left(10^9\right).$$

So $\underline{\chi}_2(1)$ is the same order of magnitude as before, $\underline{\chi}_3(1)$ has been reduced by 1 order of magnitude, $\underline{\chi}_4(1)$ has been reduced by 2 orders of magnitude and $\underline{\chi}_5(1)$ has been reduced by 3 orders of magnitude from the previous solutions. Now $\text{cond}(M) = 3.3 \times 10^{13}$, which is again a reduction of 1 order in magnitude from the previous solution. Now, MATLAB can determine the constants c_j $(j = 1, \ldots, 6)$ correct to 5.d.p. The coefficient of the reflected progressive wave is given by

$$\text{5-term:} \quad R_1^0 = -0.05395 - 0.03411i \qquad (|R_1^0| = 0.06384).$$

The above estimate for R_1^0 agrees to 5.d.p. with that given when the tolerance in the method is increased to 10^{-10}.

However, the solutions of the initial-value problem (4.55), (4.62) and (4.63) for a 6 or higher term approximation are still too large and so MATLAB cannot solve the system (4.59).

Let us now compare these n-term approximation estimates for R_1^0 where $n = 1, \ldots, 5$. From above we recall that

$$\begin{aligned}
\text{MMSE: } R_1^0 &= -0.047743 - 0.044376i \qquad (|R_1^0| = 0.065181) ,\\
\text{2-term: } R_1^0 &= -0.052240 - 0.037232i \qquad (|R_1^0| = 0.064150) ,\\
\text{3-term: } R_1^0 &= -0.053247 - 0.035397i \qquad (|R_1^0| = 0.063939) ,\\
\text{4-term: } R_1^0 &= -0.053699 - 0.034580i \qquad (|R_1^0| = 0.063869) ,\\
\text{5-term: } R_1^0 &= -0.05395 - 0.03411i \qquad (|R_1^0| = 0.06384) .
\end{aligned}$$

From these results, we can see that as we increase the number of terms in the approximation, the estimate of R_1^0 converges. We also notice that $|R_1^0|$ given by the 4-term and 5-term approximations agree to 4.d.p.

The coefficient of the first decaying wave mode evaluated at $x = 0$ given by the 2-term, 3-term, 4-term and 5-term approximations calculated using a tolerance of 10^{-6}, 10^{-6}, 10^{-9} and 10^{-9} respectively are

$$\begin{aligned}
\text{2-term: } R_1^1 &= -0.005600 + 0.003077i \qquad (|R_1^1| = 0.006390) ,\\
\text{3-term: } R_1^1 &= -0.005755 + 0.003181i \qquad (|R_1^1| = 0.006576) ,\\
\text{4-term: } R_1^1 &= -0.005813 + 0.003225i \qquad (|R_1^1| = 0.006647) ,\\
\text{5-term: } R_1^1 &= -0.00584 + 0.00324i \qquad (|R_1^1| = 0.00668) .
\end{aligned}$$

Again, we see convergence in the estimate of R_1^1 as the number of terms in the trial function is increased, with $|R_1^1|$ given by the 4-term and 5-term approximations the same to 4.d.p.

The coefficient of the second decaying wave mode evaluated at $x = 0$ given by the 3-term, 4-term and 5-term approximations calculated using a tolerance of 10^{-6}, 10^{-9} and 10^{-9} respectively are

$$\begin{aligned}
\text{3-term: } R_1^2 &= 0.000306 - 0.000613i \qquad (|R_1^2| = 0.000685) ,\\
\text{4-term: } R_1^2 &= 0.000313 - 0.000626i \qquad (|R_1^2| = 0.000700) ,\\
\text{5-term: } R_1^2 &= 0.00031 - 0.00063i \qquad (|R_1^2| = 0.00070) .
\end{aligned}$$

The convergence is again evident, with $|R_1^2|$ given by the 4-term and 5-term approximations the same to 5.d.p.

The coefficient of the second decaying wave mode evaluated at $x = 0$ given by the 4-term and 5-term approximations calculated using a tolerance of 10^{-9} are

$$\begin{aligned} \text{4-term: } R_1^3 &= -0.000059 + 0.000118i \qquad (|R_1^3| = 0.000197) \ , \\ \text{5-term: } R_1^3 &= -0.00006 \ + 0.00019i \qquad (|R_1^3| = 0.00020) \ , \end{aligned}$$

which agree to the first 4 decimal places. The coefficient of the fourth decaying wave mode evaluated at $x = 0$ given by the 5-term approximation calculated using a tolerance of 10^{-9} is

$$\text{5-term: } R_1^4 = 0.00001 \ - 0.00008i \qquad (|R_1^4| = 0.00008) \ .$$

The coefficient of the first decaying wave mode evaluated at $x = 0$ is one order of magnitude larger than the corresponding coefficient of the second decaying wave mode. As $\beta_k < \beta_{k+1}$ $(k \in \mathbb{N})$, the $(k+1)^{\text{th}}$ decaying wave mode decays away more rapidly than the k^{th} as $x \to \pm\infty$. This clearly illustrates that the first decaying wave mode is much more significant than the second decaying wave mode, which will be more significant than the third, etc.

We shall now investigate the solutions of the initial-value problem (4.55), (4.62) and (4.63) for a different choice of the parameters α_0 and τ. If we now assign the following values to α_0 and τ given by

$$\alpha_0 = 6 \ , \qquad \tau = 0.2 \ ,$$

then the maximum values of the functions β_k $(k = 1, \ldots, n-1)$ in the interval $[0, 1]$ are now

$$\beta_1(1) = 28.98 \ , \qquad \beta_2(1) = 61.67 \ , \qquad \beta_3(1) = 93.48 \ .$$

So for these values of α_0 and τ the functions β_k $(k = 1, \ldots, n-1)$ are much larger than at the previous values of α_0 and τ. Consequently, the solutions of the initial-value problem (4.55), (4.62) and (4.63) evaluated at $x = 1$ will also be larger in magnitude at these values of α_0 and τ. Indeed, using a tolerance of 10^{-9} in the Runge-Kutta method, we find for a 2-term approximation that

$$\underline{\chi}_1(1) = \begin{pmatrix} 0.129 \\ 2.454 \end{pmatrix} \times 10^4, \qquad \underline{\chi}_2(1) = \begin{pmatrix} -0.119 \\ -2.270 \end{pmatrix} \times 10^4,$$

$$\underline{\chi}_3(1) = \begin{pmatrix} 4.891 \\ 90.87 \end{pmatrix}, \qquad \underline{\chi}_4(1) = \begin{pmatrix} 0.053 \\ 1.017 \end{pmatrix} \times 10^6,$$

Now, $\text{cond}(M) = 3.9 \times 10^7$, where M is the matrix in equation (4.59), and MATLAB can determine the constants c_j $(j = 1, \ldots, 4)$ accurate to 9.d.p.

For a 3-term approximation

$$\underline{\chi}_1 \sim O(10^{12}) , \qquad \underline{\chi}_2 \sim O(10^{12}) , \qquad \underline{\chi}_3 \sim O(10^{12}),$$

$$\underline{\chi}_4 \sim O(10^{11}) , \qquad \underline{\chi}_5 \sim O(10^{12}) , \qquad \underline{\chi}_6 \sim O(10^{14}).$$

Now, $\text{cond}(M) = 4 \times 10^{16}$, where M is the matrix in equation (4.59), and we cannot now determine the constants c_j $(j = 1, \ldots, 6)$.

In this section, we have shown that as the number of decaying wave mode terms in the approximation is increased, the results given can visibly be seen to converge. We have demonstrated that the solution method we are employing to solve the BVP (4.23), (4.37) – (4.40) is restricted by the magnitude of the functions β_k $(k = 1, \ldots, n-1)$, which limits the number of terms we can use in the approximation to ϕ. We have also seen that the tolerance in the Runge-Kutta method needs to be increased as the size of the initial-value problem solutions increase in order to maintain solution accuracy. The n-term approximation should give different (and more accurate) approximations to the coefficients of the scattered waves over steep bed profiles than the MSE and the MMSE, because the decaying modes are more significant for steeper bed profiles. As the slope of the bed profile reduces, the results given by these approximations should become very similar as the effect of the decaying modes diminishes. In section 4.7, we examine the results given by these approximations as the steepness of a depth profile is varied. We show how the maximum values of the functions β_k $(k = 1, \ldots, n-1)$ in the interval $[0, 1]$ vary as the steepness of the bed is varied. We find that the steeper the bed profile, the smaller the magnitude of the functions β_k $(k = 1, \ldots, n-1)$. As the slope of the bed profile decreases, so β_k $(k = 1, \ldots, n-1)$ increase in magnitude. So, the solution method given here can be used to obtain the results given by the 2, 3 and 4-term approximations for steep bed profiles, which are the results of prime interest. We find that the results given by the 2, 3 and 4-term approximations converge to those given by

the MMSE before the bed profile becomes too mild for results to be found. These results are presented graphically in section 4.7.

4.7 Graphical results

In this section, we consider three examples where the results are best presented graphically. In the first example we plot the approximation to the free surface at two different time intervals for normal incidence. In the other two examples, we show how the amplitude of the reflected progressive wave varies with the steepness of the bed profile. We consider two shapes of bed profile – a talud and a hump, and compare results given by the MSE, MMSE, 2-term, 3-term and 4-term approximations. We also compare results given by the MSE and MMSE with the two sets of boundary conditions discussed in section 4.3.

Example 4.2

Here the depth profile is given by

$$H(x) = \frac{3}{4} + \frac{1}{4}\cos\left(2\pi x^2\right) \qquad (0 \le x \le 1) \ ,$$

which represents an asymmetric hump whose height is half the still water depth. The parameters α_0 and τ are chosen to be

$$\begin{aligned} \alpha_0 &= 2.5 \ , \\ \tau &= 0.4 \ . \end{aligned}$$

The n-term approximation to the free surface elevation is given by

$$\eta \approx \mathrm{Re}\left\{ e^{-i\sigma t} \sum_{j=0}^{n-1} \phi_j \right\} \ .$$

For an incident wave of unit amplitude from $x = -\infty$, the approximation to the free surface at time $t = 2j\frac{\pi}{\sigma}$ $(j+1 \in \mathbb{N})$ is given by

$$\eta(x,t) \approx \mathrm{Re}\left\{ \begin{array}{cc} e^{i\kappa_0 x} + R_1^0 e^{-i\kappa_0 x} + \sum_{j=1}^{n-1} R_1^j e^{\beta_j^0 x} & (x \le 0) \ , \\ \sum_{j=0}^{n-1} \phi_j(x) & (0 \le x \le 1) \ , \\ T_1^0 e^{i\kappa_1 x} + \sum_{j=1}^{n-1} T_1^j e^{-\beta_j^1 x} & (x \ge 1) \ . \end{array} \right.$$

The results displayed in Fig.4.1 were obtained by running the computer program with a tolerance of 10^{-6} in the Runge-Kutta method for the MSE, MMSE, 2-term

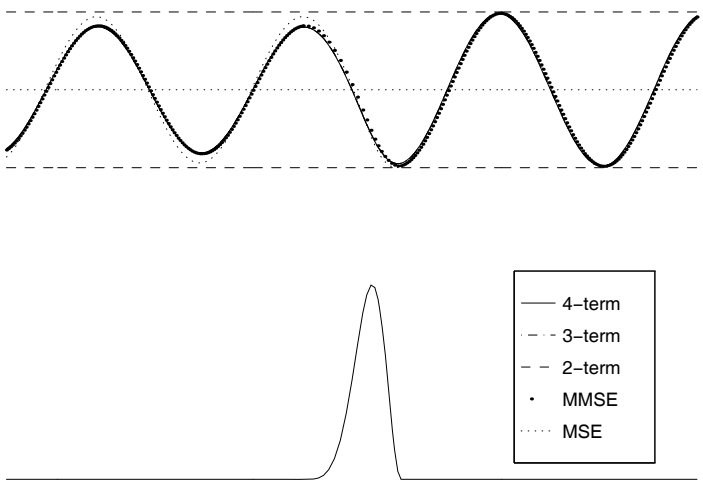

Figure 4.1: Free surface elevation

and 3-term approximations, and a tolerance of 10^{-9} for the 4-term approximation. With these tolerances, the solutions for each approximation had converged to 6.d.p. The depth profile is also displayed in Fig.4.1 and we have exaggerated the amplitude of the waves to make the figure clearer. The dashed lines represent the amplitude of the incident wave and the dotted line represents the undisturbed free surface. At this instant, we observe that destructive interference produces a wave which has an amplitude smaller than that of the incident wave in $x \leq 0$. All the decaying wave modes decay away very rapidly as they move away from the hump and the contribution they all make to the free surface shape at the left and right-hand ends in Fig.4.1 is negligible. We note that the n-term approximation to the free surface has converged (as far as one can tell by the eye) when $n = 4$, with only a small difference in results given by the MMSE and 4-term approximations. So, for these values of α_0 and τ the hump is steep enough for the decaying wave modes to make a small, but noticeable contribution.

Fig.4.2 displays the same free surface after σt has increased by $\frac{1}{3}\pi$. The diagram indicates the presence of constructive interference in $x \leq 0$. Again, there is a small difference in the results given by the MMSE and the 4-term approximation.

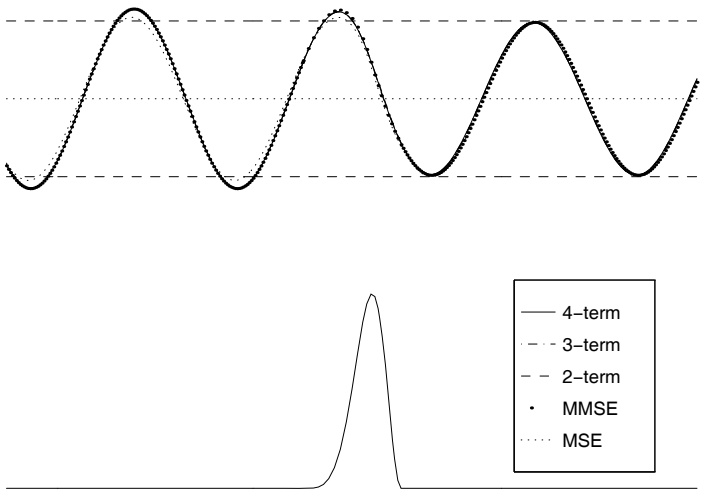

Figure 4.2: Free surface elevation after σt has increased by $\frac{1}{3}\pi$

Example 4.3

We now return to the talud problem considered by Booij [5], in which the accuracy of the mild-slope approximation was tested as the gradient of the talud varied. This was done by comparing the amplitude of the reflection coefficient ($|R_1^0|$) given by the MSE with the corresponding value computed using the full linearised theory. The boundary conditions used by Booij [5] with the MSE correspond to the set (4.41) given in section 4.3. The varying depth profile we are considering here is given by

$$H(x) = 1 - \frac{2}{3}x \qquad\qquad (0 \leq x \leq 1) \ ,$$

so at $x = 0$ and $x = 1$, where the talud meets the flat beds, the slope of the depth profile is discontinuous. In [5], the unscaled problem Booij considered had flat bed depths $h_0 = 0.6m$ and $h_1 = 0.2m$. Booij computed $|R_1^0|$ using the full linearised theory at values of a parameter W_s which denotes the length of the talud. Our parameters α_0 and τ are defined in terms of W_s by

$$\alpha_0 = \frac{W_s}{\sqrt{0.6}} \ , \qquad \tau = \frac{0.6}{W_s}, \qquad \text{so that} \quad \alpha_0 = \frac{\sqrt{0.6}}{\tau} \ .$$

Returning to the definitions of α_0 and τ, we recall that

$$\alpha_0 = \frac{\sigma l}{\sqrt{g h_0}} , \qquad \tau = h_0/l .$$

So with α_0 and τ given in terms of W_s as above, we see that

$$\sqrt{0.6}\alpha_0 = \frac{\sigma^2}{g} l , \qquad \frac{\tau}{0.6} = \frac{1}{\frac{\sigma^2}{g} l} .$$

It follows that varying W_s is equivalent to varying the length l of the talud, and therefore the steepness of the talud at each fixed value of $\frac{\sigma^2}{g}$, the deep water wave number. Following Booij [5], we seek results for our new approximation for values of W_s from 0.1 to 6 at intervals of 0.05. As W_s varies from 0.1 to 6, $\alpha_0\tau = \sqrt{0.6}$ and τ decreases monotonically. Therefore, the functions β_k $(k = 1, \ldots, n-1)$, the roots of the relations

$$-(\alpha_0\tau)^2 H = (\beta_k \tau H)\tan(\beta_k \tau H) \qquad (k \in \mathbb{N}) ,$$

monotonically increase as W_s increases. Note that the minimum depth in this example occurs at $x = 1$, and so the maximum value of β_k $(k = 1, \ldots, n-1)$ in the interval $[0, 1]$ is at $x = 1$. When $W_s = 0.1$, we find that

$$\beta_1(1) = 1.54 , \qquad \beta_2(1) = 3.13 , \qquad \beta_3(1) = 4.70 , \qquad \beta_4(1) = 6.28 .$$

When $W_s = 6$, we find that

$$\beta_1(1) = 92.30 , \qquad \beta_2(1) = 187.54 , \qquad \beta_3(1) = 282.11 , \qquad \beta_4(1) = 376.51 .$$

We saw in section 4.6 that when the maximum value of β_k $(k = 1, \ldots, n-1)$ was greater than 60, solutions of the boundary-value problem could not be found. Therefore as W_s increases, there will be a value of W_s at which the function β_1 is large enough to make the solutions of the initial-value problem for the 2-term approximation too large for the system (4.59) to be solved to a minimum accuracy. The minimum accuracy we require is three decimal places. For the 3-term approximation, the value of W_s at which the system (4.59) cannot be solved to this minimum accuracy will be smaller than that for the 2-term as $\beta_2 > \beta_1$, and so on for the 4,5,..-term approximations.

Using the solution procedure outlined in sections 4.5 and 4.6, it turns out that for the 2-term approximation, when $W_s = 4.35$, $\beta_1(1) = 65.54$,

cond$(M) = 3.9 \times 10^{15}$ and equation (4.59) cannot be solved to the minimum accuracy we have specified. When $W_s = 2.15$, $\beta_2(1) = 66.58$ and the results given by the 3-term approximation cannot be found to the minimum accuracy for $W_s \geq 2.15$. When $W_s = 1.45$, $\beta_3(1) = 68.18$ and the results given by the 4-term approximation cannot be found to the minimum accuracy for $W_s \geq 1.45$. For all the n-term approximations, we initially use a tolerance in the Runge-Kutta method of 10^{-6} which rises to 10^{-11} as W_s increases, in accordance with the size of the solutions of the initial- value problem. The initial-value problem solutions obtained therefore have all converged to at least 4 significant figures. Remember that for the MSE and MMSE we do not have a problem with the initial-value problem solutions growing because these approximations do not contain any exponentially growing/decaying wave modes. Therefore, for the MSE and MMSE we use a tolerance of 10^{-6} in the Runge-Kutta method over the whole W_s range which gives solutions accurate to 6.d.p.

The first set of results we give, are those given by the MSE and MMSE with the old set (4.41) and new set (4.42) of boundary conditions. These are presented in Fig.4.3. It is clear from the graphs that the results given by both the MSE and MMSE with the new set of boundary conditions (4.42) are much closer to the amplitude of the reflection coefficient Booij [5] computed using full linearised theory. The results given by the MMSE closely agree with all the computed results for the full linearised theory. The results given by the MSE closely agree with the computed results for the full linearised theory for $W_s > 0.4$, which corresponds to taluds with gradient up to 1. This implies that the MSE can give reliable results for taluds with a maximum gradient of up to 1, rather than a maximum gradient of up to $\frac{1}{3}$ which Booij [5] suggested. The results given by the MSE with boundary conditions (4.42) begin to vary from the full linear ones for small W_s because the terms $O(\nabla^2 h,\ |\nabla h|^2)$ that were neglected in this approximation are now clearly not negligible. The results given by the MMSE are much closer to the full linear results for these small values of W_s (as one would expect), as no terms of $O(\nabla^2 h,\ |\nabla h|^2)$ have been neglected. As W_s tends to zero, α_0 tends to zero, which is equivalent to the wavelength becoming much larger than the water depth. In other words, the limit as W_s tends to zero is the shallow water limit.

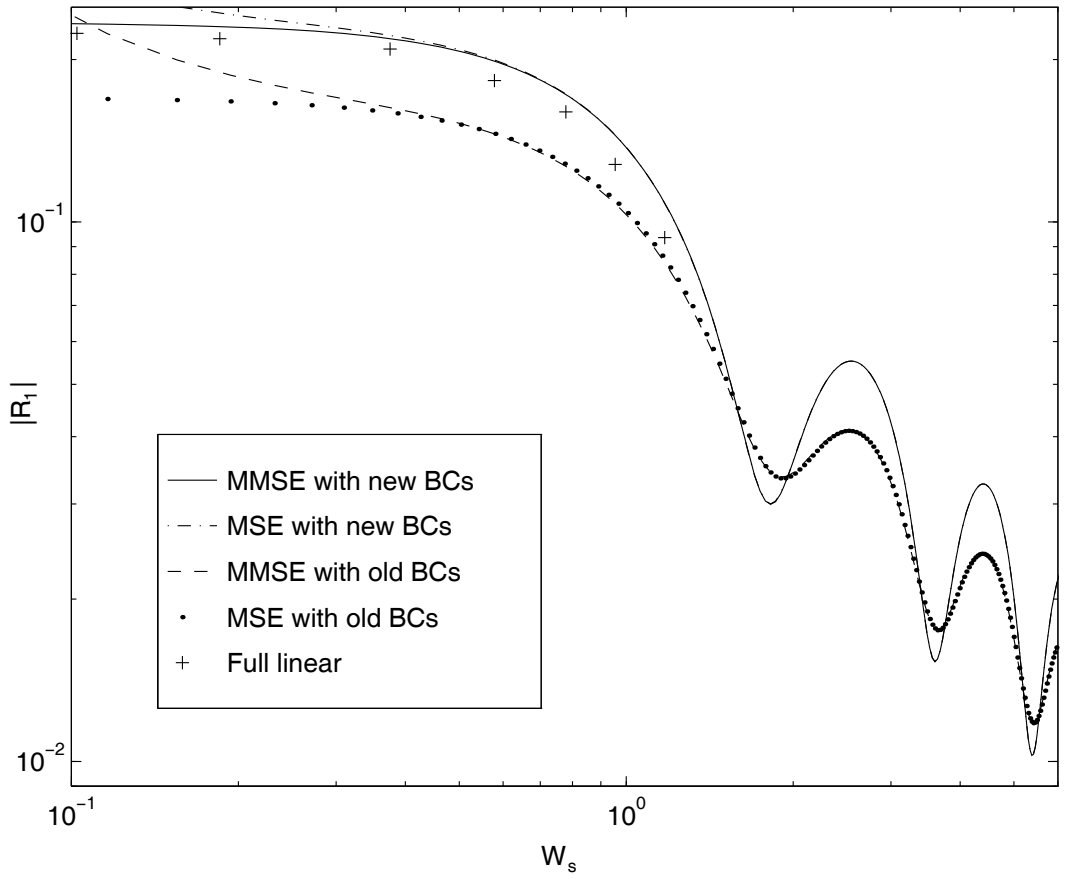

Figure 4.3: Reflected amplitude over the depth profile $H(x)=1-\frac{2}{3}x$ $(0\leq x\leq 1)$.

Also as W_s tends to zero, the talud is tending to a step, and so the amplitude of the reflection coefficient should tend to the exact value of the reflection coefficient for wave incidence on a step in shallow water which Lamb [28] derived, namely

$$|R_1^0| = \frac{\sqrt{h_0}-\sqrt{h_1}}{\sqrt{h_0}+\sqrt{h_1}} = 0.268,$$

in the present case. It can be seen from Fig.4.3 that when $W_s = 0.1$, the MMSE with the new boundary conditions (4.42) gives

$$|R_1^0| = 0.236\ ,$$

which is quite close to Lamb's result, and certainly much closer than any of the other approximations. From the evidence in Fig.4.3, we conclude that the approach used in section 4.3 to derive the boundary conditions is the correct approach. Notice also from Fig.4.3 that the amplitude of the oscillations of $|R_1^0|$

given by the MSE and MMSE with the new boundary conditions (4.42) is much larger than that given with the old boundary conditions (4.41). Booij [5] claimed that the results given by the full linear theory and the MSE with the old boundary conditions (4.41) were in 'good agreement' for $W_s > 1.2$. He does not publish any values of $|R_1^0|$ for full linearised theory for $W_s > 1.2$ to confirm this claim, but from the evidence in Fig.4.3 it is reasonable to suppose that these results would be much closer to those given with the new boundary conditions (4.42) rather than those given by the old ones as claimed.

In Fig.4.4 we present the results obtained from the boundary-value problem

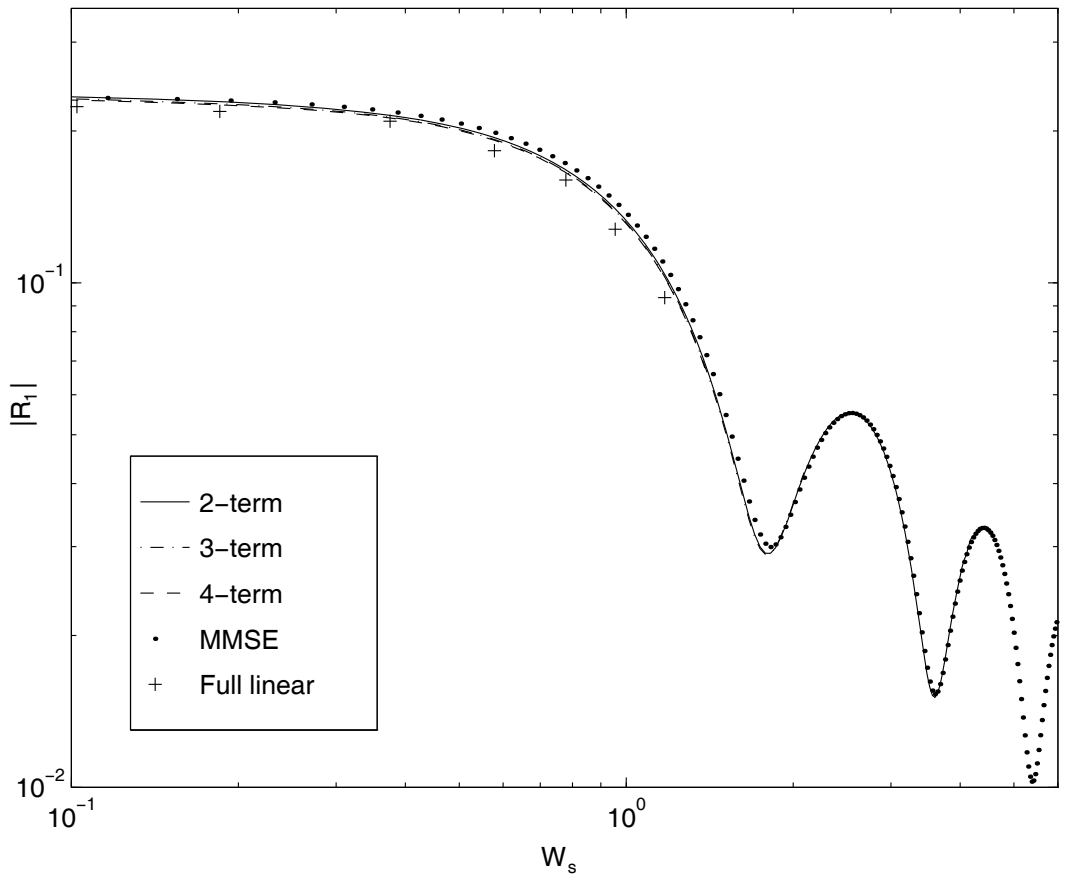

Figure 4.4: Reflected amplitude over the depth profile $H(x) = 1 - \frac{2}{3}x$ $(0 \leq x \leq 1)$.

(4.23), (4.37) – (4.38) for the MMSE, 2-term, 3-term and 4-term approximations. It is clear from the graph, that as the number of terms in the trial function is increased, the closer the results become to the full linear ones. The results given by the 2-term approximation have converged to those given by the MMSE

when $W_s > 1.6$, which corresponds to taluds with gradient less than $\frac{1}{4}$. In other words, taluds with gradients of up to $\frac{1}{4}$ are mild enough to make the contribution from the first (and largest) decaying mode negligible. Therefore, it is not of great importance that we cannot find results for the 2-term approximation for $W_s > 4.35$, as the results will be the same as those given by the MMSE which we can find for $W_s > 4.35$.

For $W_s > 1.4$, that is, for gradients less than $\frac{2}{7}$, the results given by the 3-term approximation have converged to those given by the 2-term approximation. So the contribution from the second decaying mode becomes negligible for taluds with gradient up to $\frac{2}{7}$.

Finally, the results given by the 4-term approximation are practically the same as those given by the 3-term approximation, with no observable difference for $W_s > 0.8$, that is, for taluds with gradients less than $\frac{1}{2}$. From the similarity between the 3-term and 4-term approximation results, we conclude that the n-term approximation has essentially converged when n=4 and so we do not compute solutions for the 5-term or higher term approximations.

Rey [52] also considers this problem, by using a method which approximates the depth profile as a series of horizontal shelves separated by abrupt vertical steps. The results presented in Fig.4.4 are in good agreement with those found by Rey.

Let us now consider another problem, where the depth profile is now given by a hump.

Example 4.4

We consider a depth profile given by

$$H(x) = 2x^2 - 2x + 1 \qquad\qquad (0 \leq x \leq 1) \ .$$

This corresponds to a hump whose height is half the still water depth which has slope discontinuities at $x = 0$ and at $x = 1$, where it meets the flat beds. We wish to solve the boundary- value problem (4.23), (4.37) – (4.40) at values of a parameter ω starting at 0.05, ending at 10, with intervals of 0.05. The parameters α_0 and τ are defined in terms of ω by

$$\alpha_0 = \omega \ , \qquad \tau = \frac{1}{\omega} \ .$$

With these definitions for α_0 and τ, varying ω corresponds to varying the length l of the hump or, equivalently, to varying the steepness of the depth profile, as in Example 4.3. As ω increases, $\alpha_0\tau = 1$ and τ decreases, so (as in Example 4.3) the functions β_k $(k = 1, \ldots, n-1)$ monotonically increase. The minimum depth in this example occurs at $x = \frac{1}{2}$, and so the maximum value of β_k $(k = 1, \ldots, n-1)$ in the interval $[0, 1]$ is at $x = \frac{1}{2}$. When $\omega = 0.05$, we find that

$$\beta_1\left(\frac{1}{2}\right) = 0.30\ , \qquad \beta_2\left(\frac{1}{2}\right) = 0.62\ , \qquad \beta_3\left(\frac{1}{2}\right) = 0.94\ , \qquad \beta_4\left(\frac{1}{2}\right) = 1.25\ .$$

and when $\omega = 10$, we find that

$$\beta_1\left(\frac{1}{2}\right) = 59.50\ , \qquad \beta_2\left(\frac{1}{2}\right) = 124.06\ , \qquad \beta_3\left(\frac{1}{2}\right) = 187.43\ , \qquad \beta_4\left(\frac{1}{2}\right) = 250.53\ .$$

As in Example 4.3, as ω increases, there is a value of ω at which the function β_1 is large enough to make the solutions of the initial-value problem for the 2-term approximation too large for the system (4.59) to be to be solved to the minimum accuracy (3.d.p.). Similarly, at smaller values of ω, solutions for the 3-term and 4-term approximations will not be available. It turns out that for the 2-term approximation, when $\omega = 7.75$, $\beta_2(\frac{1}{2}) = 46.11$, $\mathrm{cond}(M) = 2.4 \times 10^{15}$ and equation (4.59) cannot be solved to the minimum accuracy we have specified. When $\omega = 3.75$, $\beta_2(\frac{1}{2}) = 46.52$ and the results given by the 3-term approximation cannot be found to the minimum accuracy for $\omega \geq 3.75$. When $\omega = 2.4$, $\beta_3(\frac{1}{2}) = 44.98$ and the results given by the 4-term approximation cannot be found to the minimum accuracy for $\omega \geq 2.4$. As in Example 4.3, for all the n-term approximations, we initially use a tolerance in the Runge-Kutta method of 10^{-6} which rises to 10^{-11} as ω increases, in accordance with the size of the solutions of the initial-value problem. Again we use a tolerance of 10^{-6} in the Runge-Kutta method for the MSE and MMSE, which gives solutions accurate to 6.d.p. over the whole ω range.

As in the previous example, the first set of results we give, are for the MSE and MMSE with the old set (4.41) and new set (4.42) of boundary conditions. These are presented in Fig.4.5. It is clear from the graphs that the results given by both the MSE and MMSE with the new set of boundary conditions (4.42) are very different to those given with the old boundary conditions (4.41). The

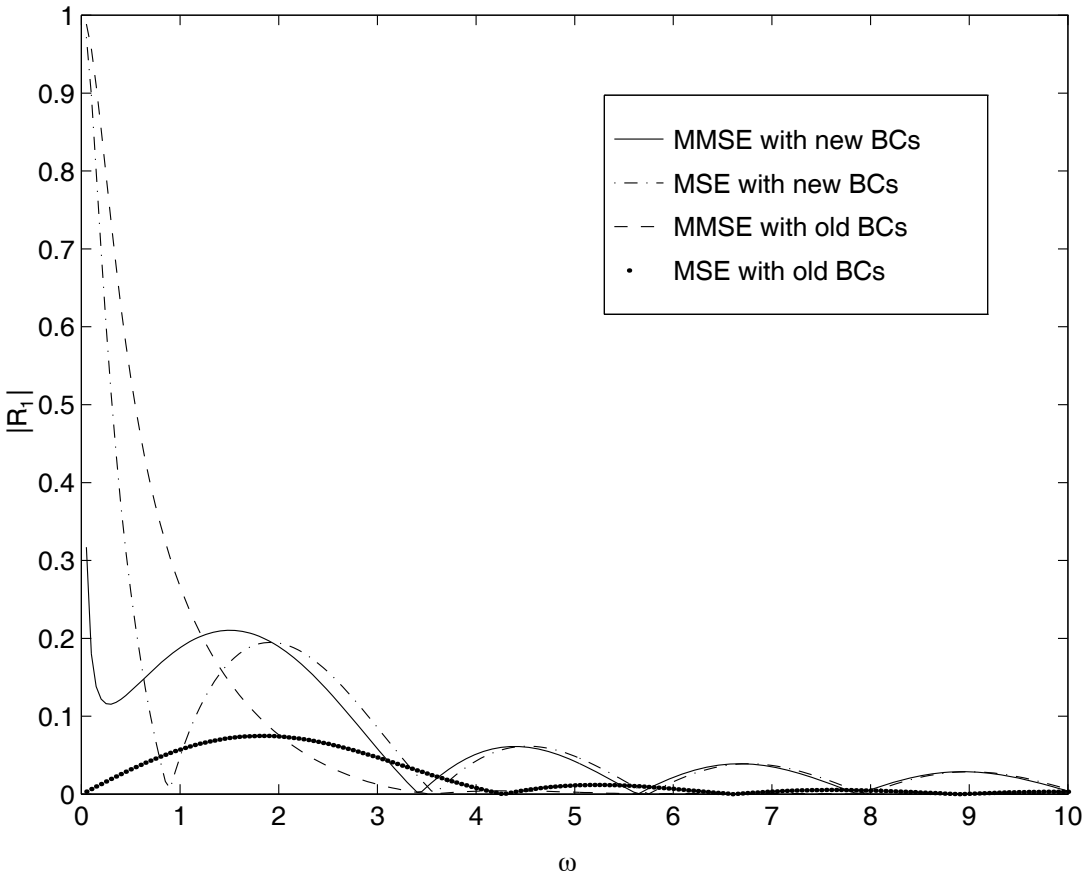

Figure 4.5: Reflected amplitude over the depth profile $H(x) = 2x^2 - 2x + 1$ $(0 \leq x \leq 1)$.

results given by the MMSE with the old boundary conditions just decay away as ω increases. Those given by the MSE with the old boundary conditions make small oscillations. For $\omega > 9$ the MMSE results with the new boundary conditions have practically converged to those given by the MSE. There is a clear overall decreasing trend in these results which is because as ω increases the physical water depth becomes equal to a large number of wavelengths and consequently less energy is reflected. The behaviour in the results as ω tends to zero is a result of the modelling, because for small values of ω the hump corresponds to a submerged thin step. Decaying wave mode terms are significant in this case and as the mild-slope or modified mild-slope approximations do not contain decaying wave mode terms, we cannot expect reliable results. In Chapter 5, we find second-order accurate approximations to the reflection and transmission coefficients for the full linear wave scattering problem over a hump. We find that the results

given by the MSE and MMSE with the new boundary conditions (4.42) are very similar to these full linear results, with those given by the MMSE the closest.

In Fig.4.6 we present the results obtained from the boundary-value problem

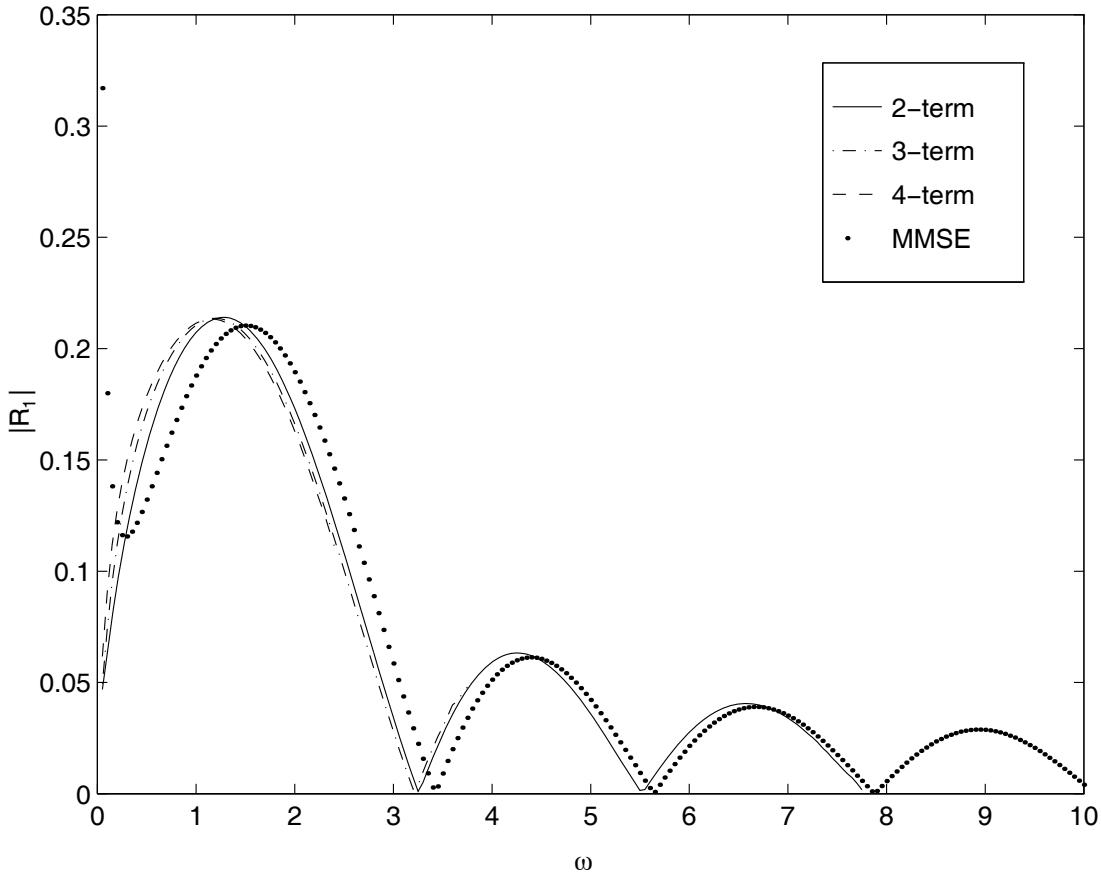

Figure 4.6: Reflected amplitude over the depth profile $H(x) = 2x^2 – 2x + 1$ $(0 \leq x \leq 1)$.

(4.23), (4.37) – (4.38) for the MMSE, 2-term, 3-term and 4-term approximations. It is clear from the graph, that as the number of terms in the trial function is increased, the results are converging. The results given by the 2-term approximation have nearly converged to those given by the MMSE when $\omega > 7.0$. In other words, for $\omega > 7.0$, the slope of the hump is mild enough to make the contribution from the first (and largest) decaying mode almost negligible. When $\omega = 3.7$, the results given by the 3-term approximation have very nearly converged to those given by the 2-term approximation. So the contribution from the second decaying mode becomes essentially negligible for $\omega > 3.7$. Finally, the results given by the 4-term have nearly converged to those given by the 3-term approximation when

$\omega = 2.4$. Therefore, the contribution from the fourth decaying mode becomes essentially negligible for $\omega > 2.4$. From the similarity between the 3-term and 4-term approximation results, we conclude that the n-term approximation has essentially converged when n=4 and so we do not compute solutions for the 5-term or higher term approximations. In this example we have not seen the same convergence in the results given by the n-term ($n > 1$) approximations as we did in the previous example. This is because the steepness of a hump of the same maximum height as a talud and the same length is effectively twice that of the talud. So unfortunately, the slope of the hump does not become mild enough for us to see the same convergence in the results given by the n-term ($n > 1$) approximations as seen in Example 4.3 before the results given by these n-term ($n > 1$) approximations become inaccurate.

For small values of ω, the hump we are considering is similar to a thin rectangular block, whose height is half the fluid depth. Mei and Black [4] considered this type of problem using full linear theory, for blocks of various width and the limiting case of a thin barrier.For small wave numbers, their results show that there is a large difference in the amplitude of the reflected wave given by a thin barrier and the blocks they considered. The results given in Fig.4.6 by the 2, 3 and 4-term approximations when $\omega = 0.05$, that is, when the flat bed depth is 20 times the length of the hump are consistent with those of Mei and Black, in the sense that they lie between the corresponding estimates Mei and Black give for the thin barrier and the narrowest block they consider, where the flat bed depth is half the length of the step.

In Chapter 5, we find that our decay mode approximation results for this hump problem are in good agreement with the results we compute using full linearised theory.

We round off this chapter by developing the theory given so far to encompass obliquely incident waves.

4.8 Obliquely incident waves

In this chapter, the theory employed so far is only for 1-dimensional problems. In other words, it applies to waves that are normally incident on depth profiles which are independent of y. We shall now generalise this to allow waves incident other than normally on such profiles. Consider a plane wave train arriving from $x = -\infty$ whose direction of propagation makes an angle θ_0 to the normal to the y axis. Let the angle which the transmitted wave makes to the normal be denoted by θ_1, where $\theta_1 \neq \theta_0$ in general.

If the fluid depth in $x < 0$ is less than that in $x > 1$ then $\theta_1 > \theta_0$ (Mei [37], for example). We note that there exists a critical angle θ_{crit} which for any incident wave with angle of incidence in the interval $\left[\theta_{\text{crit}}, \frac{\pi}{2}\right]$ total reflection occurs – a well-known result in optics. We do not consider these total reflection problems here as this would require us to derive alternative boundary conditions, with which we are not concerned. We shall consider wave scattering problems in which part of the incident wave is reflected and part of it is transmitted. If the fluid depth in $x < 0$ is greater than than that in $x > 1$, that is, if $h_0 > h_1$, then $\theta_1 < \theta_0$ – this is the case depicted in Fig. 4.7 In this case the incident wave

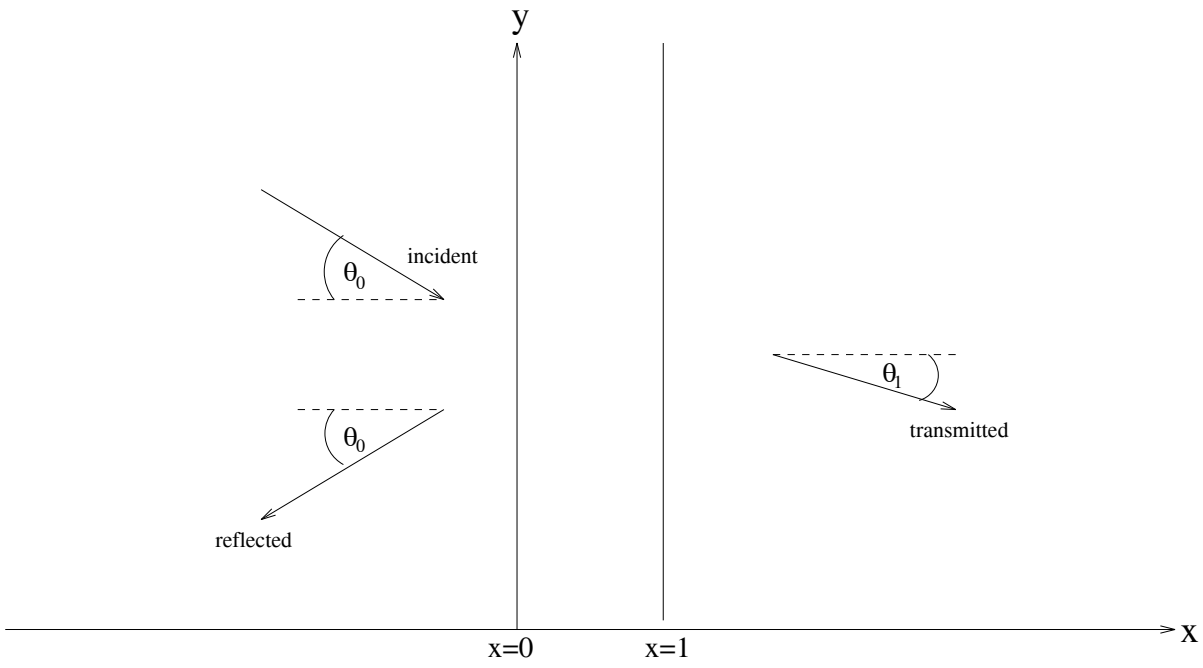

Figure 4.7: Top view of an obliquely incident wave approaching a talud for $h_0 > h_1$.

is always transmitted whatever the angle of incidence. For an oblique incidence problem as depicted in Fig. 4.7, we can follow the same procedure used in section 4.1 to see that the approximation to the free surface elevation η is given by

$$\eta \approx Re\left\{ e^{-i\sigma t} \sum_{k=0}^{n-1} \tilde{\phi}_k \right\} \ .$$

Here the functions $\tilde{\phi}_k = \tilde{\phi}_k(x,y)$ $(k = 0, \ldots, n-1)$, after scaling, satisfy

$$U_k \left(\nabla^2 \tilde{\phi}_k - {\beta_k}^2 \tilde{\phi}_k \right) + \sum_{j=0}^{n-1} \left\{ F_{jk} \frac{\partial \tilde{\phi}_j}{\partial x} + G_{jk} \tilde{\phi}_j \right\} = 0 \qquad (k = 0, \ldots, n-1) \ , \quad (4.64)$$

with $U_k = U_k(x)$, $\beta_k = \beta_k(x)$, $F_{jk} = F_{jk}(x)$ and $G_{jk} = G_{jk}(x)$ $(j,k = 0, \ldots, n-1)$, defined by (4.24) and (4.30) respectively, since $H = H(x)$.

The wave numbers κ_0 and κ_1 of the incident and the scattered progressive waves can be calculated from the dispersion relation (4.26) once the parameters α_0 and τ have been prescribed. Similarly, the corresponding terms β_k^0 and β_k^1 $(k = 1, \ldots, n-1)$ of the scattered decaying wave modes can be calculated from (4.25). The incident and scattered waves have an x and y component, with the incident wave components in the x and y directions having wave numbers $\kappa_0 \cos\theta_0$ and $\kappa_0 \sin\theta_0$ respectively. As the depth profile H is independent of y, the y component of the waves cannot change across the talud. In other words, $\forall\ (x,y) \ \in \ \mathbb{R}^2$

$$\tilde{\phi}_k(x,y) = \phi_k(x) e^{i\kappa_0 y \sin\theta_0} \qquad (k = 0, \ldots, n-1) \ , \quad (4.65)$$

for some $\phi_k(x)$ $(k = 0, \ldots, n-1)$. Substituting (4.65) into (4.64) and dividing through by $e^{i\kappa_0 y \sin\theta_0}$ gives

$$U_k \left(\phi_k'' - \left({\kappa_0}^2 \sin^2\theta_0 + {\beta_k}^2 \right) \phi_k \right) + \sum_{j=0}^{n-1} \left\{ F_{jk} \phi_j' + G_{jk} \phi_j \right\} = 0 \quad (k = 0, \ldots, n-1), \quad (4.66)$$

with the prime denoting differentiation with respect to x. This equation reduces to our original coupled equation (4.23) in the event of an incident wave of normal incidence. The asymptotic behaviour of ϕ_k $(k = 0, \ldots, n-1)$ can be summarised by

$$\phi_0(x) = \begin{cases} e^{i\kappa_0 x \cos\theta_0} + R_0 e^{-i\kappa_0 x \cos\theta_0} & x \leq 0 \ , \\ \\ T_0 e^{i\kappa_T x} & x \geq 1 \ , \end{cases} \quad (4.67)$$

$$\phi_k(x) = \begin{cases} R_k e^{\beta_k^0 x \cos\theta_0} & x \leq 0 \quad (k = 1, \ldots, n-1) \ , \\ \\ T_k e^{-\beta_k^T x} & x \geq 1 \quad (k = 1, \ldots, n-1) \ . \end{cases} \tag{4.68}$$

Here, κ_T is the x-component of the wave number of the transmitted progressive wave, and β_k^T $(k = 1, \ldots, n-1)$ are the x-components of the corresponding terms of the transmitted decaying wave modes. The procedure outlined in section 4.3 can be used to derive the boundary conditions for ϕ_k $(k = 0, \ldots, n-1)$ from equations (4.67) and (4.68). The transmitted progressive wave has wave number κ_1 and we know in advance that its y-component is $\kappa_0 \sin\theta_0$. Therefore

$$\kappa_T = \sqrt{{\kappa_1}^2 - {\kappa_0}^2 \sin^2\theta_0} \ .$$

Similarly, the y-component of the functions $\beta_1^1, \ldots, \beta_{n-1}^1$ is $\kappa_0 \sin\theta_0$ and therefore

$$\beta_k^T = \sqrt{(\beta_k^1)^2 + {\kappa_0}^2 \sin^2\theta_0} \qquad (k = 1, \ldots, n-1) \ .$$

We can also deduce from the above work that θ_1, the angle between the normal to the y-axis and the direction of the transmitted wave, is given by

$$\kappa_0 \sin\theta_1 = \kappa_1 \sin\theta_0 \ .$$

This is analogous to a well-known result in optics known as Snell's law and this determines whether $\theta_0 \leq \theta_1$ or $\theta_0 \geq \theta_1$.

We can now use the numerical methods outlined in section 4.5 to solve equation (4.66) together with its appropriate boundary conditions. The required solutions $\tilde{\phi}_k$ $(k = 0, \ldots, n-1)$ are then found using equation (4.65). We return to the problem considered in section 4.7, where we gave plots of the approximation to the free surface for a plane wave incident normally on the depth profile

$$H(x) = \frac{3}{4} + \frac{1}{4}\cos\left(2\pi x^2\right) \qquad (0 \leq x \leq 1) \ ,$$

with parameter values

$$\begin{aligned} \alpha_0 &= 2.5 \ , \\ \tau &= 0.4 \ . \end{aligned}$$

Now suppose we have an incident wave of unit amplitude from $x = -\infty$ obliquely incident on the bed at an angle $\theta_0 = \frac{\pi}{6}$ to the normal. The graphical representations of the free surface given by the MMSE, 2-term, 3-term and 4-term

approximations are very similar, so we just present the results for the 2-term approximation here. The 2-term approximation to the free surface elevation at time $t = 2j\frac{\pi}{\sigma}$ $(j+1 \in \mathbb{N})$ is given by

$$\eta \approx \mathrm{Re}\left\{ e^{i\kappa_0 y \sin\theta_0} \left\{ \begin{array}{cc} e^{i\kappa_0 x\cos\theta_0} + R_0 e^{-i\kappa_0 x\cos\theta_0} + R_1 e^{\beta_1^0 x\cos\theta_0} & (x \le 0)\ , \\ \phi_0(x) + \phi_1(x) & (0 \le x \le 1)\ , \\ T_0 e^{i\kappa_T x} + T_1 e^{-\beta_1^T x} & (x \ge 1)\ . \end{array} \right. \right\}$$

Fig. 4.8 displays the approximation to the free surface elevation given by the 2-term approximation. To give the figure more meaning we have included the depth profile used, and the amplitude of the waves has been exaggerated to improve clarity. Notice the presence of constructive interference in $x \le 0$.

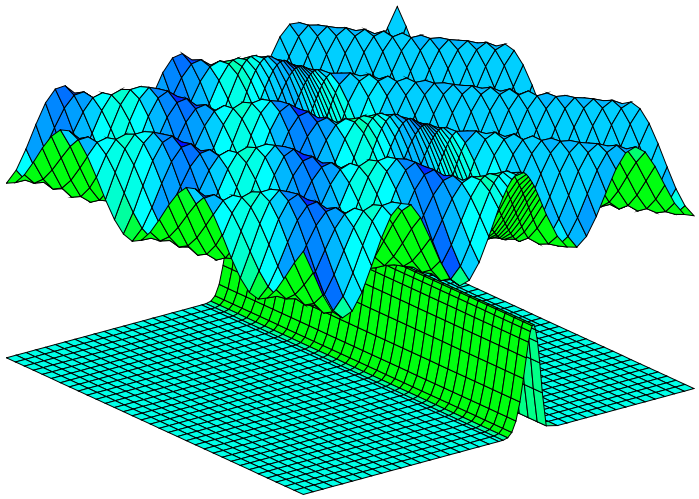

Figure 4.8: Free surface for oblique incidence given by the 2-term approximation.

In the oblique incidence problem there is a possibility that at certain values of the wave number κ and the angle of incidence θ_0, waves may propagate in the y direction with amplitude that tends to zero as $|x| \to \infty$. These 'trapped' waves therefore evade the radiation conditions used and it follows that at these parameter values the solution is non-unique.

It is clear that the numerical method that we have used to solve the boundary-value problem (4.23), (4.37) – (4.40) is restricted by the size of the functions β_k $(k = 1, \ldots, n-1)$. A major objective of any future work will be to develop a solution routine that overcomes this problem. The size of the functions β_k $(k = 1, \ldots, n-1)$ will cause problems in most numerical solution procedures of the boundary- value problem. These problems might be avoided by developing an approximate solution method to solve the integral equation equivalent to this boundary-value problem which we presented in section 4.4.

In this chapter, we have shown that by incorporating decaying wave mode terms into the formulation of the original mild-slope approximation to the velocity potential for the full linearised wave scattering problem, we can find good approximations to the velocity potential. This new approximation has been compared with two older approximations that only contain progressive wave mode terms, namely the mild-slope and modified mild-slope approximations. We have shown that for steep depth profiles, where the decaying wave modes are significant, the results given by the new approximation agreed much more closely with results Booij [5] obtained using full linear theory. From the results given in sections 4.6 and 4.7, the new 'decaying mode' approximation of the coefficients of the scattered waves is seen to essentially converge when the number of decaying wave modes included has reached three, even for the steepest bed profiles. The milder the depth profile, the fewer the number of decaying modes needed for convergence, until eventually the gradient of the depth profile becomes mild enough to make all the decaying modes negligible. In the course of developing this approximation, it has been found that the boundary conditions that have been used in the past by all authors with the mild-slope approximation are incorrect. By this, we mean that an alternative set of boundary conditions can be found which make the mild-slope approximation results agree far more closely with computed results of the full linear problem than the original ones.

Chapter 5

The full linear problem for a hump

In this chapter, the depth profiles that are considered are local elevations in an otherwise flat uniform bed, which we refer to as humps. A second-kind integral equation is derived from the full linear boundary-value problem (BVP) satisfied by the velocity potential, which was given in Chapter 2. The BVP was defined there in terms of two orthogonal horizontal co-ordinates x and y and a vertical co-ordinate z. We shall be considering the two-dimensional problem, which is independent of y, in this chapter.

Initially, as the kernel of the integral equation presents serious numerical problems to evaluate accurately, we make an approximation. The approximation, which is equivalent to one that is used in the mild-slope and modified mild-slope approximations, is to remove the decaying wave mode terms to leave just the progressive wave mode terms. This process makes the kernel of the second-kind integral equation simple to compute and Chamberlain's integral equation procedure, which was reviewed in Chapter 2, can be used to solve it very accurately. Unfortunately this approximation is found to be quite inaccurate when the results are compared with those from reliable approximations.

It is found, however, that the second-kind integral equation for the potential can be converted into a first-kind integral equation for the tangential fluid velocity. The kernel of the first-kind equation is given in terms of a Green's function whereas the kernel of the second-kind equation is given by the normal derivative

of another Green's function evaluated on the hump. It follows that the kernel in the first-kind equation is much easier to compute numerically than the kernel of the second-kind equation. It is shown that the first-kind integral equation can be derived directly from the corresponding boundary-value problem for the associated stream function. A variational principle is used to deliver approximations to the coefficients of the scattered waves which are second-order accurate compared to the approximation of the solution of the first-kind equation. The subsequent results are used to further test the accuracy of the decay mode approximation derived in Chapter 4 and also to test the accuracy of the modified mild-slope and mild-slope approximations.

5.1 A second-kind integral equation

The problem under consideration is that of finding the velocity potential $\phi = \phi(x, z)$ for waves incident from $x = \pm\infty$ on an arbitrary, that is, symmetric or asymmetric, hump of finite length l. This depth profile is such that $h(x) = h_0 \ \forall x \in (-\infty, 0] \cup [l, \infty)$ and $h(x) > h_0 \ \forall x \in (0, l)$. The problem domain is as depicted in Fig.5.1.

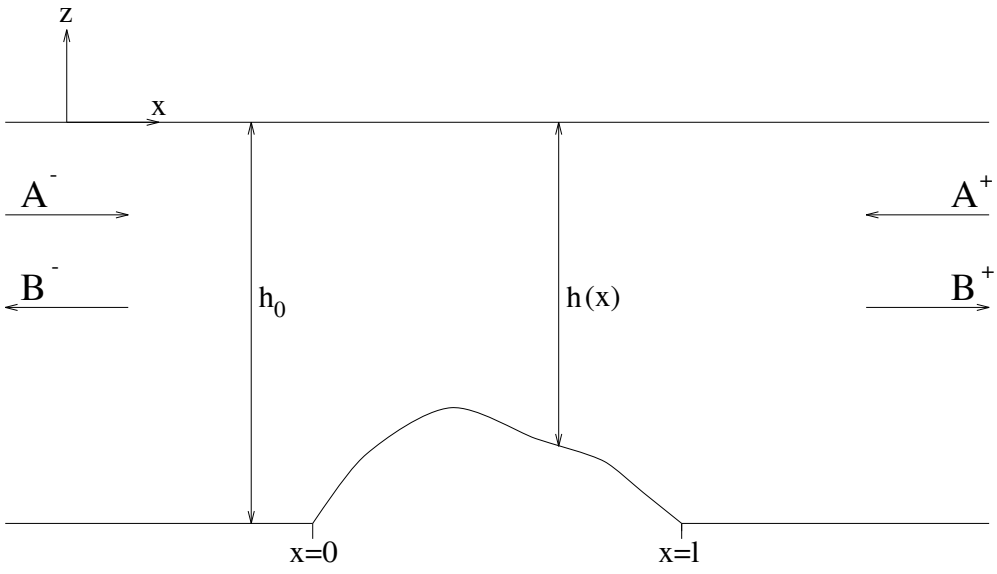

Figure 5.1: The problem domain.

From Chapter 2, we recall that in this situation ϕ satisfies

$$\begin{aligned} \hat{\nabla}^2\phi &= 0 \qquad && -h < z < 0 \ , \\ \frac{\partial\phi}{\partial z} - \nu\phi &= 0 \qquad && \text{on } z = 0 \ , \\ \frac{\partial\phi}{\partial n} &= 0 \qquad && \text{on } z = -h(x) \ , \end{aligned} \tag{5.1}$$

where $\hat{\nabla} = (\frac{\partial}{\partial x}, \frac{\partial}{\partial z})$ and $\nu = \frac{\sigma^2}{g}$, together with radiation conditions in the form

$$\phi(x,z) \sim \frac{\cosh\left(k_0(z+h_0)\right)}{\cosh\left(k_0 h_0\right)} \left[A^- e^{ik_0 x} + B^- e^{-ik_0 x}\right] \qquad \text{as } x \to -\infty \tag{5.2}$$

and

$$\phi(x,z) \sim \frac{\cosh\left(k_0(z+h_0)\right)}{\cosh\left(k_0 h_0\right)} \left[A^+ e^{-ik_0 x} + B^+ e^{ik_0 x}\right] \qquad \text{as } x \to \infty \ . \tag{5.3}$$

As discussed in Chapters 2 & 4, linearity removes the need to solve the problem for two incident waves. Therefore, for an incident wave from $x = -\infty$ ($A^+ = 0$), the coefficients of the reflected and transmitted waves are defined as

$$R_1 = \frac{B^-}{A^-} \qquad \text{and} \qquad T_1 = \frac{B^+}{A^-} \ .$$

Similarly, for an incident wave from $x = \infty$ ($A^- = 0$), the coefficients of the reflected and transmitted waves are defined as

$$R_2 = \frac{B^+}{A^+} \qquad \text{and} \qquad T_2 = \frac{B^-}{A^+} \ .$$

The coefficients of the outgoing waves $B^{\pm}$ for two incident waves are given in terms of these reflection and transmission coefficients. Following the steps used in Chapter 2, this relationship is given by

$$\begin{pmatrix} B^+ \\ B^- \end{pmatrix} = \begin{pmatrix} T_1 & R_2 \\ R_1 & T_2 \end{pmatrix} \begin{pmatrix} A^- \\ A^+ \end{pmatrix} \ ,$$

where the matrix on the right-hand side of the above equation is called the scattering matrix.

The second-kind integral equation is derived via Green's identity

$$\iint_D \left(\phi\hat{\nabla}^2 G - G\hat{\nabla}^2\phi\right) dxdz = \oint_C \left(\phi\frac{\partial G}{\partial n} - G\frac{\partial\phi}{\partial n}\right) dc \quad , \tag{5.4}$$

where the domain D and boundary C will be defined as required and where $\frac{\partial}{\partial n}$ is the outward normal derivative, which is defined as

$$\frac{\partial}{\partial n} = -\frac{\frac{\partial}{\partial z} + h'(x)\frac{\partial}{\partial x}}{\left(1 + (h'(x))^2\right)^{\frac{1}{2}}},$$

where the prime denotes differentiation with respect to x. The Green's function G is chosen to satisfy

$$\begin{aligned} \hat{\nabla}^2 G &= -\delta(x - x_0)\delta(z - z_0) && -h_0 < z < 0 , \\ \frac{\partial G}{\partial z} - \nu G &= 0 && \text{on } z = 0 , \\ \frac{\partial G}{\partial n} &= 0 && \text{on } z = -h_0 , \end{aligned} \tag{5.5}$$

together with a radiation condition ensuring that G behaves like an outgoing wave as $|x| \to \infty$. In other words,

$$G \sim e^{\pm ik_0 x} \qquad \text{as } x \to \pm\infty . \tag{5.6}$$

This Green's function is well-known and one can find derivations of its integral or series forms in Wehausen and Laitone [59] and Thorne [56]. The infinite series representation of G is given by

$$\begin{aligned} G(x, z|x_0, z_0) = {} & \frac{i}{2k_0} c_0^2 \cosh(k_0(z + h_0)) \cosh(k_0(z_0 + h_0))\, e^{ik_0|x - x_0|} \\ & + \sum_{n=1}^{\infty} \frac{1}{2B_n^0} c_n^2 \cos\left(B_n^0(z + h_0)\right) \cos\left(B_n^0(z_0 + h_0)\right) e^{-B_n^0|x - x_0|}, \end{aligned} \tag{5.7}$$

where

$$\begin{aligned} c_0^2 &= \frac{4k_0}{2k_0 h_0 + \sinh(2k_0 h_0)} , \\ c_n^2 &= \frac{4B_n^0}{2B_n^0 h_0 + \sin(2B_n^0 h_0)} \qquad (n \in \mathbb{N}) . \end{aligned}$$

Here k_0 is the root of the flat bed dispersion relation

$$\nu = k_0 \tanh(k_0 h_0) ,$$

and B_n^0 are the roots of the equation

$$-\nu = B_n^0 \tan(B_n^0 h_0) \qquad (n \in \mathbb{N}) ,$$

arranged in ascending order of magnitude.

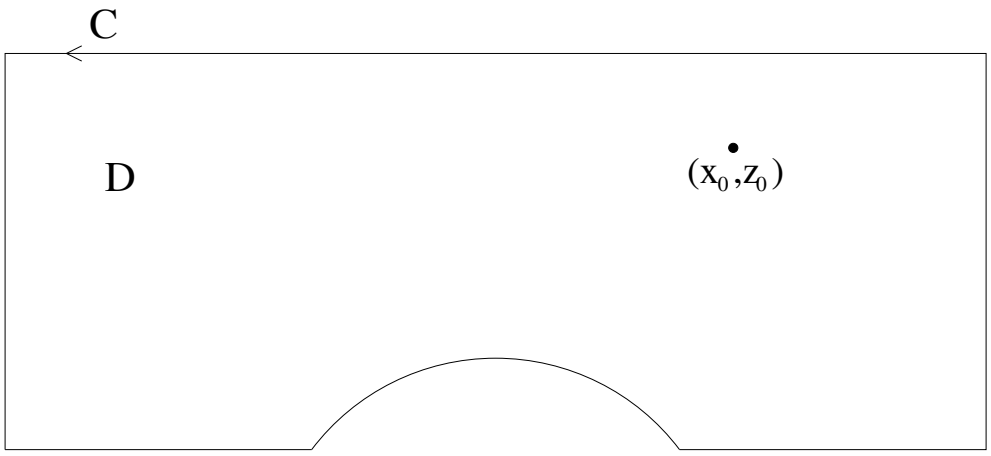

Figure 5.2: First domain used in Green's identity.

If Green's identity (5.4) is now applied to the domain depicted in Fig.5.2, where (x_0, z_0) is inside D and the vertical boundaries are assumed to be a great distance from the hump so that the radiation conditions (5.2), (5.3) and (5.6) apply there, then it is simple to show that

$$-\phi(x_0,z_0) = -\frac{\cosh\left(k_0(z_0+h_0)\right)}{\cosh\left(k_0h_0\right)}\left[A^-e^{ik_0x_0}+A^+e^{-ik_0x_0}\right]+\int_{C_h}\left[\phi\frac{\partial G}{\partial n}\right]_{z=-h(x)}dc \ ,$$

where C_h is the curved part of C. Noticing that $dc = \left(1+(h'(x))^2\right)^{\frac{1}{2}}dx$, then this equation can be written as

$$\begin{aligned}\phi(x_0,z_0) = \ & \frac{\cosh\left(k_0(z_0+h_0)\right)}{\cosh\left(k_0h_0\right)}\left[A^-e^{ik_0x_0}+A^+e^{-ik_0x_0}\right] \\ & +\int_0^l\left[\left(h'(x)\frac{\partial G}{\partial x}+\frac{\partial G}{\partial z}\right)\phi\right]_{z=-h(x)}dx \ .\end{aligned} \tag{5.8}$$

Equation (5.8) is an integral representation of $\phi(x_0, z_0)$ in terms of $\phi(x, -h(x))$ for $0 \le x \le l$, that is, in terms of ϕ evaluated on the hump. Applying Green's identity (5.4) to a slightly different domain, depicted in Fig.5.3, where (x_0, z_0) now lies on the hump, gives

$$0 = -\frac{\cosh\left(k_0(z_0+h_0)\right)}{\cosh\left(k_0h_0\right)}\left[A^-e^{ik_0x_0}+A^+e^{-ik_0x_0}\right]+\int_{C_h}\left[\phi\frac{\partial G}{\partial n}\right]_{z=-h(x)}dc+\frac{1}{2}\phi(x_0,z_0) \ .$$

Here, the left-hand side is now zero because $\hat{\nabla}^2G = \hat{\nabla}^2\phi = 0$ in D and the extra term on the right-hand side arises from the line integral around the small indentation at (x_0, z_0). The above equation is a second-kind integral equation for

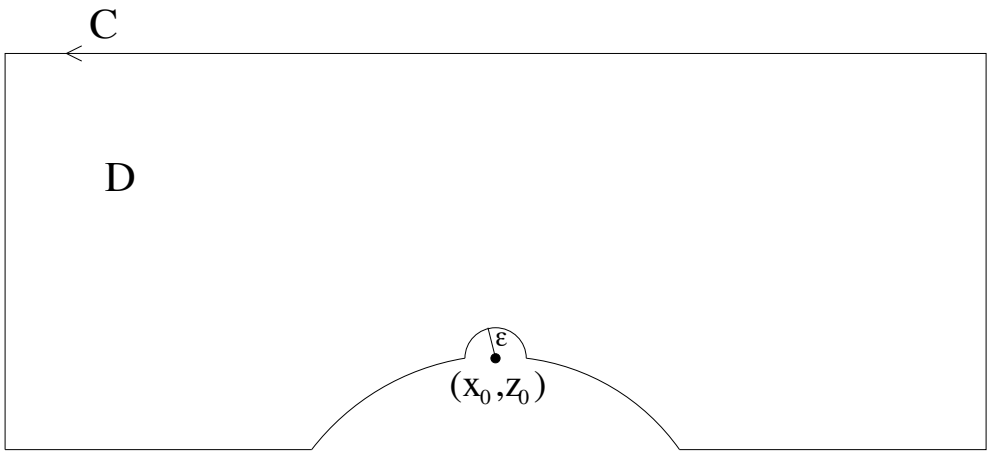

Figure 5.3: Second domain used in Green's identity.

ϕ on the hump. On the hump, $z_0 = -h(x_0)$ and so we can rewrite this equation as

$$\begin{aligned}\tfrac{1}{2}\phi(x_0,-h(x_0)) = \quad & \frac{\cosh\left(k_0(h_0-h(x_0))\right)}{\cosh\left(k_0h_0\right)}\left[A^-e^{ik_0x_0}+A^+e^{-ik_0x_0}\right] \\ & + \int_0^l \left(\left[h'(x)\frac{\partial G}{\partial x} + \frac{\partial G}{\partial z} \right]_{\substack{z=-h(x) \\ z_0=-h(x_0)}} \phi(x,-h(x)) \right) dx \quad .\end{aligned} \tag{5.9}$$

Therefore, in order to find the velocity potential in the fluid domain, the integral equation (5.9) must be solved and its solution then substituted into equation (5.8). The kernel of the above integral equation is not easy to compute numerically because the series which defines it has poor convergence properties. Hence, we wish to avoid solving this second-kind integral equation. Initially, we try making an approximation in (5.9) which simplifies the second-kind integral equation, and this process is outlined in the next section.

We finish this section by finding expressions for the coefficients of the reflected and transmitted waves in terms of the velocity potential evaluated on the hump. Suppose we have an incident wave from $x = -\infty$ (so that $A^+ = 0$), then if, in equation (5.8), we take the limit $x_0 \to -\infty$ and compare the result with the appropriate radiation condition (5.2) for ϕ, we find that the reflection coefficient is given by

$$\begin{aligned}R_1 = \frac{B^-}{A^-} = \frac{c_0^2\cosh\left(k_0h_0\right)}{2A^-}\int_0^l \Big[& -h'(x)\cosh\left(k_0(h_0-h(x))\right) \\ & +i\sinh\left(k_0(h_0-h(x))\right)\Big] e^{ik_0x}\phi(x,-h(x))\,dx.\end{aligned} \tag{5.10}$$

Similarly, by taking the limit $x_0 \to \infty$, we find that the transmission coefficient is given by

$$T_1=\frac{B^+}{A^-}=1+\frac{c_0^2\cosh(k_0h_0)}{2A^-}\int_0^l \Big[h'(x)\cosh(k_0(h_0-h(x))) \\ +i\sinh(k_0(h_0-h(x)))\Big]e^{-ik_0x}\phi(x,-h(x))\,dx. \tag{5.11}$$

For an incident wave from $x=\infty$ (so that $A^-=0$) by the same process as above, we find that the coefficients of the reflected and transmitted waves are given by

$$R_2=\frac{B^+}{A^+}=\frac{c_0^2\cosh(k_0h_0)}{2A^+}\int_0^l \Big[h'(x)\cosh(k_0(h_0-h(x))) \\ +i\sinh(k_0(h_0-h(x)))\Big]e^{-ik_0x}\phi(x,-h(x))\,dx \tag{5.12}$$

and

$$T_2=\frac{B^-}{A^+}=1+\frac{c_0^2\cosh(k_0h_0)}{2A^+}\int_0^l \Big[-h'(x)\cosh(k_0(h_0-h(x))) \\ +i\sinh(k_0(h_0-h(x)))\Big]e^{ik_0x}\phi(x,-h(x))\,dx. \tag{5.13}$$

5.2 An approximation

The mild-slope and modified mild-slope approximations to the velocity potential are derived on the basis that decaying modes are negligible. It is our intention to make an approximation in the same spirit as these approximations in the integral equation (5.9). Therefore, the approximation we make in (5.9) is to omit all the decaying wave mode terms in the Green's function. The resulting approximation $\tilde{\phi}(x_0,-h(x_0))$ to $\phi(x_0,-h(x_0))$ on the hump is the solution of the integral equation

$$\tfrac{1}{2}\phi_0(x_0)= \frac{\cosh(k_0(h_0-h(x_0)))}{\cosh(k_0h_0)}\left[A^-e^{ik_0x_0}+A^+e^{-ik_0x_0}\right] \\ +\frac{c_0^2}{2}\cosh(k_0(h_0-h(x_0)))\int_0^l\Big[\mathrm{sgn}(x_0-x)h'(x)\cosh(k_0(h_0-h(x))) \\ +i\sinh(k_0(h_0-h(x)))\Big]e^{ik_0|x-x_0|}\phi_0(x)dx, \tag{5.14}$$

where $\phi_0(x)=\tilde{\phi}(x,-h(x))$, and the sgn function is defined by

$$\mathrm{sgn}(x_0-x)=\begin{cases} 1 & x_0>x\ , \\ -1 & x_0<x\ . \end{cases}$$

The approximation to the velocity potential in the fluid is given by

$$\begin{aligned}\tilde{\phi}(x_0,z_0) = & \frac{\cosh\left(k_0(z_0+h_0)\right)}{\cosh\left(k_0h_0\right)}\left[A^-e^{ik_0x_0}+A^+e^{-ik_0x_0}\right] \\ & +\frac{c_0^2}{2}\cosh(k_0(z_0+h_0))\int_0^l\Big[\operatorname{sgn}(x_0-x)h'(x)\cosh(k_0(h_0-h(x))) \\ & \qquad +i\sinh(k_0(h_0-h(x)))\Big]e^{ik_0|x-x_0|}\phi_0(x)dx. \end{aligned} \tag{5.15}$$

We shall refer to this new approximation to the velocity potential as the integral approximation.

Therefore, in order to find the approximation $\tilde{\phi}(x_0,z_0)$ to the velocity potential in the fluid, we must solve the second-kind integral equation (5.14) and substitute its solution into equation (5.15). The kernel of the second-kind integral equation (5.14) is discontinuous at $x = x_0$, which will cause problems in numerical integration routines if we attempt to solve this integral equation as it stands. These problems are avoided by using a variable change and some straightforward manipulation to give a new second-kind integral equation whose kernel is continuous.

We define a new function $\zeta = \zeta(x)$ by

$$\zeta(x) = \frac{1}{2}\phi_0(x)\operatorname{sech}\left(k_0(h_0-h(x))\right)\cosh\left(k_0h_0\right) \ . \tag{5.16}$$

Then equation (5.14) can be rewritten as

$$\begin{aligned}\zeta(x_0) = & \left[A^-e^{ik_0x_0}+A^+e^{-ik_0x_0}\right] \\ & +c_0^2\int_0^l\Big[\operatorname{sgn}(x_0-x)h'(x)\cosh^2(k_0(h_0-h(x))) \\ & \qquad +\tfrac{i}{2}\sinh(2k_0(h_0-h(x)))\Big]e^{ik_0|x-x_0|}\zeta(x)dx. \end{aligned} \tag{5.17}$$

We now differentiate the above integral equation twice with respect to x_0 to find the boundary-value problem satisfied by ζ. Differentiating (5.17) once gives

$$\begin{aligned}\zeta'(x_0) = & \ ik_0\left[A^-e^{ik_0x_0}-A^+e^{-ik_0x_0}\right]+2c_0^2h'(x_0)\cosh^2\left(k_0(h_0-h(x_0))\right)\zeta(x_0) \\ & +ik_0c_0^2\int_0^{x_0}\Big[h'(x)\cosh^2(k_0(h_0-h(x)))+\tfrac{i}{2}\sinh(2k_0(h_0-h(x)))\Big]e^{ik_0(x_0-x)}\zeta(x)dx \\ & +ik_0c_0^2\int_{x_0}^l\Big[h'(x)\cosh^2(k_0(h_0-h(x)))-\tfrac{i}{2}\sinh(2k_0(h_0-h(x)))\Big]e^{ik_0(x-x_0)}\zeta(x)dx, \end{aligned}$$

where the prime denotes differentiation with respect to x_0. Differentiating this equation for ζ' gives

$$\zeta''(x_0) - 2u(x_0)\zeta'(x_0) = \left[2\left(u'(x_0) - k_0 v(x_0)\right) - {k_0}^2\right]\zeta(x_0) \qquad (0 < x_0 < l), \quad (5.18)$$

where

$$u(x_0) = c_0^2 h'(x_0)\cosh^2\left(k_0(h_0 - h(x_0))\right)$$

and

$$v(x_0) = \frac{1}{2}c_0^2 \sinh\left(2k_0(h_0 - h(x_0))\right) \ .$$

From equation (5.17) and the equation for ζ' we deduce that ζ satisfies the boundary conditions

$$\begin{aligned} \zeta'(0) + ik_0\zeta(0) &= 2ik_0A^- + 2u(0)\zeta(0) \ , \\ \zeta'(l) - ik_0\zeta(l) &= -2ik_0A^+e^{-ik_0l} + 2u(l)\zeta(l) \ , \end{aligned}$$

where the functions are evaluated at $x_0 = 0+$ and $x_0 = l-$.

By writing the differential equation (5.18) satisfied by ζ in self-adjoint form, we see that the boundary-value problem satisfied by ζ is of the same form as the boundary-value problem which arises from both the mild-slope and modified mild-slope approximations to the velocity potential. We can therefore use Chamberlain's [7] integral equation procedure, which was reviewed in Chapter 2, to find highly accurate estimates of ζ and thus the reflection and transmission coefficients given by our integral approximation.

Using the same scaling procedure as used in Chapter 2, which is briefly summarised as

$$\hat{x} = \frac{x}{l}, \ U(\hat{x}) = lu(l\hat{x}), \ V(\hat{x}) = lv(l\hat{x}), \ H(\hat{x}) = \frac{1}{h_0}h(l\hat{x}), \ \hat{\zeta}(\hat{x}) = \frac{1}{\sigma l^2}\zeta(l\hat{x}),$$

and discarding the accents, the differential equation (5.18) in terms of these dimensionless quantities is

$$\zeta''(x_0) - 2U(x_0)\zeta'(x_0) = \left[2\left(U'(x_0) - \kappa_0 V(x_0)\right) - {\kappa_0}^2\right]\zeta(x_0) \qquad (0 < x_0 < 1), \quad (5.19)$$

where

$$U(x_0) = C_0^2\tau H'(x_0)\cosh^2\left(\kappa_0\tau(1 - H(x_0))\right) \ ,$$

$$V(x_0) = \tfrac{1}{2}C_0^2 \sinh\left(2\kappa_0\tau(1 - H(x_0))\right) \ ,$$

$$C_0^2 = \frac{4\kappa_0}{2\kappa_0\tau + \sinh\left(2\kappa_0\tau\right)} \ ,$$

and $\kappa_0 = k_0 l$ is the positive real root of

$$\alpha_0{}^2 \tau = \kappa_0 \tanh(\kappa_0 \tau) \ ,$$

and where α_0 and τ are two dimensionless parameters given by

$$\alpha_0 = \frac{\sigma l}{\sqrt{g h_0}} \quad , \quad \tau = h_0 / l \ .$$

We need to convert (5.19) into self-adjoint form, which is done by introducing an integrating factor J given by

$$\begin{aligned} J(x_0) &= \exp\left(-2\int_0^{x_0} U(x)dx\right) \\ &= \exp\left(\frac{C_0^2}{2\kappa_0}\left[2\kappa_0\tau(1-H(x_0)) + \sinh(2\kappa_0\tau(1-H(x_0)))\right]\right) . \end{aligned} \tag{5.20}$$

The self-adjoint form of equation (5.19) is then given by

$$\left(J(x_0)\zeta'(x_0)\right)' = J(x_0)\left[2\left(U'(x_0) - \kappa_0 V(x_0)\right) - \kappa_0{}^2\right]\zeta(x_0) \ . \tag{5.21}$$

This equation is of the same form as the mild-slope equation which was given in Chapters 2 & 4. Therefore, we can solve this equation using the integral equation procedure Chamberlain [7] used to solve the mild-slope equation. Following this procedure, which is outlined in Chapter 2, we introduce a new variable ξ defined by

$$\xi(x_0) = \zeta(x_0)\sqrt{J(x_0)} \qquad\qquad (0 \le x_0 \le 1)$$

and find that ξ satisfies the second-kind integral equation

$$\begin{aligned} \xi(x_0) = &\left(c_1 + c_2\xi(0) + c_3\xi(1)\right) e^{i\kappa_0 x_0} \\ &+ \left(c_4 + c_5\xi(0) + c_6\xi(1)\right) e^{-i\kappa_0 x_0} \qquad\qquad (0 < x_0 < 1) \ , \\ &- \frac{i}{2\kappa_0}\int_0^1 e^{i\kappa_0|x_0 - t|}\rho(t)\xi(t)\ dt \end{aligned} \tag{5.22}$$

where

$$\rho(t) = \frac{J''(t)}{2J(t)} - \left(\frac{J'(t)}{2J(t)}\right)^2 + 2\left(U'(t) - \kappa_0 V(t)\right)$$

and where the constants c_j $(j = 1, \ldots, 6)$ are given by

$$\begin{aligned} c_1 &= A^-, \qquad c_2 = -\frac{i\tau}{2\kappa_0} C_0^2 H'(0+), \qquad c_3 = 0 \ , \\ c_4 &= A^+, \qquad c_5 = 0, \qquad\qquad\quad c_6 = \frac{i e^{i\kappa_0}}{2\kappa_0}\tau C_0^2 H'(1-) \ . \end{aligned}$$

From the definition of the integrating factor J, it is simple to see that the above equation for ρ can be rewritten as

$$\rho(t) = U'(t) + U^2(t) - 2\kappa_0 V(t) \ . \tag{5.23}$$

Notice that ρ is continuous for $t \in (0,1)$ and so the kernel in the second-kind integral equation (5.22) for ξ is also continuous.

The coefficients of the reflected and transmitted waves for our integral approximation are given by replacing ϕ in the definitions (5.10) – (5.13) of the reflection and transmission coefficients for the full linear problem by our integral approximation to ϕ, namely ϕ_0. It is then simple to see that the reflection and transmission coefficients for our integral approximation are given in terms of ξ, the solution of the integral equation (5.22), as follows.

For an incident wave from $x = -\infty$ (so that $A^+ = 0$), the coefficients of the reflected and transmitted waves are given by

$$R_1 = \frac{\xi(0)}{A^-} - 1 \ ,$$
$$T_1 = \frac{\xi(1)}{A^-} e^{-i\kappa_0} \ .$$

For an incident wave from $x = \infty$ (so that $A^- = 0$), the coefficients of the reflected and transmitted waves are given by

$$R_2 = \frac{\xi(1) e^{-i\kappa_0}}{A^+} - e^{-2i\kappa_0} \ ,$$
$$T_2 = \frac{\xi(0)}{A^+} \ .$$

We now use Chamberlain's [7] procedure to find approximations to these reflection and transmission coefficients given by the integral approximation, which are second-order accurate compared to the estimate of the solution ξ of the integral equation (5.22). We compare the results given by the integral approximation with the corresponding results given by the mild-slope and modified mild-slope approximations. We shall use the new boundary conditions derived in Chapter 4 with both the modified mild-slope and mild-slope equations.

Example 5.1

Suppose that a wave of unit amplitude is incident from $x = -\infty$ on a hump whose scaled depth profile is given by

$$H(x) = x^2 - x + 1 \qquad\qquad (0 \le x \le 1) \ .$$

This corresponds to a hump whose height is one quarter of the still-water depth and whose slope is discontinuous at $x = 0$ and at $x = 1$, where it meets the flat beds. We choose parameter values

$$\alpha_0 = 2 \ ,$$
$$\tau = 0.2 \ .$$

Using a 3-dimensional trial space we find that for the integral approximation

$$\text{maximum error in } |R_1| = 7.9 \times 10^{-9} \ ,$$
$$R_1 = 0.1681 + 0.1641i \ ,$$
$$|R_1| = 0.2350 \ .$$

Similarly, using a 3-dimensional trial space we find that for the mild-slope approximation gives

$$\text{maximum error in } |R_1| = 4.6 \times 10^{-14} \ ,$$
$$R_1 = 0.0883 + 0.0727i \ ,$$
$$|R_1| = 0.1143 \ .$$

Finally, using a 3-dimensional trial space we find that for the modified mild-slope approximation gives

$$\text{maximum error in } |R_1| = 5.2 \times 10^{-14} \ ,$$
$$R_1 = 0.0920 + 0.0735i \ ,$$
$$|R_1| = 0.1177 \ .$$

It is clear that the integral approximation predicts a much larger reflected amplitude than either the mild-slope or modified mild-slope approximations.

We now consider an example where we find solutions given by the modified mild-slope, mild-slope and integral approximations as we vary the steepness of the hump depth profile.

Example 5.2

We consider a depth profile given by

$$H(x) = 2x^2 - 2x + 1 \qquad\qquad (\leq x \leq 1) \ .$$

This corresponds to a hump whose height is half the still-water depth which has slope discontinuities at $x = 0$ and at $x = 1$, where it meets the flat beds. We

seek solutions given by the modified mild-slope, mild-slope and integral approximations at values of a parameter ω starting at 0.05, finishing at 10, with intervals of 0.05. The parameters α_0 and τ are defined in terms of ω by

$$\alpha_0 = \omega \ , \qquad \tau = \frac{1}{\omega} \ .$$

We have already considered this problem for the new 'decaying mode' approximation in Chapter 4 and recall that with these definitions for α_0 and τ, varying ω corresponds to varying the length l of the hump, which translates to varying the steepness of the depth profile.

We use the 'cheap' solution method given in Chapter 3 to find results for each approximation imposing the usual two significant figure tolerance in the error. The results are depicted in Fig. 5.4. The reflected amplitude given by

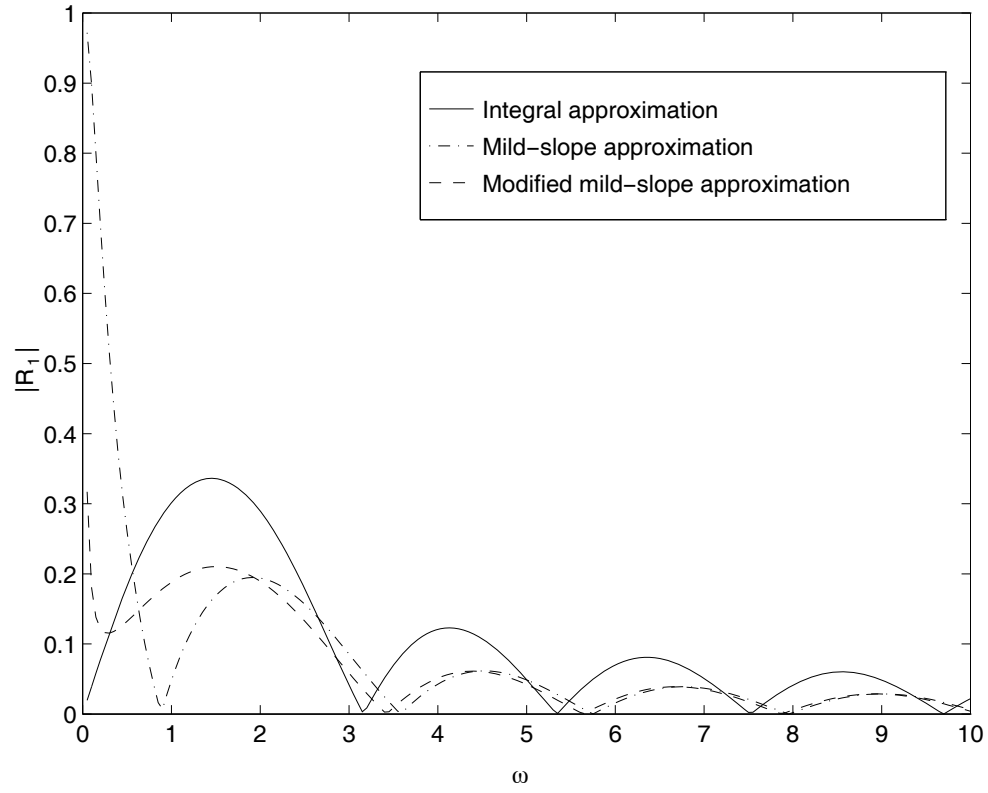

Figure 5.4: Reflected amplitude over the depth profile $H(x) = 2x^2 – 2x + 1$ $(0 \leq x \leq 1)$.

the integral approximation has much higher peaks than the corresponding peaks given by the modified mild-slope and mild-slope approximations. The number of peaks in the reflected amplitude given by all three approximations is the same,

and for large values of $\omega(\omega > 7)$, that is, as the slope of the hump becomes milder, the reflected amplitude given by the new integral approximation is closer to that given by the other two approximations.

The evidence given by these two examples clearly suggests that the integral approximation $\tilde{\phi}$ to ϕ which was derived by omitting all the decaying wave mode terms in the kernel of the second-kind integral equation (5.9), is not equivalent to either the modified mild-slope or the mild-slope approximations. From the evidence given in Chapter 4 for Booij's [5] talud problem, we saw that both the modified mild-slope and the mild-slope approximations gave good approximations to the full linear results. When decaying modes were added to the approximation, the results became even closer to the full linear ones that Booij had computed. Similarly, we expect that the results given in Chapter 4 by the new 'decaying mode' approximation for this current hump problem are tending to those given by full linear theory as the number of decaying modes is increased. From Fig.4.6 in Chapter 4, we see that the height of the peaks in the amplitude of the reflected wave for this scattering problem given by the new 'decaying mode' approximations and the modified mild-slope and mild-slope approximations are very similar. As the peaks in the amplitude of the reflected wave given by the integral approximation are nearly twice the height of the peaks given by both the modified mild-slope and mild-slope approximations, then we conclude that the integral approximation is a poor approximation to the full linear problem.

If we recall how we made the integral approximation, it is really quite surprising that the integral approximation produces recognisable results at all. We approximated the kernel of the integral equation (5.9), which is an infinite series, with just the first term of this series. From the results we have obtained, it is clear that this estimate of the infinite series is quite poor, a not surprising fact.

Instead of trying to improve the approximation in the full linear integral equation (5.9), we find that accurate estimates of the solutions of the full linear problem itself can be obtained. This is achieved by firstly converting the second-kind integral equation (5.9) for the velocity potential on the hump into a first-kind integral equation for the tangential fluid velocity on the hump.

5.3 A first-kind integral equation

We now return to the full linearised problem which was stated in section 5.1. The Green's identity domain under consideration is as depicted in Fig.5.5. In this pic-

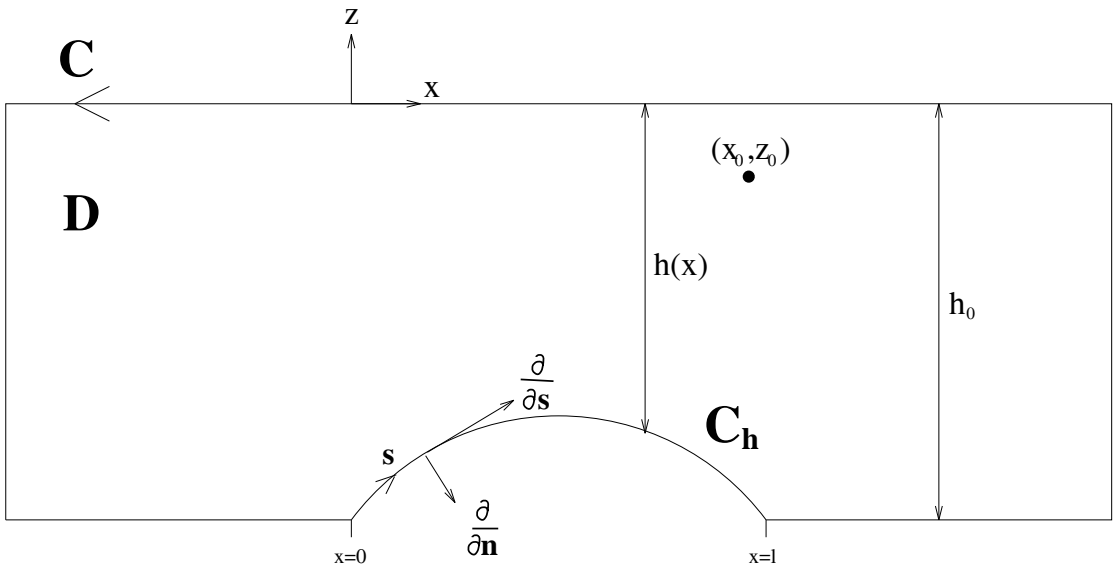

Figure 5.5: The Green's identity domain.

ture, $\frac{\partial}{\partial n}$ denotes the outward normal derivative, $\frac{\partial}{\partial s}$ the tangential derivative and s the arc length along C_h, the curved part of C, measured from $x = 0, z = -h_0$. The outward unit normal was defined in Chapter 2 in terms of two orthogonal horizontal co-ordinates x and y and a vertical co-ordinate z. For the problem domain we are considering, which is independent of y, the outward unit normal $\underline{n}$ at (x, z) on C_h is given by

$$\underline{n} = -\frac{1}{(1 + (h'(x))^2)^{\frac{1}{2}}} (h'(x),\ 1) \ ,$$

where the prime denotes differentiation with respect to x. The unit tangent $\underline{s}$ at (x, z) on C_h is given by

$$\underline{s} = \frac{1}{(1 + (h'(x))^2)^{\frac{1}{2}}} (1,\ -h'(x)) \ .$$

It follows that the normal and tangential derivatives at (x, z) on C_h are given by

$$\frac{\partial}{\partial n} = \frac{-1}{(1 + (h'(x))^2)^{\frac{1}{2}}} \left[\frac{\partial}{\partial z} + h'(x) \frac{\partial}{\partial x} \right]$$

and

$$\frac{\partial}{\partial s} = \frac{1}{(1+(h'(x))^2)^{\frac{1}{2}}}\left[\frac{\partial}{\partial x} - h'(x)\frac{\partial}{\partial z}\right] \ .$$

Taking the normal derivative of equation (5.8), the integral representation of the velocity potential in the fluid, gives

$$\begin{aligned}\frac{\partial\phi}{\partial n_0}(x_0,z_0) = \ & \frac{\partial}{\partial n_0}\left[\frac{\cosh\left(k_0(z_0+h_0)\right)}{\cosh\left(k_0h_0\right)}\left[A^-e^{ik_0x_0}+A^+e^{-ik_0x_0}\right]\right] \\ & -\frac{\partial}{\partial n_0}\int_{C_h}\left[\phi\frac{\partial G}{\partial n}\right]_{z=-h(x)} ds \end{aligned} \qquad (x_0,z_0) \text{ in } D \ .$$

The exponential term in the infinite series (5.7) for G guarantees that G is an infinitely differentiable function of (x,z) and (x_0,z_0) for $(x,z) \neq (x_0,z_0)$. As (x_0,z_0) is in D and (x,z) is on C_h, then we can take $\frac{\partial}{\partial n_0}$ under the integral in the above equation to give

$$\begin{aligned}\frac{\partial\phi}{\partial n_0}(x_0,z_0) = \ & \frac{\partial}{\partial n_0}\left[\frac{\cosh\left(k_0(z_0+h_0)\right)}{\cosh\left(k_0h_0\right)}\left[A^-e^{ik_0x_0}+A^+e^{-ik_0x_0}\right]\right] \\ & -\int_{C_h}\left[\phi\frac{\partial^2 G}{\partial n_0\partial n}\right]_{z=-h(x)} ds \ , \end{aligned} \qquad (5.24)$$

where (x_0,z_0) is in D.

Notice that the Green's function G defined by (5.7) can be written as

$$G(x,z|x_0,z_0) = f(x-x_0,z+z_0+2h_0) + f(x-x_0,z-z_0) \ , \qquad (5.25)$$

where

$$f(x,z) = \frac{i}{4k_0}c_0^2\cosh\left(k_0z\right)e^{ik_0|x|} + \sum_{n=1}^{\infty}\frac{1}{4B_n^0}c_n^2\cos\left(B_n^0z\right)e^{-B_n^0|x|} \ .$$

As G is a Green's function, singular at $(x,z)=(x_0,z_0)$, it follows that the function $f(x-x_0,z-z_0)$ is a Green's function, singular at $(x,z)=(x_0,z_0)$, satisfying

$$\hat{\nabla}^2 f(x,z) = -\delta(x)\delta(z) \qquad -h_0 < z < 0 \ .$$

The function $f(x-x_0,z+z_0+2h_0)$ is regular in D, that is, it satisfies Laplace's equation at all points in D. We now define a new function $L = L(x,z|x_0,z_0)$ by

$$L(x,z|x_0,z_0) = f(x-x_0,z+z_0+2h_0) - f(x-x_0,z-z_0) \ .$$

It follows that L is also a Green's function in the sense that

$$\hat{\nabla}^2 L = \delta(x-x_0)\delta(z-z_0) \qquad -h_0 < z < 0 \ .$$

Notice that G behaves like a line source near (x_0, z_0) and L behaves like a line sink near (x_0, z_0). From the definition of f it is simple to see that L is given by the infinite series

$$\begin{aligned} L\,(x,z|x_0,z_0) = \ & \frac{i}{2k_0}c_0^2 \sinh\left(k_0(z+h_0)\right)\sinh\left(k_0(z_0+h_0)\right) e^{ik_0|x-x_0|} \\ & -\sum_{n=1}^{\infty} \frac{1}{2B_n^0} c_n^2 \sin\left(B_n^0(z+h_0)\right)\sin\left(B_n^0(z_0+h_0)\right) e^{-B_n^0|x-x_0|}. \end{aligned} \tag{5.26}$$

Lemma 5.1 *Suppose $G = G(x,z|x_0,z_0)$ and $L = L(x,z|x_0,z_0)$ are defined by (5.7) and (5.26) respectively. Then $\frac{\partial G}{\partial n}$ and $\frac{\partial L}{\partial s}$ satisfy*

$$\frac{\partial}{\partial n_0}\left(\frac{\partial G}{\partial n}\right) = \frac{\partial}{\partial s_0}\left(\frac{\partial L}{\partial s}\right) \quad \textit{and} \quad \frac{\partial}{\partial s_0}\left(\frac{\partial G}{\partial n}\right) = -\frac{\partial}{\partial n_0}\left(\frac{\partial L}{\partial s}\right)$$

for all (x,z) and (x_0,z_0) provided $(x,z) \neq (x_0,z_0)$. (In this sense $\frac{\partial G}{\partial n}$ and $\frac{\partial L}{\partial s}$ can be thought of as conjugate functions.)

Proof

This follows directly from finding the above derivatives of the infinite series (5.7) and (5.26) for G and L.

It follows from Lemma 5.1, that equation (5.24) can be rewritten as

$$\begin{aligned} \frac{\partial \phi}{\partial n_0}(x_0,z_0) = \ & \frac{\partial}{\partial n_0}\left[\frac{\cosh\left(k_0(z_0+h_0)\right)}{\cosh\left(k_0h_0\right)}\left[A^- e^{ik_0x_0} + A^+ e^{-ik_0x_0}\right]\right] \\ & -\frac{\partial}{\partial s_0}\int_{C_h}\left[\phi\frac{\partial L}{\partial s}\right]_{z=-h(x)} ds \ , \end{aligned} \tag{5.27}$$

where (x_0,z_0) is in D. The right hand side of the above equation can be rewritten as the tangential derivative of a function by noticing that

$$\begin{aligned} & \frac{\partial}{\partial n_0}\left[\frac{\cosh\left(k_0(z_0+h_0)\right)}{\cosh\left(k_0h_0\right)}\left[A^- e^{ik_0x_0} + A^+ e^{-ik_0x_0}\right]\right] = \\ & \qquad \frac{\partial}{\partial s_0}\left[\frac{i\sinh\left(k_0(z_0+h_0)\right)}{\cosh\left(k_0h_0\right)}\left[A^- e^{ik_0x_0} - A^+ e^{-ik_0x_0}\right]\right]. \end{aligned}$$

Therefore, equation (5.27) can be written as

$$\frac{\partial \phi}{\partial n_0}(x_0,z_0) = \frac{\partial}{\partial s_0}\left[\frac{i\sinh(k_0(z_0+h_0))}{\cosh\left(k_0h_0\right)}\left[A^- e^{ik_0x_0} - A^+ e^{-ik_0x_0}\right] - \int_{C_h}\left[\phi\frac{\partial L}{\partial s}\right]_{z=-h(x)} ds\right], \tag{5.28}$$

where (x_0, z_0) is in D. Integration by parts gives

$$\int_{C_h} \left[\phi \frac{\partial L}{\partial s}\right]_{z=-h(x)} ds = \Big[\phi L\Big]_{C_h} - \int_{C_h} \left[L \frac{\partial \phi}{\partial s}\right]_{z=-h(x)} ds \ .$$

The velocity potential is certainly bounded on the bed and from the infinite series (5.26) for L it is clear that

$$L(0, -h_0|x_0, z_0) = L(l, -h_0|x_0, z_0) = 0 \qquad \forall\ (x_0, z_0) \text{ in } D \ .$$

Therefore for (x_0, z_0) in D

$$\int_{C_h} \left[\phi \frac{\partial L}{\partial s}\right]_{z=-h(x)} ds = - \int_{C_h} \left[L \frac{\partial \phi}{\partial s}\right]_{z=-h(x)} ds \ .$$

Equation (5.28) can now be written as

$$\frac{\partial \phi}{\partial n_0}(x_0, z_0) = \frac{\partial}{\partial s_0}\left[\frac{i \sinh(k_0(z_0+h_0))}{\cosh(k_0 h_0)}\left[A^- e^{ik_0 x_0} - A^+ e^{-ik_0 x_0}\right] + \int_{C_h}\left[L\frac{\partial \phi}{\partial s}\right]_{z=-h(x)} ds\right],$$

where (x_0, z_0) is in D. If we now let (x_0, z_0) tend to a point on C_h, then this equation becomes

$$0 = \frac{\partial}{\partial s_0}\left[\frac{i \sinh(k_0(z_0+h_0))}{\cosh(k_0 h_0)}\left[A^- e^{ik_0 x_0} - A^+ e^{-ik_0 x_0}\right] + \int_{C_h}\left[L\frac{\partial \phi}{\partial s}\right]_{z=-h(x)} ds\right],$$

where (x_0, z_0) is on C_h. Integrating this equation with respect to s_0 gives

$$c = \frac{i \sinh(k_0(h_0 - h(x_0)))}{\cosh(k_0 h_0)}\left[A^- e^{ik_0 x_0} - A^+ e^{-ik_0 x_0}\right] + \int_{C_h}\left[L\frac{\partial \phi}{\partial s}\right] ds \qquad (0 \le x_0 \le l), \quad (5.29)$$

where c is a constant to be found.

In the neighbourhood of a corner of angle α, of a boundary on which $\frac{\partial \phi}{\partial n}$ takes prescribed continuous values, the velocity potential ϕ is given as the sum of the bounded separation solutions near $r = 0$ by

$$\phi = \phi_0 + \sum_{j=1}^{\infty} a_j r^{\frac{j\pi}{\alpha}} \cos\left(\frac{j\pi\theta}{\alpha}\right) \qquad 0 \le \theta \le \alpha \ , \qquad (5.30)$$

where r, θ are polar co-ordinates relative to the corner, a_j $(j \in \mathbb{N})$ are constants and ϕ_0 has prescribed values on $\theta = 0$ and $\theta = \alpha$. We consider the case when $\frac{\partial \phi}{\partial n} = 0$ on the boundary as depicted in Fig.5.6. It follows that the tangential derivative of ϕ on the boundary $\theta = \alpha$ is

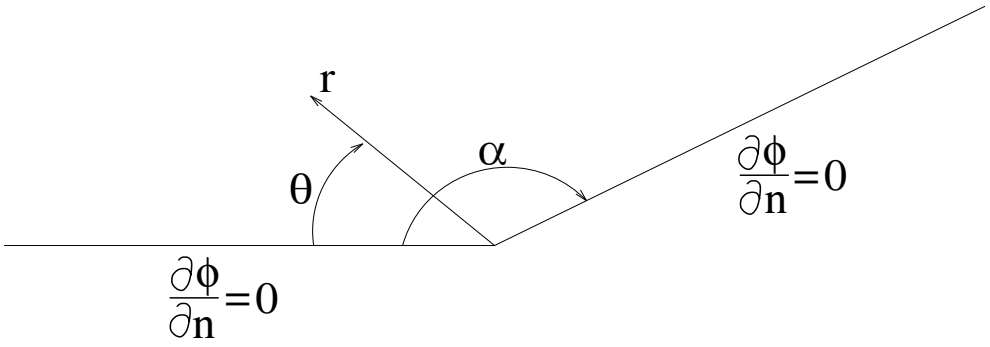

Figure 5.6: Polar co-ordinate system at a corner.

$$\left.\frac{\partial\phi}{\partial s}\right|_{\theta=\alpha} = \left.\frac{\partial\phi}{\partial r}\right|_{\theta=\alpha} = \frac{\pi}{\alpha}\sum_{j=1}^{\infty}(-1)^j a_j j r^{\frac{j\pi}{\alpha}-1} \to 0 \text{ as } r \to 0 \text{ since } 0 < \alpha < \pi \ .$$

The same result clearly holds on the boundary $\theta = 0$. Therefore, as the depth profiles C_h that we are considering are all humps (so that $\alpha < \pi$), it follows that $\frac{\partial\phi}{\partial s}$ evaluated on C_h is zero, and therefore bounded, at the ends of the hump, that is, at $x = 0$ and $x = l$. It follows that as $L(x, z|0, -h_0) = 0$ for (x, z) on C_h, then

$$\left[\int_{C_h}\left[L\frac{\partial\phi}{\partial s}\right]ds\right]_{x_0=0} = 0 \ .$$

Substituting $x_0 = 0$ in (5.29) then gives $c = 0$ and so it follows that the tangential fluid velocity evaluated on the hump satisfies the first-kind integral equation

$$\int_{C_h}\left[L\frac{\partial\phi}{\partial s}\right]ds + \frac{i\sinh(k_0(h_0-h(x_0)))}{\cosh(k_0h_0)}\left[A^-e^{ik_0x_0} - A^+e^{-ik_0x_0}\right] = 0 \qquad (0 \le x_0 \le l). \quad (5.31)$$

Notice that in the fluid the stream function ψ associated with the velocity potential ϕ is such that

$$\frac{\partial\phi}{\partial x} = \frac{\partial\psi}{\partial z} \qquad \text{and} \qquad \frac{\partial\phi}{\partial z} = -\frac{\partial\psi}{\partial x} \ , \quad (5.32)$$

provided the derivatives exist, and on the bed ψ is related to ϕ by

$$\frac{\partial\phi}{\partial n} = \frac{\partial\psi}{\partial s} \qquad \text{and} \qquad \frac{\partial\phi}{\partial s} = -\frac{\partial\psi}{\partial n} \ , \quad (5.33)$$

as long as the derivatives exist. In other words, ϕ and ψ are related by the Cauchy-Riemann equations in any orthogonal co-ordinate system. We can now rewrite (5.31) in terms of the normal derivative of ψ evaluated on the hump as

$$\int_{C_h}\left[L\frac{\partial\psi}{\partial n}\right]ds \ - \ \frac{i\sinh(k_0(h_0-h(x_0)))}{\cosh(k_0h_0)}\left[A^-e^{ik_0x_0} - A^+e^{-ik_0x_0}\right] = 0 \qquad (0 \le x_0 \le l).$$

This first-kind integral equation for $\frac{\partial \psi}{\partial n}$ evaluated on C_h looks like the result of applying Green's identity (5.4) to ψ and L. Indeed, in the next section we show that this is precisely the case and therefore we can give a much more direct derivation of equation (5.31) than we did in this section.

5.4 A direct derivation of the first-kind integral equation

Let us recall that the problem domain we are considering is as depicted in Fig.5.1, and that the time independent velocity potential ϕ satisfies

$$\begin{aligned} \hat{\nabla}^2 \phi &= 0 \qquad && -h < z < 0 \,, \\ \frac{\partial \phi}{\partial z} - \nu \phi &= 0 \qquad && \text{on } z = 0 \,, \\ \frac{\partial \phi}{\partial n} &= 0 \qquad && \text{on } z = -h(x) \,, \end{aligned}$$

where $\hat{\nabla}^2 = \frac{\partial^2}{\partial x^2} + \frac{\partial^2}{\partial z^2}$ and $\nu = \frac{\sigma^2}{g}$, together with the radiation conditions

$$\phi(x,z) \sim \frac{\cosh\left(k_0(z+h_0)\right)}{\cosh\left(k_0 h_0\right)} \left[A^- e^{ik_0 x} + B^- e^{-ik_0 x}\right] \qquad \text{as } x \to -\infty$$

and

$$\phi(x,z) \sim \frac{\cosh\left(k_0(z+h_0)\right)}{\cosh\left(k_0 h_0\right)} \left[A^+ e^{-ik_0 x} + B^+ e^{ik_0 x}\right] \qquad \text{as } x \to \infty \,.$$

From equations (5.32) and (5.33), it follows that ψ satisfies

$$\left.\begin{aligned} \hat{\nabla}^2 \psi &= 0 \qquad && -h < z < 0 \,, \\ \frac{\partial^2 \psi}{\partial z^2} - \nu \frac{\partial \psi}{\partial z} &= 0 \qquad && \text{on } z = 0 \,, \\ \psi &= 0 \qquad && \text{on } z = -h(x) \,, \end{aligned}\right\} \tag{5.34}$$

together with the radiation conditions

$$\psi(x,z) \sim \frac{i \sinh\left(k_0(z+h_0)\right)}{\cosh\left(k_0 h_0\right)} \left[A^- e^{ik_0 x} - B^- e^{-ik_0 x}\right] \qquad \text{as } x \to -\infty \tag{5.35}$$

and

$$\psi(x,z) \sim \frac{i \sinh\left(k_0(z+h_0)\right)}{\cosh\left(k_0 h_0\right)} \left[-A^+ e^{-ik_0 x} + B^+ e^{ik_0 x}\right] \qquad \text{as } x \to \infty \,. \tag{5.36}$$

Note that the stream function is arbitrary to within a constant and we have chosen $\psi = 0$ on $z = -h(x)$, that is, we have chosen the streamline $\psi = 0$ to be the bed. We have also expressed the radiation conditions on ψ at $x = \pm\infty$ in terms of the coefficients of the incident and scattered waves. It follows that the coefficients of the reflected and transmitted waves due to an incident wave from either $x = \infty$ or $x = -\infty$ are as given in section 5.1 by equations (5.10) – (5.13). We shall show later that the reflection and transmission coefficients can be expressed in terms of $\frac{\partial \psi}{\partial n}$ evaluated on C_h.

We shall now derive the first-kind integral equation via Green's identity

$$\iint_D \left(\psi \hat{\nabla}^2 L - L\hat{\nabla}^2\psi\right) dxdz = \oint_C \left(\psi \frac{\partial L}{\partial n} - L\frac{\partial \psi}{\partial n}\right) dc \quad , \tag{5.37}$$

where D is the domain with boundary C depicted in Fig.5.5. Following the work in the previous section, the Green's function L is chosen to satisfy

$$\hat{\nabla}^2 L = \delta(x - x_0)\delta(z - z_0) \qquad -h_0 < z < 0 \ , \tag{5.38}$$

$$\frac{\partial^2 L}{\partial z^2} - \nu \frac{\partial L}{\partial z} = 0 \qquad \text{on } z = 0 \ , \tag{5.39}$$

$$L = 0 \qquad \text{on } z = -h_0 \ , \tag{5.40}$$

together with a radiation condition that L behaves like an outgoing wave as $|x| \to \infty$. In other words,

$$L \sim e^{\pm ik_0 x} \qquad \text{as } x \to \pm\infty \ . \tag{5.41}$$

We have already shown that the Green's function L defined by the infinite series (5.26) satisfies (5.38). From equation (5.26) it is clear that L also satisfies conditions (5.39) – (5.41).

The structure of the Green's function L given by (5.26) is unusual, in that L is not defined in terms of an orthogonal sequence on $-h_0 < z < 0$ because

$$\int_{-h_0}^{0} \sin\left(B_i^0(z+h_0)\right) \sin\left(B_j^0(z+h_0)\right) dz = \frac{-1}{B_i^0} \cos\left(B_i^0 h_0\right) \sin\left(B_j^0 h_0\right) \neq 0 \qquad (i \neq j).$$

This raises the question of whether the Green's function L satisfying (5.38) – (5.41) can be determined without first finding the Green's function G given by (5.7). We can show that L is indeed given by (5.26) without first finding G by

considering a fourier series expansion for $\frac{\partial L}{\partial z}$, given by

$$\frac{\partial L}{\partial z}(x,z|x_0,z_0) = \sum_{n=0}^{\infty} d_n(x|x_0,z_0)v_n(z) \ .$$

Here $v_0(z) = c_0\cosh(k_0(z+h_0))$, $v_n(z) = c_n\cos(B_n^0(z+h_0))$ $(n \in \mathbb{N})$, and the functions d_n $(n+1 \in \mathbb{N})$ are to be found. All the other functions are defined earlier in this chapter.

Integrating the above expression for $\frac{\partial L}{\partial z}$ with respect to z gives

$$\begin{aligned} L\,(x,z|x_0,z_0) = \ & \frac{1}{k_0}d_0(x|x_0,z_0)c_0\sinh\left(k_0(z+h_0)\right) \\ & + \sum_{n=1}^{\infty}\frac{1}{B_n^0}d_n(x|x_0,z_0)c_n\sin\left(B_n^0(z+h_0)\right) \ , \end{aligned}$$

where there is no constant of integration because we require $L = 0$ on $z = -h_0$. It is clear that L as defined above also satisfies the free surface condition (5.39).

From Chapter 4, we know that the sequence $\{v_n \ : \ n+1 \in \mathbb{N}\}$ is orthonormal for $z \in [-h_0, 0]$. Therefore, the unknown functions d_n are given by

$$d_n(x|x_0,z_0) = \int_{-h_0}^{0}\frac{\partial L}{\partial z}(x,z|x_0,z_0)v_n(z)dz \qquad (n+1 \in \mathbb{N}) \ . \tag{5.42}$$

Integration by parts gives

$$\begin{aligned} d_0(x|x_0,z_0) &= \frac{c_0}{k_0}\sinh\left(k_0h_0\right)\frac{\partial L}{\partial z}\bigg|_{z=0} - \frac{1}{k_0}\int_{-h_0}^{0}\frac{\partial^2 L}{\partial z^2}w_0(z)dz \ , \\ d_n(x|x_0,z_0) &= \frac{c_n}{B_n^0}\sin\left(B_n^0h_0\right)\frac{\partial L}{\partial z}\bigg|_{z=0} - \frac{1}{B_n^0}\int_{-h_0}^{0}\frac{\partial^2 L}{\partial z^2}w_n(z)dz \qquad (n \in \mathbb{N}), \end{aligned} \tag{5.43}$$

where $w_0(z) = c_0\sinh(k_0(z+h_0))$ and $w_n(z) = c_n\sin(B_n^0(z+h_0))$ $(n \in \mathbb{N})$. Differentiating (5.42) twice with respect to x and then integrating the result by parts gives

$$\begin{aligned} d_0''(x|x_0,z_0) &= c_0\cosh\left(k_0h_0\right)\frac{\partial^2 L}{\partial x^2}\bigg|_{z=0} - k_0\int_{-h_0}^{0}\frac{\partial^2 L}{\partial x^2}w_0(z)dz \ , \\ d_n''(x|x_0,z_0) &= c_n\cos\left(B_n^0h_0\right)\frac{\partial^2 L}{\partial x^2}\bigg|_{z=0} + B_n^0\int_{-h_0}^{0}\frac{\partial^2 L}{\partial x^2}w_n(z)dz \qquad (n \in \mathbb{N}), \end{aligned} \tag{5.44}$$

where the prime denotes differentiation with respect to x.

From (5.38), it follows that

$$\int_{-h_0}^{0}\left(\hat{\nabla}^2 L\right)w_n(z)dz \ = \delta(x-x_0)w_n(z_0) \qquad (n+1 \in \mathbb{N}) \ . \tag{5.45}$$

Substituting equations (5.43) and (5.44) into (5.45) and employing the equations $\nu = k_0 \tanh(k_0 h_0)$ and $-\nu = B_n^0 \tan(B_n^0 h_0)$ $(n \in \mathbb{N})$, we find that

$$d_0'' + {k_0}^2 d_0 - c_0 \cosh(k_0 h_0)\left[\frac{\partial^2 L}{\partial x^2} + \nu \frac{\partial L}{\partial z}\right]\Big|_{z=0} = -\delta(x - x_0) k_0 w_0(z_0),$$

$$d_n'' - \left(B_n^0\right)^2 d_n - c_n \cos\left(B_n^0 h_0\right)\left[\frac{\partial^2 L}{\partial x^2} + \nu \frac{\partial L}{\partial z}\right]\Big|_{z=0} = \delta(x - x_0) B_n^0 w_n(z_0) \quad (n \in \mathbb{N}).$$

As (x_0, z_0) is in D, then $\hat{\nabla}^2 L = 0$ on $z = 0$ and so as L satisfies the surface condition (5.39) then it also satisfies the surface condition

$$\frac{\partial^2 L}{\partial x^2} + \nu \frac{\partial L}{\partial z} = 0 \qquad \text{on } z = 0 \ .$$

Therefore, the unknown functions d_n $(n + 1 \in \mathbb{N})$ satisfy the ordinary differential equations

$$d_0'' + {k_0}^2 d_0 = -\delta(x - x_0) k_0 w_0(z_0) \ ,$$

$$d_n'' - \left(B_n^0\right)^2 d_n = \delta(x - x_0) B_n^0 w_n(z_0) \qquad (n \in \mathbb{N}).$$

These equations can be solved using variation of parameters to give

$$d_0(x|x_0, z_0) = \begin{cases} L_0 e^{ik_0 x} + M_0 e^{-ik_0 x} & x < x_0 \ , \\ L_0 e^{ik_0 x} + M_0 e^{-ik_0 x} - \dfrac{w_0(z_0)}{2i}\left(e^{ik_0(x-x_0)} - e^{-ik_0(x-x_0)}\right) & x > x_0 \end{cases}$$

and, for $n \in \mathbb{N}$,

$$d_n(x|x_0, z_0) = \begin{cases} L_n e^{B_n^0 x} + M_n e^{-B_n^0 x} & x < x_0 \ , \\ L_n e^{B_n^0 x} + M_n e^{-B_n^0 x} + \dfrac{w_n(z_0)}{2}\left(e^{B_n^0(x-x_0)} - e^{-B_n^0(x-x_0)}\right) & x > x_0 \ . \end{cases}$$

Imposing the radiation condition (5.41) gives the unknown constants in the above expressions. It follows that

$$d_0(x|x_0, z_0) = \frac{i}{2} c_0 \sinh(k_0(z_0 + h_0))\, e^{ik_0|x - x_0|}$$

and

$$d_n(x|x_0, z_0) = -\frac{1}{2} c_n \sin\left(B_n^0(z_0 + h_0)\right) e^{-B_n^0|x - x_0|} \qquad (n \in \mathbb{N}) \ .$$

Therefore, the Green's function L satisfying (5.38) – (5.41) is given by

$$\begin{aligned} L(x, z|x_0, z_0) = \ & \frac{i}{2k_0} c_0^2 \sinh(k_0(z + h_0)) \sinh(k_0(z_0 + h_0))\, e^{ik_0|x - x_0|} \\ & - \sum_{n=1}^{\infty} \frac{1}{2B_n^0} c_n^2 \sin\left(B_n^0(z + h_0)\right) \sin\left(B_n^0(z_0 + h_0)\right) e^{-B_n^0|x - x_0|}. \end{aligned}$$

The method that we have used to construct L here can be used to construct the Green's function G given by (5.7). Notice that L and G are only defined for $-h_0 < z < 0$. Hence, it is clear that these two Green's functions are not suitable to be used with other types of depth profiles that satisfy $h(x) = h_0 \ \forall x \in (-\infty, 0] \cup [l, \infty)$, such as ripples in the sea bed or a trench, as h_0 is no longer the greatest fluid depth. The issue of finding the Green's functions L and G for depth profiles corresponding to ripples and trenches is a separate problem and is not pursued here. This is the reason why we just consider hump depth profiles in this chapter.

If Green's identity (5.37) is now applied to the domain depicted in Fig.5.5, where (x_0, z_0) is inside D and the vertical boundaries are assumed to be a great distance from the hump, so that the radiation conditions (5.35), (5.36) and (5.41) apply there, then

$$\begin{aligned}\psi(x_0,z_0) = &\int_{-\infty}^{0}\left[-\psi\frac{\partial L}{\partial z}+L\frac{\partial\psi}{\partial z}\right]\Bigg|_{z=-h_0}dx+\int_{C_h}\left[\psi\frac{\partial L}{\partial n}-L\frac{\partial\psi}{\partial n}\right]\Bigg|_{z=-h(x)}ds\\ &+\int_{l}^{\infty}\left[-\psi\frac{\partial L}{\partial z}+L\frac{\partial\psi}{\partial z}\right]\Bigg|_{z=-h_0}dx+\int_{-h_0}^{0}\left[\psi\frac{\partial L}{\partial x}-L\frac{\partial\psi}{\partial x}\right]\Bigg|_{x=\infty}dz\\ &+\int_{-\infty}^{\infty}\left[\psi\frac{\partial L}{\partial z}-L\frac{\partial\psi}{\partial z}\right]\Bigg|_{z=0}(-dx)+\int_{0}^{-h_0}\left[-\psi\frac{\partial L}{\partial x}+L\frac{\partial\psi}{\partial x}\right]\Bigg|_{x=-\infty}(-dz)\,.\end{aligned}\tag{5.46}$$

As $\psi = 0$ on $z = -h(x) \ \forall x \in (-\infty, \infty)$ and $L = 0$ on $z = -h_0$, then the first and third integrals in (5.46) are zero. The fifth integral in (5.46) is non-zero because ψ and L satisfy a second-order boundary condition at the surface $z = 0$. This integral is given by

$$\begin{aligned}-\int_{-\infty}^{\infty}\left[\psi\frac{\partial L}{\partial z}-L\frac{\partial\psi}{\partial z}\right]\Bigg|_{z=0}dx &= 2\left[A^{-}e^{ik_0x}\ L\big|_{\substack{z=0\\x=-\infty}}-A^{+}e^{-ik_0x}\ L\big|_{\substack{z=0\\x=\infty}}\right],\\ &= 2\left[\frac{ic_0^2}{2k_0}\frac{\sinh\left(k_0(z_0+h_0)\right)}{\operatorname{cosech}\left(k_0h_0\right)}\left[A^{-}e^{ik_0x_0}-A^{+}e^{-ik_0x_0}\right]\right].\end{aligned}$$

The sum of the fourth and sixth integrals in the right hand side of (5.46) is given

by

$$\int_{-h_0}^{0}\left[\psi\frac{\partial L}{\partial x}-L\frac{\partial\psi}{\partial x}\right]\Big|_{x=\infty}dz+\int_{0}^{-h_0}\left[-\psi\frac{\partial L}{\partial x}+L\frac{\partial\psi}{\partial x}\right]\Big|_{x=-\infty}(-dz)$$

$$=\frac{-2k_0}{\cosh(k_0h_0)}\int_{-h_0}^{0}\left[A^-e^{ik_0x}\,L|_{x=-\infty}-A^+e^{-ik_0x}\,L|_{x=\infty}\right]\sinh(k_0(z+h_0))\,dz$$

$$=\frac{-2k_0}{\cosh(k_0h_0)}\left[\frac{-ic_0^2}{2k_0}\frac{\left[A^-e^{ik_0x_0}-A^+e^{-ik_0x_0}\right]}{\mathrm{cosech}(k_0(z_0+h_0))}\frac{(2k_0h_0-\sinh(2k_0h_0))}{4k_0}\right].$$

Substituting these expressions for the integrals into (5.46) gives

$$\psi(x_0,z_0)=\frac{ic_0^2}{2k_0}\frac{\left[A^-e^{ik_0x_0}-A^+e^{-ik_0x_0}\right]}{\mathrm{cosech}(k_0(z_0+h_0))}\left[2\sinh(k_0h_0)+\frac{2k_0h_0-\sinh(2k_0h_0)}{2\cosh(k_0h_0)}\right]$$
$$-\int_{C_h}\left[L\frac{\partial\psi}{\partial n}\right]\Big|_{z=-h(x)}ds\quad,$$

which simplifies to

$$\psi(x_0,z_0)=\frac{i\sinh(k_0(z_0+h_0))}{\cosh(k_0h_0)}\left[A^-e^{ik_0x_0}-A^+e^{-ik_0x_0}\right]-\int_{C_h}\left[L\frac{\partial\psi}{\partial n}\right]\Big|_{z=-h(x)}ds\quad.$$

If we now let (x_0,z_0) tend to a point on C_h, then this equation reduces to the first-kind integral equation for $\frac{\partial\psi}{\partial n}$ evaluated on C_h that was derived in the previous section, namely

$$\int_{C_h}\left[L\frac{\partial\psi}{\partial n}\right]ds-\frac{i\sinh(k_0(h_0-h(x_0)))}{\cosh(k_0h_0)}\left[A^-e^{ik_0x_0}-A^+e^{-ik_0x_0}\right]=0\qquad(0\le x_0\le l).$$

From equation (5.33) which relates ϕ and ψ on the bed, we can rewrite this first-kind equation as

$$\int_{C_h}\left[L\frac{\partial\phi}{\partial s}\right]ds+\frac{i\sinh(k_0(h_0-h(x_0)))}{\cosh(k_0h_0)}\left[A^-e^{ik_0x_0}-A^+e^{-ik_0x_0}\right]=0\qquad(0\le x_0\le l),$$

or equivalently as

$$\int_0^l\left[L|_{\substack{z=-h(x)\\ z_0=-h(x_0)}}\frac{\partial\phi}{\partial x}(x,-h(x))\right]dx$$
$$+\frac{i\sinh(k_0(h_0-h(x_0)))}{\cosh(k_0h_0)}\left[A^-e^{ik_0x_0}-A^+e^{-ik_0x_0}\right]=0\qquad(0\le x_0\le l).\tag{5.47}$$

If the boundary-value problem (5.1) – (5.3) for ϕ has a unique solution, then it is given by solving the above first-kind integral equation.

Evans [16], whilst considering water wave scattering by a shelf, showed that as the point (x, z) approaches (x_0, z_0),

$$G \approx \frac{1}{2\pi}\left[\log\left\{(x-x_0)^2+(z-z_0)^2\right\}^{\frac{1}{2}} + \log\left\{(x-x_0)^2+(z+z_0+2h_0)^2\right\}^{\frac{1}{2}}\right] ,$$

where the notation $f \approx g$ means that $\frac{\partial(f-g)}{\partial n}$ is bounded for all points on the shelf. This result holds for any bed contours including humps. The above result can also be deduced from equation (5.25), where we expressed G as a sum of two infinite series. It is simple to show that on a hump, as $(x, z) \to (x_0, z_0)$ then

$$\frac{\partial}{\partial n}\left[\log\left\{(x-x_0)^2+(z-z_0)^2\right\}^{\frac{1}{2}}\right] = \frac{-1}{2R(x_0)} ,$$

where

$$R(x_0) = \frac{(1+(h'(x_0))^2)^{\frac{3}{2}}}{h''(x_0)}$$

is the radius of curvature of C_h at $(x_0, -h(x_0))$. Therefore, the above normal derivative is bounded for all $x_0 \in [0, l]$. The other logarithm given above is only singular on C_h at $(x_0, z_0) = (0, -h_0)$ and $(x_0, z_0) = (l, -h_0)$. It is simple to show that at these points the value of $\frac{\partial}{\partial n}\left[\log\left\{(x-x_0)^2+(z+z_0+2h_0)^2\right\}^{\frac{1}{2}}\right]$ is $\frac{-1}{2R(0+)}$ and $\frac{-1}{2R(l-)}$ respectively.

It follows that, except for discrete values of the parameters of the problem for which the homogeneous form of the second-kind integral equation (5.9) satisfied by ϕ on C_h has non-trivial solutions, the second-kind integral equation (5.9) has a unique solution and therefore so does the boundary-value problem (5.1) – (5.3) for ϕ.

It is possible that there are discrete values of the parameters of the problem for which the homogeneous form of the second-kind integral equation (5.9) has non-trivial solutions, which corresponds to trapped modes over the hump. However, in all the problems we have considered there has been no evidence of such modes, nor do we expect them for these bed geometries.

We have derived a first-kind integral equation for the tangential velocity $\frac{\partial\phi}{\partial s}$ on C_h. We actually want to find approximations to the coefficients of the reflected and transmitted waves due to a wave incident on the hump. These coefficients were defined earlier by equations (5.10) – (5.13) in terms of ϕ evaluated on the hump. We can rewrite these equations in terms of $\frac{\partial\phi}{\partial s}$ evaluated on the hump as follows.

For an incident wave from $x = -\infty$, the coefficient of the reflected wave was defined as

$$R_1 = \frac{c_0^2 \cosh(k_0 h_0)}{2A^-} \int_0^l \Big[-h'(x) \cosh(k_0(h_0 - h(x))) + i \sinh(k_0(h_0 - h(x))) \Big] e^{ik_0 x} \phi(x, -h(x))\, dx.$$

Integration by parts gives

$$R_1 = \frac{c_0^2 \cosh(k_0 h_0)}{2A^- k_0} \left[\Big[\phi(x, -h(x)) e^{ik_0 x} \sinh(k_0(h_0 - h(x))) \Big]_0^l - \int_0^l e^{ik_0 x} \sinh(k_0(h_0 - h(x))) \frac{\partial \phi}{\partial x}(x, -h(x)) dx \right].$$

As ϕ is bounded on C_h, that is, on the hump, then R_1 is given in terms of the tangential velocity on the hump by

$$R_1 = -\frac{c_0^2 \cosh(k_0 h_0)}{2A^- k_0} \int_0^l e^{ik_0 x} \sinh(k_0(h_0 - h(x))) \frac{\partial \phi}{\partial x}(x, -h(x)) dx \quad .$$

Similarly, the transmission coefficient is defined by

$$T_1 = 1 + \frac{c_0^2 \cosh(k_0 h_0)}{2A^- k_0} \int_0^l e^{-ik_0 x} \sinh(k_0(h_0 - h(x))) \frac{\partial \phi}{\partial x}(x, -h(x)) dx \quad .$$

For an incident wave from $x = \infty$, the coefficients of the resulting reflected and transmitted waves are given by

$$R_2 = \frac{c_0^2 \cosh(k_0 h_0)}{2A^+ k_0} \int_0^l e^{-ik_0 x} \sinh(k_0(h_0 - h(x))) \frac{\partial \phi}{\partial x}(x, -h(x)) dx$$

and

$$T_2 = 1 - \frac{c_0^2 \cosh(k_0 h_0)}{2A^+ k_0} \int_0^l e^{ik_0 x} \sinh(k_0(h_0 - h(x))) \frac{\partial \phi}{\partial x}(x, -h(x)) dx \quad .$$

We are now ready to solve the first-kind integral equation for $\frac{\partial \phi}{\partial s}$ evaluated on C_h, given by (5.47), for a wave incident from either $x = \pm\infty$, and hence calculate the coefficients of the resulting reflected and transmitted waves. We do this using a variational approach, after we have non-dimensionalised the problem.

5.5 Non-dimensionalisation

We use the same scaling procedure as used in previous chapters, which is briefly summarised as follows. Let

$$\begin{aligned} \hat{x} &= \frac{x}{l} \ , \\ \hat{z} &= \frac{z}{h_0} \ , \\ H(\hat{x}) &= \frac{1}{h_0} h(l\hat{x}) \ , \\ \hat{\phi}(\hat{x},\hat{z}) &= \frac{1}{\sigma l^2}\phi(l\hat{x}, h_0\hat{z}) \ . \end{aligned}$$

Then, after discarding the accents from these definitions to simplify the notation, the first-kind integral equation (5.47) may be written in non-dimensional form as

$$\begin{aligned} &\int_0^1 \Big[L\big|_{\substack{z=-H(x)\\ z_0=-H(x_0)}} \chi(x) \Big] dx \\ &\qquad + \frac{i\sinh\left(\kappa_0\tau(1-H(x_0))\right)}{\cosh\left(\kappa_0\tau\right)} \Big[A^- e^{i\kappa_0 x_0} - A^+ e^{-i\kappa_0 x_0} \Big] = 0 \qquad (0 \le x_0 \le 1), \end{aligned} \tag{5.48}$$

where $\chi(x) = \frac{\partial\phi}{\partial x}(x, -H(x))$ and A^- (A^+) is the amplitude of the incident wave from $x = -\infty$ ($x = \infty$). The Green's function L is now redefined to be

$$\begin{aligned} L\left(x,z|x_0,z_0\right) = \ & \frac{i}{2\kappa_0} C_0^2 \sinh\left(\kappa_0\tau(z+1)\right)\sinh\left(\kappa_0\tau(z_0+1)\right) e^{i\kappa_0|x-x_0|} \\ & - \sum_{n=1}^{\infty} \frac{1}{2\beta_n^0} C_n^2 \sin\Big(\beta_n^0\tau(z+1)\Big)\sin\Big(\beta_n^0\tau(z_0+1)\Big) e^{-\beta_n^0|x-x_0|}, \end{aligned}$$

where

$$C_0^2 = \frac{4\kappa_0}{2\kappa_0\tau + \sinh\left(2\kappa_0\tau\right)} \ , \qquad C_n^2 = \frac{4\beta_n^0}{2\beta_n^0\tau + \sin\left(2\beta_n^0\tau\right)} \ (n \in \mathbb{N}) \ ,$$

$\kappa_0 = k_0 l$ is the positive, real root of

$$\alpha_0{}^2\tau = \kappa_0 \tanh\left(\kappa_0\tau\right) \ ,$$

$\beta_n^0 = B_n^0 l$ ($n \in \mathbb{N}$) are the positive real roots of

$$-\alpha_0{}^2\tau = \beta_n^0 \tan\Big(\beta_n^0\tau\Big) \ \ (n \in \mathbb{N}) \ ,$$

arranged in ascending order of magnitude and where α_0 and τ are two dimensionless parameters given by

$$\alpha_0 = \frac{\sigma l}{\sqrt{g h_0}} \ , \qquad \tau = h_0/l \ .$$

The coefficients of the reflected and transmitted waves due to an incident wave from $x = -\infty$ are given by

$$R_1 = -\frac{C_0^2 \cosh(\kappa_0\tau)}{2A^-\kappa_0} \int_0^1 e^{i\kappa_0 x} \sinh(\kappa_0\tau(1-H(x)))\,\chi(x)dx \quad , \tag{5.49}$$

$$T_1 = 1 + \frac{C_0^2 \cosh(\kappa_0\tau)}{2A^-\kappa_0} \int_0^1 e^{-i\kappa_0 x} \sinh(\kappa_0\tau(1-H(x)))\,\chi(x)dx \quad , \tag{5.50}$$

and for an incident wave from $x = \infty$ are given by

$$R_2 = \frac{C_0^2 \cosh(\kappa_0\tau)}{2A^+\kappa_0} \int_0^1 e^{-i\kappa_0 x} \sinh(\kappa_0\tau(1-H(x)))\,\chi(x)dx \quad , \tag{5.51}$$

$$T_2 = 1 - \frac{C_0^2 \cosh(\kappa_0\tau)}{2A^+\kappa_0} \int_0^1 e^{i\kappa_0 x} \sinh(\kappa_0\tau(1-H(x)))\,\chi(x)dx \quad . \tag{5.52}$$

5.6 A variational principle

We start this section by recasting the first-kind integral equation (5.48) on the Hilbert space $L_2(0,1)$, which is the set of all equivalence classes of complex-valued Lebesgue measurable functions ζ satisfying the condition $\int_0^1 |\zeta|^2 < \infty$. This space has pointwise operations with inner product defined by $(f,g) = \int_0^1 f\overline{g}$ and norm defined by $\|f\| = \sqrt{(f,f)}$ (Young [60]). This space includes functions $f \neq 0$ where $\|f\| = 0$, so equivalence classes of functions are considered to re-establish the norm. Two functions f and g are said to be equivalent if they are unequal only on a set of measure zero, such a set being one which can be covered by a sequence of arbitrarily small open intervals. Two equivalent functions are written $f = g$ (a.e.), that is, f and g are equal almost-everywhere. All function equalities in the Hilbert space are meant in this almost-everywhere sense.

We now introduce an operator K defined by

$$(K\psi)(x_0) = \int_0^1 k(x_0,x)\psi(x)dx \qquad (0 \le x_0 \le 1) \ , \tag{5.53}$$

where $k(x_0,x)$, the kernel of K, is defined by

$$\begin{aligned} k(x_0,x) = {} & \frac{i}{2\kappa_0} C_0^2 \sinh(\kappa_0\tau(1-H(x))) \sinh(\kappa_0\tau(1-H(x_0)))\, e^{i\kappa_0|x-x_0|} \\ & -\sum_{n=1}^{\infty} \frac{1}{2\beta_n^0} C_n^2 \sin\Big(\beta_n^0\tau(1-H(x))\Big) \sin\Big(\beta_n^0\tau(1-H(x_0))\Big)\, e^{-\beta_n^0|x-x_0|}. \end{aligned} \tag{5.54}$$

It is quite simple to show that if

$$f_n(x_0,x) = \frac{1}{2\beta_n^0} C_n^2 \sin\Big(\beta_n^0\tau(1-H(x))\Big) \sin\Big(\beta_n^0\tau(1-H(x_0))\Big)\, e^{-\beta_n^0|x-x_0|} \qquad (n \in \mathbb{N}) \ ,$$

then

$$\begin{aligned}\|f_n\| &= \sqrt{\int_0^1 \int_0^1 |f_n(x_0,x)|^2 \, dx dx_0} \\ &\leq \frac{1}{(2\beta_n^0)^{\frac{3}{2}}} C_n^2 \left(2 + \frac{1}{\beta_n^0}(e^{-2\beta_n^0} - 1)\right)^{\frac{1}{2}} < \infty \qquad (n \in \mathbb{N}).\end{aligned}$$

Hence $f_n \in L_2(0,1) \times L_2(0,1)$ $\forall n \in \mathbb{N}$.

Now $\forall n \in \mathbb{N}$, C_n^2 is bounded and for a fixed τ, $\beta_n^0 \sim \frac{n\pi}{\tau} + O(\frac{1}{n})$ as $n \to \infty$ (see Wehausen and Laitone [59], for example). Therefore, it follows that $\sum_{n=1}^{\infty} \|f_n\|$ converges and hence $\sum_{n=1}^{\infty} f_n$ converges in $L_2(0,1) \times L_2(0,1)$. Hence

$$k\,(x_0,x) = \sum_{n=0}^{\infty} f_n\,(x_0,x)$$

converges in $L_2(0,1) \times L_2(0,1)$, where

$$f_0(x_0,x) = \frac{i}{2\kappa_0} C_0^2 \sinh(\kappa_0 \tau (1 - H(x))) \sinh(\kappa_0 \tau (1 - H(x_0)))\, e^{i\kappa_0 |x - x_0|} \ .$$

We also have that for all $n \in \mathbb{N}$, the functions f_n are continuous and are therefore measurable and

$$\begin{aligned}\|k\,(x_0,x)\| &= \sqrt{\int_0^1 \int_0^1 |k(x_0,x)|^2 \, dx dx_0} \\ &\leq \sum_{n=0}^{\infty} \sqrt{\int_0^1 \int_0^1 |f_n(x_0,x)|^2 \, dx dx_0} < \infty \ ,\end{aligned}$$

and so k is called an L_2-kernel on $[0,1] \times [0,1]$. From Porter and Stirling [51], it follows that the operator K defined by (5.53) is a bounded linear map from $L_2(0,1)$ to itself and that K is a compact operator and so is not invertible. The adjoint operator K^* of K is a unique bounded linear map from $L_2(0,1)$ to itself with the property that

$$\forall \psi, \zeta \in L_2(0,1) \qquad (K\psi, \zeta) = (\psi, K^*\zeta) \ .$$

As k is an L_2-kernel, the adjoint operator K^* is given by

$$(K^*\psi)\,(x_0) = \int_0^1 \overline{k(x,x_0)} \psi(x) dx \qquad (0 \leq x_0 \leq 1) \ .$$

The proof of this result can be found in Porter and Stirling [51]. From the definition (5.54) of the kernel k, we can see that $k(x,x_0) = k(x_0,x)$ and $k(x,x_0) \neq \overline{k(x,x_0)}$ and so k is called complex symmetric.

The first-kind integral equation (5.48) can now be written as an operator equation in $L_2(0,1)$ by defining g as

$$g(x_0) = -\frac{i\sinh\left(\kappa_0\tau(1-H(x_0))\right)}{\cosh\left(\kappa_0\tau\right)}\left[A^- e^{i\kappa_0 x_0} - A^+ e^{-i\kappa_0 x_0}\right] \ .$$

Then χ is the solution of

$$K\chi = g \tag{5.55}$$

in $L_2(0,1)$.

Notice that if we now define χ_- to be the solution of (5.55) for a wave of unit amplitude incident from $x = -\infty$ (requiring $A^- = 1, A^+ = 0$ in (5.55)), then the reflection coefficient R_1 is given by

$$R_1 = -\frac{iC_0^2\cosh^2\left(\kappa_0\tau\right)}{2\kappa_0}\left(\chi_-, \overline{g}_-\right) \ , \tag{5.56}$$

where

$$g_-(x_0) = -\frac{i\sinh\left(\kappa_0\tau(1-H(x_0))\right)}{\cosh\left(\kappa_0\tau\right)}e^{i\kappa_0 x_0} \ .$$

Similarly, if we now define χ_+ to be the solution of (5.55) for a wave of unit amplitude incident from $x = \infty$ (requiring $A^- = 0, A^+ = 1$ in (5.55)), then the reflection coefficient R_2 is given by

$$R_2 = -\frac{iC_0^2\cosh^2\left(\kappa_0\tau\right)}{2\kappa_0}\left(\chi_+, \overline{g}_+\right) \ , \tag{5.57}$$

where

$$g_+(x_0) = \frac{i\sinh\left(\kappa_0\tau(1-H(x_0))\right)}{\cosh\left(\kappa_0\tau\right)}e^{-i\kappa_0 x_0} \ .$$

Now $(\chi, \overline{g})$ is the integral of the product of χ, the solution of the operator equation (5.55), and its free term g. We can find a variational principle that will give a second-order estimate to $(\chi, \overline{g})$ compared to the estimate of the solution of χ of (5.55).

Consider the functional $J: \ L_2(0,1) \to \mathbb{C}$ given by

$$J(p) = 2(p, \overline{g}) - (Kp, \overline{p}) \ . \tag{5.58}$$

It is simple to establish that $J(\chi) = (\chi, \overline{g})$, so that given an approximation p to χ, $J(p)$ delivers an approximation to $(\chi, \overline{g})$.

Lemma 5.2 *The functional $J(p)$ defined by (5.58) is stationary at $p = \chi$, the solution of (5.55), with stationary value $(\chi, \overline{g})$.*

Proof

Suppose that $p = \chi + \delta\chi$ where $\delta\chi$ represents the error in this approximation to χ. Then

$$\begin{aligned} J(p) &= J(\chi + \delta\chi) \\ &= (\chi, \overline{g}) + 2(\delta\chi, \overline{g}) - (K\chi, \overline{\delta\chi}) - (K\delta\chi, \overline{\chi}) - (K\delta\chi, \overline{\delta\chi}) \\ &= (\chi, \overline{g}) + 2(\delta\chi, \overline{g - K\chi}) - (K\delta\chi, \overline{\delta\chi}) \qquad \text{(as } k \text{ is complex symmetric)} \\ &= (\chi, \overline{g}) + O\left(\|\delta\chi\|^2\right) \ . \end{aligned}$$

Hence J is stationary at $p = \chi$ with stationary value equal to $(\chi, \overline{g})$. Therefore, using a given first-order accurate approximation p to χ in the functional J delivers a second-order accurate approximation $J(p)$ to $(\chi, \overline{g})$.

We now need to consider the choice of our approximation to χ. In other words, given the integral equation $K\chi = g$, how do we choose p such that $p \approx \chi$?

We choose the trial function p in the form

$$p(x) = \sum_{j=1}^{N} a_j \psi_j(x) \ , \tag{5.59}$$

where the constants $a_j \in \mathbb{C}$ $(j = 1, \ldots, N)$ are unknown and ψ_j $(j = 1 \ldots, N)$ are orthogonal functions that satisfy the same boundary conditions at $x = 0$ and $x = 1$ as χ, that is, they satisfy

$$\psi_j(0) = \chi(0) \qquad \text{and} \qquad \psi_j(1) = \chi(1) \qquad (j = 1, \ldots, N) \ .$$

We have already shown in section 5.3 that $\frac{\partial \phi}{\partial s}$ evaluated at the ends of C_h is zero. In other words, $\chi(0) = 0$ and $\chi(1) = 0$. Consequently, we choose

$$\psi_j(x) = \sin(j\pi x) \qquad (j = 1, \ldots, N) \ . \tag{5.60}$$

The approximation $p = \sum_{j=1}^{N} a_j \psi_j$ to the solution χ of the first-kind integral equation (5.55) is therefore an element of the sub-space E_n of $L_2(0, 1)$ which is spanned by the orthogonal functions ψ_j $(j = 1, \ldots, N)$ given by (5.60).

The constants $a_j \in \mathbb{C}$ $(j = 1, \ldots, N)$ are determined by using the fact that the variational principle $\delta J = 0$ is stationary at $p = \chi$. Therefore, we choose p so that

$$\frac{\partial J}{\partial a_j} = 0 \qquad\qquad (j = 1, \ldots, N) \; .$$

Hence the unknown constants $a_j \in \mathbb{C}$ $(j = 1, \ldots, N)$ satisfy the N simultaneous, linear equations

$$\sum_{j=1}^{N} a_j \, (K\psi_j, \psi_n) = (\psi_n, \overline{g}) \qquad\qquad (n = 1, \ldots, N) \; . \tag{5.61}$$

We can actually evaluate the functional J without needing to find explicitly the approximation to χ. This procedure is given in Porter and Stirling ([51] p.268-269), where the stationary value is expressed as the quotient of the determinants of two $N \times N$ matrices. The entries in the j^{th} column of each matrix correspond to an inner product involving ψ_j. If we did not require to know the values of the constants a_j $(j = 1, \ldots, N)$, then the advantage of this method for evaluating the stationary value of J is that it is not necessary to solve the set of simultaneous equations (5.61). However, in our problem we want to know the approximation to χ so that we can calculate the norm of the residual error of the first-kind integral equation, that is, calculate

$$\left\| g - \sum_{j=1}^{N} a_j K\psi_j \right\| \; .$$

This norm gives an indication of the accuracy of the approximation Kp to $K\chi$.

Unfortunately, even if we show that $\left\| g - \sum_{j=1}^{N} a_j K\psi_j \right\|$ decreases as the dimension of the trial space N increases, it does not follow that the approximation $p = \sum_{j=1}^{N} a_j \psi_j$ converges to χ as N increases because K is not invertible. However, if we show that $\left\| g - \sum_{j=1}^{N} a_j K\psi_j \right\|$ decreases as N increases, then this gives an indication that p may be converging to χ. The unavailability of a proof that $p = \sum_{j=1}^{N} a_j \psi_j$ converges to χ as $N \to \infty$ is the price we have to pay by choosing to solve the computationally attractive first-kind integral equation (5.48) for χ rather than the computationally difficult second-kind integral equation (5.9) for ϕ evaluated on C_h.

We can obtain second-order accurate approximations to the transmission coefficients directly from the second-order accurate approximations to the reflection coefficients using the symmetry relations these coefficients satisfy. It may be

shown, by a simple application of Green's identity to ϕ and its complex conjugate for an incident wave from $x = -\infty$, that

$$|R_1|^2 + |T_1|^2 = 1 \ . \tag{5.62}$$

Similarly, by applying Green's identity to ϕ and its complex conjugate for an incident wave from $x = \infty$, it may be shown that

$$|R_2|^2 + |T_2|^2 = 1 \ . \tag{5.63}$$

Applying Green's identity to ϕ for an incident wave from $x = -\infty$ and to ϕ for an incident wave from $x = \infty$ gives

$$T_1 = T_2 \ . \tag{5.64}$$

Finally, applying Green's identity to ϕ for an incident wave from $x = -\infty$ and the complex conjugate of ϕ for an incident wave from $x = \infty$ gives

$$T_1 \overline{R_2} = -R_1 \overline{T_2} \ . \tag{5.65}$$

These relationships are well-known, with (5.62) first derived by Kreisel [27] and the remainder derived by Newman [42].

From equations (5.62)–(5.65), it is simple to deduce that

$$|R_1| = |R_2| \tag{5.66}$$

and

$$\delta R_1 + \delta R_2 = 2\delta T_1 + (2n+1)\pi \qquad (n \in \mathbb{Z}) \ , \tag{5.67}$$

where δz is the argument of the complex number z.

Once we have calculated the second-order accurate approximations (5.56) and (5.57) to R_1 and R_2 respectively, the second-order accurate approximation to T_1 is given by substituting these values into equations (5.62) and (5.67). The second-order approximation to T_2 is then given by equation (5.64).

We are now in a position to show how we implement this solution process.

5.7 Numerical solution method

In order to determine the approximation to the reflection coefficients and to χ, we see from equation (5.61) that we need to calculate the inner products

$$(\psi_j, \overline{g}) \qquad\qquad (j = 1, \ldots, N)$$

and

$$(K\psi_j, \psi_n) \qquad\qquad (j, n = 1, \ldots, N) \ .$$

In the previous section, we proved that the series for the kernel k of the operator K converged in $L_2(0,1) \times L_2(0,1)$. It follows that we can swap the order of integration and summation in $K\psi_j$. In other words, $K\psi_j$ can be written as

$$\begin{aligned}(K\psi_j)(x_0) = {} & \frac{iC_0^2}{2\kappa_0} w_0(x_0) \int_0^1 w_0(x) e^{i\kappa_0|x-x_0|} \psi_j(x) dx \\ & - \sum_{n=1}^{\infty} \frac{1}{2\beta_n^0} C_n^2 w_n(x_0) \int_0^1 w_n(x) e^{-\beta_n^0|x-x_0|} \psi_j(x) dx \end{aligned} \qquad (j = 1, \ldots, N),$$

where the functions $w_n(x)$ $(n+1 \in \mathbb{N})$ are defined by

$$\begin{aligned} w_0(x) &= \sinh\left(\kappa_0 \tau (1 - H(x))\right) \ , \\ w_n(x) &= \sin\left(\beta_n^0 \tau (1 - H(x))\right) \qquad\qquad (n \in \mathbb{N}) \ . \end{aligned}$$

The advantage of writing $K\psi_j$ in the above form is that by integrating before taking the sum, we avoid the numerical problem of calculating the kernel of K at $x = x_0$, where the kernel is logarithmically singular. We find that we only need to take 40 terms in the infinite series for $K\psi_j$ for the series to converge to 3.d.p. for any values of the parameters α_0 and τ. This feature is illustrated in the results section.

For ease of computation, we rewrite the functions $K\psi_j$ and inner products $(K\psi_j, \psi_n)$ $(j, n = 1, \ldots, N)$ in terms of real-valued integrals. Since

$$ie^{i|x-x_0|} = i\cos(x - x_0) - \sin(|x - x_0|) \qquad\qquad \forall x, x_0 \in \mathbb{R} \ ,$$

and $\psi_j \in \mathbb{R}$ $(j = 1, \ldots, N)$, then we can write $K\psi_j$ in real and imaginary parts as

$$(K\psi_j)(x_0) = (K_r\psi_j)(x_0) + i\,(K_i\psi_j)(x_0) \qquad\qquad (j = 1, \ldots, N) \ ,$$

where

$$(K_r\psi)(x_0) = -\left\{\frac{C_0^2}{2\kappa_0}w_0(x_0)\int_0^1 w_0(x)\sin(\kappa_0|x-x_0|)\,\psi(x)dx + \sum_{n=1}^{\infty}\frac{C_n^2}{2\beta_n^0}w_n(x_0)\int_0^1 w_n(x)e^{-\beta_n^0|x-x_0|}\psi(x)dx\right\}$$

and

$$(K_i\psi)(x_0) = \frac{C_0^2}{2\kappa_0}w_0(x_0)\left\{\cos(\kappa_0 x_0)\int_0^1 w_0(x)\cos(\kappa_0 x)\psi(x)dx + \sin(\kappa_0 x_0)\int_0^1 w_0(x)\sin(\kappa_0 x)\psi(x)dx\right\} .$$

Similarly, we write $(K\psi_j,\psi_n)$ $(j,n=1,\ldots,N)$ in terms of real and imaginary parts as

$$(K\psi_j,\psi_n) = (K_r\psi_j,\psi_n) + i\,(K_i\psi_j,\psi_n) \qquad (j,n=1,\ldots,N) .$$

Finally we express $(\psi_j,\overline{g})$ $(j,n=1,\ldots,N)$ in terms of real and imaginary parts. For a wave of unit amplitude incident from $x=-\infty$ $(A^+=0)$, we write

$$(\psi_j,\overline{g}) = \left(\psi_j,\overline{g}_-\right) = [(\psi_j,f_1) - i\,(\psi_j,f_2)] \qquad (j=1,\ldots,N) \tag{5.68}$$

and for a wave of unit amplitude incident from $x=\infty$ $(A^-=0)$, we write

$$(\psi_j,\overline{g}) = \left(\psi_j,\overline{g}_+\right) = [(\psi_j,f_1) + i\,(\psi_j,f_2)] \qquad (j=1,\ldots,N) , \tag{5.69}$$

where the functions f_1 and f_2 are given by

$$f_1(x) = \frac{\sinh(\kappa_0\tau(1-H(x)))}{\cosh(\kappa_0\tau)}\sin(\kappa_0 x) \quad \text{and} \quad f_2(x) = \frac{\sinh(\kappa_0\tau(1-H(x)))}{\cosh(\kappa_0\tau)}\cos(\kappa_0 x).$$

It is clear that once the real-valued inner products on the right-hand side of (5.68) have been calculated to give $\left(\psi_j,\overline{g}_-\right)$ $(j=1,\ldots,N)$, then as these are the same inner products that appear in the right-hand side of (5.69), we can find $\left(\psi_j,\overline{g}_+\right)$ $(j=1,\ldots,N)$ without calculating any more inner products. In other words, we only have to find a solution for a wave incident from $x=-\infty$, and we can then find the solution for a wave incident from $x=\infty$ without having to calculate any more inner products.

The functions $K_r\psi$ and $K_i\psi$ can only be approximated at a finite number of points x_0. Therefore, the approximations $p=\sum_{j=1}^N a_j\psi_j$ and $Kp=\sum_{j=1}^N a_jK\psi_j$

are only known at a finite number of points. We use 10 point composite Gauss-Legendre quadrature to calculate the integrals because it delivers highly accurate answers very economically for well-behaved integrands. Details of this quadrature rule can be found in Johnson and Riess [24], for example.

Chamberlain [7] used Gauss-Legendre quadrature to calculate

$$I(x_0) = \int_0^1 f(x) \sin\left(\kappa_0 |x - x_0|\right) dx \ ,$$

where f and its first derivative are continuous, real-valued functions. He found that the quadrature rule was hampered by the presence of the slope discontinuity which exists in the integrand at $x = x_0$. Chamberlain showed that an efficient remedy is given by writing

$$I(x_0) = \int_0^1 \left(f(x) - f(x_0)\right) \sin\left(\kappa_0 |x - x_0|\right) dx + f(x_0) \int_0^1 \sin\left(\kappa_0 |x - x_0|\right) dx \ . \quad (5.70)$$

The integrand in the first term of the right-hand side has a continuous first derivative and the integral in the second term can be found explicitly and is given by

$$\int_0^1 \sin\left(\kappa_0 |x - x_0|\right) dx = \frac{2}{\kappa_0} \left[1 - \cos\left(\frac{1}{2}\kappa_0\right) \cos\left(\kappa_0 (x_0 - \frac{1}{2})\right)\right] \ .$$

Details of how this process improves the performance of the quadrature rule are given in Chamberlain [7]. Similarly, we write

$$\int_0^1 f(x) e^{-\beta |x - x_0|} dx = \int_0^1 \left(f(x) - f(x_0)\right) e^{-\beta |x - x_0|} dx + f(x_0) \int_0^1 e^{-\beta |x - x_0|} dx \ , \quad (5.71)$$

so that the integrand in the first term on the right-hand side has a continuous first derivative and the integral in the second term is given by

$$\int_0^1 e^{-\beta |x - x_0|} dx = \frac{1}{\beta} \left[2 - \left(e^{-\beta x_0} + e^{-\beta (1 - x_0)}\right)\right] \ .$$

The integration routine in our computer program therefore calculates the integrals in $K_r \psi$ by using (5.70) and (5.71).

The solution process is now clear. Once the depth profile H and the parameters α_0 and τ have been chosen, we calculate the functions $K_r \psi_j$ and $K_i \psi_j$ $(j = 1, \ldots, N)$. The inner products $(K\psi_j, \psi_n)$ $(j, n = 1, \ldots, N)$ are then calculated by evaluating their component real-valued inner products. Similarly, $(\psi_j, \overline{g})$

$(j = 1, \ldots, N)$ are calculated for an incident wave from $x = -\infty$ and from $x = \infty$. We then substitute these inner products into equation (5.61) and solve it to give the constants a_j $(j = 1, \ldots, N)$. We then find the approximations to the reflection and transmission coefficients, formulate $p = \sum_{j=1}^{N} a_j \psi_j$ and $Kp = \sum_{j=1}^{N} a_j K\psi_j$ and evaluate the residual of the first-kind integral equation, that is, evaluate $\|Kp - g\|$.

5.8 Results

In this section we find approximations to the reflection and transmission coefficients of the scattered waves due to a wave of unit amplitude incident from either $x = -\infty$ or $x = \infty$ on a variety of hump depth profiles. In the first example we give numerical results and illustrate the convergence of $K\psi_j$ where $j \in (1, \ldots, N)$ and the convergence of the approximation to the reflection coefficient as the number of terms in the series for K is increased. After concluding that 40 terms in the series gives sufficiently accurate results, we then illustrate the convergence of the approximation to the reflection coefficient and its modulus as the number of terms in the trial function is increased. Finally, we present some graphical results, compare them to results from previous model equations, such as the mild-slope equation, and give some conclusions.

Example 5.3

Suppose that C_h is given by the depth profile

$$H(x) = x^2 - x + 1 \qquad (0 \leq x \leq 1) \ .$$

This corresponds to a hump whose height is one quarter of the still-water depth with slope discontinuities at $x = 0$ and $x = 1$. We choose parameter values

$$\alpha_0 = 2 \qquad \text{and} \qquad \tau = 0.2 \ .$$

Firstly, we shall examine the convergence of $K_r\psi_j = \sum_{n=0}^{M} K_n^r \psi_j$, where

$$\left(K_0^r \psi_j\right)(x_0) = -\frac{C_0^2}{2\kappa_0} w_0(x_0) \int_0^1 w_0(x) \sin(\kappa_0 |x - x_0|) \psi_j(x) dx$$

and

$$\left(K_n^r \psi_j\right)(x_0) = -\frac{C_n^2}{2\beta_n^0} w_n(x_0) \int_0^1 w_n(x) e^{-\beta_n^0 |x - x_0|} \psi_j(x) dx \qquad (n = 1, \ldots, M) \ ,$$

as M is increased.

Instead of showing the convergence of $(K_r\psi_j)(x_0)$ for chosen values of x_0 in $[0,1]$, we show the convergence of $\|K_r\psi_j\|$ as M increases, to give an overall

M	$\left\|\sum_{n=0}^{M-1} K_n^r\psi_1\right\|$	$\left\|\sum_{n=0}^{M} K_n^r\psi_1\right\|$	$\left\|\sum_{n=0}^{M-1} K_n^r\psi_3\right\|$	$\left\|\sum_{n=0}^{M} K_n^r\psi_3\right\|$
10	0.023965	0.024160	0.015655	0.015851
20	0.024793	0.024819	0.016441	0.016463
30	0.025027	0.025046	0.016667	0.016687
40	0.025154	0.025161	0.016791	0.016797
50	0.025224	0.025230	0.016859	0.016865
60	0.025274	0.025277	0.016907	0.016910
70	0.025307	0.025310	0.016940	0.016943
80	0.025333	0.025335	0.016966	0.016967
90	0.025353	0.025355	0.016985	0.016986
100	0.025369	0.025371	0.017001	0.017002

Table 5.1: Illustrating the convergence of $\left\|\sum_{n=0}^{M} K_n^r\psi_j\right\|$ $(j = 1, 3)$.

impression of the convergence of $(K_r\psi_j)(x_0)$ in $[0,1]$ as M increases. Table 5.1 gives $\left\|\sum_{n=0}^{M-1} K_n^r\psi_j\right\|$ and $\left\|\sum_{n=0}^{M} K_n^r\psi_j\right\|$ for $j = 1$ and $j = 3$ as M takes values from 10 to 100. We can see from Table 5.1 that for this depth profile and parameter values, $\|K_r\psi_j\|$ $(j = 1, 3)$ converges quite slowly, but has converged to 3.d.p. when $M = 40$.

Now let us examine the convergence of the approximation to the reflection coefficient as M increases. Table 5.2 gives the approximation to the reflection coefficient R_1 delivered by a 4-term and an 8-term trial approximation as M takes values from 10 to 100. It is clear from Table 5.2 that when $M = 40$, the approximation to the reflection coefficient delivered by the 4-term trial function has converged to 3.d.p. and that given by the 8-term trial function has practically converged to 3.d.p. as well. Similarly, we find that for all choices of the parameters α_0 and τ of interest and all depth profiles tested, using $M = 40$ in the series for K_r gives an approximation to the reflection coefficient which has converged to

M	R_1 $(4-term)$	R_1 $(8-term)$
10	$0.095878 + 0.078823i$	$0.094665 + 0.078163i$
20	$0.094260 + 0.076531i$	$0.093248 + 0.075982i$
30	$0.093712 + 0.075775i$	$0.092755 + 0.075256i$
40	$0.093435 + 0.075395i$	$0.092503 + 0.074890i$
50	$0.093268 + 0.075168i$	$0.092352 + 0.074671i$
60	$0.093156 + 0.075016i$	$0.092250 + 0.074525i$
70	$0.093076 + 0.074908i$	$0.092177 + 0.074421i$
80	$0.093016 + 0.074827i$	$0.092122 + 0.074342i$
90	$0.092970 + 0.074764i$	$0.092080 + 0.074282i$
100	$0.092932 + 0.074713i$	$0.092046 + 0.074233i$

Table 5.2: Illustrating the convergence of the approximation to R_1 as M increases.

3.d.p. for any number of terms in the trial function p. Therefore, for the results presented in the rest of this section, we use $M = 40$ in the series for K_r.

We now examine the behaviour of the approximation to the reflection coefficient R_1 as we increase the number of terms in the trial function. Table 5.3 gives the approximations to R_1, $|R_1|$ and $\|Kp - g\|$ as the number of terms (N) in the trial function is increased. From Table 5.3, it is clear that a 10-term trial function

M	R_1	$\lvert R_1\rvert$	$\|Kp - g\|$
2	$0.096 + 0.077i$	0.123	0.0079
4	$0.093 + 0.075i$	0.120	0.0041
6	$0.093 + 0.075i$	0.119	0.0026
8	$0.093 + 0.075i$	0.119	0.0018
10	$0.092 + 0.075i$	0.119	0.0013
12	$0.092 + 0.075i$	0.119	0.0010
14	$0.092 + 0.075i$	0.119	0.0008

Table 5.3: Illustrating the convergence of the approximation to R_1 as N increases.

delivers an approximation to the reflection coefficient that has converged to 3.d.p. We also note from Table 5.3 that as the number of terms in the trial function is increased, so the norm of the residual error in the first-kind integral equation, $\|Kp - g\|$, decreases. This gives an indication that p may be converging to χ.

For all other hump depth profiles and values of parameters α_0 and τ, we have found that a 10-term trial function gives an approximation to the reflection and transmission coefficients that is correct to 3.d.p., in the sense that the estimates of $K_r\psi_j$ $(j = 1, \ldots, N)$ have converged to 3.d.p. This accuracy is quite satisfactory and so the results given in the rest of this section are obtained using a 10-term trial-function.

The approximation to the reflection coefficient R_2 for this problem is

$$R_2 = -0.114 + 0.034i \ .$$

Using the method described in Section 5.6, we find that the transmission coefficients are given by

$$T_1 = T_2 = 0.974 + 0.194i \ .$$

In Table 5.4, we compare the reflection and transmission coefficients of the scattered waves given by the mild-slope (MSE), modified mild-slope (MMSE) with both sets of boundary conditions, which were given in Chapter 4, and the n-term $(n = 2, 3)$ trial approximations, which were derived in Chapter 4, with the estimates we have obtained for full linear theory. It is clear from Table 5.4 that the results given by the MSE and MMSE with the new boundary conditions are in much better agreement with the estimates we have obtained for full linear theory than the results given by the MSE and MMSE with the old boundary conditions. We can also see that as we increase the number of decaying modes in the approximation to the full linear velocity potential, the results become closer to those obtained for full linear theory.

We now compare the estimates to the solutions of the full linear problem with those given by the above mentioned approximate models over a range of parameter values. In the first example, we return to the wave scattering problem for a hump that was considered in Chapter 4.

Approximation	R_1	T_1
Full linear	$0.092 + 0.075i$	$0.974 + 0.194i$
3-term	$0.0927 + 0.0727i$	$0.9757 + 0.1916i$
2-term	$0.0917 + 0.0736i$	$0.9747 + 0.1899i$
MMSE (new)	$0.0920 + 0.0735i$	$0.9751 + 0.1878i$
MSE (new)	$0.0883 + 0.0727i$	$0.9727 + 0.2021i$
MMSE (old)	$0.0867 + 0.0673i$	$0.9786 + 0.1741i$
MSE (old)	$0.0829 + 0.0663i$	$0.9763 + 0.1885i$

Table 5.4: A comparison of estimates of R_1 and T_1.

Example 5.4

The depth profile is given by

$$H(x) = 2x^2 - 2x + 1 \qquad\qquad (0 \leq x \leq 1) \ .$$

This corresponds to a hump whose height is half the still-water depth which has slope discontinuities at $x = 0$ and at $x = 1$, where it meets the flat beds. We seek solutions given by the mild-slope, modified mild-slope and n-term ($n = 2, 3, 4$) approximations and estimates to the solutions of full linear problem at values of a parameter ω starting at 0.05, finishing at 10, with intervals of 0.05. The parameters α_0 and τ are defined in terms of ω by

$$\alpha_0 = \omega \ , \qquad \tau = \frac{1}{\omega} \ .$$

With these definitions for α_0 and τ, varying ω corresponds to varying the length l of the hump, which corresponds to varying the steepness of the depth profile.

Using a 10-term trial function to give estimates of the reflection and transmission coefficients for the full linear problem, we find that the maximum value of $\|Kp - g\|$ over the whole ω range is 5.8×10^{-3}.

The graphs of $|R_1|$ against ω given using full linear theory, MSE and MMSE with the new and the old boundary conditions are presented in Fig.5.7. It is clear from the graphs that the results given by both the MSE and MMSE with the new set of boundary conditions are very much closer to those estimated for

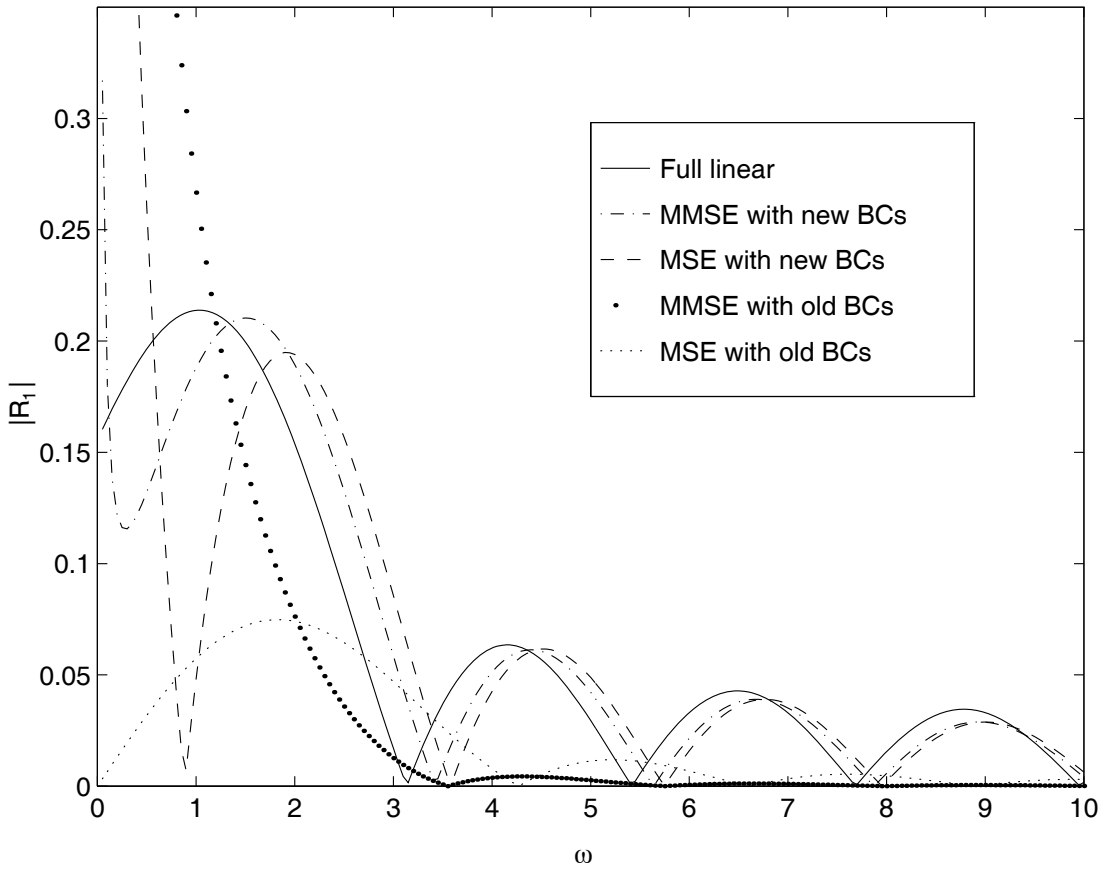

Figure 5.7: Reflected amplitude over the depth profile $H(x) = 2x^2 - 2x + 1$ $(0 \leq x \leq 1)$.

the full linear problem, than the results given by the MSE and MMSE with the old boundary conditions. Indeed, the results given by the MSE and MMSE with the old boundary conditions bear little resemblance to the full linear results. From this evidence and that given in Chapter 4 for Booij's [5] talud problem, we conclude that the new boundary conditions are the appropriate boundary conditions to use with the MSE and MMSE.

The results given by the MMSE with the new boundary conditions are the closest to the full linear results, as expected, and give good agreement with the full linear results for $\omega > 4.5$. However, the results given by the MSE with the new boundary conditions only agree with the full linear results as well as the results given by the MMSE when $\omega > 8$. This illustrates that the MMSE gives results in good agreement with the full linear results for humps with up to nearly twice the maximum gradient that can be used with the MSE to give results that

are in good agreement with full linear theory.

In Fig.5.8 we present the graphs of $|R_1|$ against ω given using full linear theory and the MMSE, 2-term, 3-term and 4-term approximations. It is clear from the

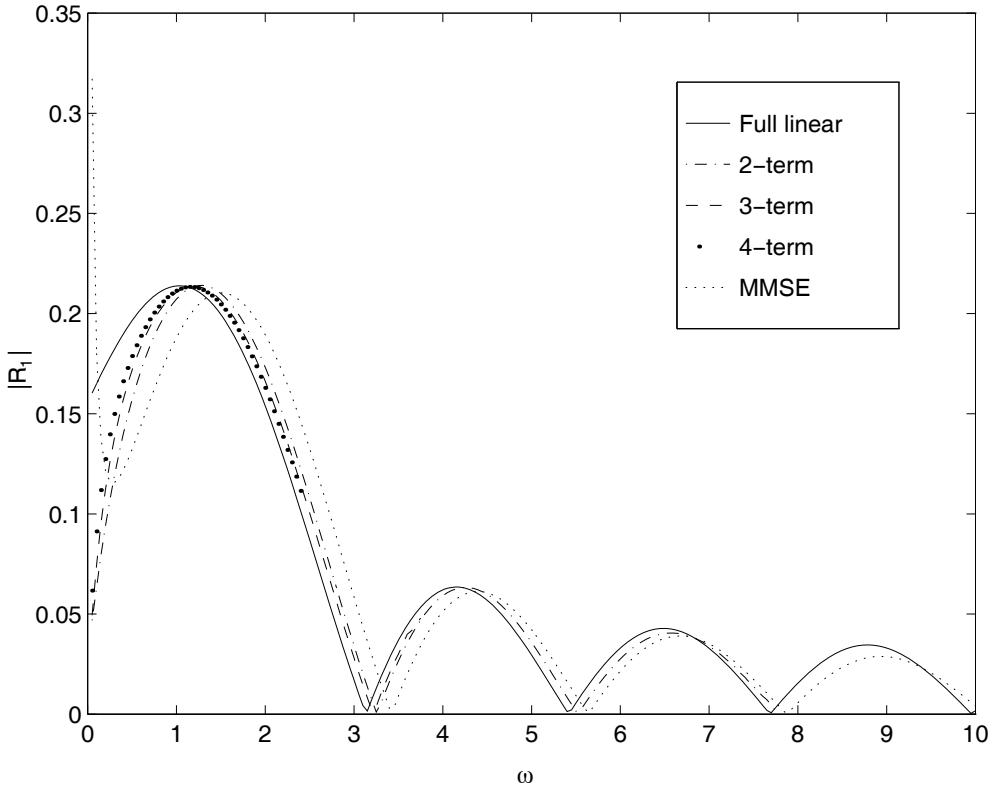

Figure 5.8: Reflected amplitude over the depth profile $H(x) = 2x^2$–$2x$+1 $(0 \leq x \leq 1)$.

graph that, as the number of terms in the n-term approximation is increased, the closer the results become to the full linear ones. For $\omega > 4$, the slope of the hump is mild enough for the 2-term approximation to give good estimates to the full linear solutions. Similarly, the 3- and 4-term approximations gives good estimates of the full linear solutions when $\omega > 2.5$ and $\omega > 1$ respectively.

As a final example, we consider a hump which is smoothly joined to the flat beds at $x = 0$ and $x = 1$. Remember from Chapter 4 that in this case the old and new boundary conditions for the MSE and MMSE are the same.

Example 5.5

We consider a depth profile given by

$$H(x) = \frac{3}{4} + \frac{1}{4}\cos(2\pi x) \qquad (0 \leq x \leq 1) \ ,$$

which corresponds to a hump whose height is half the still-water depth. We seek solutions given by the mild-slope, modified mild-slope and n-term ($n = 2, 3, 4$) approximations and estimates of the solutions of full linear problem at values of a parameter ω starting at 0.05, finishing at 10, with intervals of 0.05. The parameters α_0 and τ are defined in terms of ω by

$$\alpha_0 = \omega \ , \qquad \tau = \frac{1}{\omega} \ .$$

Again, with these definitions for α_0 and τ, varying ω corresponds to varying the steepness of the depth profile.

Using a 10-term trial function to give estimates of the reflection and transmission coefficients for the full linear problem, we find that the maximum value of $\|Kp - g\|$ over the whole ω range is 3.4×10^{-3}.

In Fig.5.9 we present the graphs of $|R_1|$ against ω estimated using full linear theory and the MSE, MMSE, 2-term, 3-term and 4-term approximations. Again,

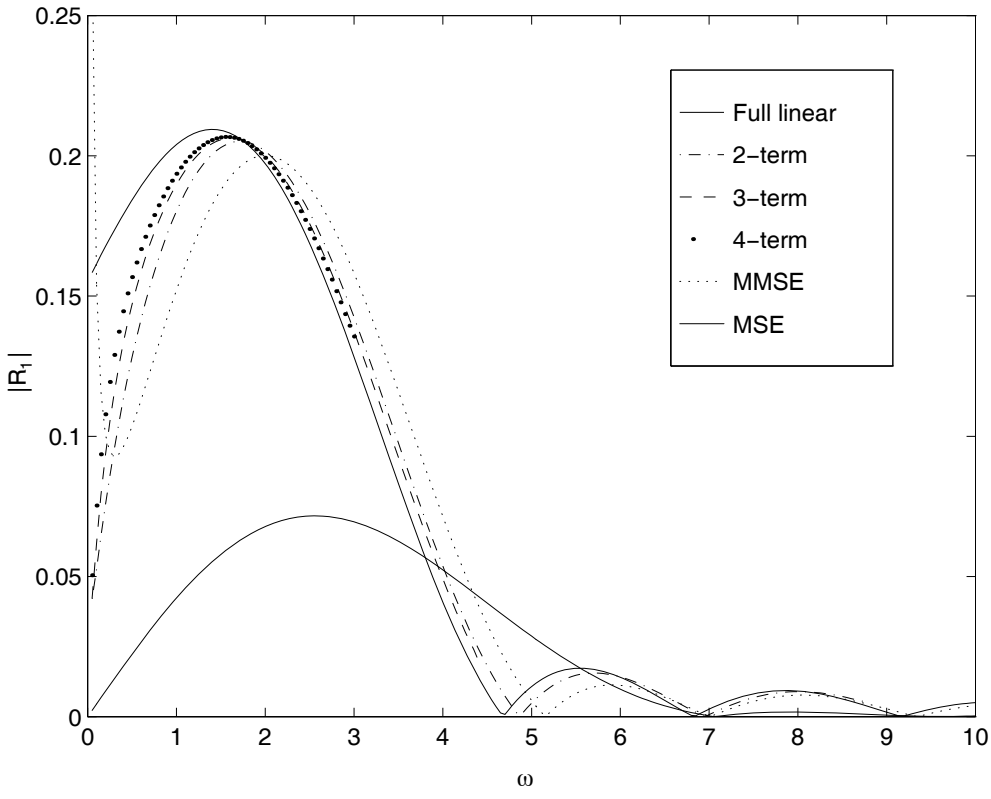

Figure 5.9: Reflected amplitude for depth profile $H(x) = \frac{3}{4} + \frac{1}{4}\cos(2\pi x)$ $(0 \leq x \leq 1)$.

it is clear from the graph that, as the number of terms in the n-term approxima-

tion is increased, the closer the results become to the full linear ones. The results given by the MSE over the whole ω range are quite poor. The results given by the MMSE are much closer to the full linear results than those given by the MSE and give good agreement with the full linear results for $\omega > 6.5$. However, for $\omega < 6.5$, it is clear that the slope of the hump is large enough to warrant the inclusion of decaying modes in the approximation to the velocity potential. As usual, we see that the greater the slope of the hump becomes, the more decaying modes we need to use in the approximation to the velocity potential. As there is little difference in the results given by the 3-term and 4-term approximations, we do not calculate results for the 5-term approximation. Again, we notice that the results given by the n-term approximation converge to those given by the $(n-1)$-term approximation as ω decreases, that is, as the slope of the hump becomes milder.

In this chapter, we have shown how to obtain estimates of the coefficients of the scattered waves due to waves incident from $x = \pm\infty$ on hump depth profiles for full linear theory. A new first-kind integral equation for the tangential fluid velocity $\frac{\partial \phi}{\partial s}$ on the hump has been derived and a variational approach has been used to generate approximations to the coefficients of the scattered waves which are second-order accurate compared to the approximation of the solution of the first-kind equation. We have shown that estimates of the reflection coefficient can be determined to 3.d.p. using 40 terms in the infinite series of the kernel in the first-kind equation and a 10-term trial function. Results have been presented of how the estimate of the modulus of the reflection coefficient for the full linear model varies as the slope of the hump is varied. These results were compared with the corresponding results given by earlier approximations to the full linear model, namely the mild-slope, modified mild-slope and the n-term approximations, which were derived in Chapter 4. Further evidence was found to support the evidence given in Chapter 4, that the new boundary conditions derived in Chapter 4, were the appropriate ones to use with the MSE and MMSE. We also showed that the

mild-slope and modified mild-slope approximations give good agreement with the full linear results for humps with mild slopes, and that as the slope of the hump becomes large, decaying wave mode terms are required in the approximation to gives results that are in good agreement with the full linear results.

These estimates of the solutions of the full linear wave scattering problem over humps will provide an invaluable new test to the accuracy of any new approximation to wave scattering by an arbitrary sea bed.

Summary and Further Work

In this thesis the scattering of a train of small amplitude harmonic surface waves on water by undulating one- and quasi-one-dimensional bed topography has been investigated.

After re-establishing the full linear boundary-value problem satisfied by the velocity potential for the scattering of waves by varying topography in Chapter 2, three approximations to this problem were given, namely the mild-slope, Eckart and linearised shallow water approximations. A highly accurate integral equation method given by Chamberlain [7] which can be used to solve these approximate problems was then reviewed.

In Chapter 3, several extensions to the work appearing in Chamberlain [7] & [8] were presented. A new integral equation method was developed which solves the mild-slope, Eckart and linearised shallow water equations over a range of their parameters in less than one half of the CPU time required by previously implemented integral equation procedures. Eckart's approximation was also investigated and improved and, as a by-product, a new, explicit and very accurate approximation to the solution of the dispersion relation was also found. Finally, after rederiving the symmetry relations satisfied by the reflection and transmission coefficients given by these approximations, we showed that these coefficients satisfy the symmetry relations even when they are inaccurately calculated, an unexpected property.

In Chapter 4, we derived a new approximation to wave scattering that included both decaying and progressive wave mode terms. This new approximation was compared with two older approximations that only contain progressive wave mode terms, namely the mild-slope and modified mild-slope approximations. We showed that for steep depth profiles, where the decaying wave modes are signifi-

cant, the results given by the new approximation agreed much more closely with the results Booij [5] obtained using full linear theory. The maximum number of decaying modes used in the new approximation was three. This was because the difference in the results obtained using two and three decaying modes in the new approximation was only very small for even the steepest depth profiles. In other words, the results given by the new approximation had essentially converged for the steepest depth profiles when the number of decaying modes included had reached three. The less steep the depth profile, the fewer the number of decaying modes required for convergence until eventually the gradient of the depth profile becomes mild enough to make all the decaying modes negligible. The solution method, in which the governing system of second-order differential equations was converted into a first-order system and then solved using a Runge-Kutta procedure, could not be used for some values of the parameters of the problem, which correspond to mild bed profiles. Further work is required here to find a more robust solution method. This could possibly be achieved by using a finite difference method to solve the second-order system of differential equations and associated boundary conditions. Alternatively, developing an approximate solution method to solve the integral equation system equivalent to this boundary-value problem is another possibility.

More work is still required to determine the properties of the reflection and transmission coefficients given by the new 'decaying mode' approximation. The estimates we have calculated of these coefficients satisfy the usual symmetry relations. However, a proof that the exact coefficients or any estimates of them satisfy these symmetry relations has not yet been found. Chamberlain [8] developed a decomposition method for the modified mild-slope and mild-slope equations which allows wave scattering by complex bed profiles to be deduced from wave scattering over simple bed profiles which together make up the complex bed profile. This process is built around the symmetry relations satisfied by the reflection and transmission coefficients. It seems likely that such a method could be developed for the 'decaying mode' approximation too, once the properties of the reflection and transmission coefficients have been determined.

In the course of developing the 'decaying mode' approximation, a new set

of boundary conditions was derived for the mild-slope and modified mild-slope equations. Previously, the boundary conditions for these equations had been obtained by enforcing the continuity of the approximation to the free surface and its slope at the ends of the varying depth region. The new boundary conditions arise from enforcing the continuity of the approximation to the velocity potential and its horizontal velocity throughout the fluid at the ends of the varying depth region. The results given by the mild-slope and modified mild-slope equations with these new boundary conditions are in much better agreement with results that have been computed using full linear theory and results that have been found by using a type of approximation in the full linear wave scattering problem different to the ones that have been used in this thesis. The modified mild-slope equation together with these new boundary conditions can be derived from a variational principle. The details of this process are the subject of a paper by Porter and Staziker (in preparation).

Finally, we showed how to obtain estimates of the coefficients of the scattered waves due to plane wave incidence on hump depth profiles for full linear theory. A new first-kind integral equation for the tangential fluid velocity on the hump was derived and a variational approach used to generate approximations to the reflection coefficients which are second-order accurate compared to the approximation of the solution of the first-kind equation. The symmetry relations satisfied by the reflection and transmission coefficients were then used to calculate the transmission coefficients. An alternative variational principle can be found which gives approximations to both the reflection and transmission coefficients. However, this alternative process is computationally more expensive than the method used because a larger trial space is required. The reflection coefficient was determined to three decimal places using the first 40 terms of the infinite series which defines the kernel in the first-kind equation and a 10-term trial function. Further work to remove the logarithmic singularity in the infinite series will improve the convergence of this series and thus improve computational efficiency. These estimates of the solutions of the full linear wave scattering problem over humps provide an invaluable new test of the accuracy of any new approximation to wave scattering by an arbitrary sea bed.

The modified mild-slope approximation to the velocity potential is derived by using a 1-term plane wave trial function in a variational principle. The results obtained give good agreement with full linear theory for all but the steepest of depth profiles. An apparently similar approximation in the variational principle which was used for the first-kind integral equation is to omit all the decaying wave mode terms in the series for the kernel, so that only the first term in the series is used. However the results obtained by this approximation are poor and we find that the amplitude of the reflected wave increases as the water depth increases which is exactly opposite to the behaviour of the exact solution. So the following question arises: what approximation in the variational principle for the first-kind integral equation corresponds to the modified mild-slope approximation? Further work is clearly required here to fully understand this approximation process. Once it is understood, it could be used in other more complicated integral equations arising from wave scattering, such as that derived by Evans [16] for scattering by a shelf of arbitrary profile. So far this second-kind integral equation has not been solved due to the extremely complicated form of the kernel. If an approximation equivalent to the modified mild-slope approximation could be made in a variational principle, which is equivalent to solving this equation, then not only could powerful solution techniques such as reiteration be used to solve the approximate equation, but it could also be possible to find explicit bounds on the error incurred by making the approximation.

Bibliography

Bibliography

[1] E. F. Bartholomeusz. The reflexion of long waves at a step. *Proc. Camb. Phil. Soc.*, 54:106–118, 1958.

[2] J. C. W. Berkhoff. Computation of combined refraction-diffraction. In *Proc. 13th Int. Conf. on Coastal Eng.*, pages 471–490. Vancouver, Canada, ASCE, New York, N. Y., July 1973.

[3] J. C. W. Berkhoff. Mathematical models for simple harmonic linear water waves. Rep. W 154-iv, Delft Hydr., 1976.

[4] J. L. Black and C. C. Mei. Scattering of surface waves by rectangular obstacles in waters of finite depth. *J. Fluid Mech.*, 38:499–511, 1969.

[5] N. Booij. A note on the accuracy of the mild-slope equation. *Coastal Engineering*, 7:191–203, 1983.

[6] P. G. Chamberlain. *Wave Propagation on Water of Uneven Depth.* PhD thesis, University of Reading, 1991.

[7] P. G. Chamberlain. Wave scattering over uneven depth using the mild-slope equation. *Wave Motion*, 17:267–285, 1993.

[8] P. G. Chamberlain. Symmetry relations and decomposition for the mild-slope equation. *J. Eng. Math.*, 29:121–140, 1995.

[9] P. G. Chamberlain and D. Porter. The modified mild-slope equation. *J. Fluid Mech.*, 1995a. (to appear).

[10] P. G. Chamberlain and D. Porter. Decomposition methods for wave scattering by topography with application to ripple beds. *Wave Motion*, 1995b. (to appear).

[11] K. W. E. Chu and D. Porter. The solution of two wave-diffraction problems. *J. Eng. Math.*, 20:63–72, 1986.

[12] A. G. Davies and A. D. Heathershaw. Surface-wave propagation over sinusoidally varying topography. *J. Fluid Mech.*, 144:419–443, 1984.

[13] W. R. Dean. On the reflection of surface waves by a submerged plane barrier. *Proc. Camb. Phil. Soc.*, 41:231–238, 1945.

[14] B. A. Ebersole. Refraction-diffraction model for linear water waves. *Journal of Waterway, Port, Coastal and Ocean Engineering*, 111(6):939–953, 1985.

[15] C. Eckart. The propagation of gravity waves from deep to shallow water. In *Gravity Waves: (Proc. NBS Semicentennial Symp. on Gravity Waves,NBS, June 15-18, 1951)*, pages 165–175, Washington: National Bureau of Standards, 1952.

[16] D. V. Evans. The application of a new source potential to the problem of the transmission of water waves over a shelf of arbitrary profile. *Proc. Camb. Phil. Soc.*, 71:391–410, 1972.

[17] D. V. Evans. A note on the total reflexion or transmission of surface waves in the presence of parallel obstacles. *J. Fluid Mech.*, 67:465–472, 1975.

[18] D. V. Evans and C. A. N. Morris. Complementary approximations to the solution of a problem in water waves. *J. Inst. Math. Applics.*, 10:1–9, 1972.

[19] E. Fehlberg. Klassiche runge-kutta formeln vierter und niedregerer ordnung mit schrittweiten-kontrolle und ihre anwendung auf warmeleitungs-probleme. *Computing*, 6:61–71, 1970.

[20] G. F. Fitz-Gerald. The reflexion of plane gravity waves travelling in water of variable depth. *Phil. Trans. Roy. Soc.*, A286:49–89, 1976.

[21] G. E. Forsythe, M. A. Malcolm, and C. B. Moler. *Computer Methods for Mathematical Computations*. Prentice-Hall, 1977.

[22] J. Harband. Propagation of long waves over water of slowly varying depth. *J. Eng. Math.*, 11:97–119, 1977.

[23] R. J. Jarvis. The scattering of surface waves by two vertical plane barriers. *J. Inst. Math. Applics.*, 7:207–215, 1971.

[24] R. J. Johnson and R. D. Riess. *Numerical Analysis*. Addison-Wesley, 2nd edition, 1982.

[25] I. G. Jonsson, O. Skovgaard, and O. Brink-Kjaer. Diffraction and refraction calculations for waves incident on an island. *Journal of Marine Research*, 34:469–496, 1976.

[26] J. T. Kirby. A general wave equation for waves over rippled beds. *J. Fluid Mech.*, 162:171–186, 1986.

[27] G. Kreisel. Surface waves. *Quart. Appl. Math.*, VII(1):21–44, 1949.

[28] H. Lamb. *Hydrodynamics 6th Ed.* Cambridge University Press, 1932.

[29] J. D. Lambert. *Numerical Methods in Ordinary Differential Equations*. Wiley, 1992.

[30] C. C. Lautenbacher. Gravity wave refraction by islands. *J. Fluid Mech.*, 41:655–672, 1970.

[31] B. Li and K. Anastasiou. Efficient elliptic solvers for the mild-slope equation using the multigrid technique. *Coastal Engineering*, 16:245–266, 1992.

[32] C. Lozano and R. E. Meyer. Leakage and response of waves trapped by round islands. *The physics of fluids*, 19:1075–1088, 1976.

[33] J. C. Luke. A variational principle for a fluid with a free surface. *J. Fluid Mech.*, 27:395–397, 1967.

[34] C. Macaskill. Reflexion of water waves by a permeable barrier. *J. Fluid Mech.*, 95:141–157, 1979.

[35] S. R. Massel. Hydrodynamics of coastal zones. *Elsevier Oceanography Series*, 48, 1989.

[36] S. R. Massel. Extended refraction-diffraction equation for surface waves. *Coastal Engineering*, 19:97–126, 1993.

[37] C. C. Mei. *The applied dynamics of ocean surface waves*. Wiley Interscience publishers, 1983.

[38] R. E. Meyer. Surface wave reflection by underwater ridges. *Journal of Physical Oceanography*, 9(1):150–157, 1979.

[39] J. W. Miles. Surface wave scattering matrix for a shelf. *J. Fluid Mech.*, 28(4):755–767, 1967.

[40] J. W. Miles. Variational approximations for gravity waves in water of variable depth. *J.Fluid.Mech*, 232:681–688, 1991.

[41] J. N. Newman. Propagation of water waves past long two-dimensional obstacles. *J. Fluid Mech.*, 23:23–29, 1965a.

[42] J. N. Newman. Propagation of water waves over an infinite step. *J. Fluid Mech.*, 23(2):399–415, 1965b.

[43] J. N. Newman. Interaction of water waves with two closely spaced vertical obstacles. *J. Fluid Mech.*, 66:97–106, 1974.

[44] J. N. Newman. Numerical solutions of the water-wave dispersion relation. *Applied Ocean Research*, 12(1):14–18, 1990.

[45] T. J. O'Hare and A. G. Davies. A new model for surface wave propagation over undulating topography. *Coastal Engineering*, 18:251–266, 1992.

[46] T. J. O'Hare and A. G. Davies. A comparison of two models for surface-wave propagation over rapidly varying topography. *Applied Ocean Research*, 15:1–11, 1993.

[47] D. Porter. The transmission of surface waves through a gap in a vertical barrier. *Proc. Camb. Phil. Soc.*, 71:411–421, 1972.

[48] D. Porter. The radiation and scattering of surface waves by vertical barriers. *J. Fluid Mech.*, 63(4):625–634, 1974.

[49] D. Porter. Approximate solutions to a multiple barrier diffraction problem. Applied Mathematics Report 79/1, University of Reading, 1979.

[50] D. Porter. Wave diffraction around breakwaters. Rep. IT 200, Hydraulics Research Station, Wallingford, Oxon., December 1979.

[51] D. Porter and D. S. G. Stirling. *Integral Equations.* Cambridge University Press, 1990.

[52] V. Rey. Propagation and local behaviour of normally incident gravity waves over varying topography. *European J. Mechanics (B/Fluids)*, 11:213–232, 1992.

[53] M. Roseau. Contribution à la théorie des ondes liquides de gravité en profondeur variable. No. 275, Publications Scientifiques et Techniques du Ministère de l'Air, Paris, 1952.

[54] R. Smith and T. Sprinks. Scattering of surface waves by a conical island. *J. Fluid Mech.*, 72:373–384, 1975.

[55] J. J. Stoker. *Water Waves.* Interscience publishers, 1957.

[56] R. C. Thorne. Multipole expansions in the theory of surface waves. *Proc. Camb Phil. Soc*, 49:707–716, 1953.

[57] E. O. Tuck. Transmission of water-waves through small apertures. *J. Fluid Mech.*, 49:65–74, 1971.

[58] F. Ursell. The effect of a fixed vertical barrier on surface waves in deep water. *Proc. Camb. Phil. Soc.*, 43:374–382, 1947.

[59] J. V. Wehausen and E. V. Laitone. *Surface waves*, pages 446–778. Handbuch der Physik, Springer Verlag, 1960.

[60] N. Young. *An introduction to Hilbert space.* Cambridge University Press, 1983.